

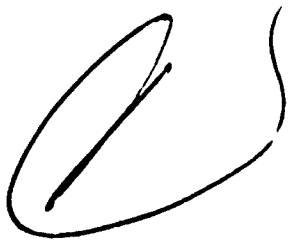
UNCLASSIFIED

AD NUMBER
AD829895
NEW LIMITATION CHANGE
TO Approved for public release, distribution unlimited
FROM Distribution authorized to U.S. Gov't. agencies and their contractors; Administrative/Operational Use; Feb 1968. Other requests shall be referred to Director, Air Force Aero Propulsion Laboratory, Wright-Patterson AFB, OH, 45433.
AUTHORITY
AFAPL ltr, 21 Sep 1971

THIS PAGE IS UNCLASSIFIED

AD829895

AFAPL-TR-65-45  
Part VII



# ROTOR-BEARING DYNAMICS DESIGN TECHNOLOGY

## Part VII: The Three Lobe Bearing and Floating Ring Bearing

J. Lund

Mechanical Technology Incorporated

TECHNICAL REPORT AFAPL-TR-65-45, PART VII

February 1968

This document is subject to special export controls and each transmittal to foreign governments or foreign national may be made only with prior approval of the Air Force Aero Propulsion Laboratory (APFL), Wright-Patterson Air Force Base, Ohio 45433.

AD 829895  
DSG FILE COPY

Air Force Aero Propulsion Laboratory  
Air Force Systems Command  
Wright-Patterson Air Force Base, Ohio

DDC  
RECEIVED  
MAR 29 1968  
B

Best Available Copy

279

**AFAPL-TR-65-45**

**Part VII**

# **ROTOR-BEARING DYNAMICS DESIGN TECHNOLOGY**

**Part VII: The Three Lobe Bearing and Floating Ring Bearing**

**J. Lund**

**Mechanical Technology Incorporated**

**TECHNICAL REPORT AFAPL-TR-65-45, PART VII**

**February 1968**

This document is subject to special export controls and each transmittal to foreign governments or foreign national may be made only with prior approval of the Air Force Aero Propulsion Laboratory (APFL), Wright-Patterson Air Force Base, Ohio 45433.

**Air Force Aero Propulsion Laboratory  
Air Force Systems Command  
Wright-Patterson Air Force Base, Ohio**

FOREWORD

This report was prepared by Mechanical Technology Incorporated, 968 Albany-Shaker Road, Latham, New York 12110 under USAF Contract No. AF33(615)-3238. The contract was initiated under Project No. 3048, Task No. 304806. The work was administered under the direction of the Air Force Aero Propulsion Laboratory, with Mr. Micheal R. Chasman (AFPL) acting as project engineer.

This report covers work conducted from 1 August 1966 to 1 August 1967.

This report was submitted by the authors for review on 31 August 1967. Prior to assignment of a AFAPL document number, this report was identified by the contractor's designation MTI 67TR47. This report is Part VII of final documentation issued in multiple parts.

This technical report has been reviewed and is approved.

  
ARTHUR V. CHURCHILL, Chief

Fuels, Lubrication and Hazards Branch  
Support Technology Division  
Air Force Aero Propulsion Laboratory

### ABSTRACT

This volume treats three special bearing types selected for study because of their favorable stability characteristics and, hence, their potential for use in high speed rotating machinery applications. The three bearing types are:

- a. The Three Lobe Journal Bearing
- b. The Floating Sleeve Bearing with an Incompressible Lubricant
- c. The Floating Sleeve Bearing with a Compressible Lubricant.

In the floating sleeve bearings, the ring is prevented from rotating but is otherwise free to move. The ring is floated by pressurizing the outer film of the bearing. In the case of a compressible lubricant, the inner film is pressurized as well.

The volume gives extensive design data in form of charts and tables from which the bearing dimensions can be obtained for a given application. Data are given for bearing flow, friction power loss and the speed at which hydrodynamic instability sets in. In addition, two computer programs accompany the volume, and instructions and listings of the programs are included. The programs may be used to obtain data for cases not covered by the presented design data.

This document is subject to special export controls and each transmittal to foreign governments or foreign nationals may be made only with prior approval of the Air Force Aero Propulsion Laboratory (APFL), Wright-Patterson Air Force Base, Ohio 45433.

TABLE OF CONTENTS

	<u>Page</u>
INTRODUCTION .....	1
THE THREE LOBE JOURNAL BEARING .....	5
THE HYDRODYNAMIC-HYDROSTATIC RING BEARING .....	15
THE HYBRID-HYDROSTATIC RING BEARING .....	25
APPENDIX I:    The Static and Dynamic Performance of a Partial Arc Bearing with Turbulent Film .....	95
APPENDIX II:   The Static and Dynamic Performance of the Three Lobe Bearing with Turbulent Film .....	119
APPENDIX III:  The Stiffness and the Damping of a Hydrostatic Bearing with an Incompressible Lubricant .....	127
APPENDIX IV:   The Stability of the Hydrodynamic - Hydrostatic Ring Bearing with an Incompressible Lubricant .....	147
APPENDIX V:    The Stiffness and the Damping of a Hybrid Journal Bearing with a Compressible Lubricant .....	155
APPENDIX VI:   The Stability of the Hybrid-Hydrostatic Ring Bearing with a Compressible Lubricant .....	177
APPENDIX VII:  Computer Program - The Static and Dynamic Performance of a Lobed Bearing with Turbulent Film .....	179
APPENDIX VIII: Computer Program - The Performance and Stability of a Hybrid Journal Bearing with Flexible, Damped Support ...	231
REFERENCES .....	267

## ILLUSTRATIONS

<u>Figure</u>		<u>Page</u>
1	The 3 Lobe Bearing, Schematic -----	42
2	The Hydrodynamic-Hydrostatic Ring Bearing, Schematic -----	43
3	The Hybrid-Hydrostatic Ring Bearing, Schematic -----	44
4	3 Lobe Bearing, Vertical Rotor, $\frac{L}{D} = \frac{1}{2}$ , Stability Map -----	45
5	3 Lobe Bearing, Vertical Rotor, $\frac{L}{D} = 1$ , Stability Map -----	46
6	3 Lobe Bearing, Vertical Rotor, $\frac{L}{D} = \frac{1}{2}$ , Friction -----	47
7	3 Lobe Bearing, Vertical Rotor, $\frac{L}{D} = 1$ , Friction -----	48
8	3 Lobe Bearing, Preload = 0.5, $\frac{L}{D} = \frac{1}{2}$ , Stability Map -----	49
9	3 Lobe Bearing, Preload = 0.5, $\frac{L}{D} = 1$ , Stability Map -----	50
10	3 Lobe Bearing, Preload = 0.5, $\frac{L}{D} = \frac{1}{2}$ , Friction -----	51
11	3 Lobe Bearing, Preload = 0.5, $\frac{L}{D} = 1$ , Friction -----	52
12	3 Lobe Bearing, Preload = 0.5, $\frac{L}{D} = \frac{1}{2}$ , Minimum Film Thickness ---	53
13	3 Lobe Bearing, Preload = 0.5, $\frac{L}{D} = 1$ , Minimum Film Thickness ---	54
14	3 Lobe Bearing, Preload = 0.5, $\frac{L}{D} = \frac{1}{2}$ , Flow -----	55
15	3 Lobe Bearing, Preload = 0.5, $\frac{L}{D} = 1$ , Flow -----	56

Illustrations (Continued)

<u>Figure</u>		<u>Page</u>
16	Hydrodynamic-Hydrostatic Ring Bearing, $R_e = 0, \frac{CK}{W} = 0.7$ , Stability Map -----	57
17	Hydrodynamic-Hydrostatic Ring Bearing, $R_e = 0, \frac{CK}{W} = 0.4$ , Stability Map -----	58
18	Hydrodynamic-Hydrostatic Ring Bearing, $R_e = 0, \frac{CK}{W} = 0.1$ , Stability Map -----	59
19	Hydrodynamic-Hydrostatic Ring Bearing, $R_e = 30,000, \frac{CK}{W} = 0.7$ , Stability Map -----	60
20	Hydrodynamic-Hydrostatic Ring Bearing, $R_e = 30,000, \frac{CK}{W} = 0.4$ , Stability Map -----	61
21	Hydrodynamic-Hydrostatic Ring Bearing, $R_e = 30,000, \frac{CK}{W} = 0.1$ , Stability Map -----	62
22	Hydrostatic Bearing, Incompressible, Single Plane Admission, Stiffness -----	63
23	Hydrostatic Bearing, Incompressible, Double Plane Admission, Stiffness -----	64
24	Hydrostatic Bearing, Incompressible, Single Plane Admission, Damping -----	65
25	Hydrostatic Bearing, Incompressible, Double Plane Admission, Damping -----	66

Illustrations (Continued)

<u>Figure</u>		<u>Page</u>
26	Hydrostatic Bearing, Incompressible, Flow -----	67
27	Hybrid-Hydrostatic Ring Bearing, $\frac{P_s}{P_a} = 2, \frac{CK_o}{(P_s - P_a)LD} = 0.24$ , Stability Map -----	68
28	Hybrid-Hydrostatic Ring Bearing, $\frac{P_s}{P_a} = 2, \frac{CK_o}{(P_s - P_a)LD} = 0.24$ , Instability Frequency -----	69
29	Hybrid-Hydrostatic Ring Bearing, $\frac{P_s}{P_a} = 2, \frac{CK_o}{(P_s - P_a)LD} = 0.18$ , Stability Map -----	70
30	Hybrid-Hydrostatic Ring Bearing, $\frac{P_s}{P_a} = 2, \frac{CK_o}{(P_s - P_a)LD} = 0.18$ , Instability Frequency -----	71
31	Hybrid-Hydrostatic Ring Bearing, $\frac{P_s}{P_a} = 2, \frac{CK_o}{(P_s - P_a)LD} = 0.09$ , Stability Map -----	72
32	Hybrid-Hydrostatic Ring Bearing, $\frac{P_s}{P_a} = 2, \frac{CK_o}{(P_s - P_a)LD} = 0.09$ , Instability Frequency -----	73
33	Hybrid-Hydrostatic Ring Bearing, $\frac{P_s}{P_a} = 5, \frac{CK_o}{(P_s - P_a)LD} = 0.24$ , Stability Map -----	74
34	Hybrid-Hydrostatic Ring Bearing, $\frac{P_s}{P_a} = 5, \frac{CK_o}{(P_s - P_a)LD} = 0.24$ , Instability Frequency -----	75
35	Hybrid-Hydrostatic Ring Bearing, $\frac{P_s}{P_a} = 5, \frac{CK_o}{(P_s - P_a)LD} = 0.18$ , Stability Map -----	76

Illustrations (Continued)

<u>Figure</u>	<u>Page</u>
36 Hybrid-Hydrostatic Ring Bearing, $\frac{P_s}{P_a} = 5, \frac{CK_o}{(P_s - P_a)LD} = 0.18$ , Instability Frequency -----	77
37 Hybrid-Hydrostatic Ring Bearing, $\frac{P_s}{P_a} = 5, \frac{CK_o}{(P_s - P_a)LD} = 0.09$ , Stability Map -----	78
38 Hybrid-Hydrostatic Ring Bearing, $\frac{P_s}{P_a} = 5, \frac{CK_o}{(P_s - P_a)LD} = 0.09$ , Instability Frequency -----	79
39 Hybrid-Hydrostatic Ring Bearing, $\frac{P_s}{P_a} = 10, \frac{CK_o}{(P_s - P_a)LD} = 0.24$ , Stability Map -----	80
40 Hybrid-Hydrostatic Ring Bearing, $\frac{P_s}{P_a} = 10, \frac{CK_o}{(P_s - P_a)LD} = 0.24$ , Instability Frequency -----	81
41 Hybrid-Hydrostatic Ring Bearing, $\frac{P_s}{P_a} = 10, \frac{CK_o}{(P_s - P_a)LD} = 0.18$ , Stability Map -----	82
42 Hybrid-Hydrostatic Ring Bearing, $\frac{P_s}{P_a} = 10, \frac{CK_o}{(P_s - P_a)LD} = 0.18$ , Instability Frequency -----	83
43 Hybrid-Hydrostatic Ring Bearing, $\frac{P_s}{P_a} = 10, \frac{CK_o}{(P_s - P_a)LD} = 0.09$ , Stability Map -----	84
44 Hybrid-Hydrostatic Ring Bearing, $\frac{P_s}{P_a} = 10, \frac{CK_o}{(P_s - P_a)LD} = 0.09$ , Instability Frequency -----	85
45 Hydrostatic Bearing, Compressible, $\frac{P_s}{P_a} = 1.25$ , Stiffness -----	86

Illustrations (Continued)

<u>Figure</u>		<u>Page</u>
46	Hydrostatic Bearing, Compressible, $\frac{P_s}{P_a} = 2$ , Stiffness -----	87
47	Hydrostatic Bearing, Compressible, $\frac{P_s}{P_a} = 5$ , Stiffness -----	88
48	Hydrostatic Bearing, Compressible, $\frac{P_s}{P_a} = 10$ , Stiffness -----	89
49	Hydrostatic Bearing, Compressible, $\frac{P_s}{P_a} = 1.25$ , Damping -----	90
50	Hydrostatic Bearing, Compressible, $\frac{P_s}{P_a} = 2$ , Damping -----	91
51	Hydrostatic Bearing, Compressible, $\frac{P_s}{P_a} = 5$ , Damping -----	92
52	Hydrostatic Bearing, Compressible, $\frac{P_s}{P_a} = 10$ , Damping -----	93
53	Hydrostatic Bearing, Compressible, Flow -----	94
54	Geometry of Partial Arc Bearing -----	97
55	Finite Difference Grid -----	103
56	Finite Difference Grid Lines -----	104
57	Three Lobe Bearing -----	119
58	Geometry of Single Lobe -----	119
59	Axial Strip -----	131
60	Axial Strip -----	134
61	Hydrodynamic-Hydrostatic Ring Bearing -----	147

Illustrations (Continued)

<u>Figure</u>		<u>Page</u>
62	Axial Strip -----	164
63	Feeding Hole -----	205

LIST OF TABLES

	<u>Page</u>
Table 1: 3 Lobe Bearing, Vertical Rotor .....	37
Table 2: 3 Lobe Bearing, Preload: $\delta = 0.5$ .....	39
Table 3: Plain Cylindrical Bearing .....	41

**BLANK PAGE**

### SYMBOLS

$a$	Orifice radius (or radius of laminar restrictor tube), inch
$B$	Damping coefficient, lbs.sec/inch
$B_o$	Damping coefficient for outer film, lbs.sec/inch
$B_{xx}, B_{xy}, B_{yx}, B_{yy}$	Damping coefficients for bearing, lbs.sec/inch
$B_{rr}, B_{rt}, B_{tr}, B_{tt}$	Damping coefficients for bearing, lbs.sec/inch
$\bar{B}_B$	Dimensionless effective bearing film damping
$C$	Radial clearance, inch
$C_o$	Radial clearance for outer film, inch
$C_D$	Discharge coefficient or vena contracta coefficient
$C_f$	Coefficient of friction
$D$	Journal diameter, inches
$D_o$	Diameter of outer bearing, inch
$d$	Feeder hole diameter, inch
$e$	Journal center eccentricity, inch
$e_B$	Eccentricity of journal center with respect to bearing center, inch
$e_o$	Journal center eccentricity, steady-state, inch
$F_f$	Friction force, lbs.
$F_r, F_t$	Radial and tangential components of bearing force, lbs.
$F_x, F_y$	Vertical and horizontal components of bearing force, lbs.
$F_{x0}, F_{y0}$	Static components of $F_x$ and $F_y$ , lbs.
$f_r$	= $F_r/SW$ (Appendix I) or = $F_r/P_a LD$ (Appendix V)
$f_t$	= $F_t/SW$ (Appendix I) or = $F_t/P_a LD$ (Appendix V)
$G_x, G_z$	Turbulent flow coefficients, see Ref. 1

$G$	$= G_z / G_x$
$G_0, G_1, G_2$	Defined by Eq. (A-19), Appendix I
$G_0, G_1, G_2$	Defined through Eqs. (E-17) to (E-19), Appendix V
$H$	$= h^{3/2} G_x^{1/2}$
$H_0, H_1, H_2$	Defined by Eq. (A-18), Appendix I
$H_1, H_2$	Defined by Eq. (C-56), Appendix III
$\bar{h}$	Film thickness, inch
$h$	$= \bar{h}/C$ , dimensionless film thickness
$i$	$= \sqrt{-1}$
$i, j$	Finite difference indices, Appendix I
$j$	$= \sqrt{-1}$ , Appendix V
$K$	Spring coefficient, lbs/inch
$K_o$	Spring coefficient for outer film, lbs/inch
$K_{xx}, K_{xy}, K_{yx}, K_{yy}$	Spring coefficients for bearing, lbs/inch
$K_{rr}, K_{rt}, K_{tr}, K_{tt}$	Spring coefficients for bearing, lbs/inch
$\bar{K}_B$	Dimensionless effective bearing film stiffness
$K_R$	Stiffness of shaft, lbs/inch
$K_{eff}$	Effective bearing film stiffness, lbs/inch
$L$	Bearing length, inch
$L_o$	Length of outer bearing, inch
$L_1$	Distance between admission planes, inch
$L_2$	$= L - L_1$ , inch
$l$	Length of feeder hole, inch
$M$	Journal mass (half rotor mass for rigid rotor), lbs.sec <sup>2</sup> /inch
$M_B$	Mass flow into bearing from one feeder hole, lbs.sec/inch
$M_c$	Mass flow through feeder hole orifice, lbs.sec/inch

$\bar{M}$	Total bearing mass flow, lbs.sec/inch
$M_R$	Mass of rotor disc, lbs.sec <sup>2</sup> /inch
$m$	Dimensionless mass flow (Eq. (C-13), App. III or Eq. (E-31), App. V)
$m$	Number of finite difference increments
$N$	Rotor speed, rps
$\bar{N}$	Rotor speed, rpm
$n$	Number of feeder holes
$n$	Number of finite difference increments on half bearing length
$\bar{P}$	Film pressure, psi
$P$	Dimensionless film pressure
$P_s$	Supply pressure, psi
$P_a$	Ambient pressure, psi
$\bar{P}'_c$	Film pressure at rim of feeder hole, psi
$Q$	Bearing flow, inch <sup>3</sup> /sec
$Q_x$	Flow in circumferential direction, inch <sup>3</sup> /sec.
$Q_z$	Side flow, inch <sup>3</sup> /sec.
$q$	Dimensionless flow (Eq. (C-47), App. III or Eq. (E-40), App. V)
$R$	Journal radius, inch
$R_o$	Radius of outer bearing, inch
$R_e$	$= \rho R \omega C / \mu$ , Reynolds number for bearing
$R_h$	$= \rho R \omega h / \mu = h R_e$ , local Reynolds number for film
$R$	Gas constant, inch <sup>2</sup> /sec <sup>2</sup> °R
$r$	Distance of lobe centers from bearing center, 3 lobe bearing, inch

$r_p$	Distance of lobe center from bearing center, inch
$S$	$= \mu NDL \left(\frac{R}{C}\right)^2 / W$ , Sommerfeld number
$T$	Total temperature of film, °F.
$t$	Time, seconds
$W$	Static load on bearing, lbs
$V$	$= P_s / P_a$ , supply pressure ratio
$V_c$	Feeder hole volume
$x, y$	Journal center amplitudes, inch
$z$	Axial coordinate, inch
$\gamma$	$= \frac{v}{\omega}$ , frequency ratio
$\delta$	$= a^2 / dC$ , inherent compensation factor
$\delta$	$= r/C$ , preload
$\delta_p$	$= r_p / C$ , preload for lobe p
$\epsilon$	$= e/C$ , eccentricity ratio
$\epsilon_B$	$= e_B / C$ , eccentricity ratio for bearing
$\epsilon_p$	Eccentricity ratio for lobe p
$\epsilon_0$	Eccentricity ratio, steady-state
$\zeta$	$= z/R$
$\theta$	Angular coordinate, radians
$\theta_1, \theta_2$	Angular coordinates for leading and trailing edges of lobe, radians
$\theta_{in}$	Angle from load vector to leading edge of lobe, radians
$\theta_{out}$	Angle from load vector to trailing edge of lobe, radians
$\Lambda$	$= 6\mu\omega \left(\frac{R}{C}\right)^2 / P_a$ , compressibility number

$\Lambda$	Restrictor coefficient for incompressible flow, defined by Eq. (C-12), App. III For compressible flow, defined by Eq. (E-33), App. V
$\lambda$	Spacing factor (pressure correction factor), Eqs. (E-49) and (E-50), App. V
$\mu$	Lubricant viscosity, lbs.sec/inch <sup>2</sup>
$\nu$	Frequency, radians/sec
$\xi_1$	= $L_1/D$
$\xi_2$	= $L_2/D$
$\rho$	Mass density of lubricant, lbs.sec <sup>2</sup> /inch <sup>4</sup>
$\sigma$	Squeeze number (Eq. (C-8), App. III or Eq. (E-10), App. V)
$\tau$	Dimensionless time
$\varphi$	Attitude angle, radians
$\varphi_B$	Attitude angle for bearing, radians
$\varphi_0$	Attitude angle, steady-state, radians
$\psi_p$	Angle between load vector and preload direction for lobe p, radians
$\psi$	= PH, Appendix I
$\psi$	Defined by Eq. (C-39), Appendix III
$\psi_1, \psi_2, \psi_3, \psi_4$	Perturbations of $\psi$ = PH, Appendix I
$\psi_0', \psi_1'$	Defined by Eqs. (E-41) and (E-42), Appendix V
$\psi_0, \psi_1$	Defined by Eqs. (E-60) and (E-61), Appendix V
$\omega$	Angular speed of rotor, radians/sec.

Subscripts

0            Steady-state or static condition  
o            Outer film or outer bearing  
p            Lobe number  
c            Conditions in bearing film at rim of feeder hole  
x            In x-direction  
y            In y-direction  
i,j          Finite difference coordinates

## INTRODUCTION

The current trend towards high-speed rotating machinery in many applications has focused attention on the bearings supporting the rotor. Most conventional bearings are limited to relatively low speeds for a variety of reasons such as operating life, high friction power loss and stability, and at the present time there is no universal bearing which will eliminate all the problem areas.

The present volume analyzes three special journal bearing types which are capable of insuring stable rotor operation to rather high speeds. As conceived, the bearings assume low viscosity lubricants such as a gas or a low viscosity fluid (first, a liquid metal) in order to hold the friction power loss to an acceptable level. The three bearings are intended to provide the designer of high speed machinery with a greater variety of bearing types to choose from, a choice which at present is mostly limited to the tilting pad journal bearing.

The volume gives extensive design data in form of charts and tables from which the dimensions and performance data of the bearings can be obtained. Several numerical examples are included to illustrate the actual use of the data in making a design. Furthermore, two computer programs accompany the volume, and instructions for using the programs and listings of the programs are given.

The bearing considered first is the three lobe bearing which is shown schematically in fig. 1. This bearing has been used for many years because of its known ability to suppress instability, but up to this time, no information has been available on its actual stability limit. Also, data has been lacking on the friction power loss and flow of the bearing. The influence on the bearing performance of turbulence in the bearing film is included in the investigation to cover lubricants such as liquid metals which are frequently used in space power plants or in machinery for nuclear reactors.

The major advantages of the three lobe bearing are that it is relatively simple in construction, it has no moving parts like a tilting pad bearing or a floating

sleeve bearing, it can be designed to operate stable at rather high speeds and it is also able to run with a vertical rotor or a rotor in a zero-g field which is not possible with conventional cylindrical bearings. The limitations of the bearing are its inability to accommodate any appreciable shaft misalignment unless specially mounted, and its relatively high friction power loss.

The second bearing type is of the floating sleeve variety and is shown in Figure 2. It is given the name of the hydrodynamic-hydrostatic ring bearing. The ring inserted between the journal and the outer bearing is prevented from rotating but is otherwise unrestrained. The ring is floated by pressurizing the outer film through feeder holes in the outer wall. By proper selection of bearing dimensions and operating parameters, this bearing can be designed to have a very high stability limit (theoretically, the bearing can be inherently stable if the mass of the sleeve is ignored). Furthermore, because of its construction the bearing can accommodate more shaft misalignment than the three lobe bearing. It is found, on the other hand, that to achieve the improved stability it is necessary to have a relatively big clearance in the outer film which means that the flow requirements of the bearing are quite high compared to non-pressurized bearings. Also, the friction power loss of the bearing becomes prohibitive at speeds considerably lower than the speed at which the bearing would otherwise become unstable such that the bearings high speed potential cannot be utilized fully. Even so, the bearing is a more truly high-speed bearing than the three lobe bearing.

The third bearing type is also a floating sleeve bearing and quite similar to the one considered above except that both the inner film and the outer film are pressurized and the lubricant is a gas instead of a liquid. The bearing is called the hybrid-hydrostatic ring bearing and is shown in fig. 3. It has the same desirable stability characteristics as in the previous case and because of the gaseous lubricant, the friction power loss is not nearly as serious. Hence, the hybrid-hydrostatic bearing can operate at very high speeds, say 100,000 rpm or more, depending on the application. The bearing, however, requires somewhat tighter clearances than the liquid lubricated ring bearing which means that its ability to accommodate misalignment is more restricted.

In the following, each of the three bearing types are treated in separate sections. The sections are devoted to a detailed discussion of the design procedure for the bearings and explain the use of the design charts contained in figs. 4 to 53. In addition, complete numerical examples have been worked out for each bearing type. The theoretical analyses from which the data have been obtained, are given for reference in 6 appendices in back of the volume. Two computer programs have been written, one for the three lobe bearing which also applies to the inner film of the hydrodynamic-hydrostatic ring bearing, and one for the hybrid-hydrostatic ring bearing. Manuals for the programs are given in Appendices VII and VIII.

**BLANK PAGE**

### THE THREE LOBE JOURNAL BEARING

The geometry of the 3 lobe bearing is shown schematically in figure 1. The bearing is composed of 3 circular arcs whose centers of curvature are removed from the center of the bearing by the distance  $r$ . Thus, even when the journal is centered in the bearing, the pads are loaded. In this way, the stability threshold of the bearing is raised and even a vertical rotor, or a rotor operating in a "zero-g field," can run stably which is not possible with a conventional full circular bearing. However, the improved stability threshold is paid for by an increase in friction power loss and a smaller operating minimum film thickness which makes the bearing more sensitive to impurities in the lubricant.

The journal diameter is  $D$ , its radius is  $R$  and the bearing length is  $L$ . The lobes are separated by axial grooves with an arc width of 20 degrees. The machined radial clearance of the lobes, common to all three lobes, is  $C$  such that the radius of curvature of the lobes is  $R + C$ . The preload is defined as:

$$\text{Preload: } \delta = \frac{r}{C} \quad (1)$$

Thus, when  $\delta = 0$ , the bearing becomes cylindrical and when  $\delta = 1$ , the journal touches all three lobes.

The preload is an important design parameter for the 3 lobe bearing. It strongly influences the stability threshold and the friction power loss of the bearing.

The other design parameters are the length-to-diameter ratio  $\frac{L}{D}$ , the Sommerfeld number  $S$  and the Reynolds number  $R_e$ :

$$\text{Sommerfeld Number: } S = \frac{\mu N D L}{W} \left( \frac{R}{C} \right)^2 \quad (2)$$

$$\text{Reynolds Number: } R_e = \frac{2 \pi \phi R N C}{\mu} \quad (3)$$

where:

$W$  = bearing load, lbs

$N$  = rotor speed, rps

$\mu$  = lubricant viscosity, lbs.sec/inch<sup>2</sup>

$\rho$  = lubricant mass density, lbs.sec<sup>2</sup>/inch<sup>4</sup>

For a given bearing geometry (i.e. for known values of  $\frac{L}{D}$  and  $\delta$ ) and for a given operating condition (i.e. for known values of  $S$  and  $R_e$ ), the bearing performance can be calculated as shown in the analyses in Appendices I and II. The actual calculations are carried out on a computer by means of the program described in Appendix VII where a listing and the instructions for using the program are given.

For known values of the four parameters, the bearing performance is defined by a set of dimensionless quantities:

the bearing eccentricity ratio:  $e_B = \frac{e_B}{C}$  (4)

the bearing attitude angle:  $\phi_B$  (5)

flow parameter:  $\frac{Q_x}{NDLC}$  (6)

the friction factor:  $\frac{R}{C} \frac{F_f}{W}$  (7)

the stability mass parameter:  $\frac{C^2 M \omega^2}{W}$  (8)

the instability frequency ratio:  $\gamma = \frac{\nu}{\omega}$  (9)

the dimensionless spring coefficients:  $\frac{CK_{xx}}{W}, \frac{CK_{xy}}{W}, \frac{CK_{yx}}{W}, \frac{CK_{yy}}{W}$  (10)

the dimensionless damping coefficients:  $\frac{C_{dB}_{xx}}{W}, \frac{C_{dB}_{xy}}{W}, \frac{C_{dB}_{yx}}{W}, \frac{C_{dB}_{yy}}{W}$  (11)

where:

$e_B$  = the distance between the bearing center and the journal center, inch

$Q_x$  = the total hydrodynamic leakage flow, inch<sup>3</sup>/sec

$F_f$  = the total friction force, lbs

$M$  = the mass of the journal, lbs.sec<sup>2</sup>/inch

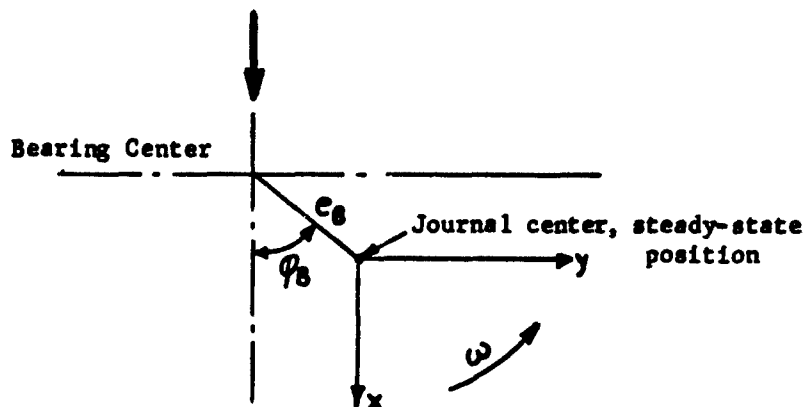
$\omega = 2\pi N$ , the angular speed of rotation, radians/sec

$\nu$  = the whirl frequency at onset of instability, radians/sec

$K_{xx}, K_{xy}, K_{yx}, K_{yy}$  = spring coefficients, lbs/inch

$B_{xx}, B_{xy}, B_{yx}, B_{yy}$  = damping coefficients, lbs.sec/inch

The x-y-coordinate system has its origin in the steady-state position of the journal center with the x-axis in the direction of the applied static load:



Under dynamic load, the journal center motion is described by the amplitudes  $x$  and  $y$ . Then the dynamic forces acting on the journal are:

$$\begin{aligned} F_x &= -K_{xx}x - B_{xx}\frac{dx}{dt} - K_{xy}y - B_{xy}\frac{dy}{dt} \\ F_y &= -K_{yx}x - B_{yx}\frac{dx}{dt} - K_{yy}y - B_{yy}\frac{dy}{dt} \end{aligned} \quad (12)$$

The 8 dynamic coefficients are used to represent the bearing in a rotor response calculation as described in Volume 5 (see also reference 3).

The hydrodynamic leakage flow,  $Q_z$ , is the sum of the end leakage flows from the lobes and also includes any net excess flow into the grooves (see Appendix VII.) To get the flow in gallons per minute (gpm), multiply  $Q_z$  by 60 and divide by 231.

Usually, the lubricant is supplied to the bearing under some pressure. The flow induced in this way (the so called "zero speed flow") must be added to the hydrodynamic leakage flow to obtain the total bearing flow.

The friction power loss can be calculated from the friction force,  $F_f$  as:

$$\text{Friction power loss} = \frac{2\pi N F_f}{6600} \quad \text{HP} \quad (13)$$

If it is assumed that all of the heat generated by the friction power loss goes into the lubricant film, the corresponding temperature rise of the lubricant can be calculated based on the obtained flow. With this temperature the operating viscosity of the lubricant can be determined.

The eccentricity ratio  $\epsilon_B$  and the attitude angle  $\phi_B$  defines the steady-state position of the journal center relative to the bearing center and the static load line (the x-axis). From this the minimum film thickness in the bearing can be determined (see Appendix II). Under almost all conditions, the minimum film thickness occurs at the bottom lobe (see fig. 1) in which case:

$$\text{Minimum Film Thickness, inch} = \min. \text{ of } \begin{cases} C [1 - \sqrt{\epsilon_B^2 + \delta^2 + 2\delta\epsilon_B \cos\phi_B}] \\ C [1 + \cos(230^\circ - \tan^{-1}(\frac{\epsilon_B \sin\phi_B}{\delta + \epsilon_B \cos\phi_B})) \sqrt{\epsilon_B^2 + \delta^2 + 2\delta\epsilon_B \cos\phi_B}] \end{cases}$$

The minimum film thickness gives a relative measure of how heavily the bearing is loaded. The acceptable lower value for the minimum film thickness depends on the condition of the lubricant.

The threshold of instability is defined through the stability mass parameter in eq. (8). It applies to a rigid rotor with total mass  $2M$  supported in two similar bearings, and the parameter defines that mass the rotor must have in order for the rotor-bearing system to be on the threshold of instability for the specified operating condition. If the actual rotor mass is bigger, the bearing is unstable. At the threshold of instability the steady-state equilibrium position of the journal is neutrally stable and the journal center whirls in an infinitesimal small closed orbit with a frequency  $\nu$ , given through the whirl frequency ratio =  $\gamma = \frac{\nu}{\omega}$ .

The stability mass parameter can also be used to determine the threshold of instability for a flexible rotor. Let the rotor consist of a shaft with stiffness

$K_R$  on which is mounted a central disc with mass  $2M_R$ .  $K_R$  and  $M_R$  are defined such that the natural frequency of the motor simply supported at the bearing centerlines is equal to  $\sqrt{K_R/M_R}$ . Then the threshold of stability is defined by the parameter:

$$\text{Stability Mass Parameter for Flexible Rotor: } \frac{CM_R\omega^2}{W} = \frac{\frac{CK_R}{W}}{\frac{CK_R}{W} + \gamma^2 \left[ \frac{CM\omega^2}{W} \right]} \left[ \frac{CM\omega^2}{W} \right]$$

where  $\frac{CM\omega^2}{W}$  and  $\gamma$  have the values obtained for the rigid motor. It is seen that the flexibility of the rotor lowers the threshold of instability.

If the rotor is not symmetric, the computer program described in Volume 5 can be used to calculate the speed at onset of instability. In this calculation, the bearing is represented by the 8 dynamic coefficients as obtained above.

The performance of the 3 lobe bearing with a preload of:  $\delta = 0.5$ , and for two values of the length-to-diameter ratio:  $L/D = 0.5$  and 1, is given in Table . The columns of the table give the values of the parameters defined above. For those conditions where no values are given for the instability frequency ratio or the stability mass parameter, the bearing is stable.

The table contains two additional quantities, namely  $Q_x/NDLC$  which is the dimensionless circumferential flow (i.e. the sum of the flows entering the three lobes from the grooves), and  $CMW/\mu DL \left( \frac{R}{C} \right)^2$  which is another dimensionless form of the stability mass parameter (it is equal to  $\frac{CM\omega^2}{W} / 4\pi^2 S$ ).

The most significant results are plotted in figs. 8 to 15. Figs. 8 and 9 give the stability mass parameter. Figs. 10 and 11 show the friction factor, figs. 12 and 13 give the minimum film thickness normalized with respect to  $C$ , and figs 14 and 15 give the flow parameter. The abscissa is in all cases the Sommerfeld number  $S$ , and each graph contains four curves corresponding to Reynolds numbers of 0, 2000, 10000 and 30,000. The curves for  $R_e = 0$  apply to laminar flow (i.e. when  $R_e < 2,000$ ).

The use of the graphs is best illustrated by an example. Let a rigid, symmetric rotor of 200 lbs. be supported in two similar 3 lobe bearings with a length-to-diameter ratio of 1/2. The lubricant is liquid potassium at 500°F. The data are:

bearing diameter:  $D = 3$  inch

bearing length;  $L = 1.5$  inch

radial clearance:  $C = 0.002$  inch

preload:  $S = 0.5$

bearing load:  $W = 100$  lbs.

Journal mass:  $M = 100/386 = 0.259$  lbs.sec<sup>2</sup>/inch

lubricant viscosity:  $\mu = 3.85 \cdot 10^{-8}$  lbs.sec/inch<sup>2</sup>

lubricant mass density:  $\rho = 7.3 \cdot 10^{-5}$  lbs.sec<sup>2</sup>/inch<sup>4</sup>

Denote the rotor speed in rpm as  $\bar{N}$ . Then:

$$R_e = \frac{2\pi \cdot 7.3 \cdot 10^{-5} \cdot 1.5 \cdot 0.002}{3.85 \cdot 10^{-8}} \cdot \frac{\bar{N}}{60} = 0.596 \cdot \bar{N}$$

$$S = \frac{3.85 \cdot 10^{-8} \cdot 3 \cdot 1.5}{100} \left( \frac{1.5}{0.002} \right)^2 \cdot \frac{\bar{N}}{60} = 1.625 \cdot 10^{-5} \cdot \bar{N}$$

$$\frac{CW^2}{W} = \frac{0.002 \cdot 0.259}{100} \left( \frac{2\pi \bar{N}}{60} \right)^2 = 5.68 \cdot 10^{-8} \bar{N}^2$$

$$Q_x = 3.896 \cdot 10^{-5} \left( \frac{Q_x}{NDLC} \right) \bar{N} \quad \text{gpm}$$

$$\text{friction power loss} = 3.17 \cdot 10^{-6} \left( \frac{RF_f}{CW} \right) \bar{N} \quad \text{HP}$$

With these relationships the bearing performance can be obtained from figs. 10, 12 and 14:

Rotor speed $\bar{N}$ , rpm	$R_e$	S	From fig. 10		From fig. 12	From fig. 14	Power loss HP	Flow gpm	Min. Film Thickness, inch
			$\frac{R}{C}$	$\frac{F_f}{W}$	$\frac{h_{min}}{C}$	$\frac{Q_x}{NDLC}$			
5,000	2,980	0.0812	5.8		0.2	1.66	0.092	0.32	0.0004
10,000	5,960	0.1625	14		0.335	0.84	0.44	0.33	0.00067
15,000	8,940	0.2438	31		0.4	0.59	1.48	0.34	0.0008
18,000	10,710	0.2925	47		0.428	0.51	2.68	0.36	0.00086

To determine the threshold of instability, plot the stability limit for the rotor in fig. 8:

$\frac{R_e}{g}$	$\bar{N}$ , rpm	$s$	$\frac{C\bar{m}^2}{W}$
2,000	3,360	0.0546	(stable)
10,000	16,800	0.273	17.9
30,000	50,400	0.819	81.5

The operating line of the rotor is given by:  $\frac{C\bar{m}^2}{W} = 215 \cdot s^2$  which is a straight line with a slope of 2 in fig. 8 because of the logarithmic scales. The operating line intersects the stability limit curve at  $\frac{C\bar{m}^2}{W} = 19$  from which the speed at onset of instability is found to be 18,300 rpm. For comparison, the instability speed of a plain cylindrical bearing can be determined from Table 3 as:

10,700 rpm for  $C = 0.002$   
Plain Cylindrical Bearing 14,260 rpm for  $C = 0.001$

This gives an indication of the stability improvement obtainable with a three lobe bearing.

If the rotor instead of being rigid is flexible and consists of a shaft on which is mounted a central disc, the threshold speed will be lowered. Let the disc weigh 200 lbs and let the shaft have a stiffness of  $10^6$  lbs/inch. The natural frequency of the rotor simply supported is:

$$\text{Natural frequency} = \sqrt{\frac{1,000,000}{200/386}} = \sqrt{\frac{500,000}{100/386}} = 1,390 \frac{\text{radians}}{\text{sec}} = 13,300 \text{ rpm}$$

The shaft stiffness to be used in eq. (15) is:  $K_R = 500,000$  lbs/inch and the half disc mass is:  $M_R = 100/386 = 0.259$  lbs.sec<sup>2</sup>/inch. Hence:

$$\frac{CK_R}{W} = \frac{0.002 \cdot 500,000}{100} = 10$$

$$\frac{C\bar{m}^2 \omega^2}{W} = 215 \cdot s^2$$

The flexible rotor has the same operating line as the rigid rotor since the mass is unchanged. The stability limit, however, is lowered. From eq. (15)

$$\frac{CM_R \omega^2}{W} = \frac{10 \cdot \frac{CM \omega^2}{W}}{10 + (0.5)^2 \frac{CM \omega^2}{W}}$$

where the instability frequency ratio has been set equal to 0.5 (for a more accurate value, use Table 2). Hence, by using fig. 8:

$R_e$	$\bar{N}$ , rpm	$S$	$\frac{CM \omega^2}{W}$ (from fig. 8)	$\frac{CM_R \omega^2}{W}$
2,000	3,360	0.0546	(stable)	(stable)
10,000	16,800	0.273	17.9	12.35
30,000	50,400	0.819	81.5	26.35

The operating line intersects the stability curve at  $\frac{CM_R \omega^2}{W} = 12$  to which corresponds a threshold speed of 14,500 rpm.

When the rotor is vertical or operates in a "zero g field", the bearing is unloaded, i.e.  $W = 0$ . Hence, the eccentricity ratio  $\epsilon_B$  is zero, and the Sommerfeld number becomes infinite and can no longer be employed as a parameter. In this case the performance parameters of eqs. (7), (8), (10) and (11) are redefined.

#### Vertical Rotor

$$\text{friction factor: } \frac{R}{C} \frac{F_f}{\mu NDL \left(\frac{R}{C}\right)^2} = \frac{1}{S} \frac{R}{C} \frac{F_f}{W} \quad (16)$$

$$\text{stability mass parameter: } \frac{1}{\mu DL \left(\frac{R}{C}\right)^2} = \frac{1}{4\pi^2 S} \frac{CM \omega^2}{W} \quad (17)$$

$$\text{dimensionless spring coefficients: } \frac{CK_{xx}}{\mu NDL \left(\frac{R}{C}\right)^2} = \frac{1}{S} \frac{CK_{xx}}{W} \quad (18)$$

$$\text{dimensionless damping coefficients: } \frac{C\omega B_{xx}}{\mu NDL \left(\frac{R}{C}\right)^2} = \frac{1}{S} \frac{C\omega B_{xx}}{W} \quad (19)$$

and similarly for  $K_{xy}$ ,  $K_{yx}$ ,  $K_{yy}$ ,  $B_{xy}$ ,  $B_{yx}$  and  $B_{yy}$ . It should be noted that for a vertical rotor:

$$K_{yy} = K_{xx}$$

$$K_{yx} = -K_{xy}$$

$$B_{yy} = B_{xx}$$

$$B_{yx} = -B_{xy}$$

Calculated performance data are given in Table 1 for a 3 lobe bearing with  $\frac{L}{D} = \frac{1}{2}$  and 1, and for 4 values of the Reynolds number. 6 preloads are considered. The stability mass parameter and the friction factor are plotted in figs. 4 to 7 as a function of the preload. Hence, for a given application the preload required to ensure stable operation is readily determined. To illustrate, consider the same rigid rotors in the previous example. From the given rotor and bearing data:

$$R_e = 0.596 \cdot \bar{N}$$

$$\frac{CMN}{\mu DL \left(\frac{R}{C}\right)^2} = \frac{MN}{2\mu L \left(\frac{R}{C}\right)^3} = \frac{0.259}{2 \cdot 3.85 \cdot 10^{-9} \cdot 1.5 \cdot \left(\frac{1.5}{0.002}\right)^3} \cdot \frac{\bar{N}}{60} = 0.886 \cdot 10^{-4} \bar{N}$$

$$\text{friction power loss} = 5.15 \cdot 10^{-11} \left( \frac{R}{C} \frac{F_f}{\mu NDL \left(\frac{R}{C}\right)^2} \right) \cdot \bar{N}^2 \quad \text{HP}$$

Thus, by using figs. 4 and 6:

$R_e$	$\bar{N}$ , rpm	$\frac{CMN}{\mu DL \left(\frac{R}{C}\right)^2}$	From Fig. 6		Power Loss, HP
			From Fig. 4 Preload: $\delta$	$\frac{R}{C} \frac{F_f}{\mu NDL \left(\frac{R}{C}\right)^2}$	
2,000	3,360	0.297	0.398	54	0.03
10,000	16,800	1.49	0.52	156	2.27
30,000	50,400	4.46	0.575	360	47.1

Hence, the rotor can operate stably at 50,000 rpm if the preload is approximately 0.6 but the friction power loss is then close to 50 HP.

It is seen that the threshold speed for the vertical rotor with a bearing preload of 0.5 is approximately 16,000 rpm which is a slight reduction of the speed determined for a horizontal rotor where the bearing is loaded.

### THE HYDRODYNAMIC-HYDROSTATIC RING BEARING

The bearing is shown schematically in figure 2. It actually consists of two bearings (two lubrication films) separated by a floating ring. The ring is restrained from rotating by a pin but is otherwise free to move. In the inner film, pressures are developed by the hydrodynamic action from the rotating journal. The outer film, which is a hydrostatic bearing, is supplied with pressurized lubricant through restricted feeder holes. In this way the bearing can be designed such that the damping from the outer film stabilizes the inner bearing thereby raising the stability limit of the bearing significantly. Furthermore, by this construction the bearings ability to accommodate misalignment is appreciably improved. On the other hand, the flow requirements of the bearing are large as discussed in the following.

The detailed analysis of the bearing is given in Appendices III and IV. The computer program described in Appendix VI is used to calculate the performance characteristics of the inner film and some typical data are given in Table 3.

The stability characteristics of the bearing are given by figures 16 to 21. The length-to-diameter ratio is equal to 1, based on the journal diameter.

The charts are based on a given outer film stiffness,  $K_o$ , and the curves give the stability mass parameter  $CW^2/W$  as a function of the damping,  $B_o$ , of the outer film. The curves are plotted for several values of the Sommerfeld number  $S$  of the inner film, and two Reynolds numbers are considered: 0 and 30,000.

The outer film stiffness and damping are used in the dimensionless forms:

$$\text{for outer film stiffness: } \frac{CK_o}{W} \quad (20)$$

$$\text{for outer film damping: } \frac{CWB_o}{W} \quad (21)$$

where:

$C$  = radial clearance of inner film, inch

$W$  = bearing load, lbs

$\omega$  = angular speed of rotation, radians/sec

$K_o$  = outer film spring coefficient, lbs/inch

$B_o$  = outer film damping coefficient, lbs.sec/inch

The stability mass parameter has been defined and discussed in the previous section on the three lobe bearing (see eq. (8)). It applies to a rigid, symmetric rotor with mass  $2M$ .

The charts, figs. 16 to 21, show that for a certain range of the outer film damping, the bearing is inherently stable. This "corridor" of inherent stability is seen to have a slope of 2 in the charts. Since the charts employ logarithmic scales, this means that for the bearing to operate in the corridor the ratio  $\frac{C_o B_o}{W} \omega^2$  is constant. This ratio is independent of speed.

In designing the bearing, the objective is to select the outer film stiffness and damping such that the bearing operates in the stable corridor. The outer film coefficients are given by the charts in figs. 22 to 25. In these charts the coefficients have the dimensionless form:

$$\text{Dimensionless stiffness: } \frac{1+\delta^2}{1+\frac{2}{3}\delta^2} \cdot \frac{C_o K_o}{P_s L_o D_o} \xi_2$$

$$\text{Dimensionless damping: } \frac{C_o B_o}{\mu L_o D_o \left(\frac{R_o}{C_o}\right)^2}$$

(note: subscript "o" is left out on the charts)

where:

$D_o$  = bearing diameter, inch

$L_o$  = bearing length, inch

$R_o$  = bearing radius, inch

$C_o$  = radial clearance of outer film, inch

$K_o$  = spring coefficient, lbs/inch

$B_o$  = damping coefficient, lbs.sec/inch

$P_s$  = lubricant supply pressure, psig

$\mu$  = lubricant viscosity, lbs.sec/inch<sup>2</sup>

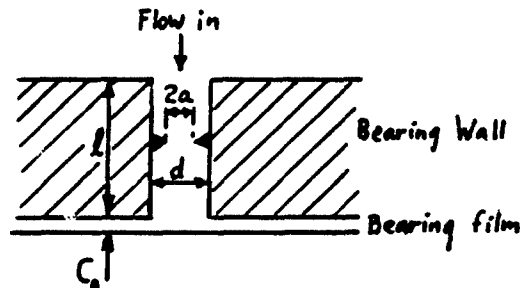
**BLANK PAGE**

The feeder holes of the bearing may either be in the centerplane of the bearing, called "single plane admission", or arranged in two planes symmetric with respect to the centerplane, called "double plane admission." If the distance between the admission planes is  $L_1$ , define:

$$\begin{aligned} L_2 &= L_0 - L_1 \\ \xi_1 &= \frac{L_1}{D_0} \\ \xi_2 &= \frac{L_2}{D_0} \end{aligned} \quad (22)$$

Hence, for single plane admission,  $\xi_1=0$  and  $\xi_2=L_0/D_0$ , whereas for double plane admission the above definitions apply.

The flow restriction may be provided by orifices or by the feeder holes themselves



If there is no orifice and the feeder hole acts as a narrow tube, the bearing is said to be laminar restricted. When the predominant flow restriction is in the orifice, the bearing is orifice restricted. Finally, the flow may be restricted in the "curtain" area formed between the rim of the feeder hole and the surface of the ring. This is called "inherent compensation." The inherent compensation factor:

$$\delta = \frac{a^2}{dC_0} \quad (24)$$

gives the ratio between the orifice area and the curtain area. When  $\delta=0$ , the feeder hole is purely orifice restricted, and when  $\delta=0$ , the flow restriction takes place in the curtain area only. For intermediate values of  $\delta$ , both restrictors are acting. For the laminar restrictor, set  $\delta=0$ .

The spacing factor  $\lambda$  accounts for the effect of the spacing of the feeder holes. Let there be  $n$  feeder holes in total (i.e. for double plane admission there are  $\frac{n}{2}$  holes per plane). Then  $\lambda$  is given by:

$$\lambda = 1 + \frac{2}{n\xi_2} \log_e \left( \frac{D}{n_p d} \right) \quad (25)$$

where  $n_p$  is the number of holes per admission plane ( $n_p = n$  or  $n_p = \frac{1}{2} n$ .) For more accurate expressions, see eqs. (C-28), (C-29), (C-33) and (C-34), Appendix III. A typical value is:  $\lambda = 1.5$ .

In the charts, figs. 16 to 21, the abscissa is the restrictor coefficient  $\Lambda_s$  which gives the ratio between the flow resistance of the bearing film and the feeder holes. It is defined as:

$$\text{Restrictor Coefficient: } \Lambda_s = \begin{cases} \frac{3\mu C_D n a^2}{C_o^3 \sqrt{\rho} P_s \sqrt{1 + \delta^2}} \lambda \xi_2 & \text{(Orifice restriction +} \\ & \text{inherent compensation)} \\ \frac{3}{8} \frac{n a^4}{C_o^3 l} \lambda \xi_2 & \text{(Laminar restriction)} \end{cases}$$

where:

- $C_D$  = discharge coefficient ( $C_D \approx 0.6$ )
- $a$  = radius of orifice or feeder hole, inch
- $\rho$  = mass density of lubricant, lbs·sec<sup>2</sup>/inch<sup>4</sup>
- $l$  = length of feeder hole, inch

and the other symbols have been defined above. It is seen that the bearing is optimized with respect to stiffness when  $\Lambda_s = 1$ .

The charts assume that the bearing is operating with no eccentricity. This assumption is valid in most cases. Furthermore, the load displacement characteristic is close to being linear such that:

$$W \approx C_o \epsilon_o K_o \quad (27)$$

where:

- $W$  = bearing load, lbs.
- $\epsilon_o$  = bearing eccentricity ratio

This relationship is valid for eccentricities up to:  $\epsilon_o \approx 0.4$  to  $0.5$ .

The bearing flow can be determined from fig. 26 where the ordinate is the dimensionless flow:

$$\frac{3Q}{P C_o^3} \cdot \lambda \xi_2$$

Here:

$$Q = \text{flow, inch}^3/\text{sec.}$$

The chart is valid for both single plane admission and double plane admission, and for any length-to-diameter ratio.

The use of the design charts is best illustrated by an example. First, it is seen from eq. (27) that:

$$\frac{C_o K_o}{W} = \frac{1}{\epsilon_o}$$

or:

$$\frac{C}{C_o} = \epsilon_o \frac{CK_o}{W} \quad (28)$$

$\epsilon_o$  should not exceed 0.4 in order for the bearing to have some load margin. Hence, the dimensionless stiffness  $\frac{CK_o}{W}$  should be chosen as large as possible

in order for  $C_o$  not to become too large which would lead to unreasonable flow requirements. On the other hand, the stability corridor narrows down with increasing outer film stiffness and eventually disappears. Thus, a compromise is necessary. In the present case, choose the largest dimensionless stiffness value given in the charts, namely  $CK_o/W = 0.7$ , which means that figs. 16 and 19 apply. To operate in the stability corridor, set  $C_{\omega} B_o/W = 0.6$  for  $C M_{\omega}^2/W = 1$  whereby the rotor will operate along a straight line with a slope of 2 in the chart. Hence:

$$B_o \sqrt{\frac{C}{M_{\omega}}} = \frac{C_{\omega} B_o/W}{(C M_{\omega}^2/W)^{1/2}} = \frac{0.6}{\sqrt{1}} = 0.6 \quad (29)$$

Let the rotor be rigid and symmetric with a weight of 200 lbs. The data for the rotor and its two bearings are:

bearing diameter:  $D = 3$  inch

bearing length:  $L = 3$  inch

outer diameter of ring:  $D_o = 3.5$  inch

lubricant viscosity:  $\mu = 3.85 \cdot 10^{-8}$  lbs·sec/inch<sup>2</sup>

lubricant mass density:  $\rho = 7.3 \cdot 10^{-5}$  lbs·sec<sup>2</sup>/inch<sup>4</sup>

bearing load:  $W = 100$  lbs.

journal mass:  $M = 100/386 = 0.259$  lbs·sec<sup>2</sup>/inch

The lubricant is liquid potassium at 500°F.

The outer bearing is chosen as a hydrostatic bearing with single plane admission and laminar restricted feeder holes. Hence, fig. 24 applies where the dimensionless damping is:

$$\frac{C_o B_o}{\mu L_o D_o \left(\frac{R_o}{C_o}\right)^2} = \frac{B_o}{2\mu L_o \left(\frac{R_o}{C_o}\right)^3} = \frac{1}{2\mu L_o \left(\frac{R_o}{C_o}\right)^3} \sqrt{\frac{MW}{C}} \cdot \frac{0.6}{\sqrt{1}} \quad (30)$$

or:

$$\left(\frac{R_o}{C_o}\right)^3 = \frac{1}{2\mu L_o} \cdot \sqrt{\frac{MW}{C}} \cdot \frac{0.6}{\sqrt{1}} \bigg/ \frac{C_o B_o}{\mu L_o D_o \left(\frac{R_o}{C_o}\right)^2} \quad (31)$$

Now, from eq.(28) it is seen that  $C/C_o < 0.4 \cdot 0.7 = 0.28$ , i.e. even if it is desired to have a small value of  $C_o$  to keep the flow down,  $C_o$  cannot be too small if  $C$  shall have a practical value. Set  $C = 0.0007$  inch and try with a dimensionless damping value of 4 (corresponds to  $\Lambda_s = 0.25$ ). Hence, from eq. (31):

$$\left(\frac{R_o}{C_o}\right)^3 = \frac{0.6}{2 \cdot 3.85 \cdot 10^{-8} \cdot 3} \cdot \sqrt{\frac{0.259 \cdot 100}{0.0007}} \bigg/ 4.0 = 1.25 \cdot 10^8$$

or:

$$\frac{R_o}{C_o} = 5 \cdot 10^2$$

i.e.

$$C_o = \frac{1.75}{500} = 0.0035 \text{ inch}$$

Since  $C/C_o = 0.0007/0.0035 = 0.2 < 0.28$ , this value of  $C_o$  can be accepted. The chosen dimensionless damping corresponds to a restrictor coefficient of:

$\Lambda_s = 0.25$ . Thus, from fig. 22:

$$\frac{C_o K_o}{P_s L_o D_o} \lambda \xi_2 = 0.28$$

Now:

$$\frac{C_o K_o}{P_s L_o D_o} \lambda \xi_2 = \frac{C_o}{C} \frac{W}{P_s L_o D_o} \lambda \xi_2 \frac{CK_o}{W} = 0.28$$

or:

$$P_s = \frac{C_o}{C} \frac{W}{L_o D_o} \lambda \xi_2 \frac{CK_o}{W} \frac{1}{0.28} \quad (32)$$

Here:  $\xi_2 = L_o/D_o$  and  $\lambda$  shall be set equal to 1.5. Thus:

$$P_s = \frac{0.0035}{0.0007} \frac{100}{3 \cdot 3.5} \cdot 1.5 \cdot \frac{3}{3.5} \cdot 0.7 \cdot \frac{1}{0.28} = 150 \text{ psig.}$$

which establishes the required supply pressure.

From the definition of the restrictor coefficient:

$$\Lambda_s = 0.25 = \frac{3}{8} \frac{na^4}{C_o^3 l} \lambda \xi_2$$

or:

$$\frac{na^4}{l} = \frac{8}{3} \frac{(0.0035)^3}{1.5 \cdot 3/3.5} = 8.89 \cdot 10^{-8}$$

Let the feeder hole have a diameter:  $d = 2a = 0.020$  inch and let the number of holes be:  $n = 10$  whereby:

$$l = 1.125 \text{ inch}$$

Check the spacing factor:

$$\lambda = 1 + \frac{2}{n \xi_2} \log_e \left( \frac{D_o}{nd} \right) = 1 + \frac{2}{10 \cdot 3/3.5} \cdot \log_e \left( \frac{3.5}{10 \cdot 0.02} \right) = 1.67$$

which is close enough to the estimated value of 1.5. It should be noted that if the obtained feeder hole dimensions are not acceptable for various reasons, the bearing can be made orifice restricted instead or a different  $\Lambda_g$ -value can be chosen which would have little influence on the selection of C and  $C_o$ . Going to a value of  $\Lambda_g = 0.5$  would reduce the required feeder hole length to  $l = 0.56$  inch, the supply pressure would become  $P_g = 105$  psig whereas the outer film clearance only would change from 0.0035 inch to 0.0034 inch. In other words, it is very important to select the proper value of the outer film clearance but the bearing is not too sensitive to even quite larger changes in the other parameters. This is quite readily deduced from eq. (31) where, for a given rotor weight, lubricant viscosity and overall bearing dimensions, the clearance  $C_o$  is pretty well defined once it is required that the bearing must operate in the stable corridor. Thus, eq. (31) can be considered to be the governing design equation with eq. (28) as a necessary condition.

From fig. 26 the dimensionless flow is found to be 0.2. Hence, the flow becomes:

$$Q = \frac{\pi \cdot P_g \cdot C^3}{3 \mu \lambda \xi_2} \cdot 0.2 = \frac{\pi \cdot 150 \cdot (0.0035)^3}{3 \cdot 3.85 \cdot 10^{-8} \cdot 1.5 \cdot 3/3.5} \cdot 0.2 = 27.2 \frac{\text{inch}^3}{\text{sec}} = 7.1 \text{ gpm}$$

This is seen to be 20 times the flow required for the three lobe bearing for the same application. However, whereas the three lobe bearing becomes unstable at 18,000 rpm, the hydrodynamic-hydrostatic bearing is stable to much higher speeds.

The actual stiffness of the hydrostatic bearing is calculated to be:

$$K_o = \frac{150 \cdot 3 \cdot 3.5}{0.0035} \cdot 0.28 = 126,000 \text{ lbs/inch}$$

The damping coefficient becomes:

$$B_o = \frac{3.85 \cdot 10^{-8} \cdot 3 \cdot 3.5}{0.0035} \cdot \left( \frac{1.75}{0.0035} \right)^2 \cdot 4.0 = 116 \frac{\text{lbs. sec}}{\text{inch}}$$

Assuming a linear load-displacement relationship, the eccentricity ratio becomes:

$$\epsilon_o = \frac{W}{C_o K_o} = \frac{100}{0.0035 \cdot 126000} = 0.227$$

which is considerably less than 0.4. Hence, the bearing should be able to withstand dynamic loads of at least the same magnitude as the static load.

From Table 3, the stability mass parameter of the inner film is found to be approximately equal to 6 with a whirl frequency ratio of 0.5. Now, the onset of instability can be likened to a resonance where:

$$v^2 = \frac{K_{eff}}{M}$$

where  $K_{eff}$  represents the effective stiffness of the inner film. Hence:

$$K_{eff} = v^2 M = \left(\frac{v}{\omega}\right)^2 \frac{C M \omega^2}{W} \cdot \frac{W}{C} = (0.5)^2 \cdot 6 \cdot \frac{100}{0.0007} = 214,000 \text{ lbs/inch}$$

The ring has an inner diameter of 3 inches and an outer diameter of 3.5 inches. Hence, its mass is:

$$\frac{\pi}{4} (3.5^2 - 3^2) \cdot 3 \cdot 0.283 = 2.17 \text{ lbs} = 0.0056 \text{ lbs} \cdot \text{sec}^2/\text{inch}$$

The natural frequency of the ring is:

$$\sqrt{\frac{214,000 + 126,000}{0.0056}} = 7,800 \frac{\text{radians}}{\text{sec}} = 75,000 \text{ rpm}$$

With an estimated instability frequency ratio of 0.5, the ring may become unstable at 150,000 rpm. This, then should be considered the top speed of the rotor to be on the safe side.

Making use of Table 3, the friction power loss of the bearing can be computed:

Rotor Speed rpm	$R_e$	$S$	Power Loss HP
20,000	4,200	5.35	9.7
40,000	8,300	10.7	64.4
60,000	12,500	16.1	195
80,000	16,700	21.4	432

Thus, even if the bearing is stable up to at least 150,000 rpm, the power loss becomes prohibitive at half that speed because of turbulence in the film.

In summary, the calculated bearing dimensions and the bearing performance data are:

journal diameter:	D = 3 inch
outer diameter of ring:	$D_o = 3.5$ inch
bearing length:	L = 3 inch
radial clearance of inner film:	C = 0.0007 inch
radial clearance of outer film:	$C_o = 0.0035$ inch
number of feeder holes for hydrostatic bearing:	n = 10
feeder hole diameter:	d = 0.020 inch
feeder hole length:	l = 1.25 inch
supply pressure for hydrostatic bearing:	$P_s = 150$ psig
bearing flow:	Q = 7.1 gpm
maximum stable speed (conservative estimate):	150,000 rpm
friction power loss: at 70,000 rpm	9.7 HP
at 40,000 rpm	64.4 HP
at 60,000 rpm	195 HP
at 80,000 rpm	432 HP

### THE HYBRID-HYDROSTATIC RING BEARING

The bearing is shown schematically in figure 3. It differs from the previously considered hydrodynamic-hydrostatic ring bearing by employing a gas as a lubricant instead of a liquid. Furthermore, both the inner and the outer film are pressurized thereby enhancing the load carrying capacity which would otherwise be rather limited with gas as a lubricant. The ring separating the inner and the outer film, is restrained from rotating but is otherwise free to follow the motions of the journal. As shown in fig. 3, the inner film is supplied with pressurized gas through feeder holes in the centerplane of the ring. The load carrying capacity of the inner film is then produced by both hydrostatic and hydrodynamic action which is known as a hybrid bearing. The outer film is purely hydrostatic and, as shown in fig. 3, consists of two bearings supplied with pressurized gas through feeder holes in a central plane. The ends of the bearings are vented to atmosphere. Figure 3 is only intended to show one possible arrangement and other designs would be possible.

The major objective of this type of bearing design is to improve the stability limit of the bearing. Furthermore, the bearing offers the advantage of being able to accommodate a larger amount of misalignment than more conventional bearing types.

The analysis of the bearing is given in Appendices V and VI. Furthermore, a computer program for calculating the bearing has been written, and the instructions for using the program and a listing of the program are given in Appendix VIII.

The stability characteristics of the bearing are given by the charts in figs. 27 to 44. Three values of the supply pressure for the inner film have been considered:

$$\frac{P_s}{P_a} = 2, 5 \text{ and } 10.$$

where:

$P_s$  = supply pressure for inner film, psia

$P_a$  = ambient pressure, psia

Furthermore, three values of the stiffness of the outer film are considered. In dimensionless form:

$$\frac{CK_o}{(P_s - P_a)LD} = 0.24, 0.18 \text{ and } 0.09 \quad (33)$$

where:

$D$  = journal diameter, inch

$L$  = bearing length, inch

$C$  = radial clearance of inner film, inch

$K_o$  = stiffness of outer film, lbs/inch

Curves are given for 7 values of the compressibility number  $\Lambda$ :

$$\Lambda = \frac{6\mu\omega}{P_a} \left( \frac{R}{C} \right)^2 = 0.3, 1, 2, 5, 10, 30 \text{ and } 100 \quad (34)$$

where:

$\mu$  = gas viscosity, lbs·sec/inch<sup>2</sup>

$\omega$  = angular speed of journal, radians/sec

The charts, figs. 27, 29, 31 --- 43, give the value of the stability mass parameter:

$$\text{Stability Mass Parameter: } \frac{CM^2}{(P_s - P_a)LD} \quad (35)$$

as a function of the dimensionless damping of the outer film:

$$\frac{CmB_o}{P_a LD} \quad (36)$$

where:

$M$  = journal mass (half the rotor mass), lbs·sec<sup>2</sup>/inch

$B_o$  = damping coefficient of outer film, lbs·sec/inch

As in the case of the hydrodynamic-hydrostatic ring bearing, it is seen that for a certain range of the outer film damping the bearing is inherently stable. The

objective when designing the bearing is to select the bearing dimensions such that the bearing operates in the "stability corridor" established by the charts.

The charts, figs. 28, 30, 37, --44, give the whirl frequency ratio:

$$\text{Whirl frequency ratio: } \frac{\nu}{\omega} \quad (37)$$

as a function of the stability mass parameter. Here:

$\nu$  = whirl frequency at onset of instability, radians/sec

These charts are used in calculating the stiffness and damping of the outer film as discussed later.

All the charts, figs. 27 to 44, are based on the following data:

length-to-diameter ratio:  $\frac{L}{D} = 1$

restrictor coefficient:  $\Lambda_s = 0.7$

Inherent compensation factor:  $\delta = 1000$

spacing factor:  $\lambda = 1.5$

eccentricity ratio:  $\epsilon = 0.02$

For  $\Lambda_s = 0.7$ , the bearing is optimized with respect to the hydrostatic stiffness. The bearing is inherently compensated (i.e. there are no orifices) to eliminate the possibility of pneumatic hammer instability. The journal is assumed to operate essentially in its concentric position but since the load is reasonably linear with displacement, the charts should be valid up to an eccentricity ratio of approximately 0.4 which covers the acceptable design range.

Figures 45 to 52 give the dimensionless stiffness and dimensionless damping of the hydrostatic outer film in the form:

$$\text{Dimensionless Stiffness: } \frac{C_o K_o}{(P_s - P_a) L_o D_o} \quad (38)$$

$$\text{Dimensionless Damping: } \frac{B_o}{\mu L_o \left( \frac{R_o}{C_o} \right)^3} \quad (39)$$

(Note: in the charts, subscript "o" has been left out).

The abscissa in the charts is the Squeeze number  $\sigma$ :

$$\text{Squeeze Number: } \sigma = \frac{12\mu\nu}{P_{so}} \left( \frac{R_o}{C_o} \right)^2 \quad (40)$$

The symbols are:

$D_o$  = outer diameter of ring, inch

$R_o$  = outer radius of ring, inch

$L_o$  = length of outer bearing, inch

$C_o$  = radial clearance of outer film, inch

$(P_s)_o$  = supply pressure for outer film, psia

$(P_a)_o$  = ambient pressure for outer film, psia

$\mu$  = gas viscosity, lbs·sec/inch<sup>2</sup>

$\nu$  = vibratory frequency, radians/sec

$K_o$  = spring coefficient of outer film, lbs/inch

$B_o$  = damping coefficient of outer film, lbs·sec/inch

The charts are valid for a single admission plane of feeder holes in the center-plane of the bearing. The feeder holes are inherently compensated ( $\delta=1000$ ) to avoid pneumatic hammer and the spacing factor is  $\lambda=1.5$ . The length-to-diameter ratio is 0.4 and four supply pressure ratios have been considered:  $P_s/P_a=1.25, 2, 5$  and  $10$ . A wide range of the restrictor coefficient is covered:

$\Lambda_s \xi_2 = 0.01, 0.02, 0.05, 0.1, 0.2, 0.5$  and  $1$ . The restrictor coefficient is defined as:

$$\Lambda_s = \frac{6\mu n d \sqrt{RT}}{P_{so} C_o^2} \quad (\text{inherent compensation}) \quad (41)$$

where:

$n$  = number of feeder holes

$d$  = feeder hole diameter, inch

$R$  = gas constant, inch<sup>2</sup>/sec<sup>2</sup> °R

$T$  = total temperature, °R

The gas flow of the outer film is given in dimensionless form in the chart, fig.

$$53: \quad \frac{6\mu R T \bar{L}_o}{\pi P_{so}^2 C_o^3 D_o} \quad (42)$$

where:

$\bar{M}$  = mass flow, lbs·sec/inch

The chart is actually valid for all length-to-diameter ratios, for both single and double plane admission, and for both orifice restriction and inherent compensation. Hence,  $\frac{L_o}{D_o}$  is replaced by  $\frac{L_2}{D} = \xi_2$  and the restrictor coefficient

is given in its general form (see Appendix V).

The use of the charts is best illustrated by an example. The or is assumed to be rigid and symmetric and it weighs: 90 lbs. The given data are:

bearing load:  $W = 45$  lbs.

journal mass:  $M = 45/386 = 0.117$  lbs·sec<sup>2</sup>/inch

journal diameter:  $D = 3$  inch

bearing length:  $L = 3$  inch

radial clearance, inner film:  $C = 0.0015$  inch

outer diameter of ring:  $D_o = 3.75$  inch

length of one outer bearing:  $L_o = 1.25$  inch

ambient pressure:  $P_a = 14.7$  psia

gas viscosity (air at 120°F):  $\mu = 2.8 \cdot 10^{-9}$  lbs·sec/inch<sup>2</sup>

gas constant (air):  $R = 2.472 \cdot 10^5$  inch<sup>2</sup>/sec<sup>2</sup> °R

total temperature:  $120 + 460 = 580$  °R

Hence:

$$RT = 1.434 \cdot 10^8 \text{ inch}^2/\text{sec}^2$$

or:

$$\sqrt{RT} = 1.198 \cdot 10^4 \text{ inch/sec}$$

The load on the bearing is 45 lbs and the bearing area is:  $L \cdot D = 3 \cdot 3 = 9$  inch<sup>2</sup>.

The load per square inch is then 5 psi which requires that the available pressure across the bearing be at least 20 psi and preferably more, i.e.:

$$P_s - P_a > 20$$

$$\text{or } \frac{P_s}{P_a} > 2.4$$

The stability charts have the dimensionless support stiffness in the form:  $CK_o / (P_s - P_a)LD$ . The eccentricity ratio of the outer film is determined from the relationship:

$$C_o \epsilon_o K_o = W \quad (43)$$

from which:

$$\epsilon_o = \frac{W}{C_o K_o} = \frac{W}{(P_s - P_a)LD} \frac{C}{C_o} \frac{(P_s - P_a)LD}{CK_o} \quad (44)$$

$\epsilon_o$  should be small and should not exceed 0.4. Thus, in order to keep the clearance ratio around 1, the dimensionless outer film stiffness should be chosen as large as possible and the supply pressure should also be kept high. Choose the largest value of the dimensionless support stiffness in the charts, namely:

$$\frac{CK_o}{(P_s - P_a)LD} = 0.24$$

Estimate that  $C/C_o \cong 1$  and set  $\epsilon_o = 0.2$  to get:

$$(P_s - P_a) = \frac{1}{\epsilon_o} \frac{C}{C_o} \frac{W}{LD} \frac{1}{0.24} = 100 \text{ psi} \quad (45)$$

or:

$$P_s = 120 \text{ psia}$$

which means:

$$\frac{P_s}{P_a} = \frac{120}{14.7} \cong 8$$

The stability charts to use for this case are then fig. 33 and fig. 39. To operate in the stability corridor it is found from the charts that the dimensionless outer film damping should be:

$$\frac{C_{dB}o}{P_a LD} = 2.5 \quad \text{at} \quad \frac{C_{MD}^2}{(P_s - P_a)LD} = 1$$

For constant support damping, the rotor will operate along a straight line with a slope of 2 in the charts as the speed increases. The corresponding damping can be found from the relationship:

$$\frac{C_0 B_0 / P_a LD}{\sqrt{C_0^2 \omega^2 / (P_s - P_a) LD}} = \frac{1}{P_a} \sqrt{\frac{C(P_s - P_a)}{MLD}} \cdot B_0 = \frac{2}{\sqrt{1}} \quad (46)$$

From figs. 50 to 53 it is seen that the dimensionless outer film damping will be around 1. Set:

$$\frac{B_0}{\mu L_0 \left(\frac{R_0}{C_0}\right)^3} = 1$$

Since there are two outer film bearings, the damping per bearing is half the required damping given in eq. (46). The damping per bearing can be expressed by means of eq. (46) as:

$$\frac{B_0}{\mu L_0 \left(\frac{R_0}{C_0}\right)^3} = 1 = \frac{1}{2} \frac{P_a}{\mu L_0 \left(\frac{R_0}{C_0}\right)^3} \cdot \sqrt{\frac{MLD}{C(P_s - P_a)}} \cdot \frac{2}{\sqrt{1}}$$

or:

$$\left(\frac{R_0}{C_0}\right)^3 = \frac{1}{2} \frac{P_a}{\mu L_0} \cdot \sqrt{\frac{MLD}{C(P_s - P_a)}} \cdot \frac{2}{\sqrt{1}} \cdot \frac{1}{1} = \frac{1}{2} \frac{14.7}{2.8 \cdot 10^{-9} \cdot 1.25} \cdot \sqrt{\frac{0.117 \cdot 3 \cdot 3}{C \cdot (120 - 14.7)}} \cdot \frac{2}{\sqrt{1}} \cdot \frac{1}{4} \quad (47)$$

Set  $C = 0.0015$  inch whereby:

$$\left(\frac{R_0}{C_0}\right)^3 = 10.84 \cdot 10^9$$

or:

$$\frac{R_0}{C_0} = 2.21 \cdot 10^3$$

i.e.

$$C_0 = \frac{1.875}{2.21} \cdot 10^{-3} = 0.00085 \text{ inch}$$

Eq. (47) (together with eqs. (44 or (45) ) must be considered the key design equation. For a given rotor-bearing system, the clearance of the outer film can only vary within a very limited range if the rotor is to operate within the stability corridor. Hence,  $C_0$  is the critical design dimension whereas the other design parameters can vary appreciably without having serious effects.

To check the estimated outer film damping, the following relationship is readily deduced:

$$\frac{C_{2D}^2}{(P_s - P_a)LD} = \frac{\Lambda^2}{72} \frac{MP_a^2}{\mu^2 L (P_s - P_a) \left(\frac{R}{C}\right)^5} \quad (48)$$

Here:

$$\frac{MP_a^2}{\mu^2 L (P_s - P_a) \left(\frac{R}{C}\right)^5} = \frac{0.117 \cdot (14.7)^2}{(2.8 \cdot 10^{-9})^2 \cdot 3 \cdot (120 - 14.7) \left(\frac{1.5}{0.0015}\right)^5} = 10.21$$

whereby:

$$\frac{C_{2D}^2}{(P_s - P_a)LD} = 0.142 \cdot \Lambda^2$$

From the definition of  $\Lambda$  and  $\sigma$  (eqs. (34) and (40) ) it is seen that:

$$\sigma = 2 \cdot \frac{\nu}{\omega} \cdot \Lambda \quad (49)$$

Making use of these relationships, figs. 34 and 40 can be employed to set up the following table:

$\Lambda$	$\frac{C_{2D}^2}{(P_s - P_a)LD}$	$B_o \rightarrow 0$		$B_o \rightarrow \infty$	
		$\frac{\nu}{\omega}$	$\sigma$	$\frac{\nu}{\omega}$	$\sigma$
2	0.567	0.5	2.0	0.5	2.0
5	3.54	0.202	2.02	0.31	3.1
10	14.2	0.105	2.10	0.185	3.7
30	128	0.036	2.16	0.075	4.5
100	1420	0.0112	2.24	0.0245	4.9

In this table,  $\frac{\nu}{\omega}$  is the instability frequency ratio obtained by interpolation between figs. 34 and 40. As seen from figs. 33 and 39, the stability corridor passes between two regions of instability, and the instability frequency is different for the two regions as shown by figs. 34 and 40. The left hand region is identified in figs. 34 and 40 as the region where  $B_o \rightarrow 0$ , and the right hand region is identified as the region where  $B_o \rightarrow \infty$ .

At the onset of instability, the journal whirls in closed orbit with frequency  $\nu$ . Hence,  $\nu$  becomes the vibratory frequency as seen by the outer film and the

stiffness and damping of the outer film must, therefore, be evaluated at the corresponding values of the Squeeze number as given in the table. Since the outer film decreases with increasing squeeze number it is only necessary to consider the Squeeze number corresponding to the left hand instability region ( $B_o \rightarrow 0$ ).

The charts, figs. 33 and 39, are based on a dimensionless support stiffness of 0.24. Hence:

$$K_o = \frac{(120-14.7) \cdot 3 \cdot 3}{0.0015} = 151,600 \text{ lbs/inch}$$

Since there are two bearings, the required stiffness per bearing is:

$$(K_o)_{\text{per bearing}} = 75,800 \text{ lbs./inch}$$

Assuming a restrictor coefficient value such that:

$$\Lambda_s \xi_2 = 0.05$$

the dimensionless stiffness per bearing is found by interpolation between figs. 47 and 48 as ( $\sigma \approx 2.2$ ):

$$\frac{C_o K_o}{(P_s - P_a)_o L_o D_o} = 0.15$$

or:

$$(P_s - P_a)_o = \frac{0.00085 \cdot 75,800}{1.25 \cdot 3.75 \cdot 0.15} = 91.6$$

Therefore:

$$P_{s0} = 106.3 \text{ psia} \approx 120 \text{ psia}$$

whereby:

$$\left( \frac{P_s}{P_a} \right)_o = 8$$

Thus, both films have the same supply pressure.

At this calculated pressure ratio, with  $\Lambda_s \xi_2 = 0.05$  and  $\sigma = 2.2$  the dimensionless damping per bearing is found from figs. 51 and 52 to be equal to the earlier assumed value of 1. Hence, the assumed value of  $\Lambda_s \xi_2 = 0.05$  is correct.

Now:

$$\xi_2 = \frac{L_o}{D_o} = \frac{1.25}{3.75} = \frac{1}{3}$$

(Note: even if the charts, figs. 45 to 52, are based on  $\xi_2=0.4$ , the dimensionless stiffness and damping are not too sensitive to variations in  $\xi_2$  and the charts may, therefore, also be used for  $\xi_2 = \frac{1}{3}$ ). Hence:

$$\Lambda_s = 0.05 \cdot 3 = 0.15$$

From the definition of  $\Lambda_s$  in eq. (41):

$$n_o d_o = \frac{P_{so} C_o^2 \Lambda_s}{6\mu \sqrt{RT}} = \frac{120 \cdot (0.00085)^2 \cdot 0.15}{6 \cdot 2.8 \cdot 10^{-9} \cdot 1.198 \cdot 10^4} = 0.0646 \text{ inch}$$

set:

$$n_o = 10$$

whereby:

$$d_o = 0.0065 \text{ inch}$$

The spacing factor becomes:

$$\lambda = 1 + \frac{2}{n_o \xi_2} \log_e \left( \frac{D_o}{n_o d_o} \right) = 3.4$$

which is higher than the value of 1.5 for which the charts are valid. This, however, has only very minor influence on the damping but the stiffness is somewhat reduced. On the other hand, the supply pressure has been set 14 psi larger than actually required which should offset the reduction due to the spacing factor.

Even so, the calculated feeder hole diameter is small and should preferably be larger (0.01 to 0.02 inches) although the obtained value can be used as is.

The mass of the ring is:

$$\frac{\pi}{4} (3.75^2 - 3.0^2) \cdot 3 \cdot 0.283 = 3.38 \text{ lbs} = 0.008755 \text{ lbs} \cdot \text{sec}^2 / \text{inch}$$

If the ring was rigidly supported, figs. 33 and 39 give:

$$\text{at } B_o = \infty : \frac{CM\omega^2}{(P_s - P_a)LD} = 1.4$$

The corresponding frequency ratio is:  $\frac{\nu}{\omega} = 0.5$ . Define an effective stiffness of the inner film by:

$$\nu^2 = \frac{K_{eff}}{M}$$

or:

$$\frac{CK_{eff}}{(P_s - P_a)LD} = \left( \frac{\nu}{\omega} \right)^2 \frac{CM\omega^2}{(P_s - P_a)LD} = 0.25 \cdot 1.4 = 0.35 \quad (50)$$

whereby:

$$K_{\text{eff}} = \frac{(120 - 14.7) \cdot 3 \cdot 3}{0.0015} \cdot 0.35 = 221,000 \text{ lbs/inch}$$

With a total outer film stiffness of:  $K_o = 151,600 \text{ lbs/inch}$ , the natural frequency of the ring is:

$$\text{Natural frequency of ring} = \sqrt{\frac{221,000 + 151,600}{0.00875}} = 6,530 \text{ radians/sec} = 62,400 \text{ rpm}$$

Assuming an instability frequency ratio of 0.5, the ring may become unstable by itself at 125,000 rpm. This is a conservative estimate but to be safe, this speed should be considered the maximum speed for the bearing.

With  $\Lambda_g \xi_2 = 0.05$ , the dimensionless flow for the outer film is found from fig. 53 to be 0.034. Hence, the flow per bearing becomes:

$$\bar{M} = \frac{\pi \cdot (120)^2 \cdot (0.00085)^3}{6 \cdot 2.8 \cdot 10^{-9} \cdot 1.434 \cdot 10^8 \cdot 0.33} \cdot 0.034 = 1.172 \cdot 10^{-6} \frac{\text{lbs} \cdot \text{sec}}{\text{inch}} = 4.52 \cdot 10^{-4} \frac{\text{lbs}}{\text{sec}} = 0.33 \text{ scfm}$$

For the two outer bearings, the flow is  $0.0009 \text{ lbs/sec} = 0.66 \text{ scfm}$ .

For the inner film,  $\Lambda_g \xi_2 = 0.7$ . Since  $\xi_2 = 1$ ,  $\Lambda_g = 0.7$  or:

$$nd = \frac{120 \cdot (0.0015)^2}{6 \cdot 2.8 \cdot 10^{-9} \cdot 1.198 \cdot 10^4} \cdot 0.7 = 0.938$$

Set  $n = 12$  whereby:

$$d = 0.076 \text{ inch}$$

The corresponding spacing factor is:  $\lambda = 1.22$  which is close to the value of  $\lambda = 1.5$  on which the charts are based.

The dimensionless flow for the inner film is determined from fig. 53 to be 0.39. Hence, the flow becomes:

$$\bar{M} = \frac{\pi \cdot (120)^2 \cdot (0.0015)^3}{6 \cdot 2.8 \cdot 10^{-9} \cdot 1.434 \cdot 10^8} \cdot 0.39 = 2.475 \cdot 10^{-5} \frac{\text{lbs} \cdot \text{sec}}{\text{inch}} = 9.55 \cdot 10^{-3} \frac{\text{lbs}}{\text{sec}} = 7.1 \text{ scfm}$$

The calculated bearing dimensions and performance data are summarized below:

total rotor weight:	$2W = 90 \text{ lbs.}$
journal diameter:	$D = 3 \text{ inch}$

outer diameter of ring:	$D_o = 3.75$ inch
length of ring:	$L = 3$ inch
length of one outer bearing:	$L_o = 1.25$ inch
radial clearance of inner film:	$C = 0.0015$ inch
radial clearance of outer film:	$C_o = 0.00085$ inch
number of feeder holes for inner film:	$n = 12$
diameter of feeder holes for inner film:	$d = 0.076$ inch
number of feeder holes for one outer bearing:	$n_o = 10$
diameter of feeder holes for outer bearing:	$d_o = 0.0065$ inch
supply pressure for both films:	$P_s = 120$ psia
flow for inner film:	7.1 scfm
flow for two outer bearings:	0.66 scfm
maximum stable speed (conservative estimate):	125,000 rpm

TABLE 1

3 LOBE BEARING, VERTICAL ROTOR

Preload		$\frac{L}{D} = \frac{1}{2}$					$\frac{CK_{xx}}{SW}$	$\frac{CK_{xy}}{SW}$	$\frac{C\omega B_{xx}}{SW}$	$\frac{C\omega B_{xy}}{SW}$
$\delta$	$R_e$	$\frac{R}{C}$	$\frac{F_f}{SW}$	$\frac{Q_z}{NDLC}$	$\frac{Q_x}{NDLC}$	$\frac{v}{\omega}$	$\frac{CK_{yy}}{SW}$	$-\frac{CK_{yz}}{SW}$	$\frac{C\omega B_{yy}}{SW}$	$-\frac{C\omega B_{yz}}{SW}$
						$\mu DL \left(\frac{R}{C}\right)$				
0.1	0	18.04	.0812	4.345	.4978	.01503	.1499	1.585	3.184	-.00577
	2000	44.55	.0892	4.351	.4983	.02122	.2150	2.536	5.090	-.0139
	10000	133.8	.0946	4.355	.4986	.04833	.4893	6.179	12.39	-.0300
	30000	306.3	.0964	4.357	.4987	.1011	1.027	13.24	26.56	-.0678
0.25	0	21.11	.1994	3.787	.4935	.07009	.6783	2.542	5.152	-.00912
	2000	47.48	.2185	3.803	.4952	.09369	.9174	3.815	7.703	-.0207
	10000	139.6	.2331	3.814	.4962	.2039	2.004	8.983	18.10	-.0432
	30000	317.7	.2381	3.818	.4965	.4206	4.143	18.96	38.18	-.0992
0.375	0	24.66	.2933	3.313	.4886	.1935	1.832	3.986	8.159	-.0171
	2000	50.77	.3207	3.337	.4918	.2464	2.367	5.732	11.66	-.0307
	10000	145.8	.3445	3.357	.4938	.5111	4.952	17.98	26.28	-.0635
	30000	329.7	.3528	3.363	.4944	1.038	10.08	27.11	54.84	-.1413
0.5	0	29.74	.3810	2.828	.4817	.5339	4.905	6.912	14.35	-.0301
	2000	55.38	.4154	2.860	.4869	.6456	6.067	9.391	19.29	-.0497
	10000	154.0	.4502	2.890	.4909	1.258	12.02	20.22	41.19	-.1015
	30000	345.2	.4628	2.900	.4921	2.501	24.01	41.66	84.65	-.2183
0.6667	0	41.48	.4817	2.156	.4673	2.521	21.78	17.61	37.69	-.1025
	2000	66.00	.5223	2.198	.4762	2.836	25.44	22.29	46.80	-.1032
	10000	170.72	.5769	2.243	.4861	4.876	45.61	44.57	91.68	-.2351
	30000	376.2	.5984	2.261	.4891	9.264	87.73	88.79	181.5	-.4849
0.75	0	52.27	.5198	1.807	.4560	6.646	54.63	32.89	72.13	-.1817
	2000	75.92	.5617	1.849	.4667	7.198	62.01	40.07	85.86	-.2182
	10000	189.6	.6301	1.904	.4832	11.27	104.1	76.51	158.3	-.4248
	30000	401.0	.6585	1.926	.4883	20.58	194.2	150.1	307.5	-.8336

TABLE 1 (Continued)

3 LOBE BEARING, VERTICAL ROTOR

$$\frac{L}{D} = 1$$

Preload $\delta$	$R_e$	$\frac{R}{C}$	$\frac{F_f}{SW}$	$\frac{Q_z}{NDLC}$	$\frac{Q_x}{NDLC}$	$\frac{v}{\omega}$	$\frac{CMN}{\mu DL (\frac{R}{C})}$	$\frac{CK_{xx}}{SW}$	$\frac{CK_{xy}}{SW}$	$\frac{C\omega B_{xx}}{SW}$	$\frac{C\omega B_{xy}}{SW}$
								$\frac{CK_{yy}}{SW}$	$-\frac{CK_{yx}}{SW}$	$\frac{C\omega B_{yy}}{SW}$	$-\frac{C\omega B_{yx}}{SW}$
0.1	0	18.04	.0434	4.318	.4968	.02665	.2584	3.343	6.729	.00256	
	2000	44.55	.0500	4.323	.4976	.03991	.3912	5.788	11.63	-.00230	
	10000	133.8	.0549	4.326	.4979	.09622	.9486	14.89	29.90	-.0141	
	30000	306.3	.0567	4.328	.4980	.2059	2.035	32.47	65.21	-.0389	
0.25	0	21.12	.1054	3.718	.4908	.1230	1.171	5.194	10.58	-.00222	
	2000	47.50	.1209	3.730	.4930	.1732	1.667	8.496	17.23	-.00881	
	10000	139.7	.1338	3.740	.4942	.4003	3.875	21.20	42.90	-.03069	
	30000	317.8	.1386	3.744	.4945	.8447	8.186	45.79	92.59	-.0619	
0.375	0	24.67	.1533	3.207	.4840	.3358	3.110	7.985	16.50	-.0115	
	2000	50.84	.1747	3.226	.4882	.4469	4.214	12.35	25.29	-.0200	
	10000	146.0	.1953	3.242	.4906	.9847	9.381	29.92	60.99	-.0477	
	30000	330.1	.2031	3.248	.4913	2.054	19.63	04.01	130.3	-.1217	
0.5	0	29.85	.1960	2.682	.4747	.9105	8.112	13.22	27.85	-.02706	
	2000	55.57	.2219	2.708	.4816	1.140	10.45	19.37	40.23	-.0374	
	10000	154.4	.2512	2.731	.4866	2.362	22.13	45.23	92.96	-.0968	
	30000	346.2	.2628	2.740	.4880	4.833	45.54	95.89	196.5	-.1957	
0.6667	0	41.89	.2405	1.954	.4560	4.141	34.01	31.05	68.09	-.0670	
	2000	66.61	.2691	1.985	.4676	4.741	40.96	41.92	89.65	-.0839	
	10000	172.2	.3122	2.017	.4807	8.586	78.42	92.94	193.3	-.1821	
	30000	379.5	.3308	2.031	.4846	16.82	156.1	193.7	399.9	-.4056	
0.75	0	53.07	.2545	1.576	.4414	10.58	81.38	54.72	124.0	-.03635	
	2000	77.07	.2824	1.605	.4554	11.57	94.80	71.23	156.4	-.1660	
	10000	187.4	.3336	1.638	.4776	18.75	169.0	152.7	319.8	-.3023	
	30000	407.2	.3573	1.653	.4848	35.18	326.7	315.0	649.7	-.6616	



TABLE 2 (continued)

$R_e$	$\epsilon_{\text{scat}}$	$\epsilon_B$	$\phi_B$	Min. Film Thickness	$S$	$\frac{R_e}{C V}$	$\frac{Q_e}{WDLG}$	$\frac{Q_e}{WDLG}$	$\frac{V}{\sigma}$	$\frac{C_{\text{DM}}^2}{V}$	$\frac{C_{\text{DM}}}{\mu\text{M}(\frac{1}{C})}$	$\frac{C_{\text{H}_2}}{V}$	$\frac{C_{\text{H}_2}}{V}$	$\frac{C_{\text{H}_2}}{V}$	$\frac{C_{\text{H}_2}}{V}$	$\frac{C_{\text{H}_2}}{V}$	$\frac{C_{\text{H}_2}}{V}$	
2000	0.02	0.645	63.32	.4785	1.003	55.84	.2242	2.705	.4813	46.40	1.172	12.26	19.84	-19.34	9.503	1.85	1.90	37.57
	0.1	.2166	62.30	.3700	.1611	9.383	.5868	2.658	.4720	12.99	2.043	4.747	-3.788	2.095	1.85	1.85	1.85	5.675
	0.15	.2987	59.66	.3006	.09359	5.750	.7980	2.614	.4450	12.26	3.317	4.869	-1.949	1.783	1.85	1.85	1.85	3.568
	0.2	.3646	56.73	.2365	.05935	3.870	.9752	2.567	.3759	15.10	6.446	5.564	4.128	1.624	1.85	1.85	1.85	2.528
	0.25	.4158	53.04	.1797	.03882	2.729	1.140	2.523	.1237	138.3	90.22	6.813	4.290	-1.151	1.624	1.85	1.85	2.333
10000	0.3	.4468	47.82	1.341	.02618	1.991	1.347	2.562	--	--	--	8.817	4.528	1.506	1.239	1.85	1.85	1.465
	0.02	.6476	65.16	.4782	.4083	63.12	.2543	2.729	.4868	39.07	2.324	10.60	19.05	-18.28	8.166	1.85	1.85	35.37
	0.1	.2275	63.92	.3662	.06666	10.60	.6207	2.681	.4885	10.52	3.996	4.062	4.921	-3.087	1.863	1.85	1.85	5.355
	0.15	.3123	61.30	.2946	.03911	6.410	.8456	2.636	.4786	9.077	5.878	4.075	4.374	-1.848	1.601	1.85	1.85	3.177
	0.2	.3792	58.17	.2294	.02504	4.264	1.033	2.586	.4574	8.574	8.672	4.472	4.205	-1.141	1.695	1.85	1.85	2.422
30,000	0.25	.4306	54.51	.1721	.01661	2.961	1.217	2.535	.3951	10.17	15.51	5.261	4.314	-1.649	1.408	1.85	1.85	1.929
	0.3	.4628	49.39	.1259	.01135	2.124	1.426	2.448	.2938	11.89	26.54	6.631	4.669	-0.264	1.145	1.85	1.85	1.337
	0.02	.6485	65.66	.4781	.1900	65.84	.2661	2.738	.4884	37.17	4.956	10.13	18.82	-17.99	7.834	1.85	1.85	34.69
	0.1	.2310	64.34	.3649	.03123	11.08	.6330	2.691	.4929	9.904	8.033	3.866	4.885	-3.051	1.797	1.85	1.85	5.301
	0.15	.3179	61.84	.2922	.01829	6.666	.8659	2.645	.4890	8.232	11.40	3.824	4.240	-1.798	1.547	1.85	1.85	3.289
0.2	.3844	58.65	.2268	.01178	4.436	1.054	2.596	.4313	7.285	15.66	4.098	4.208	-1.152	1.454	1.85	1.85	1.243	
	.4358	55.00	.1694	.00783	3.064	1.245	2.543	.4556	7.015	22.70	4.625	4.445	-0.702	1.367	1.85	1.85	1.437	
	.4683	50.16	.1229	.00533	2.176	1.460	2.547	.4764	3.946	18.76	5.473	4.750	-0.926	1.104	1.85	1.85	1.274	

TABLE 3

PLAIN CYLINDRICAL BEARING

$R_e$	$\frac{L}{D} = \frac{1}{2}$					$\frac{L}{D} = 1$				
	$\epsilon$	S	$\frac{R}{C}$	$\frac{F_f}{W}$	$\frac{CM\omega^2}{W}$	$\epsilon$	S	$\frac{R}{C}$	$\frac{F_f}{W}$	$\frac{CM\omega^2}{W}$
0	0.0907	4.778	94.74	7.202	0.0964	1.353	26.88	6.418		
	0.1578	2.654	53.14	7.039	0.1672	0.7594	15.29	6.381		
	0.2902	1.278	26.50	6.719	0.3068	0.3757	7.937	6.300		
	0.4149	0.7377	16.19	6.483	0.4366	0.2267	5.168	6.368		
	0.5138	0.4791	11.23	6.701	0.5379	0.1549	3.850	6.767		
	0.5995	0.3198	8.111	7.592	0.6246	0.1095	3.009	7.698		
	0.6777	0.2107	5.884	10.75	0.7017	0.07730	2.388	10.41		
	0.8182	0.07786	2.884	-	-	0.8365	0.03433	1.466	-	-
2,000	0.0969	2.878	148.7	6.318	0.1019	0.7948	41.13	5.716		
	0.1680	1.609	83.47	6.190	0.1766	0.4458	23.21	5.639		
	0.3075	0.7835	41.24	5.968	0.3230	0.2202	11.72	5.439		
	0.4366	0.4610	24.84	5.846	0.4578	0.1377	7.331	5.305		
	0.5365	0.3061	16.97	6.058	0.5617	0.09076	5.238	5.473		
	0.6213	0.2091	12.00	7.222	0.6495	0.06441	3.921	6.158		
	0.6977	0.1415	8.493	9.920	0.7266	0.04583	2.982	7.780		
	0.8314	0.05618	3.899	-	-	0.8562	0.02139	1.699	-	-
10,000	0.1013	1.149	180.3	5.785	0.1058	0.3133	49.20	5.288		
	0.1756	0.6440	101.3	5.667	0.1833	0.1759	27.75	5.197		
	0.3209	0.3165	50.26	5.469	0.3346	0.08720	13.98	4.952		
	0.4541	0.1891	30.48	5.381	0.4727	0.05279	8.684	4.714		
	0.5560	0.1277	20.95	5.549	0.5780	0.03624	6.146	4.532		
	0.6414	0.08900	14.91	6.464	0.6562	0.02579	4.535	4.676		
	0.7170	0.06171	10.61	8.053	0.7430	0.01836	3.377	5.031		
	0.8470	0.02595	4.830	-	-	0.8714	0.00851	1.791	-	-
30,000	0.1028	0.5313	191.5	5.664	0.1072	0.1442	51.98	5.144		
	0.1783	0.2979	107.6	5.493	0.1857	0.08102	29.33	5.056		
	0.3257	0.1469	53.46	5.302	0.3388	0.04021	14.77	4.799		
	0.4604	0.08818	32.52	5.213	0.4781	0.02441	9.174	4.543		
	0.5632	0.05992	22.43	5.357	0.5840	0.01679	6.486	4.369		
	0.6492	0.04204	16.02	6.183	0.6723	0.01197	4.777	4.314		
	0.7243	0.02941	11.45	7.458	0.7488	0.008535	3.544	4.271		
	0.8532	0.01269	5.270	-	-	0.8764	0.003933	1.839	4.648	

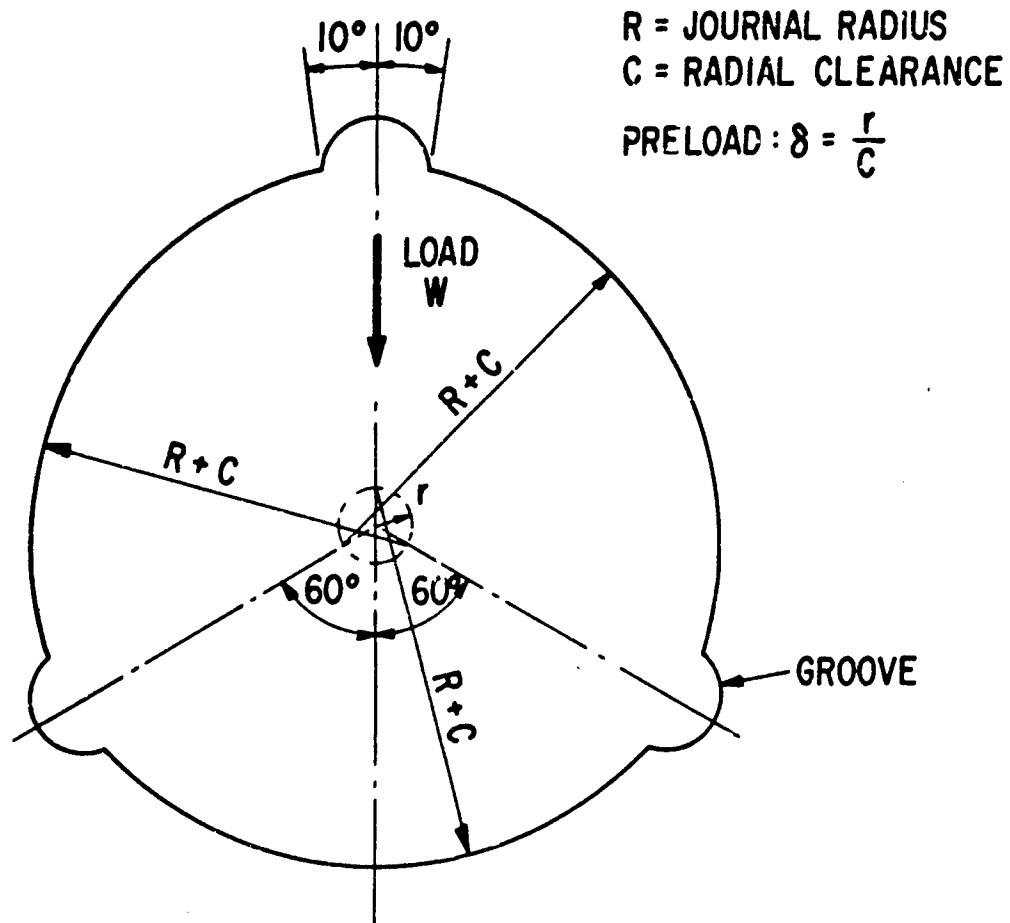


Figure 1. The 3 Lobe Bearing, Schematic

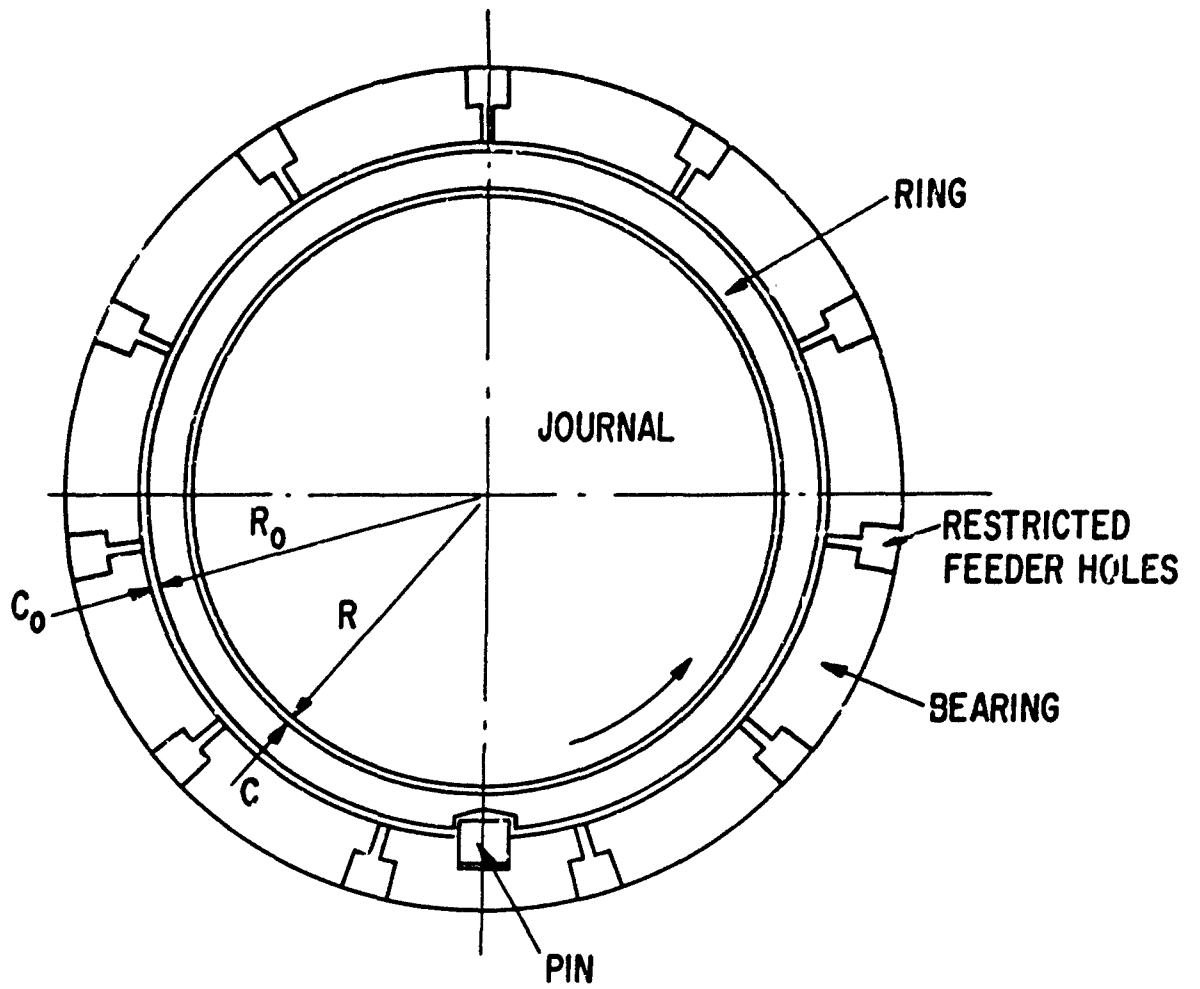


Figure 2. The Hydrodynamic-Hydrostatic Ring Bearing, Schematic

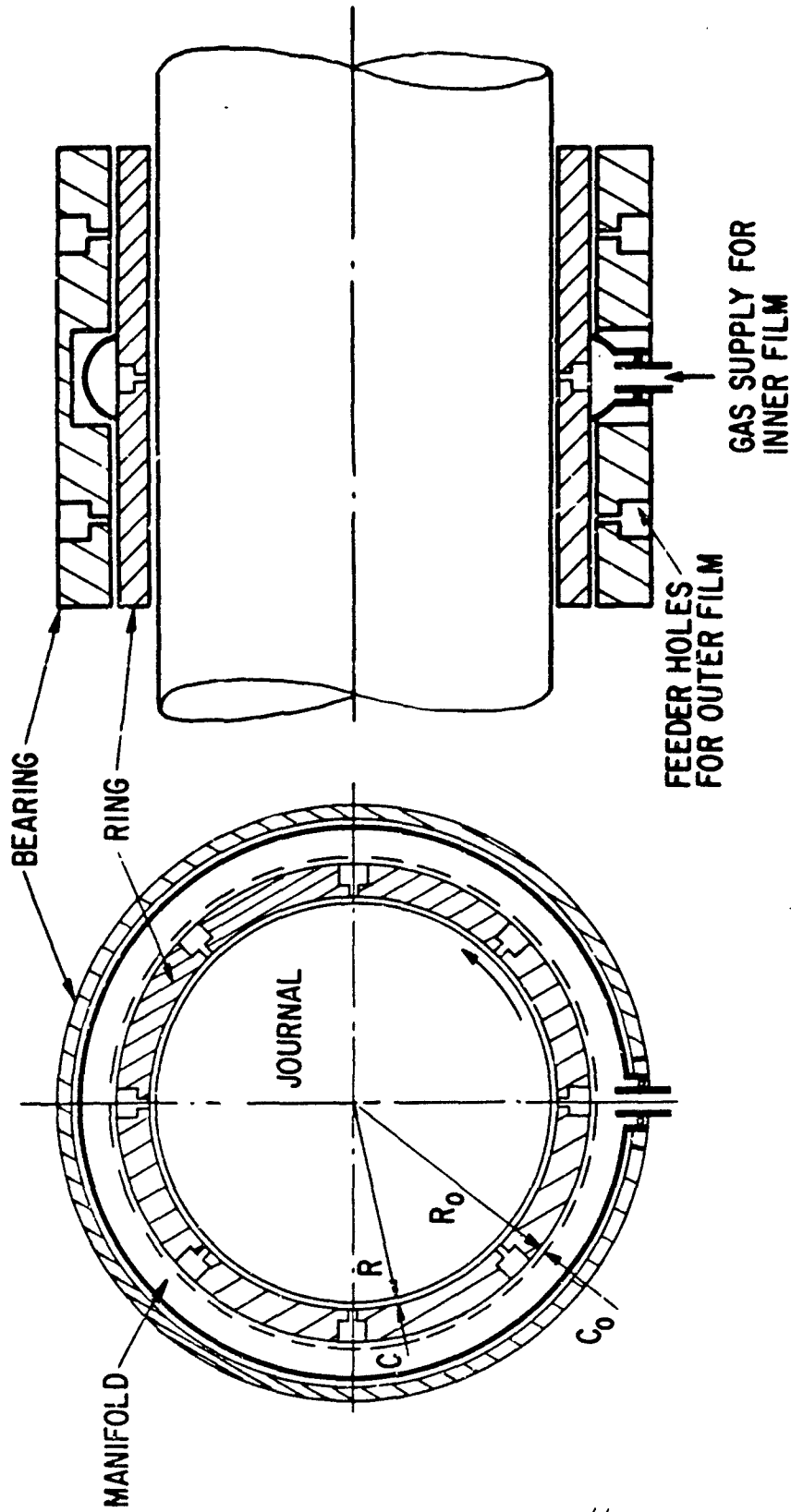


Figure 3. The Hybrid-Hydrostatic Ring Bearing, Schematic

MTI-5034

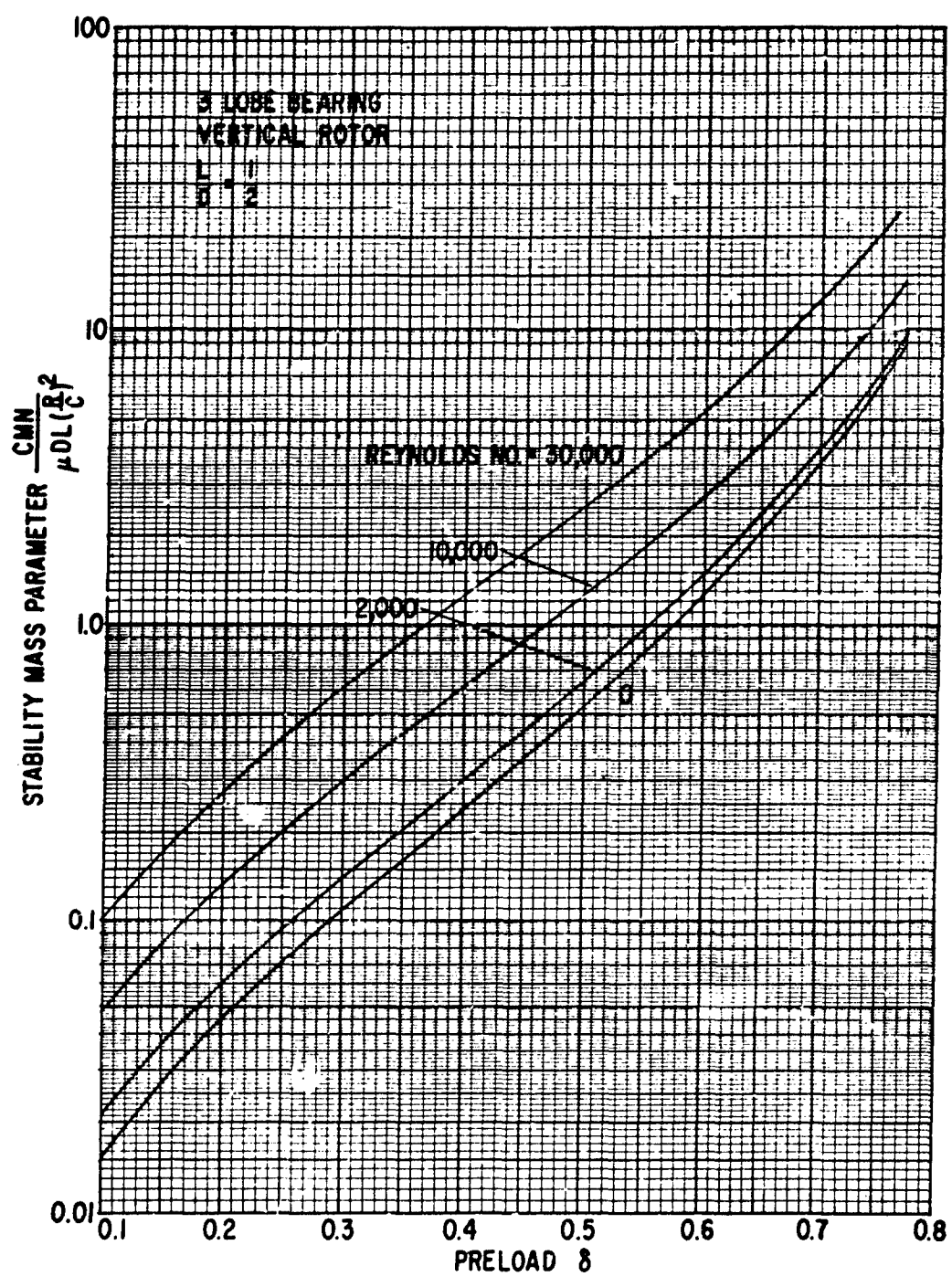


Figure 4. 3 Lobe Bearing, Vertical Rotor,  $\frac{L}{D} = \frac{1}{2}$ , Stability Map

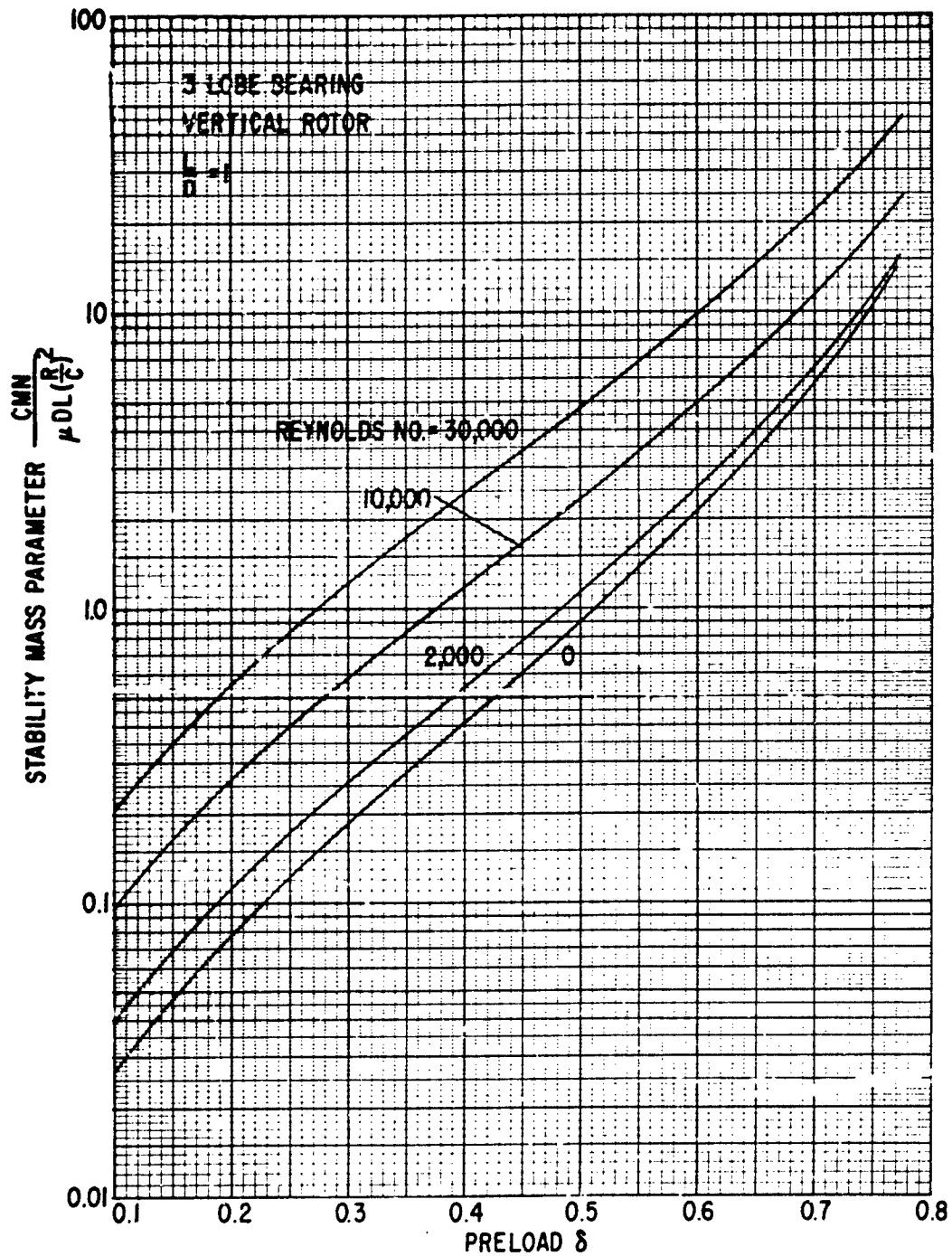


Figure 5. 3 Lobe Bearing, Vertical Rotor,  $\frac{L}{D} = 1$ , Stability Map

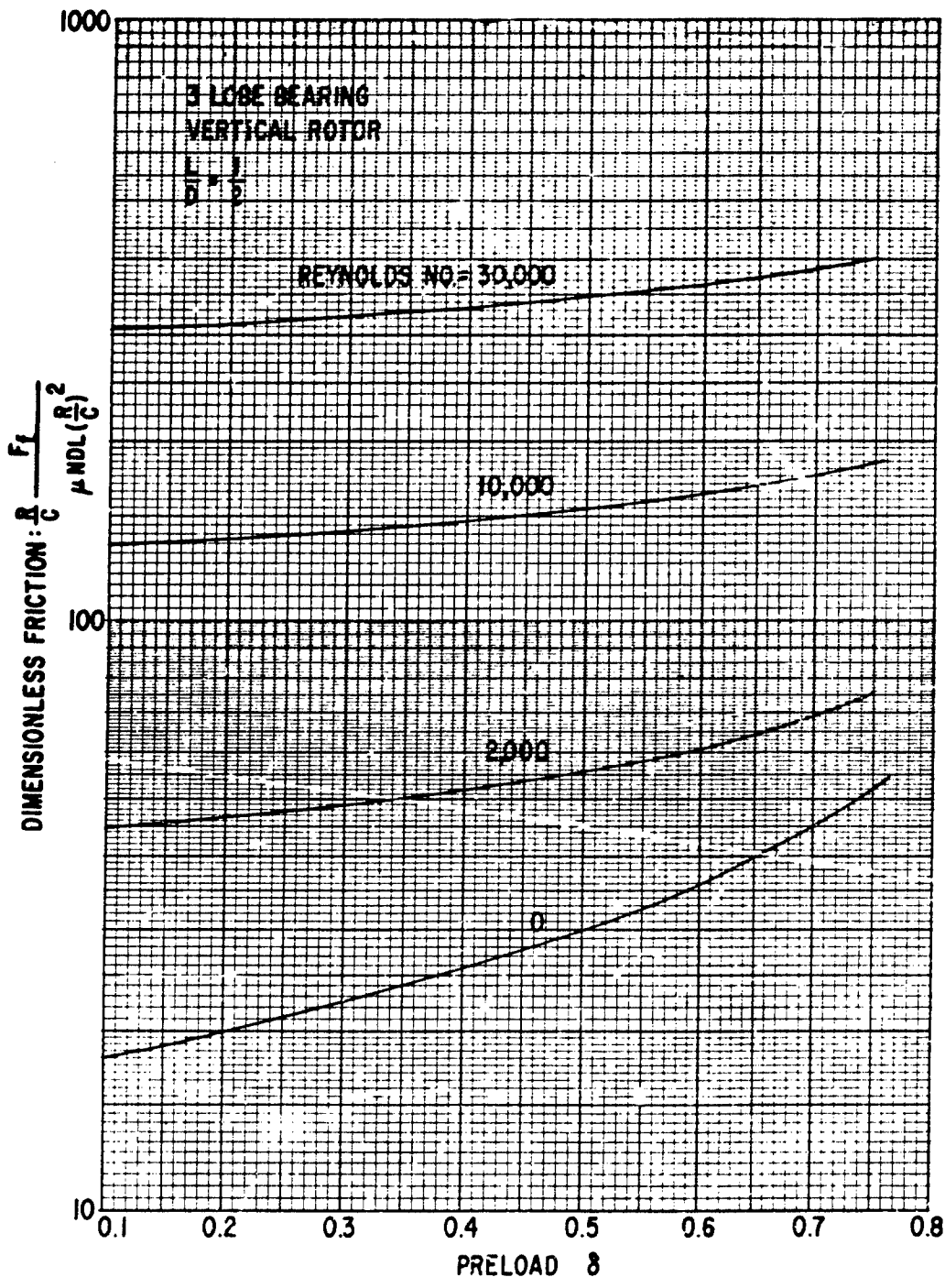


Figure 6. 3 Lobe Bearing, Vertical Rotor,  $\frac{L}{D} = \frac{1}{2}$ , Friction

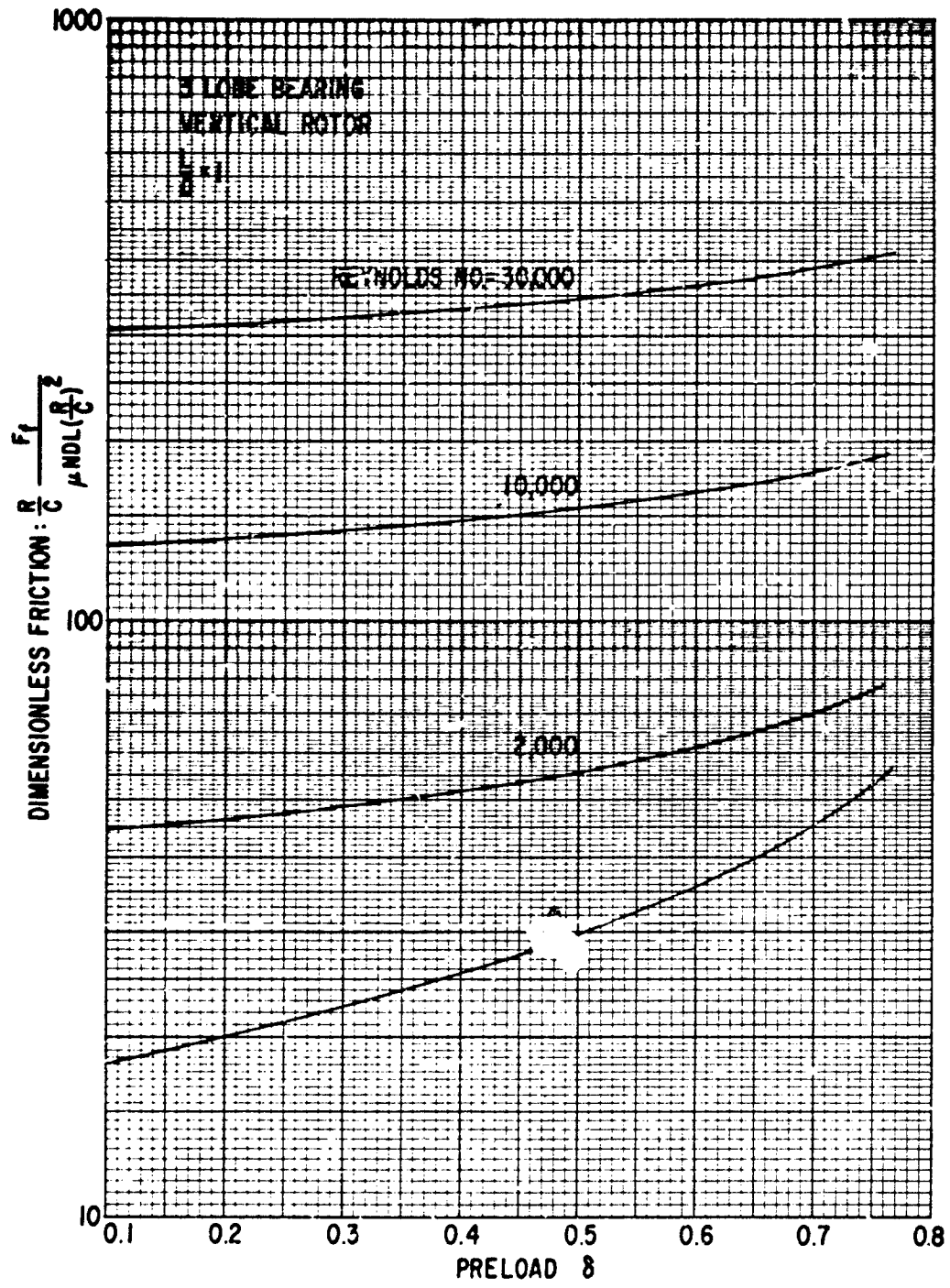


Figure 7. 3 Lobe Bearing, Vertical Rotor,  $\frac{L}{D} = 1$ , Friction

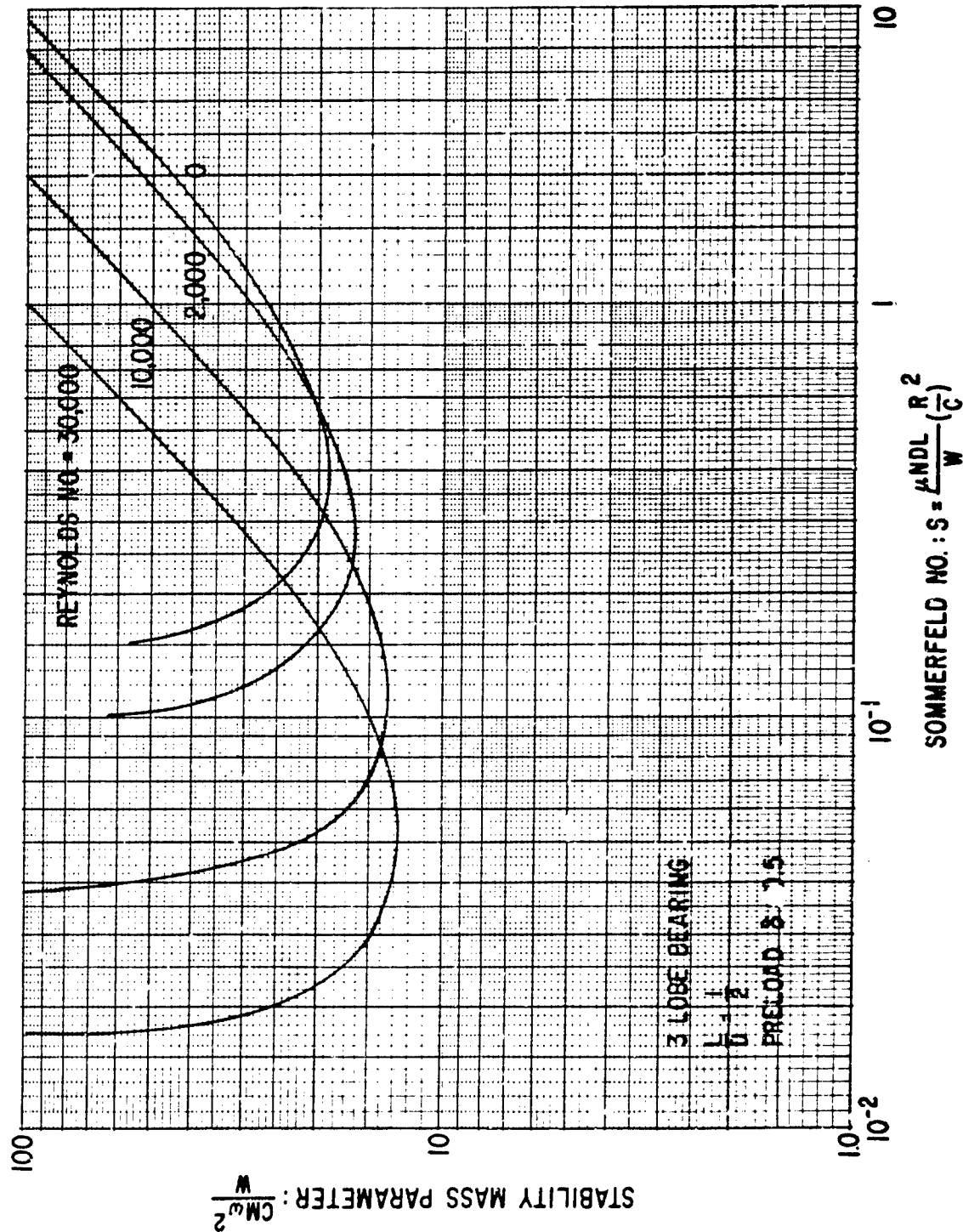


Figure 8. 3 Lobe Bearing, Preload = 0.5,  $\frac{L}{D} = \frac{1}{2}$ , Stability Map

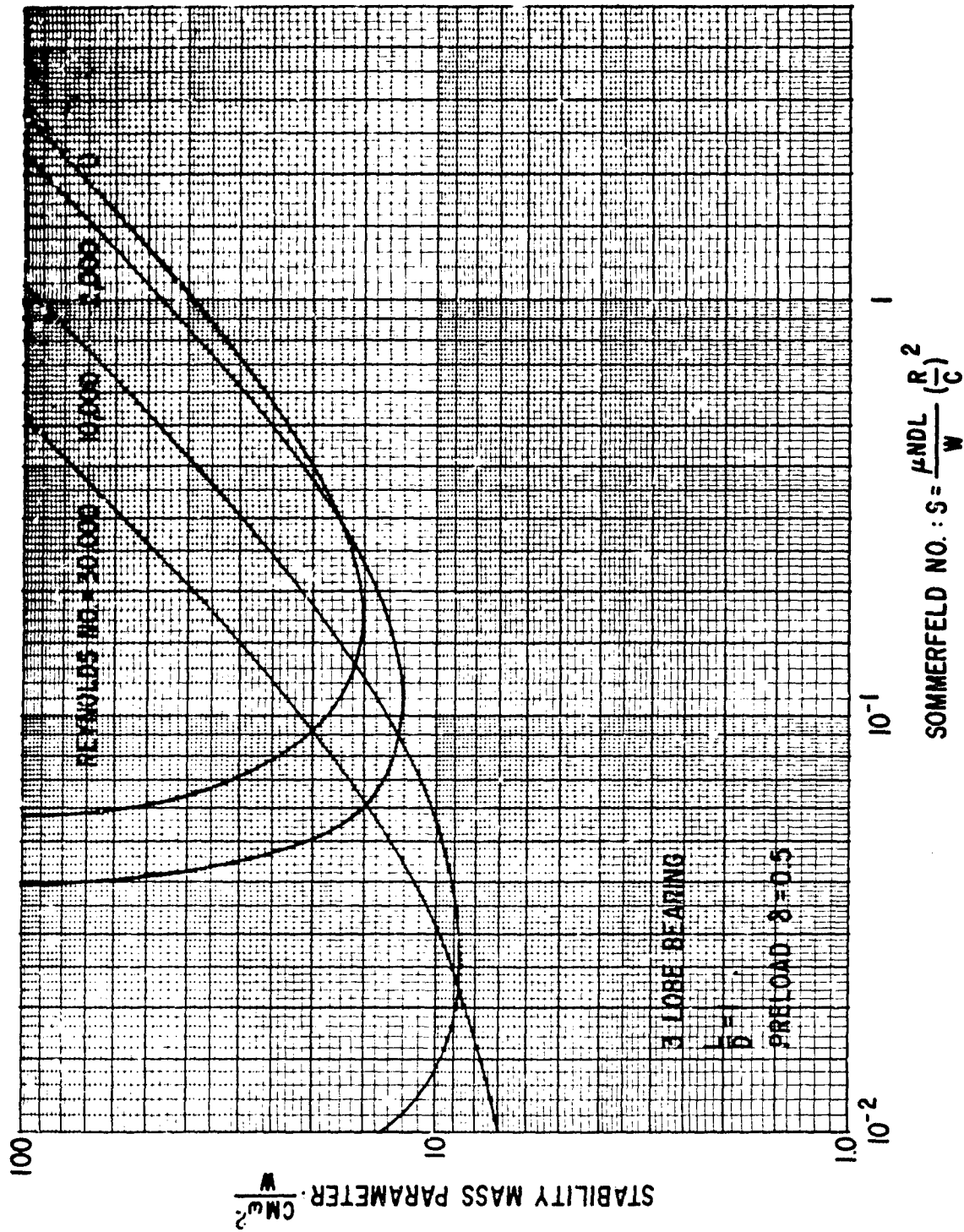


Figure 9. 3 Lobe Bearing, Preload = 0.5,  $\frac{L}{D} = 1$ , Stability Map

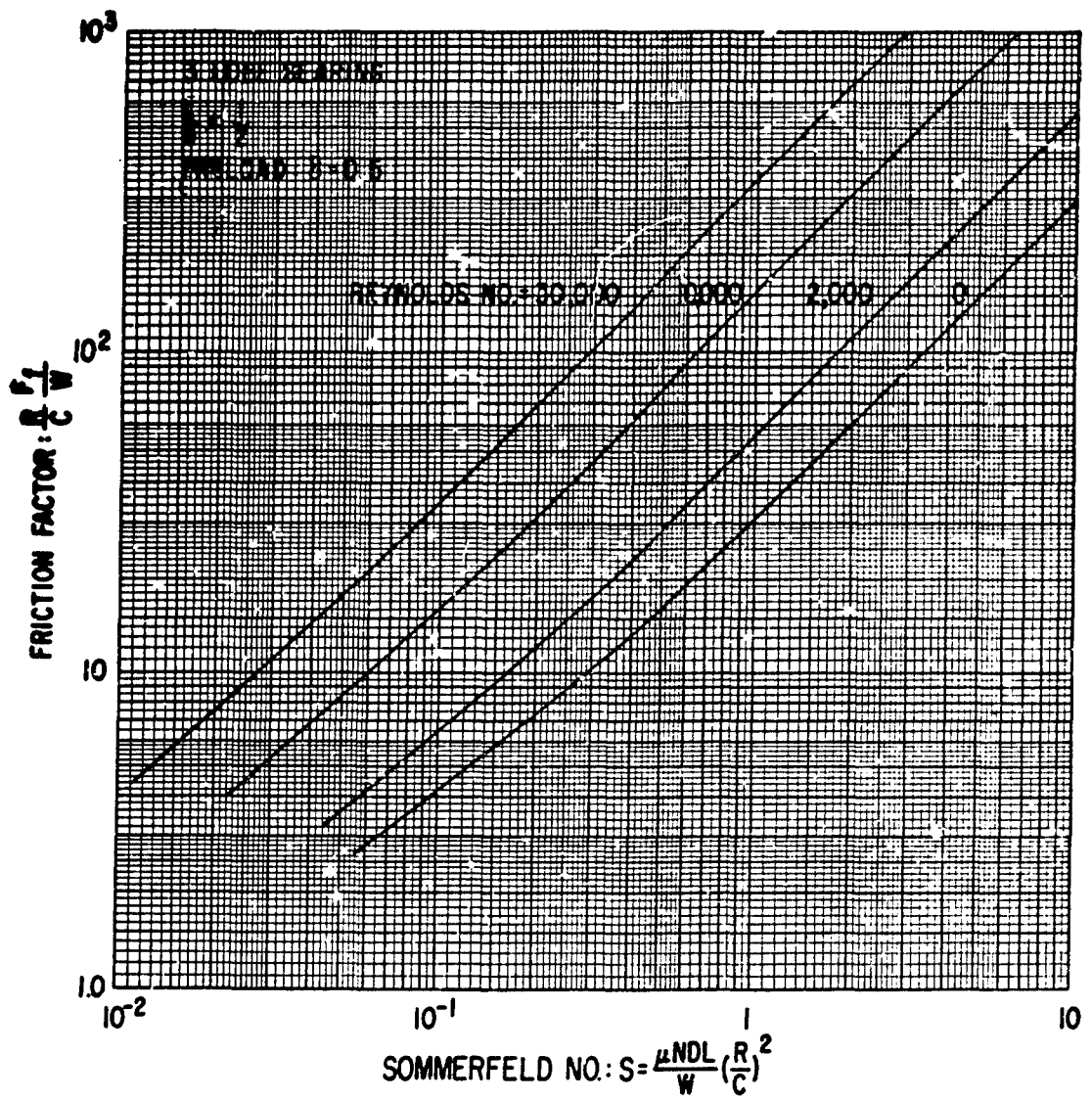


Figure 10. 3 Lobe Bearing, Preload = 0.5,  $\frac{L}{D} = \frac{1}{2}$ , Friction

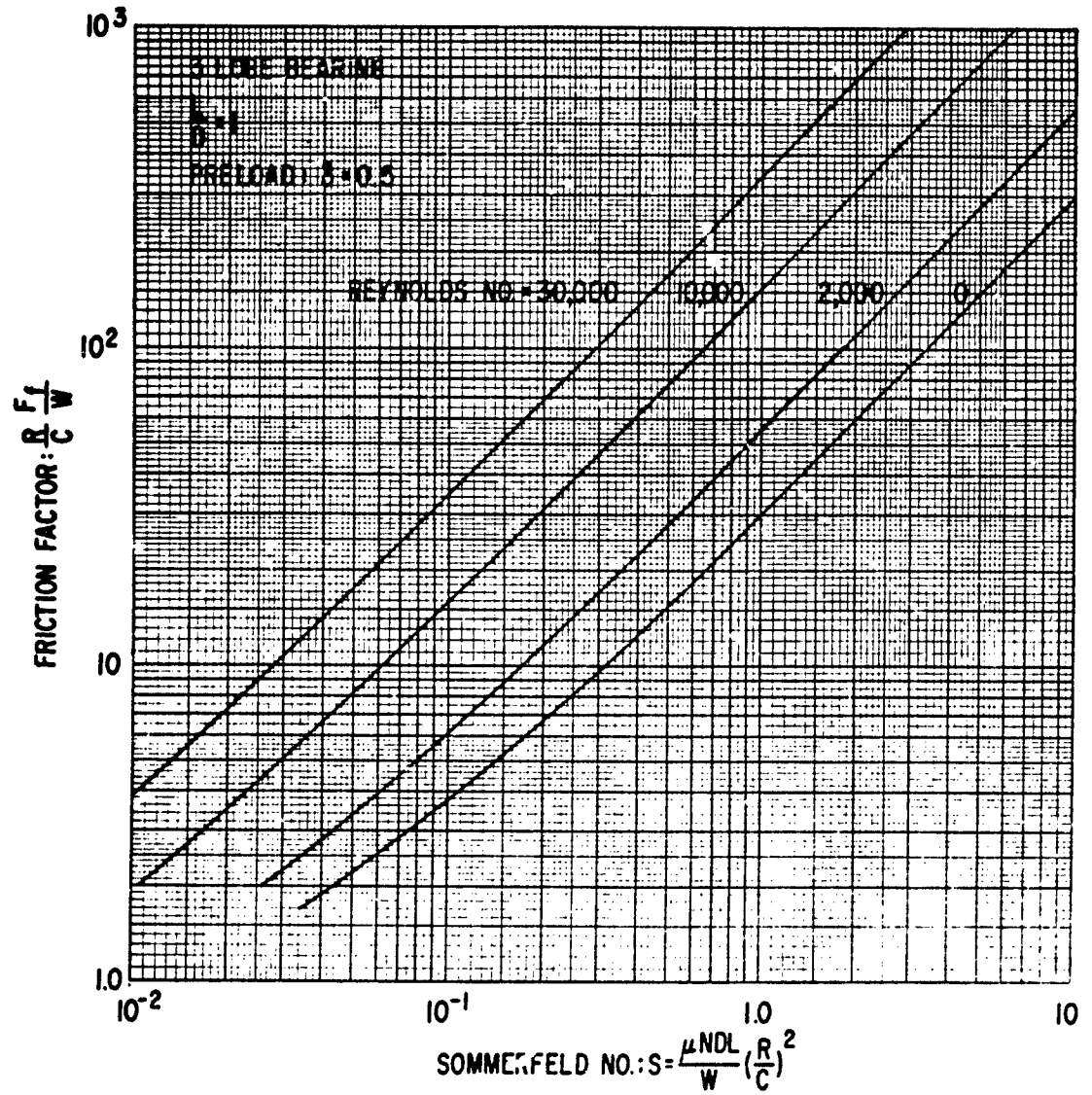


Figure 11. 3 Lobe Bearing, Preload = 0.5,  $\frac{L}{D} = 1$ , Friction

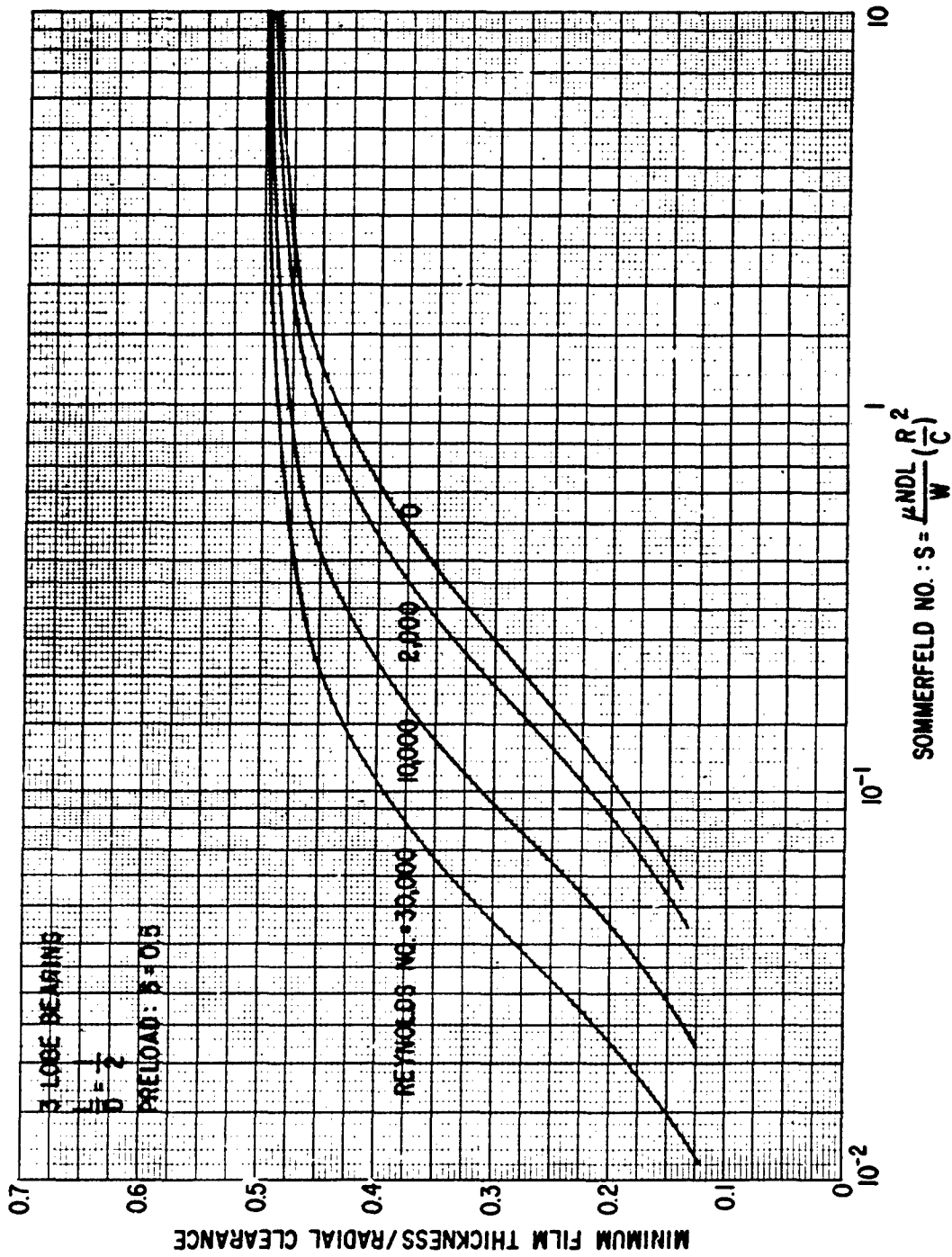


Figure 12. 3 Lobe Bearing, Preload = 0.5,  $\frac{L}{D} = \frac{1}{2}$ , Minimum Film Thickness

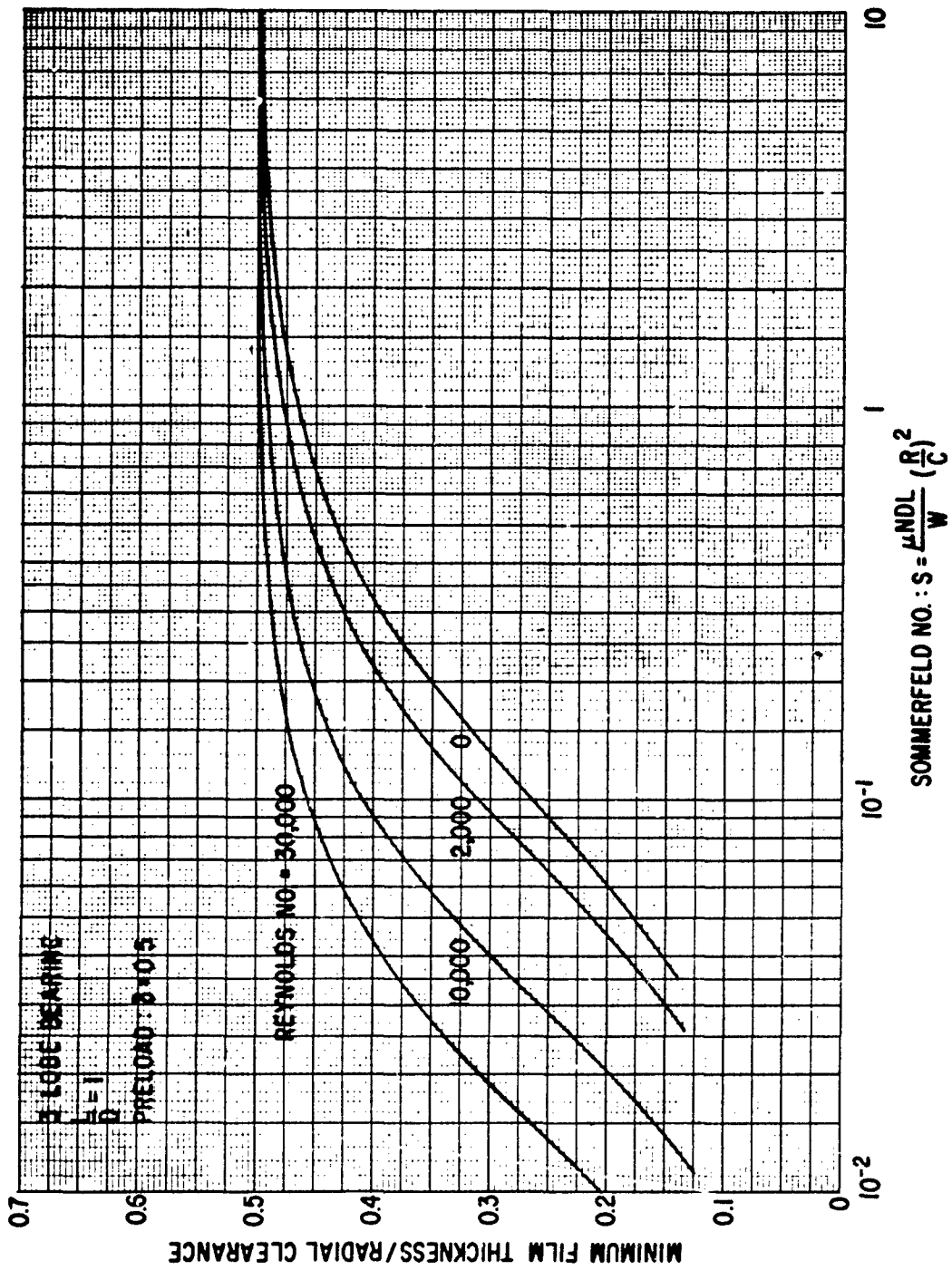


Figure 13. 3 Lobe Bearing, Preload = 0.5,  $L/D = 1$ , Minimum Film Thickness

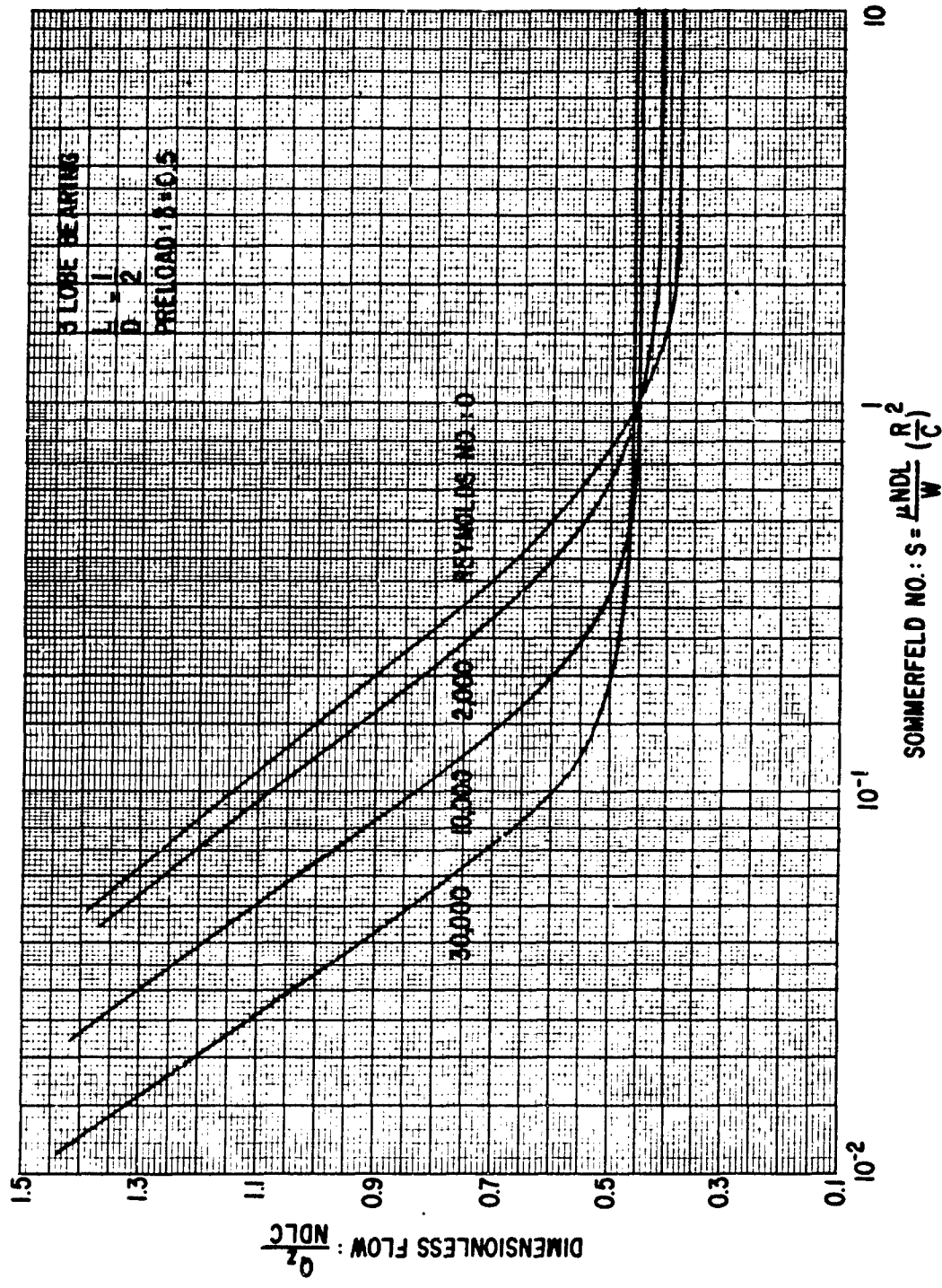


Figure 14. 3 Lobe Bearing, Preload = 0.5,  $\frac{L}{D} = \frac{1}{2}$ , Flow

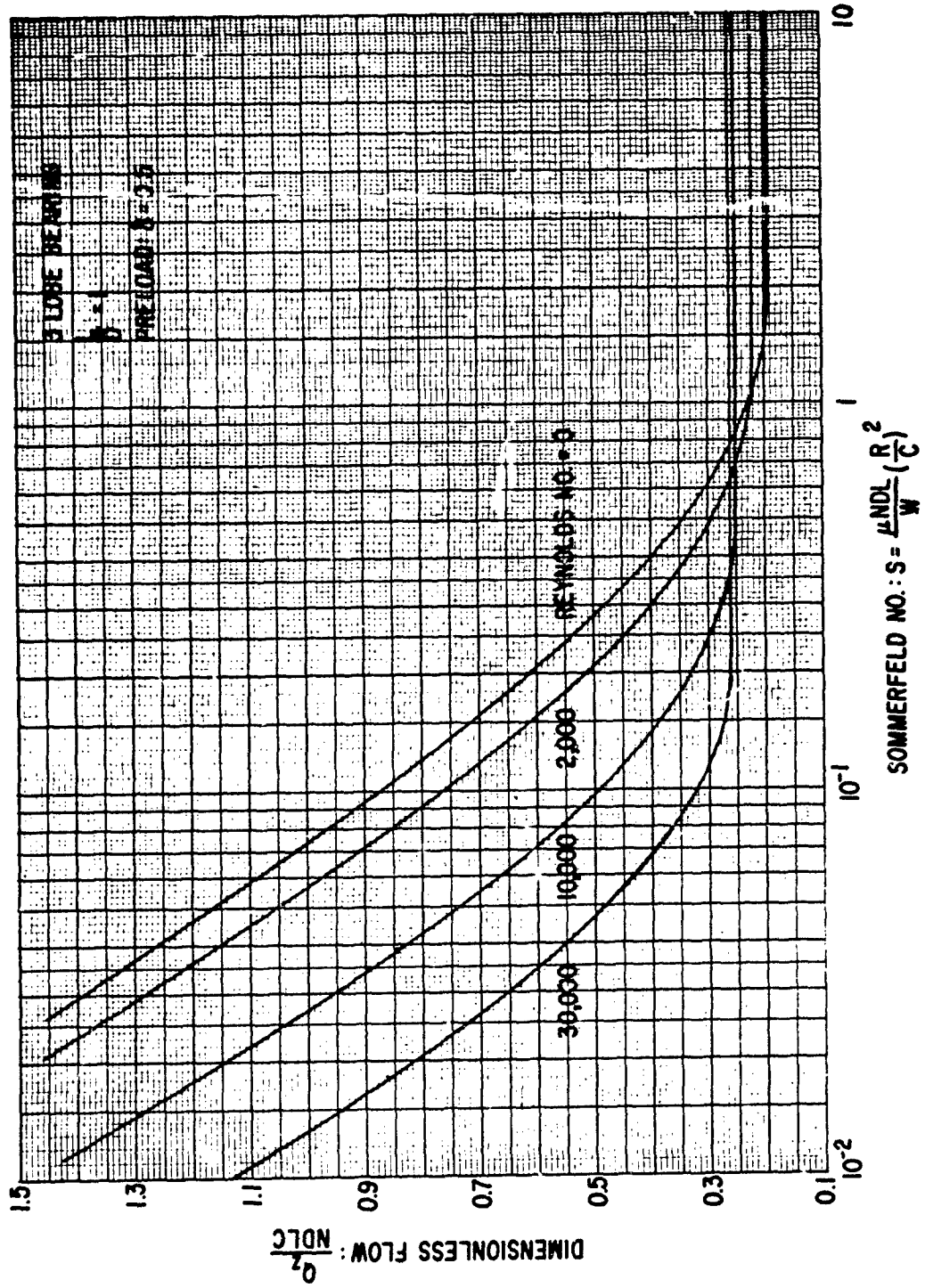


Figure 15. 3 Lobe Bearing, Preload = 0.5,  $\frac{L}{D} = 1$ , Flow

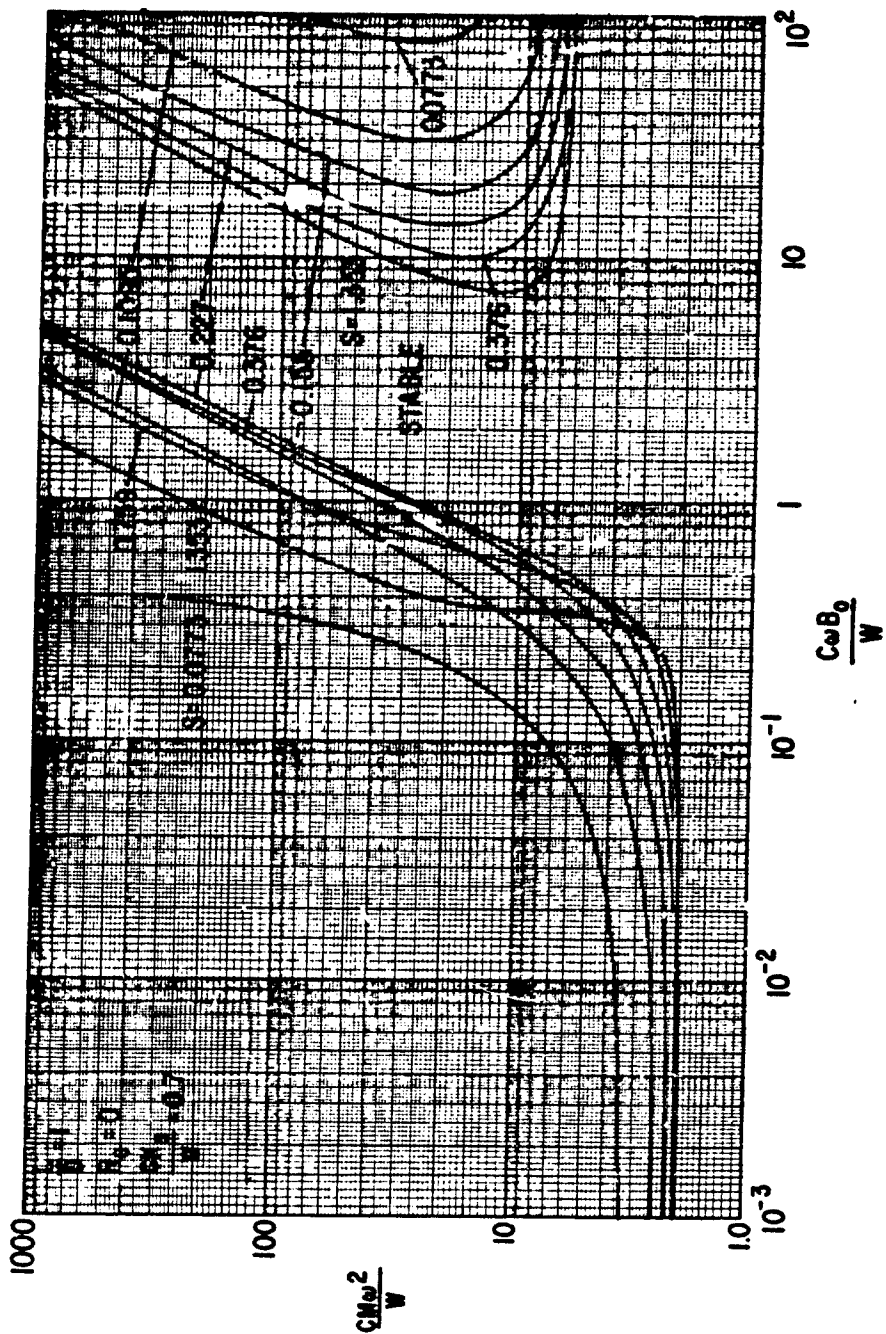


Figure 16. Hydrodynamic-Hydrostatic Bearing,  $R_e = 0$ ,  $\frac{CK}{W} = 0.7$ , Stability Map

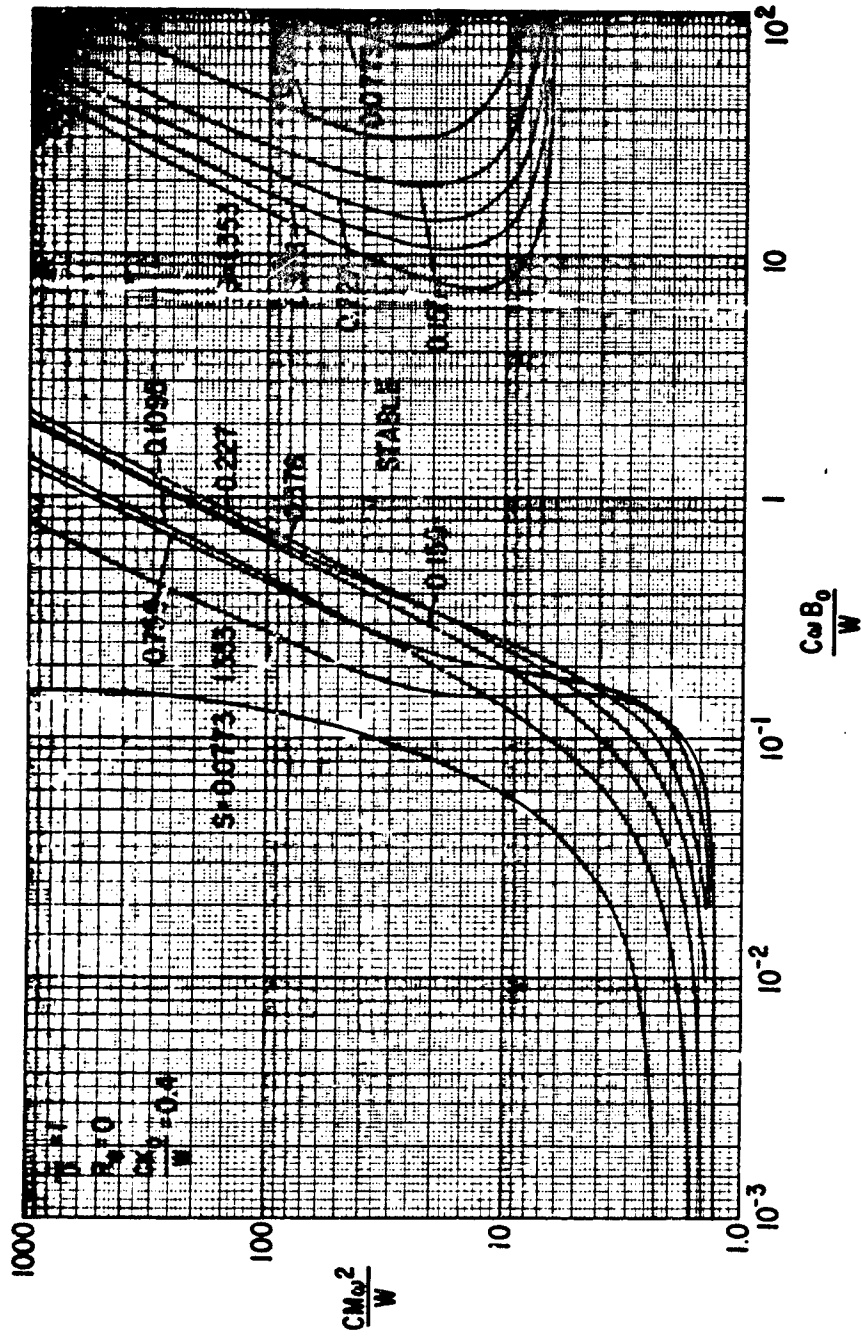


Figure 17. Hydrodynamic-Hydrostatic Ring Bearing,  $R_e = 0$ ,  $\frac{CK}{W} = 0.4$ , Stability Map

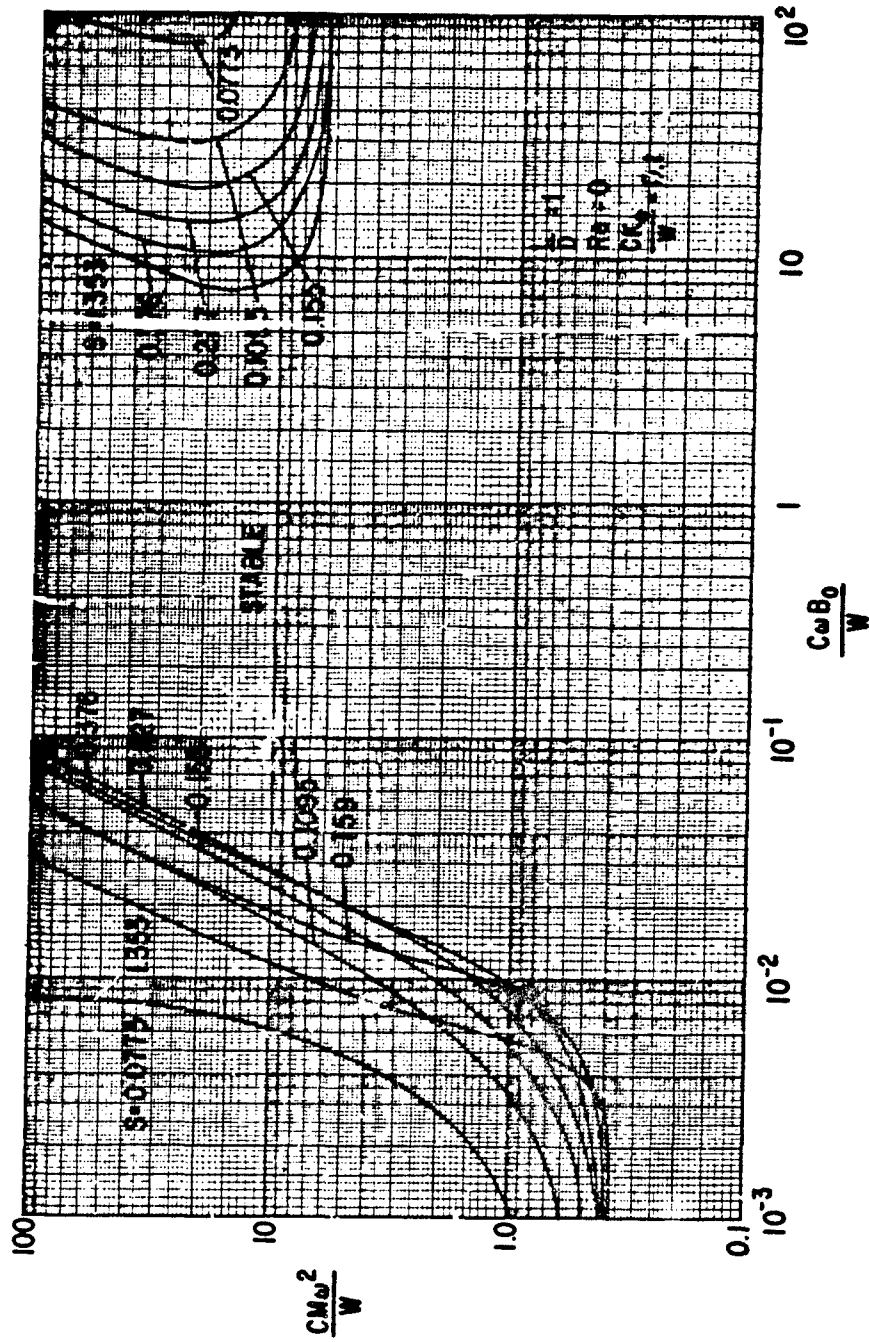


Figure 18. Hydrodynamic-Hydrostatic Ring Bearing,  $R_e = 0$ ,  $\frac{CK_0}{W} = 0.1$ , Stability Map

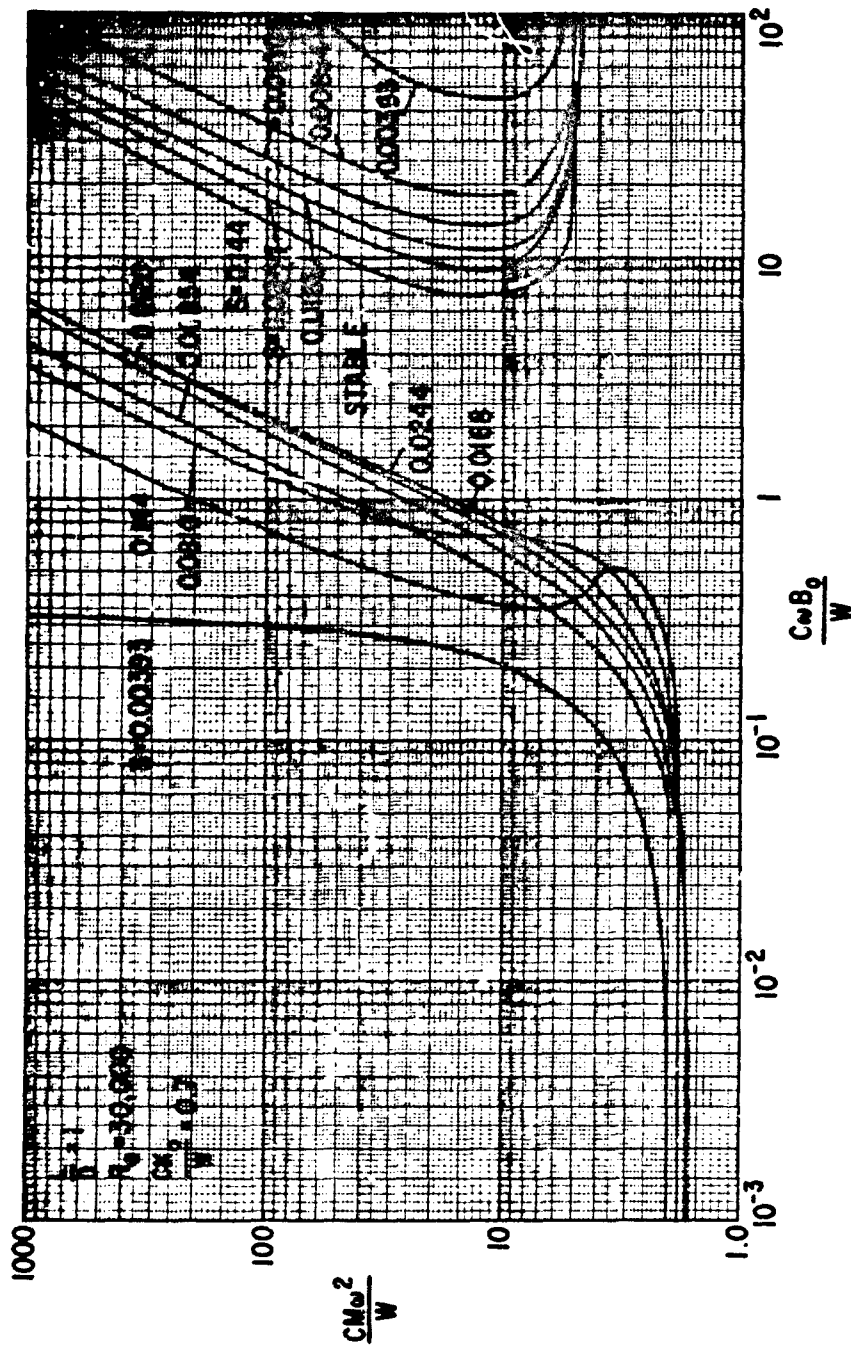


Figure 19. Hydrodynamic-Hydrostatic Ring Bearing,  $R_e = 30,000$ ,  $\frac{CK_2}{W} = 0.7$ , Stability Map

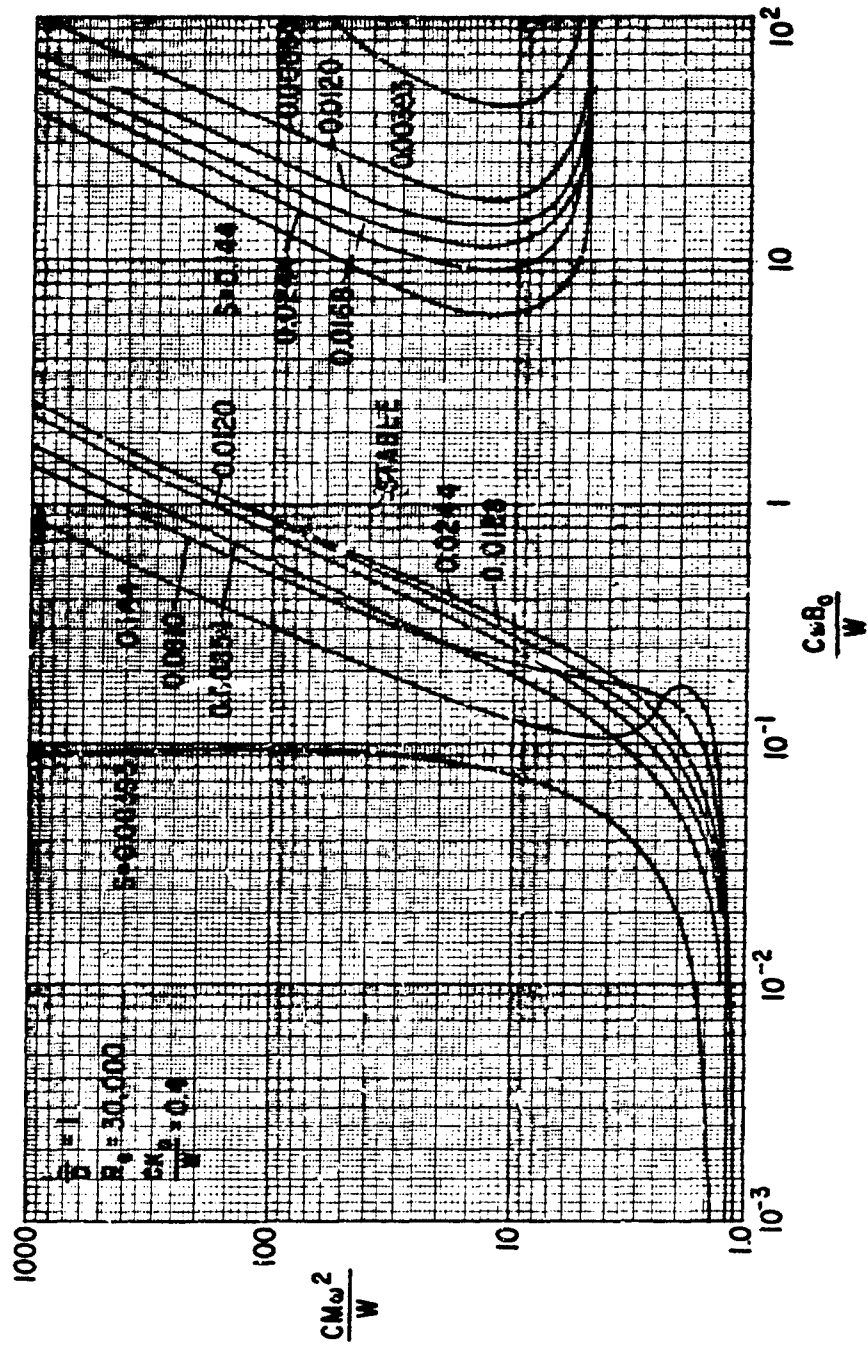


Figure 20. Hydrodynamic-Hydrostatic Ring Bearing,  $R_e = 30,000$ ,  $\frac{CK}{W} = 0.4$ , Stability Map

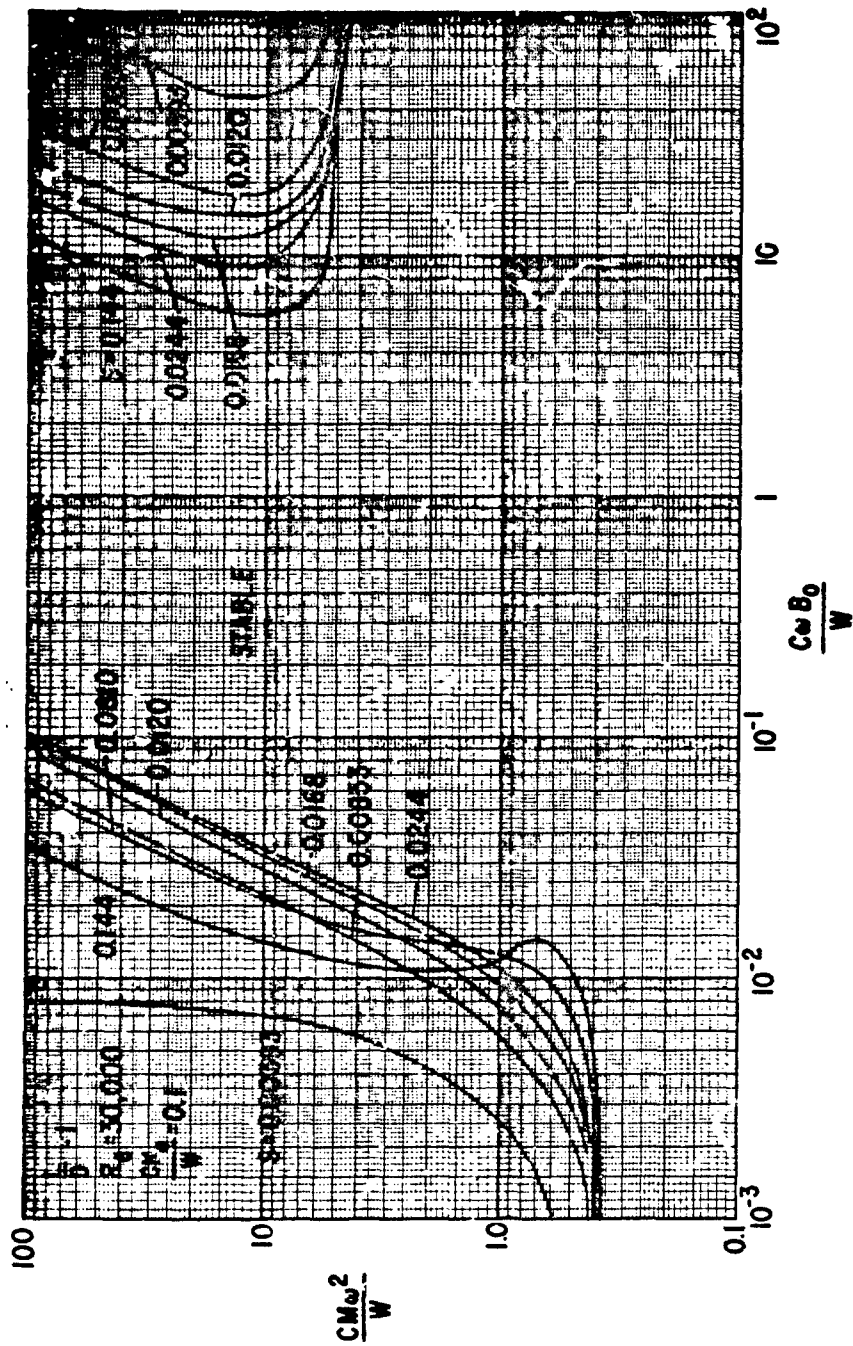


Figure 21. Hydrodynamic-Hydrostatic Ring Bearing,  $Re = 20,000$ ,  $\frac{Ck}{W} = 0.1$ , Stability Map

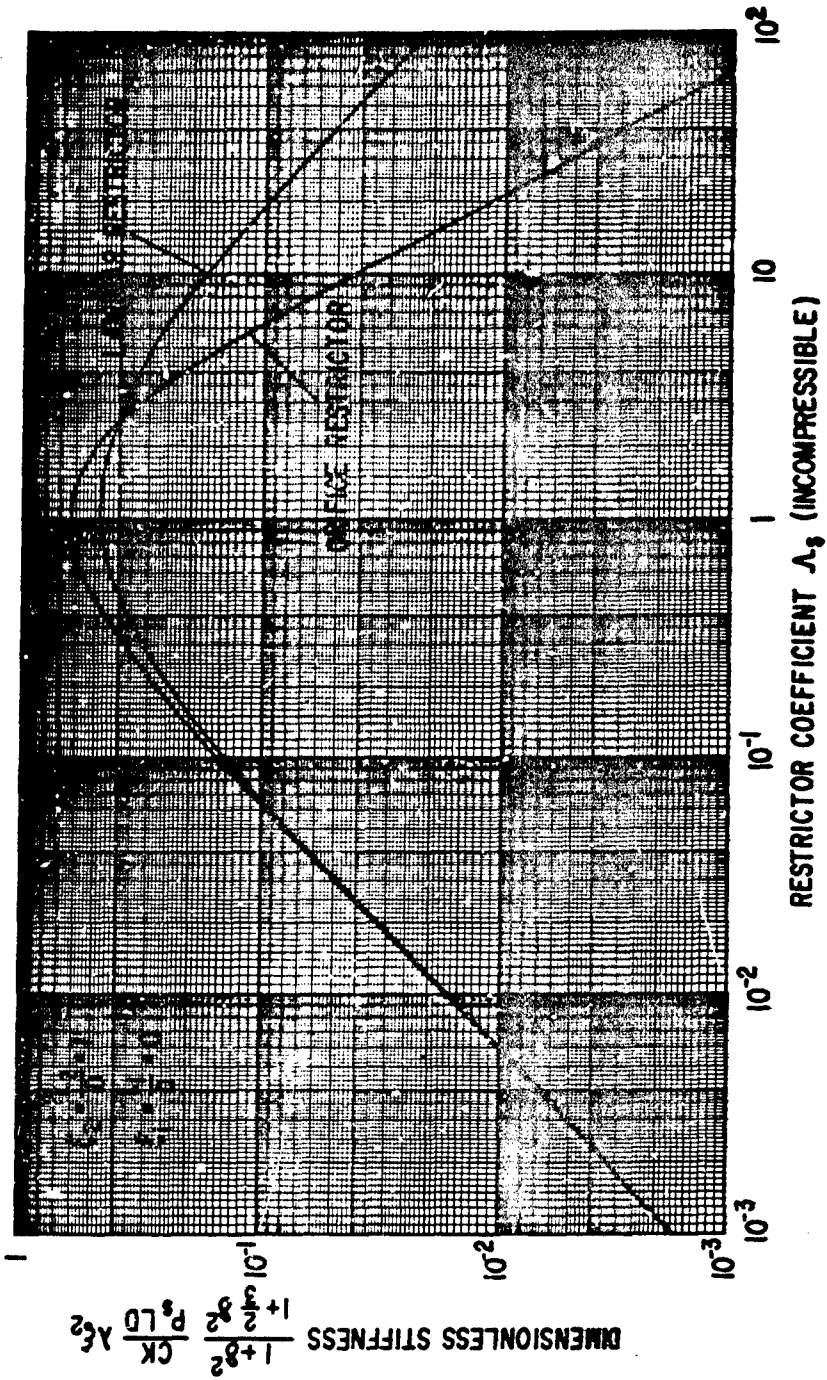


Figure 22. Hydrostatic Bearing, Incompressible, Single Plane Admission, Stiffness

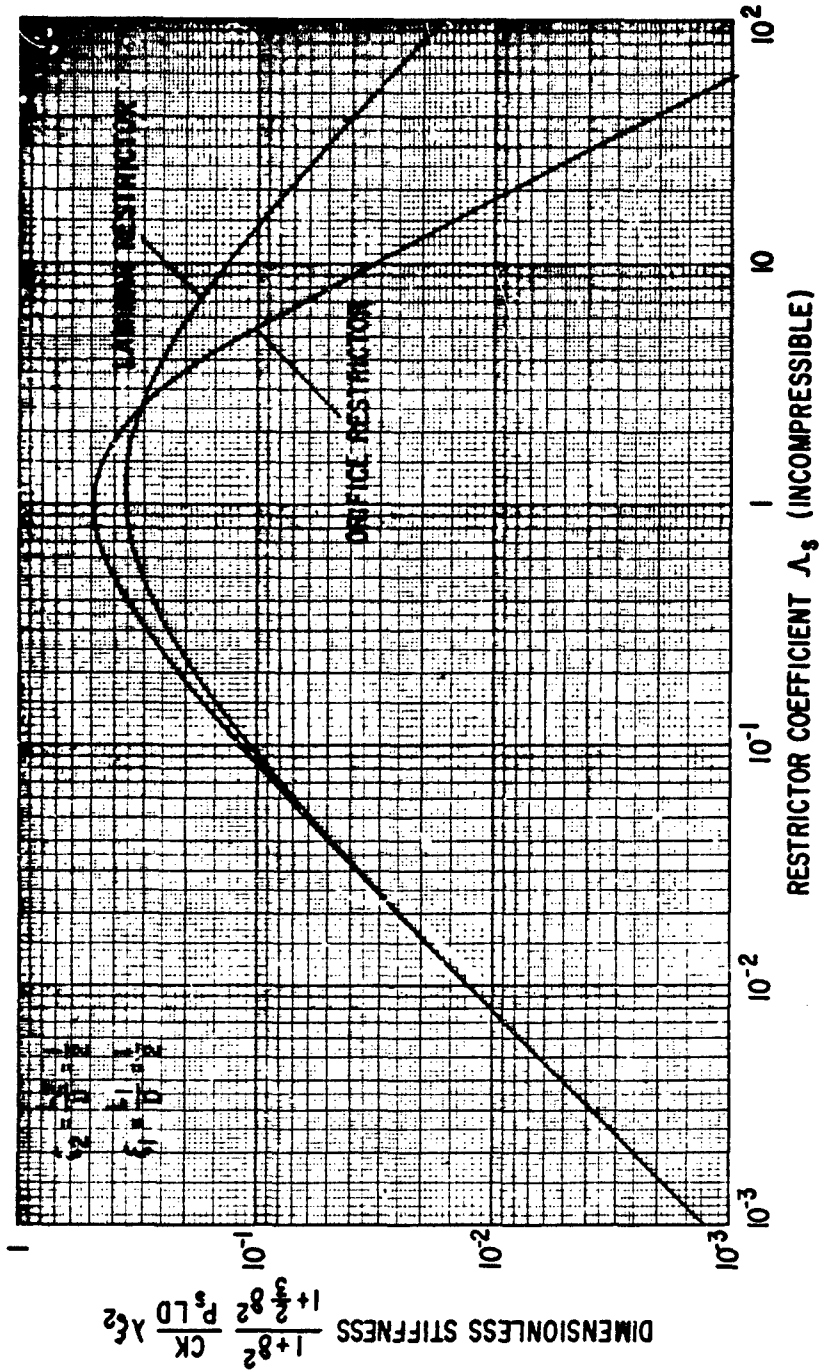


Figure 23. Hydrostatic Bearing, Incompressible, Double Plane Admission, Stiffness

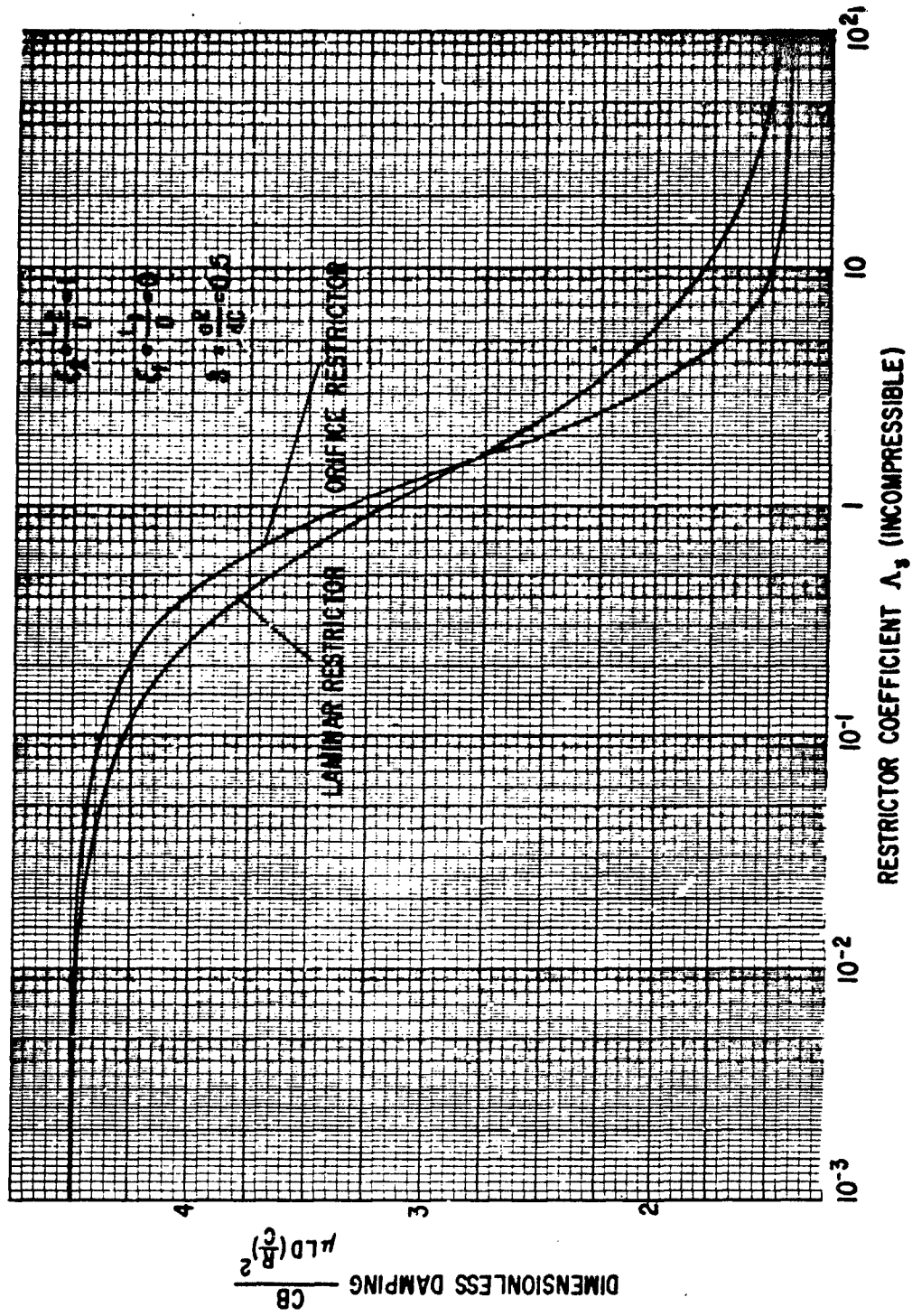


Figure 24. Hydrostatic Bearing, Incompressible, Single Plane Admission, Damping

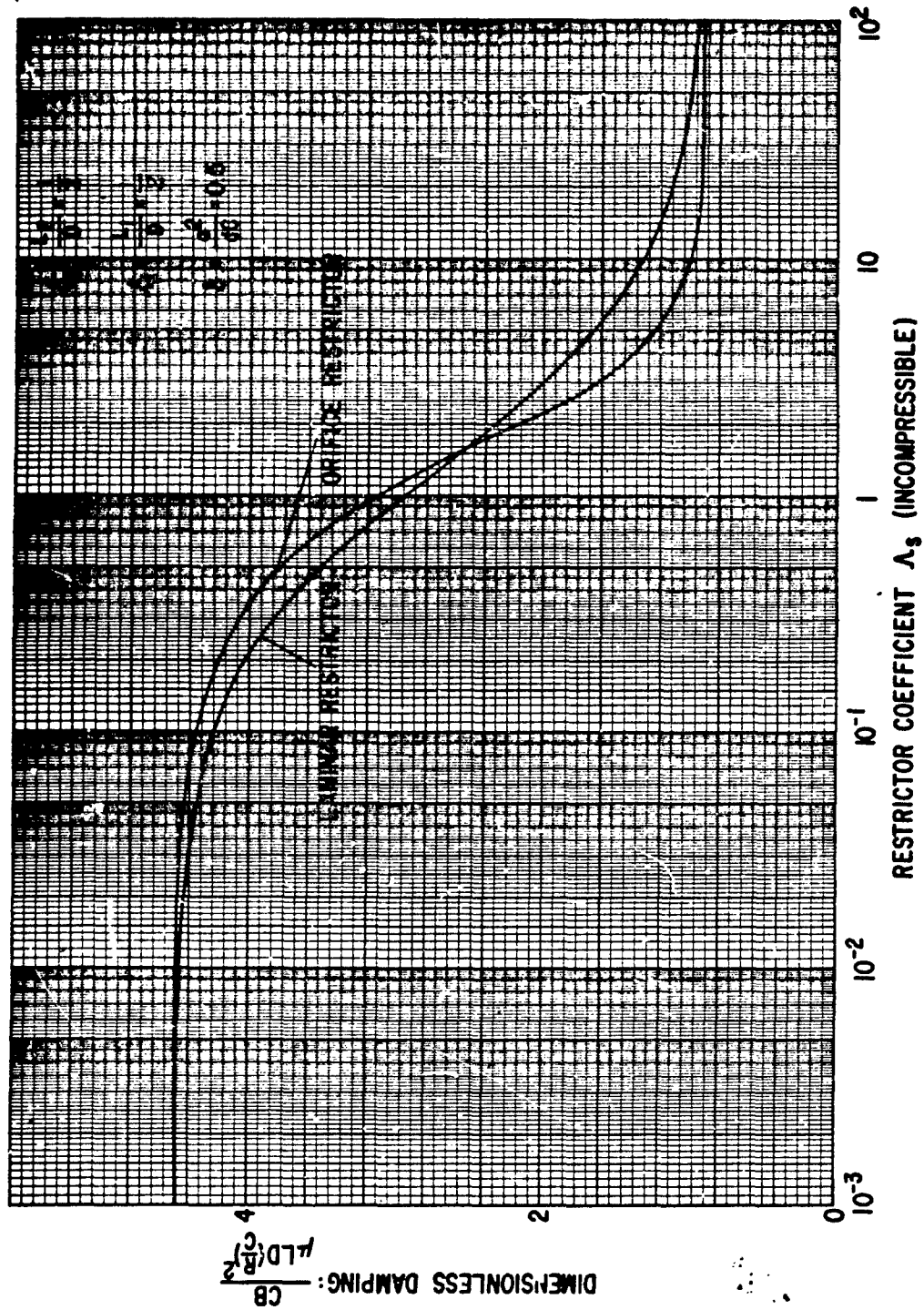


Figure 25. Hydrostatic Bearing, Incompressible, Double Plane Admission, Damping

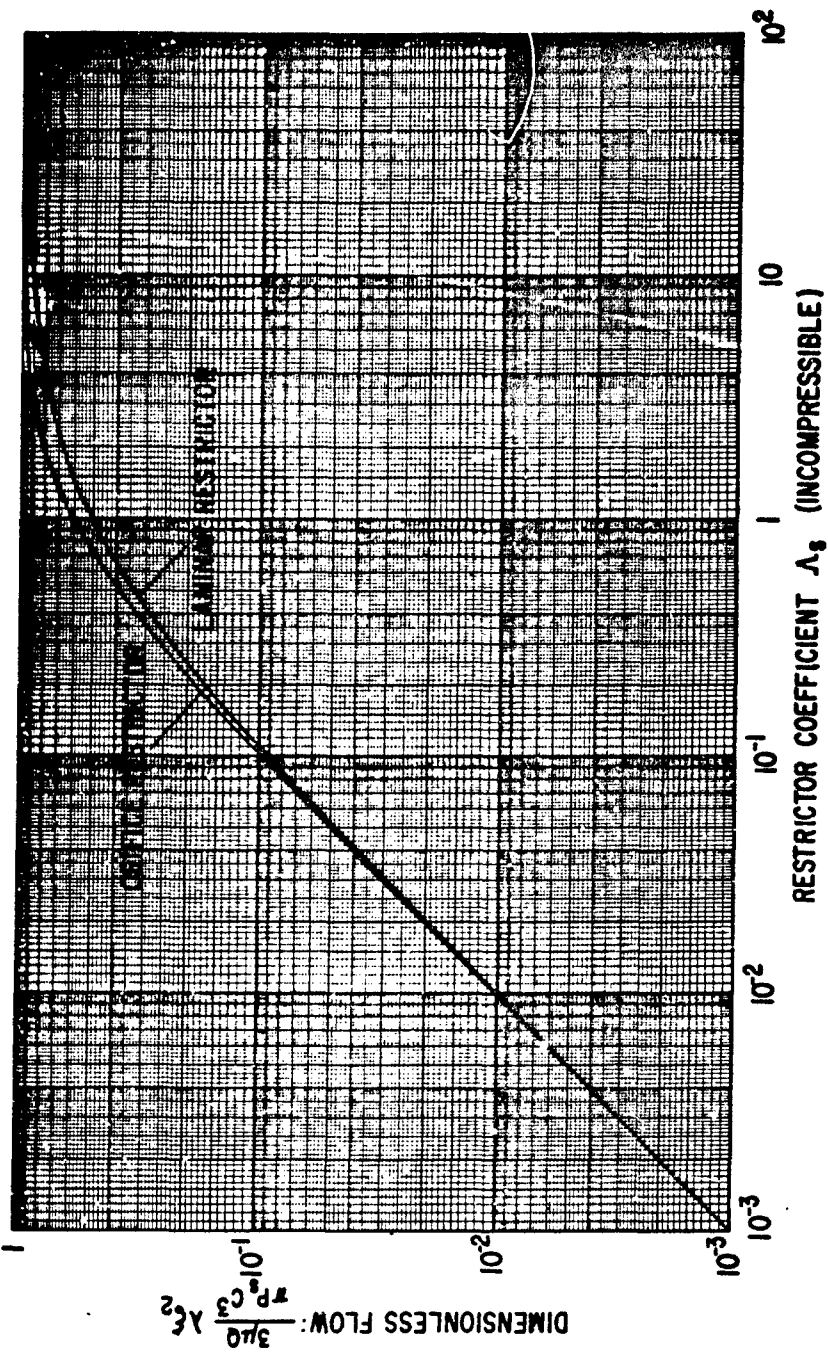


Figure 26. Hydrostatic Bearing, Incompressible, Flow

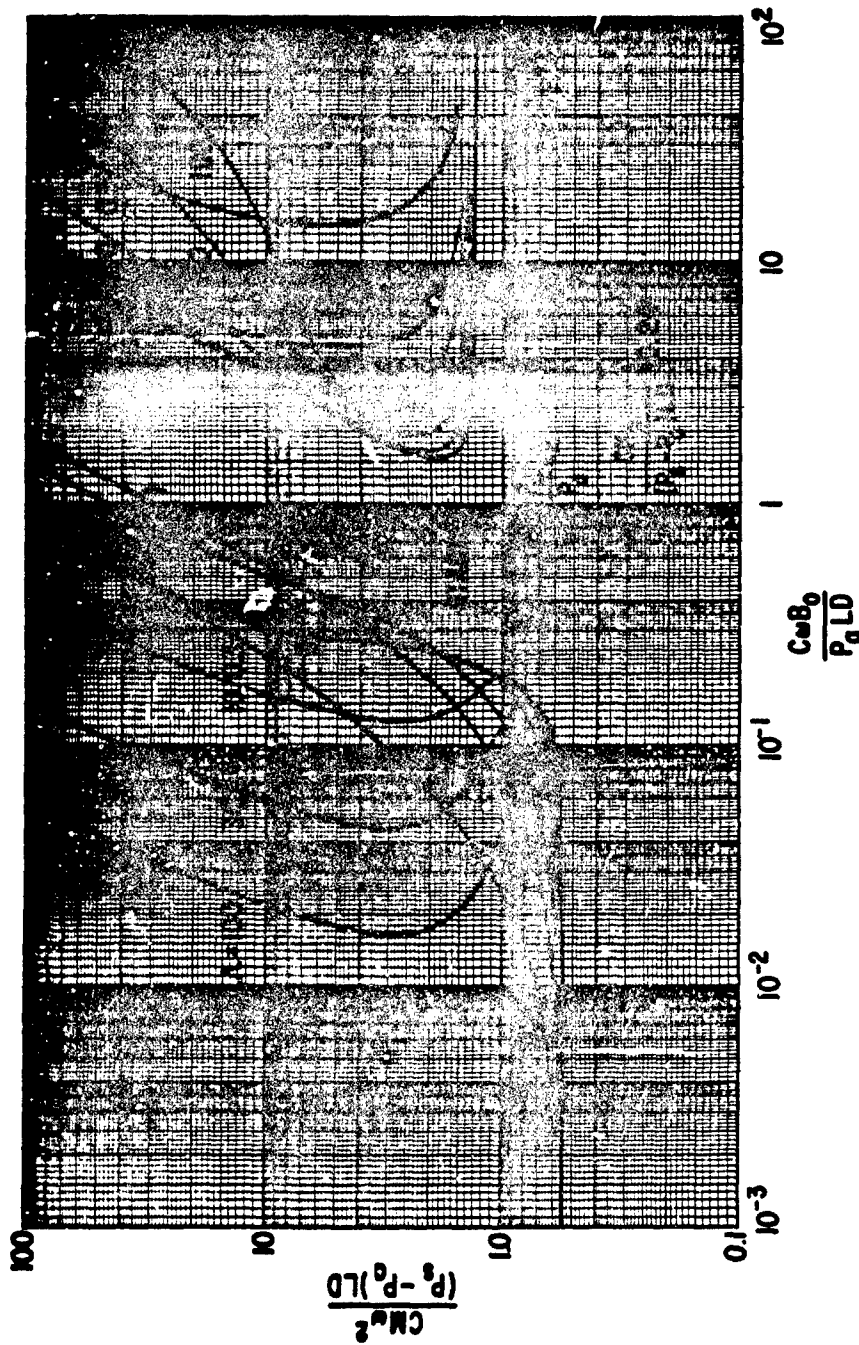


Figure 27. Hybrid-Hydrostatic Ring Bearing,  $\frac{P_s}{P_a} = 2$ ,  $\frac{CK_0}{(P_s - P_a)LD} = 0.24$ , Stability Map

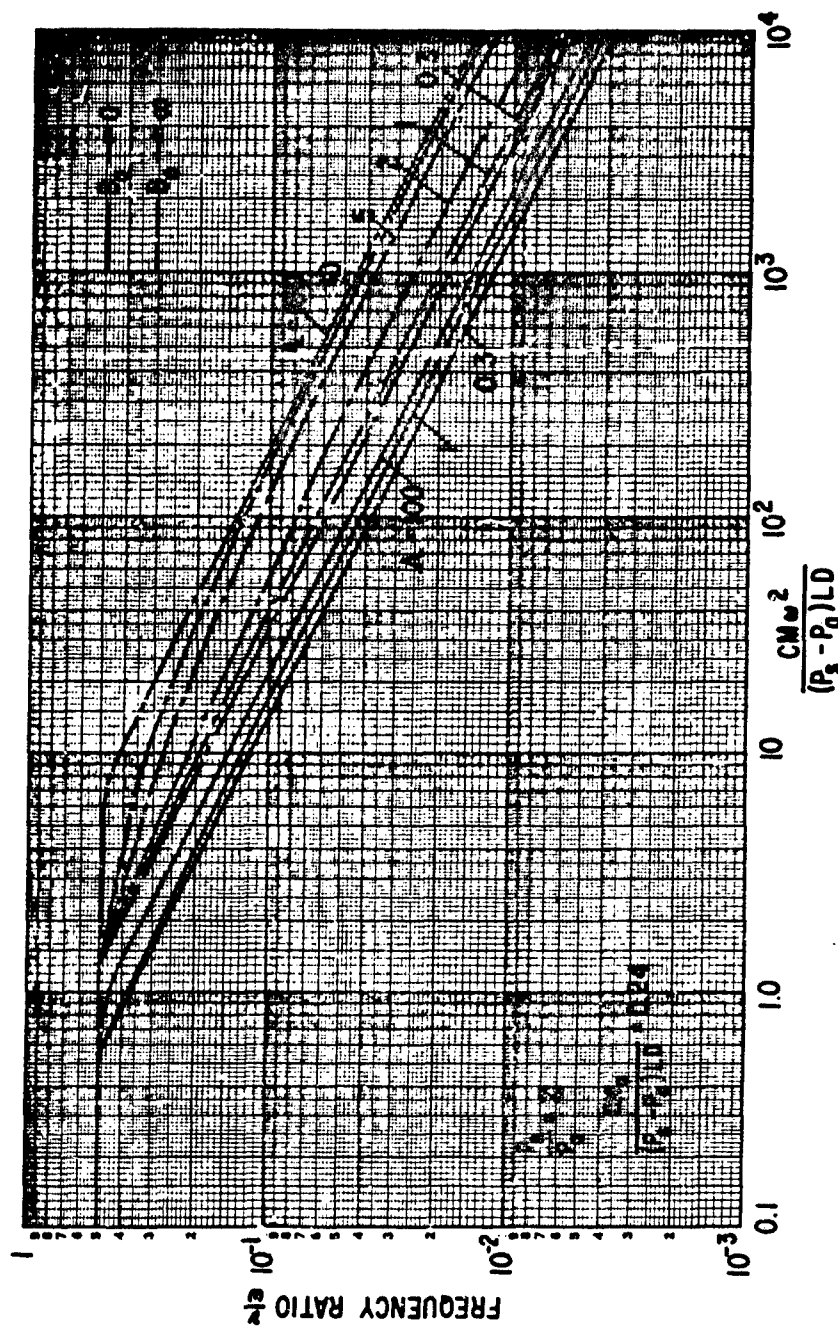


Figure 28. Hybrid-Hydrostatic Ring Bearing,  $\frac{P_s}{P_0} = 2$ ,  $\frac{CK_0}{(P_s - P_0)LD} = 0.24$ , Instability Frequency

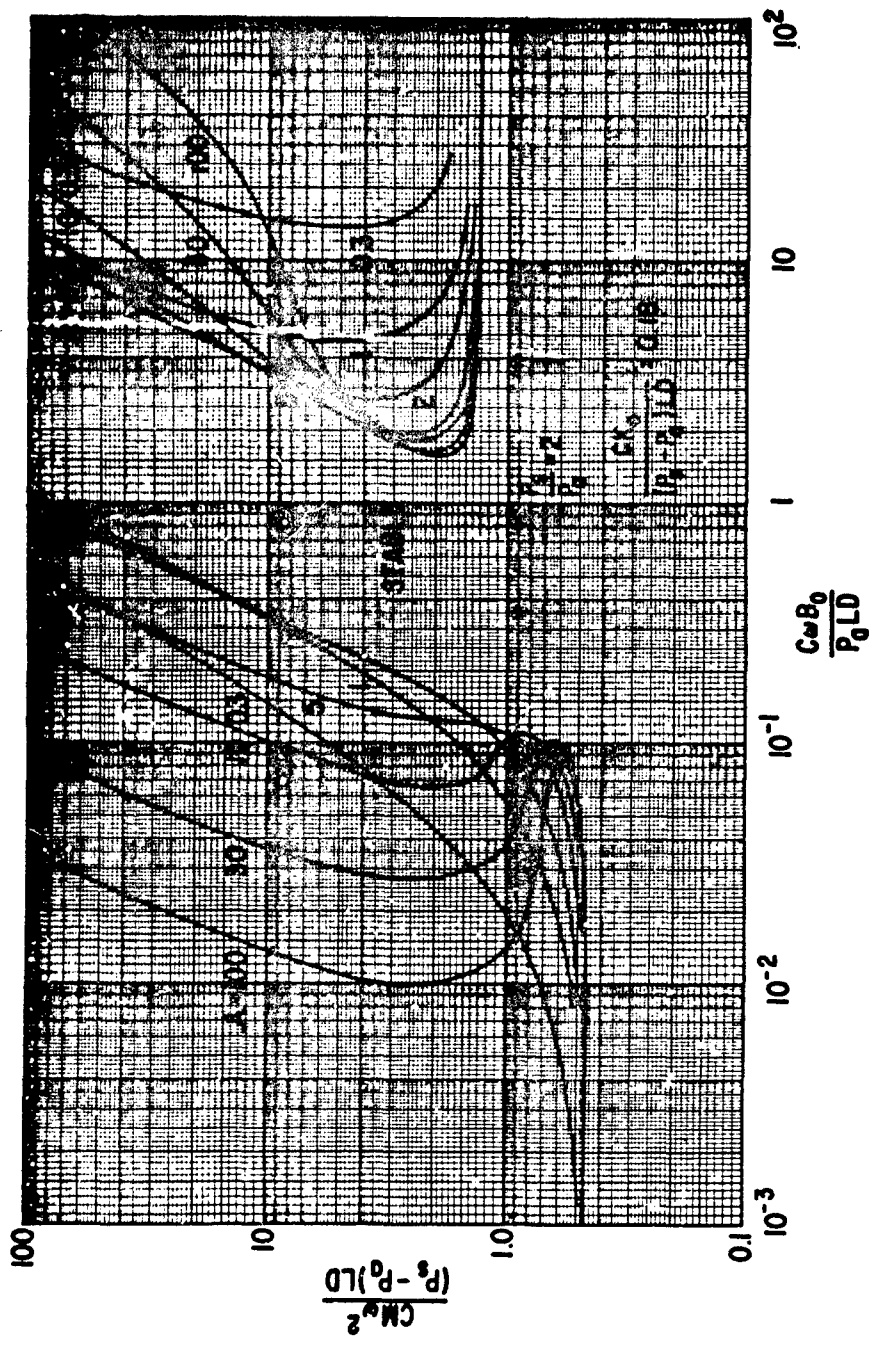


Figure 29. Hybrid-Hydrostatic Ring Bearing,  $\frac{P_s}{P_a} = 2$ ,  $\frac{CK_0}{(P_s - P_a)LD} = 0.18$ , Stability Map

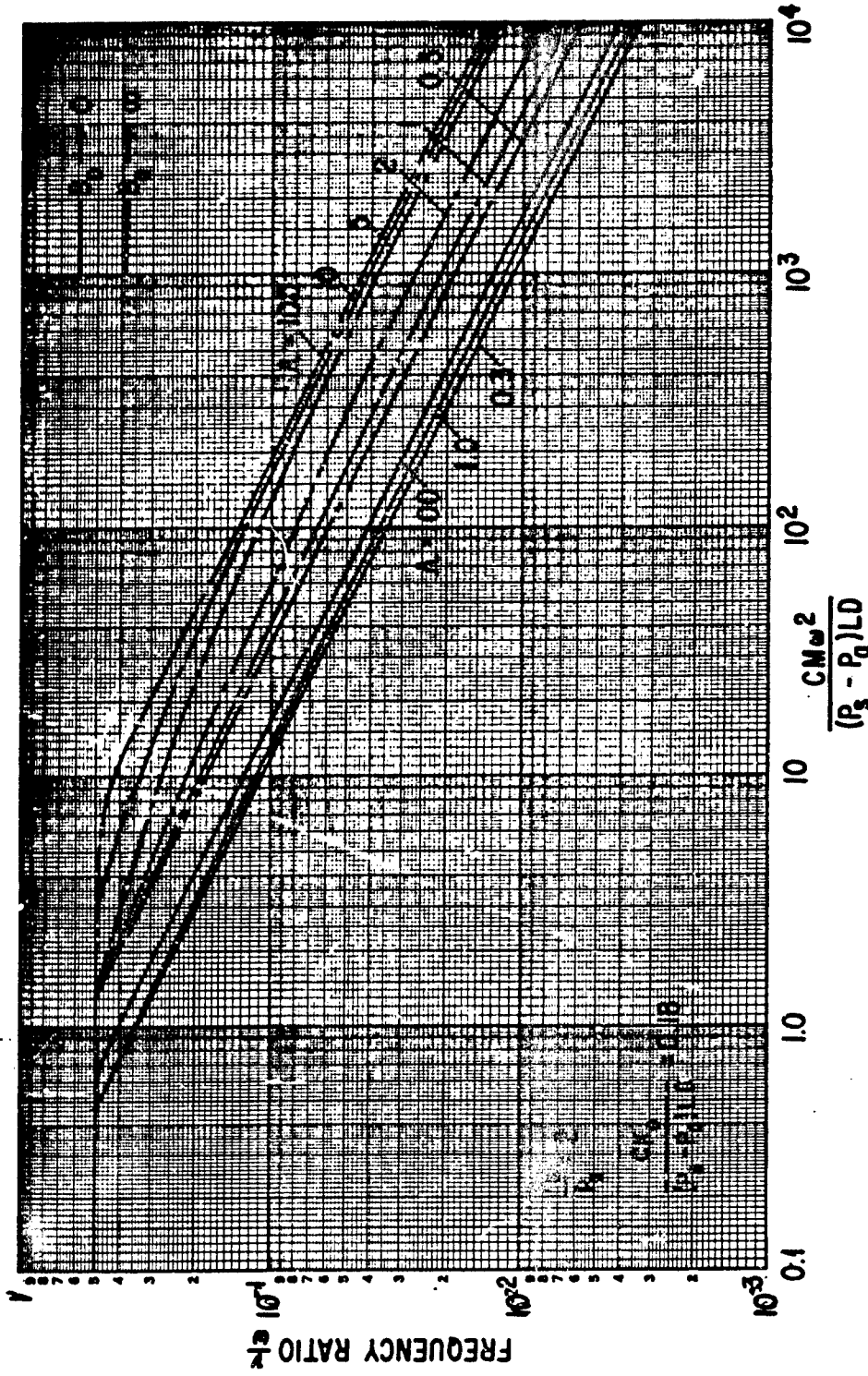


Figure 30. Hybrid-Hydrostatic Ring Bearing,  $\frac{P_s}{P_a} = 2$ ,  $\frac{CK}{(P_s - P_a)LD} = 0.18$ , Instability Frequency

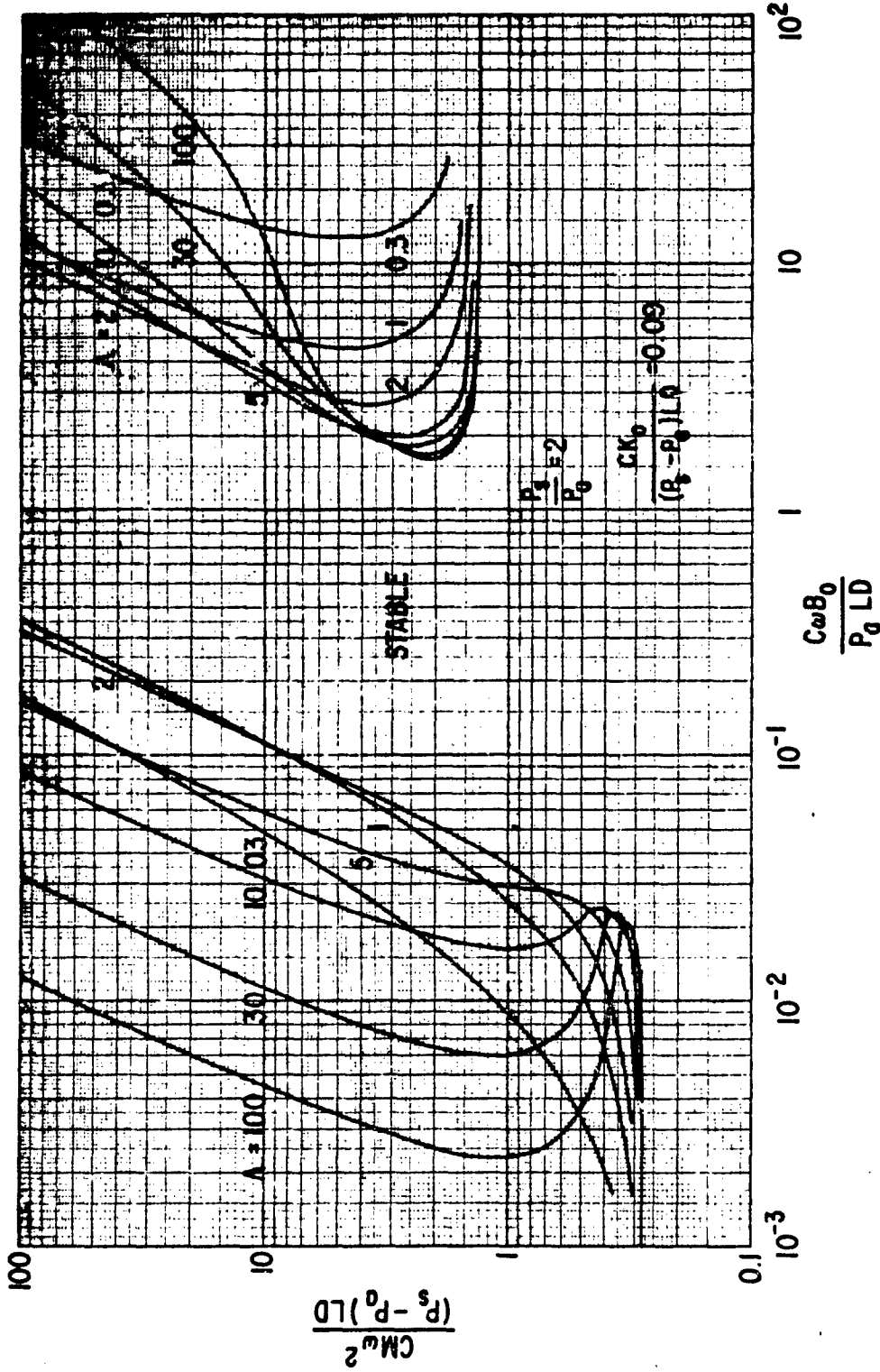


Figure 31. Hybrid-Hydrostatic Ring Bearing,  $\frac{P_s}{P_a} = 2$ ,  $\frac{CK_0}{(P_s - P_a)LD} = 0.09$ , Stability Map

HTI-5C18

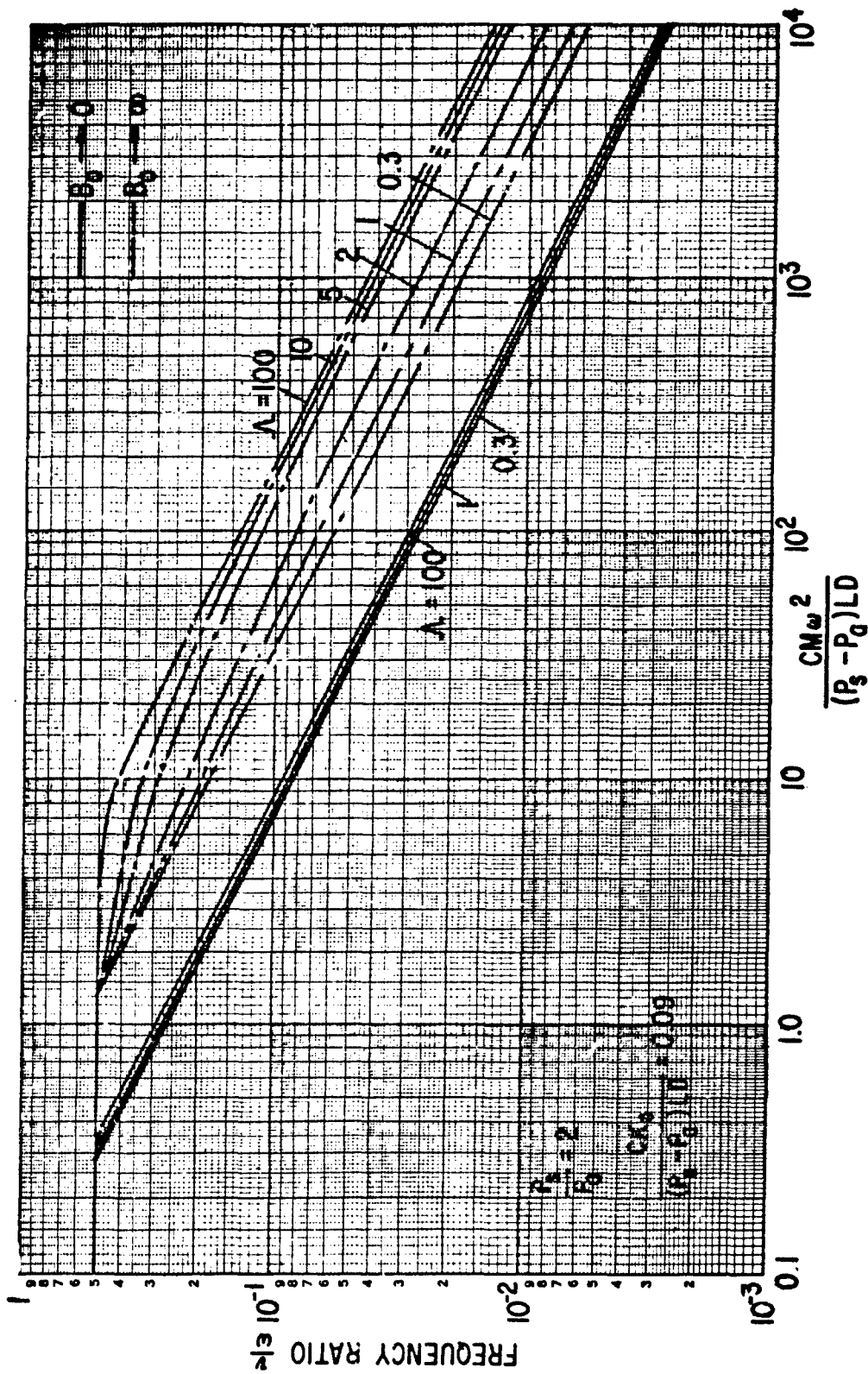


Figure 32. Hybrid-Hydrostatic Ring Bearing,  $\frac{P_s}{P_a} = 2$ ,  $\frac{Ck_0}{(P_s - P_a)LD} = 0.09$ , Instability Frequency

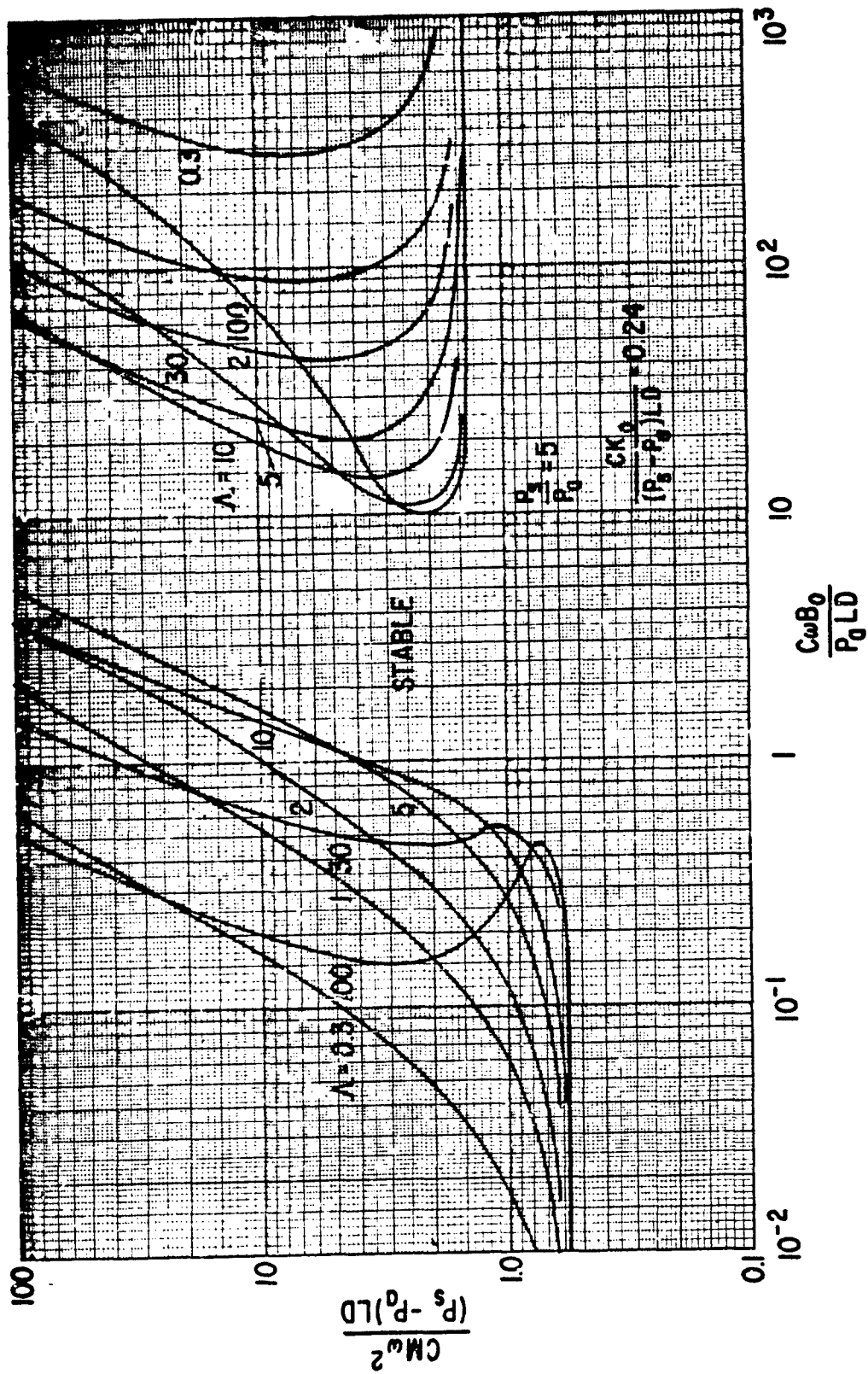


Figure 33. Hybrid-Hydrostatic Ring Bearing,  $\frac{P_s}{P_0} = 5$ ,  $\frac{CK_0}{(P_s - P_0)LD} = 0.24$ , Stability Map

MIT-5040

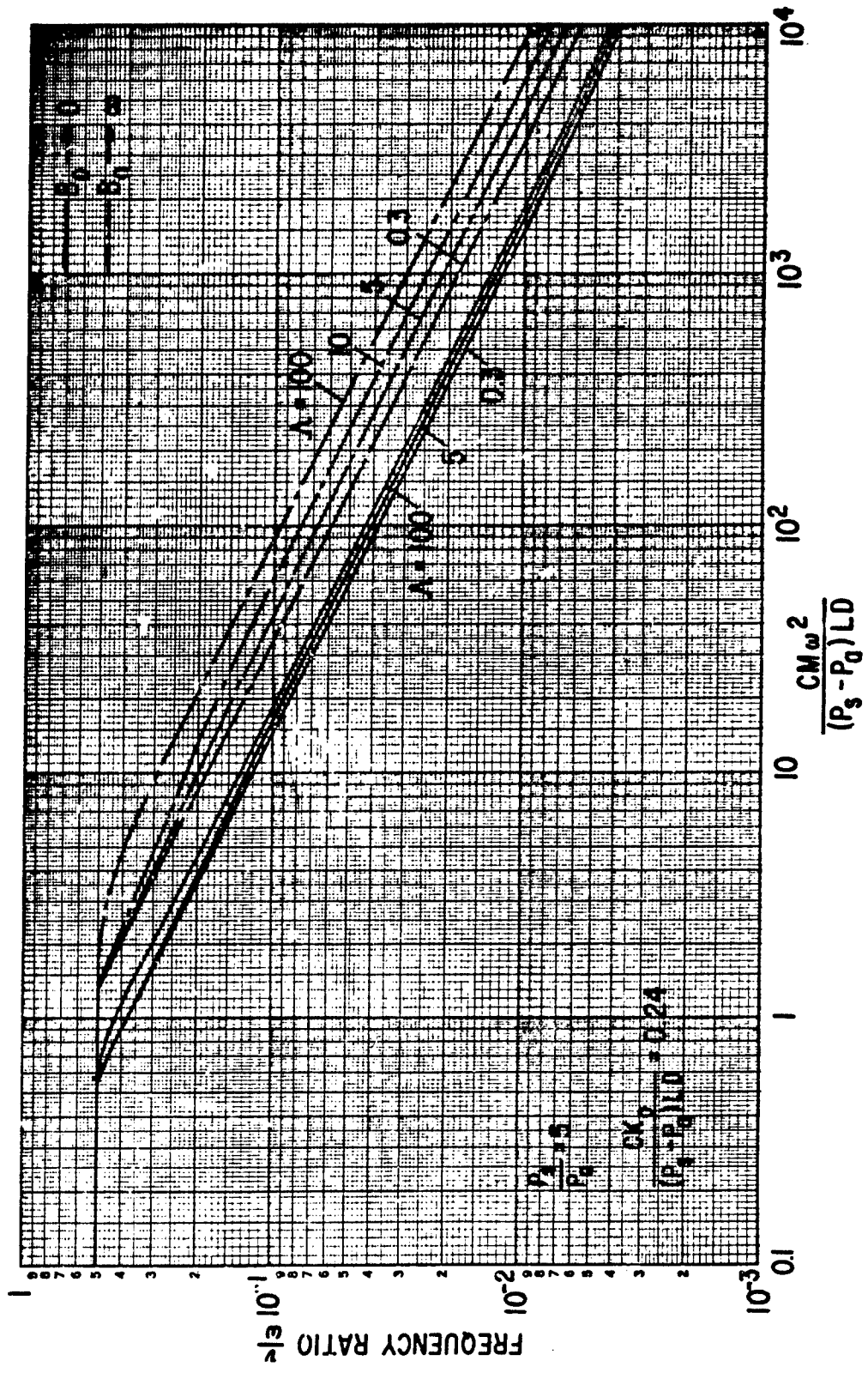


Figure 34. Hybrid-Hydrostatic Ring Bearing,  $\frac{P_s - P_0}{P_0} = 5$ ,  $\frac{CK_0}{(P_s - P_0) LD} = 0.24$ , Instability Frequency

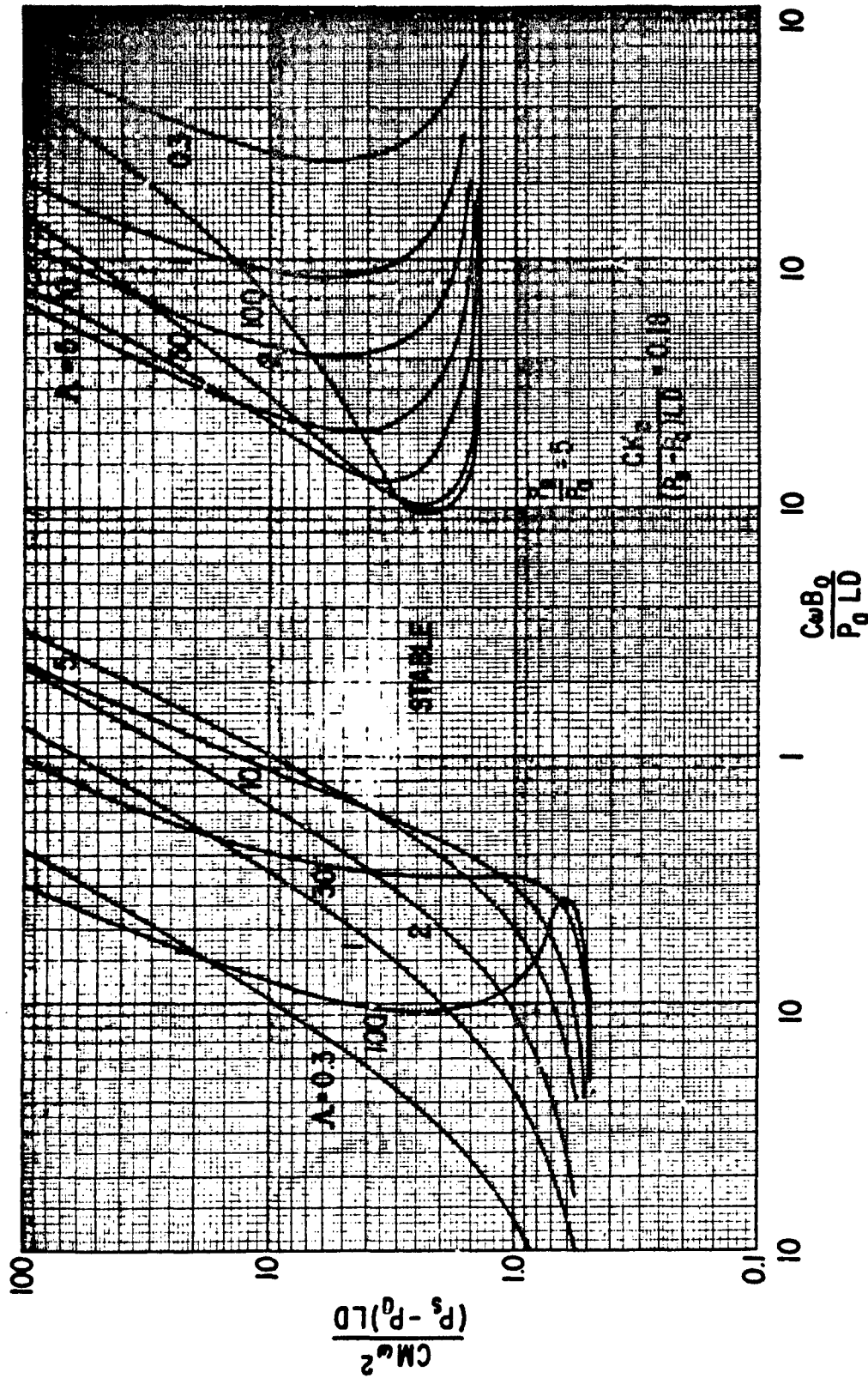


Figure 35. Hybrid-Hydrostatic Ring Bearing,  $\frac{P_s}{P_a} = 5$ ,  $\frac{CK_0}{(P_s - P_a)LD} = 0.18$ , Stability Map

NET-5042

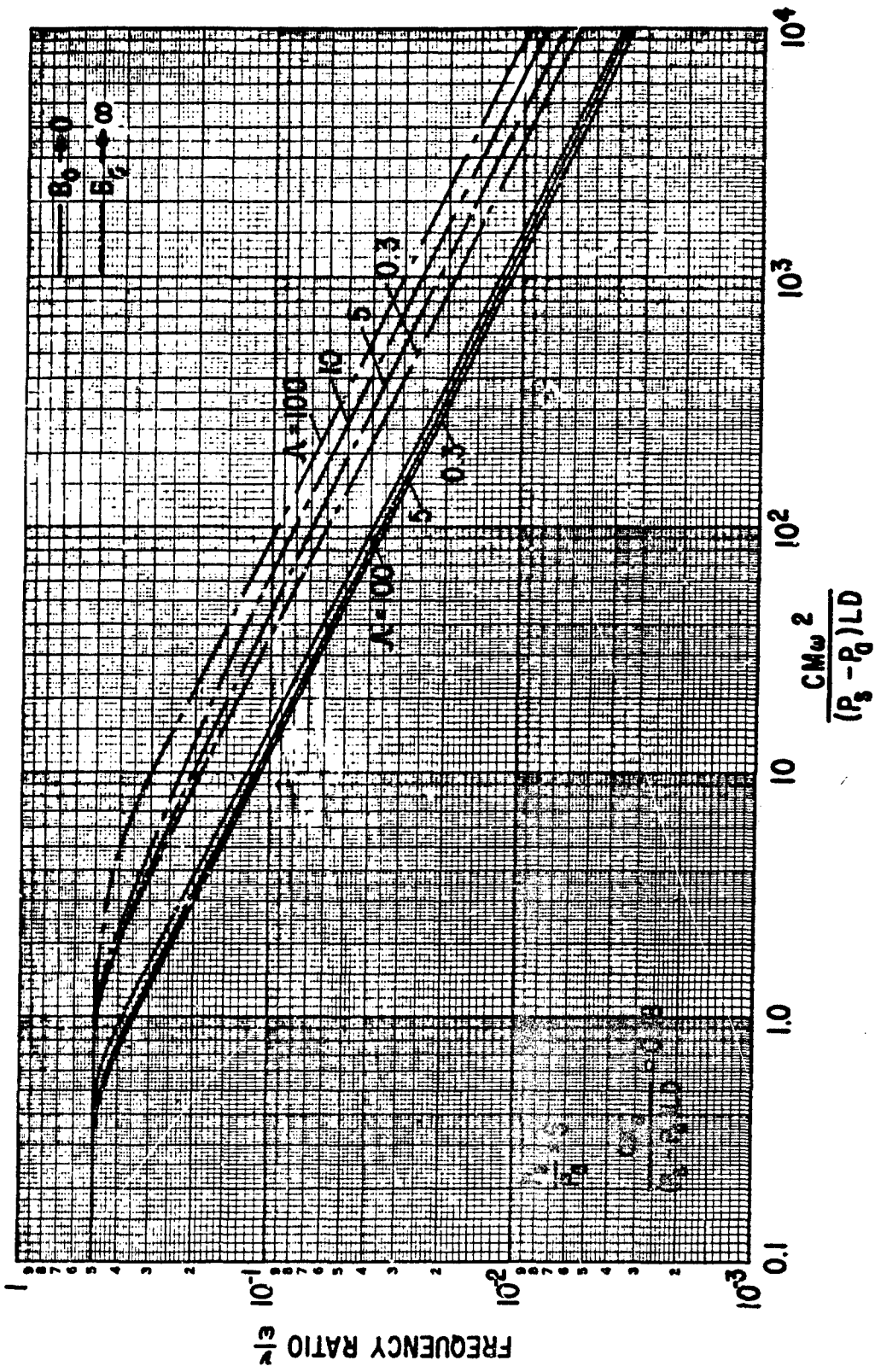


Figure 36. Hybrid-Hydrostatic Ring Bearing,  $\frac{P_s}{P_a} = 5$ ,  $\frac{CK_0}{(P_s - P_a)LD} = 0.18$ , Instability Frequency

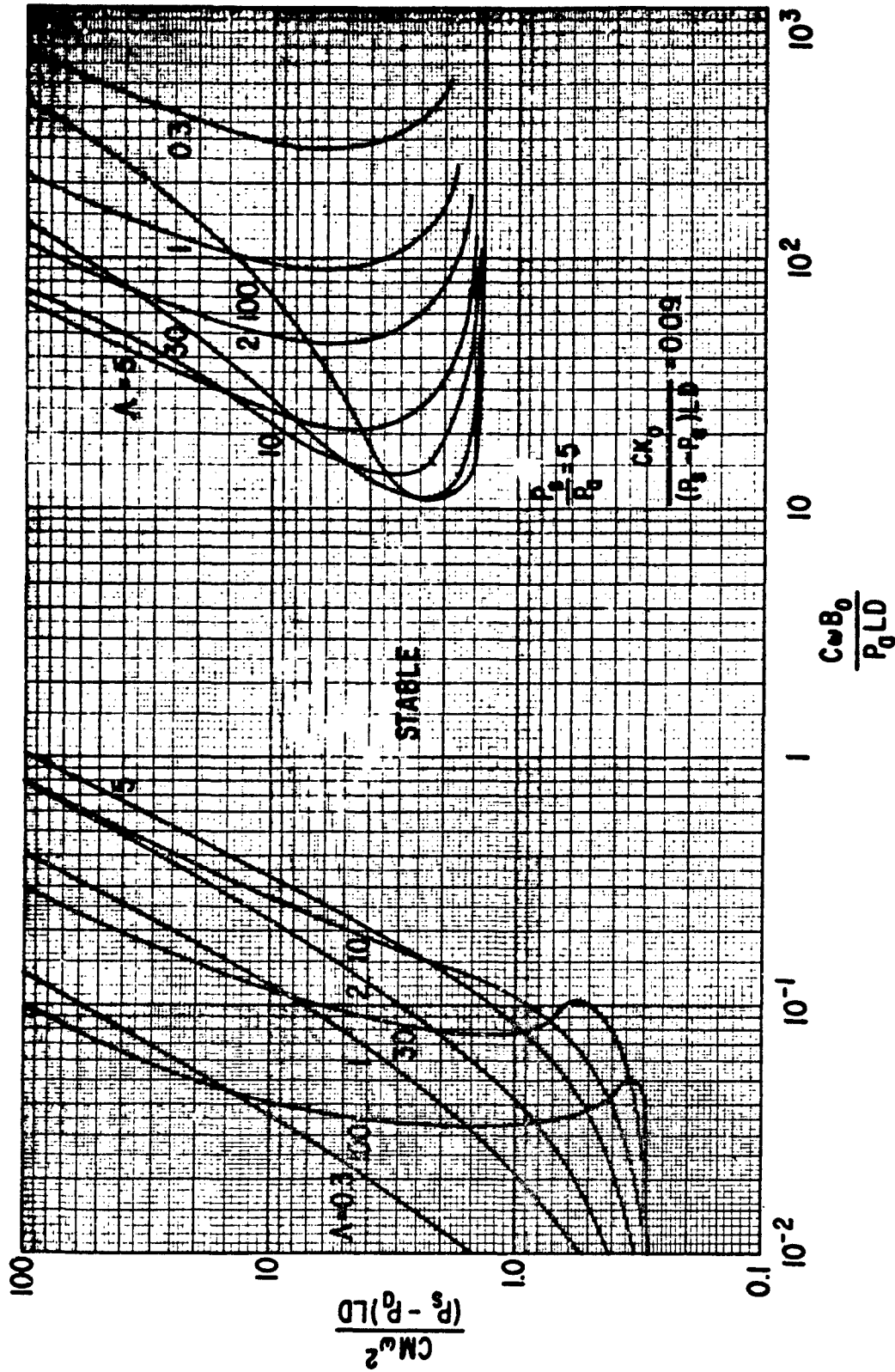


Figure 37. Hybrid-Hydrostatic Ring Bearing,  $\frac{P_s}{P_0} = 5$ ,  $\frac{CK_0}{(P_s - P_0)LD} = 0.09$ , Stability Map

MIT-3044

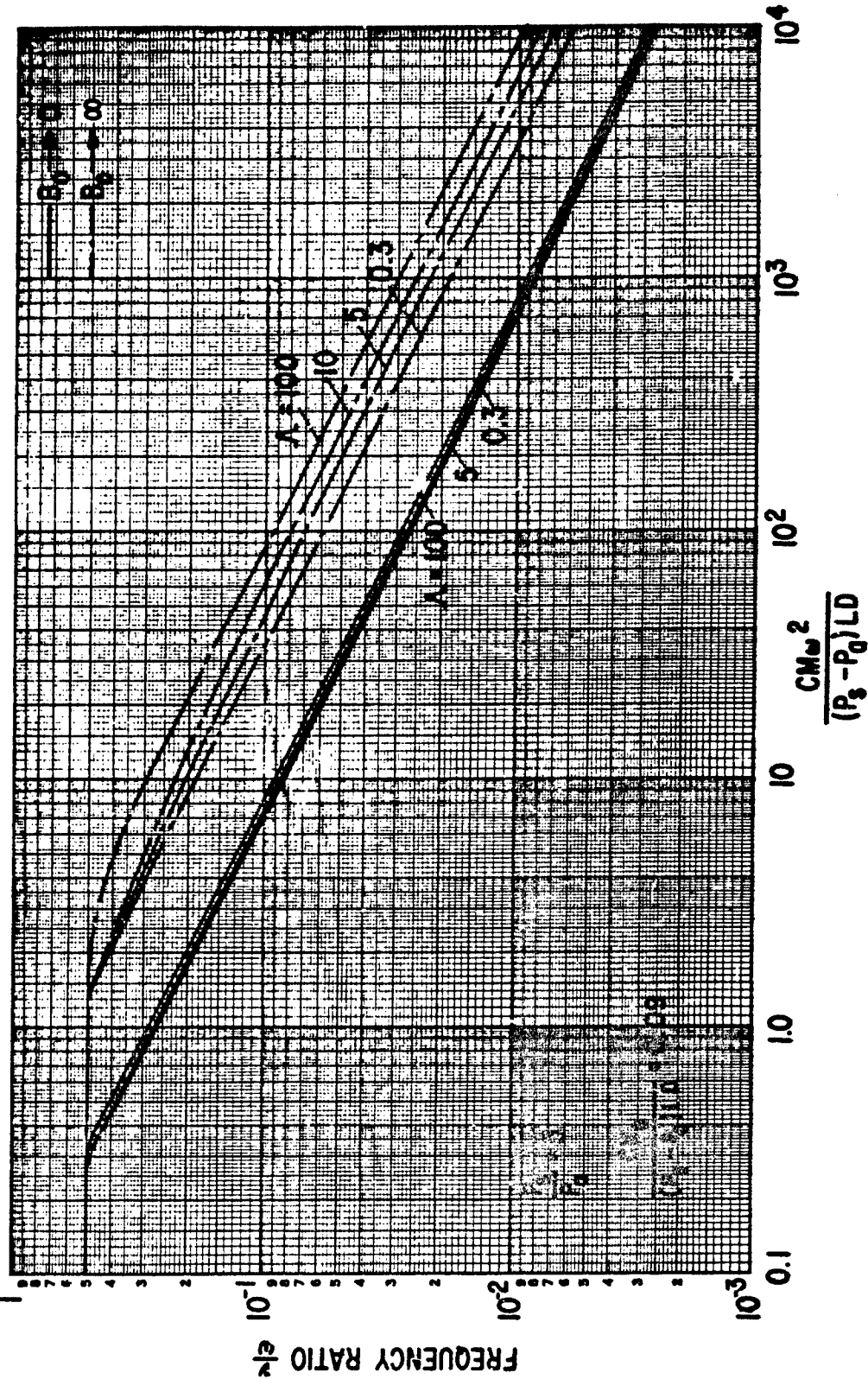


Figure 38. Hybrid-Hydrostatic Ring Bearing,  $\frac{P_3}{P_0} = 5$ ,  $\frac{CK_0}{(P_3 - P_0)LD} = 0.09$ , Instability Frequency

NET-3043

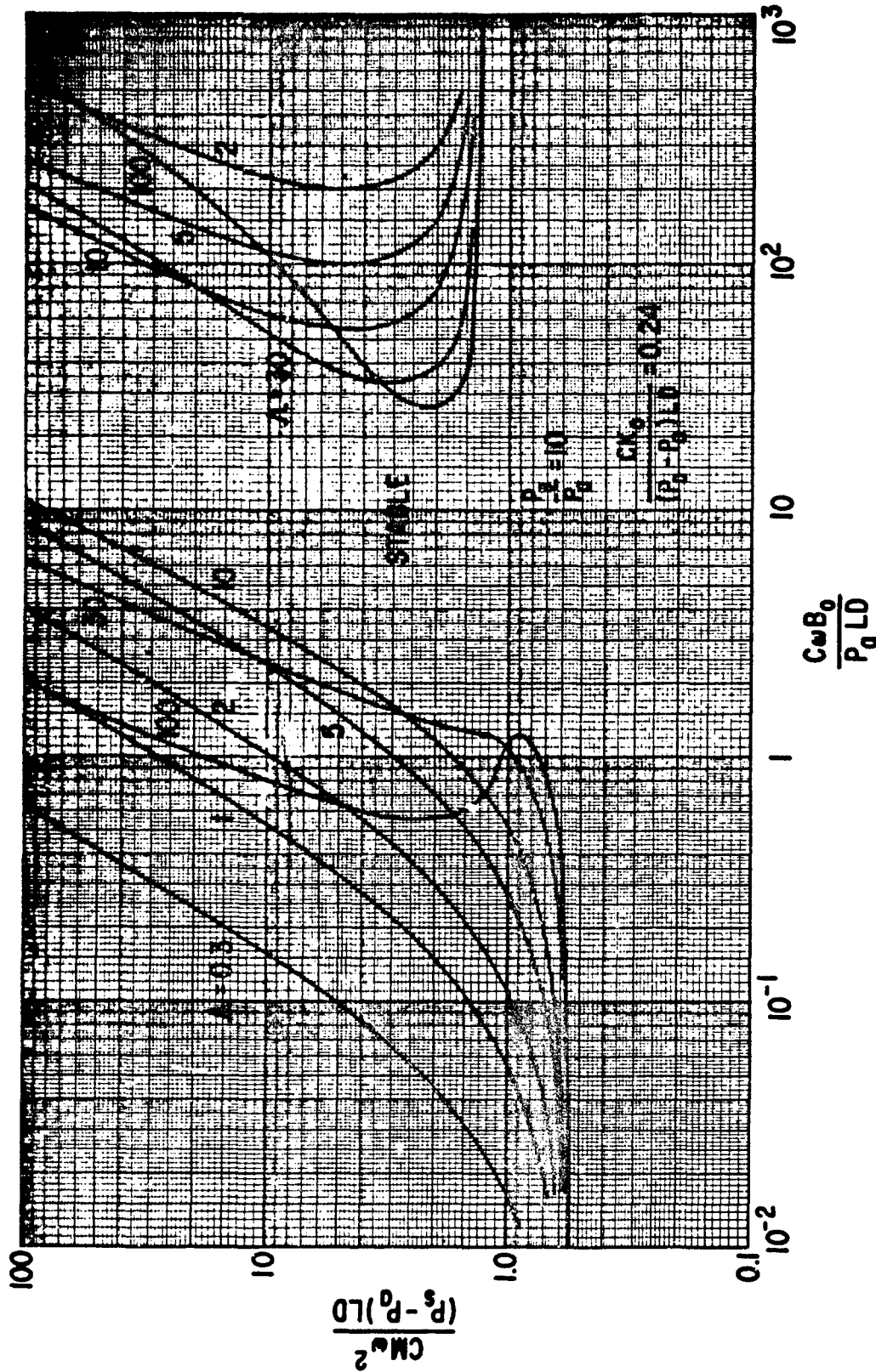


Figure 39. Hybrid-Hydrostatic Ring Bearing,  $\frac{P_s}{P_0} = 10$ ,  $\frac{CK_0}{(P_s - P_0)LD} = 0.24$ , Stability Map

MIT-5046

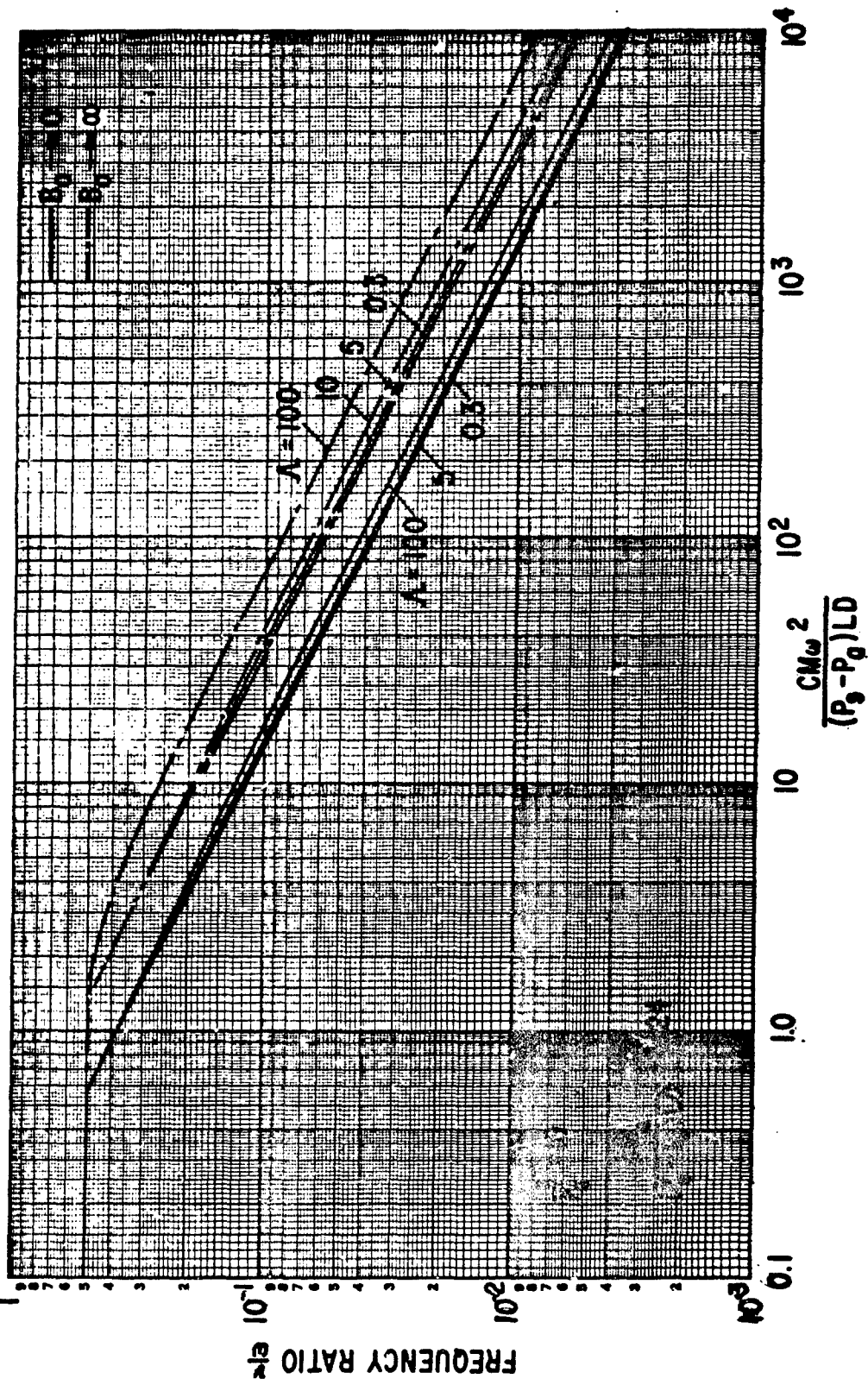


Figure 40. Hybrid-Hydrostatic Ring Bearing,  $\frac{P_s}{P_a} = 10$ ,  $\frac{CK}{(P_s - P_a)LD} = 0.24$ , Instability Frequency

MIT-5647

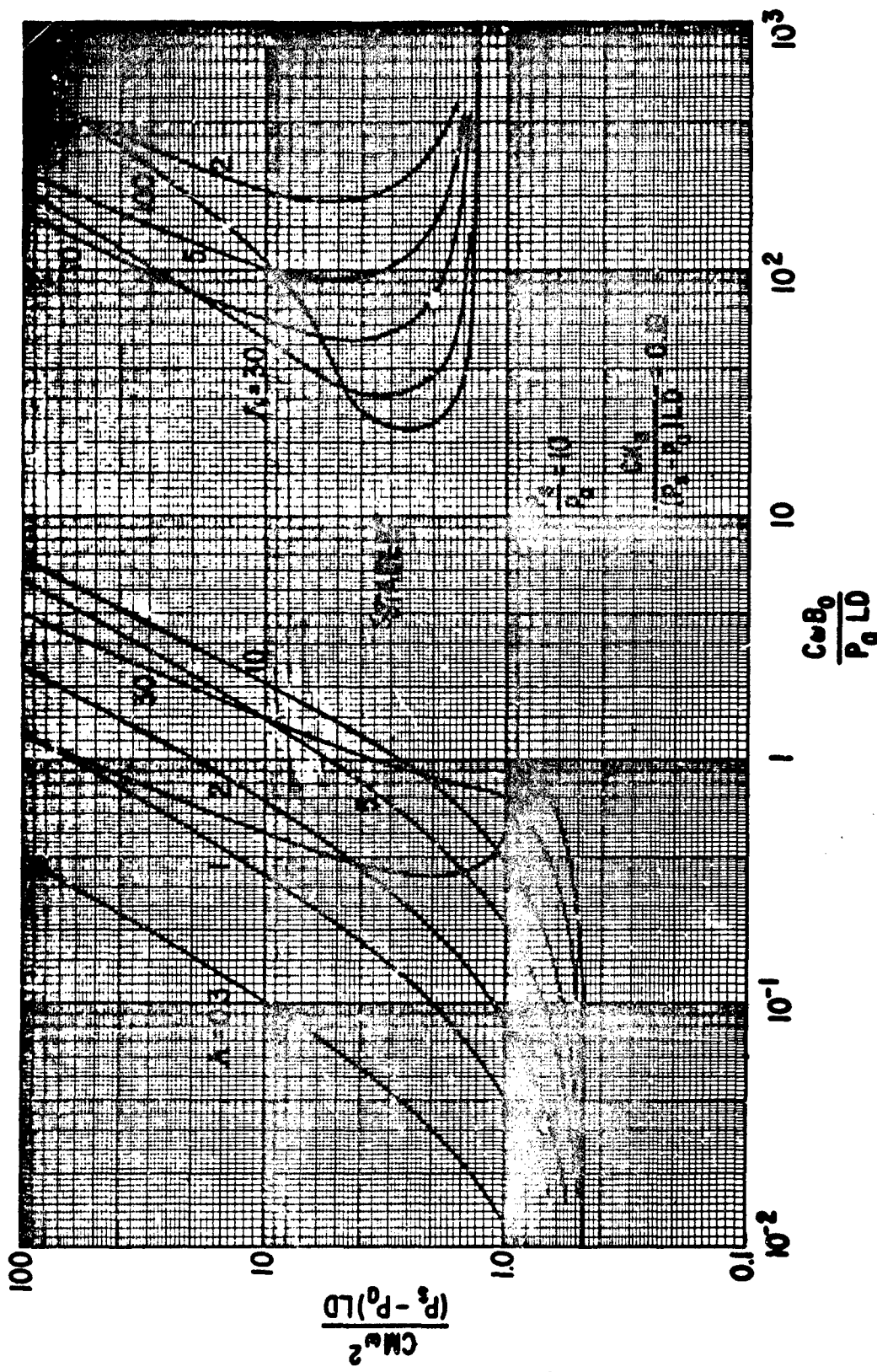


Figure 41. Hybrid-Hydrostatic Ring Bearing,  $\frac{P_e}{P_a} = 10$ ,  $\frac{Ck_o}{(P_e - P_a)LD} = 0.18$ , Stability Map

NET-5048

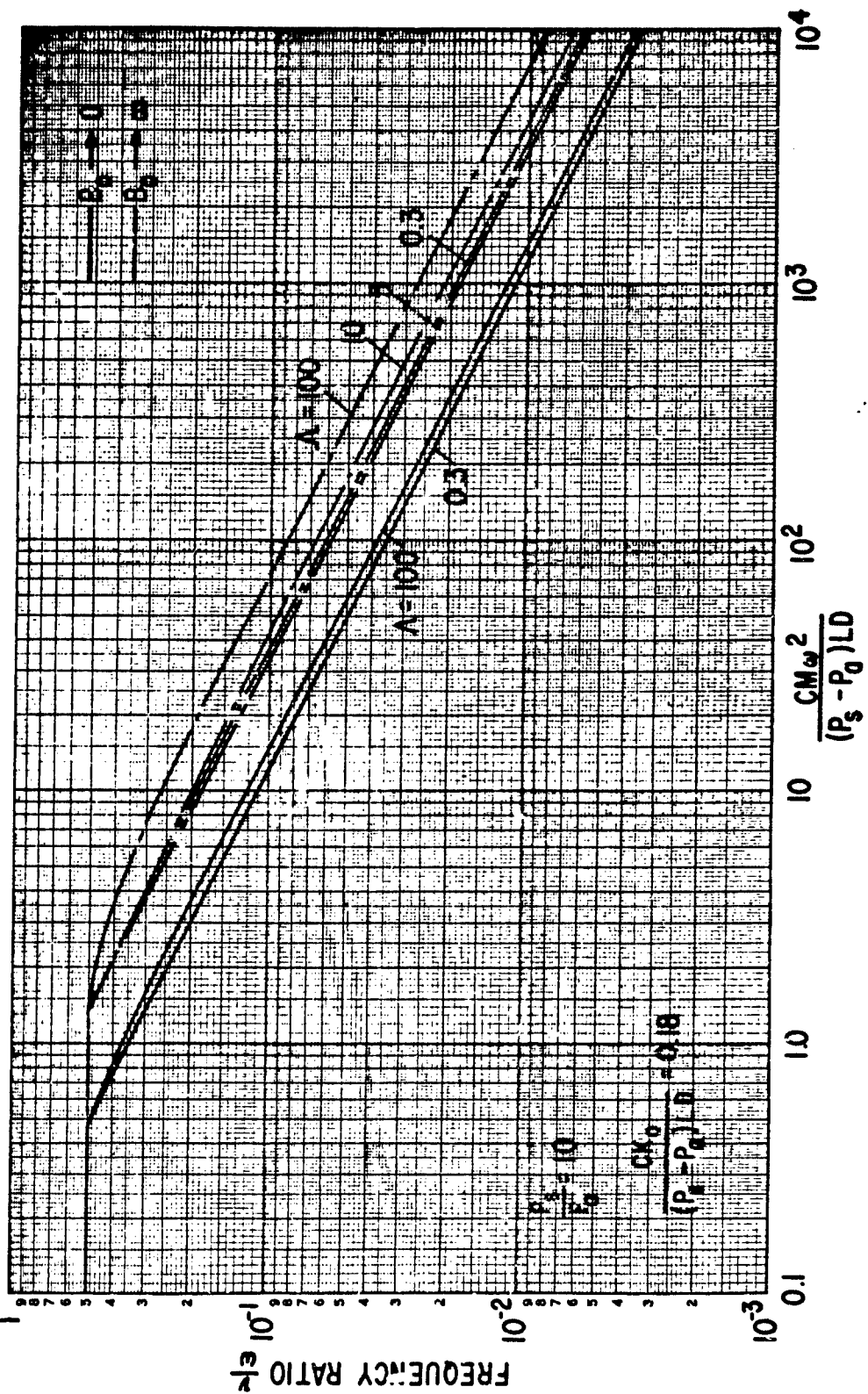


Figure 42. Hybrid-Hydrostatic Ring Bearing,  $\frac{P_s}{P_0} = 10$ ,  $\frac{CK_0}{(P_s - P_0) LD} = 0.18$ , Instability Frequency

MTI-5049

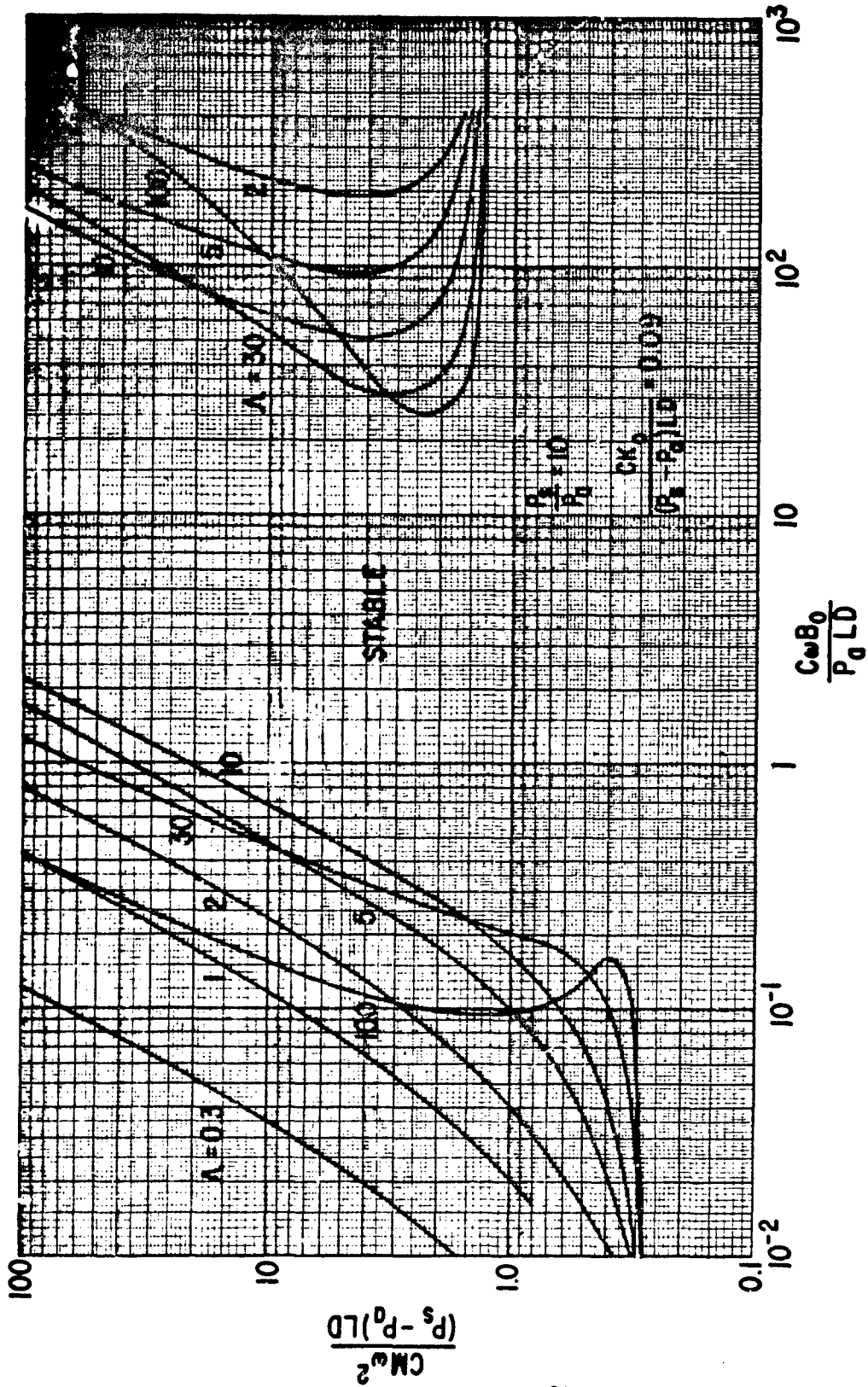


Figure 43. Hybrid-Hydrostatic Ring Bearing,  $\frac{P_s}{P_d} = 10$ ,  $\frac{CK_0}{(P_s - P_d)LD} = 0.09$ , Stability Map

MEI-5050

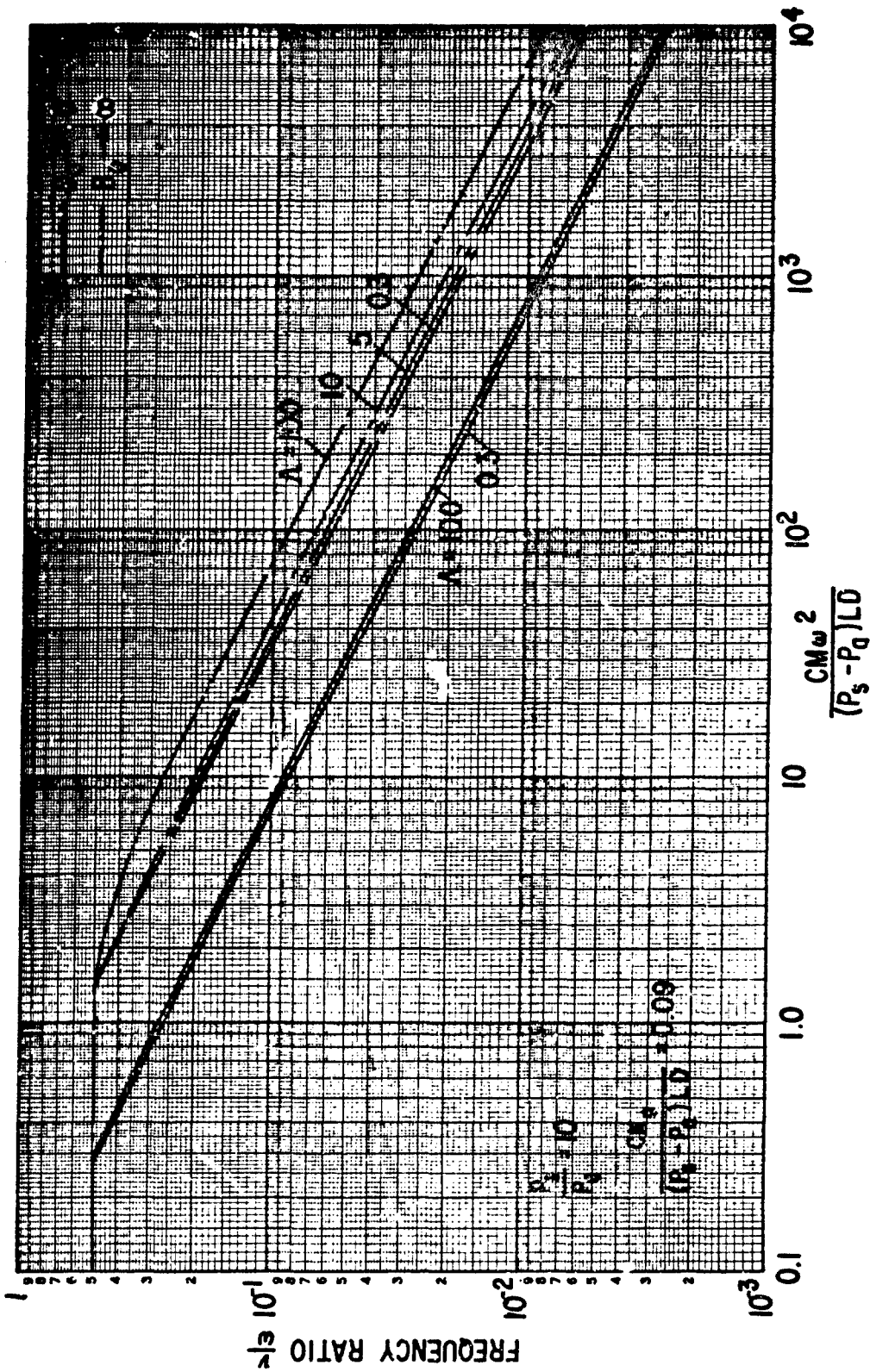


Figure 44. Hybrid-Hydrostatic Ring Bearing,  $\frac{P_a}{P_s} = 10$ ,  $\frac{CK_0}{(P_s - P_a) LD} = 0.09$ , Instability Frequency

MIT-921

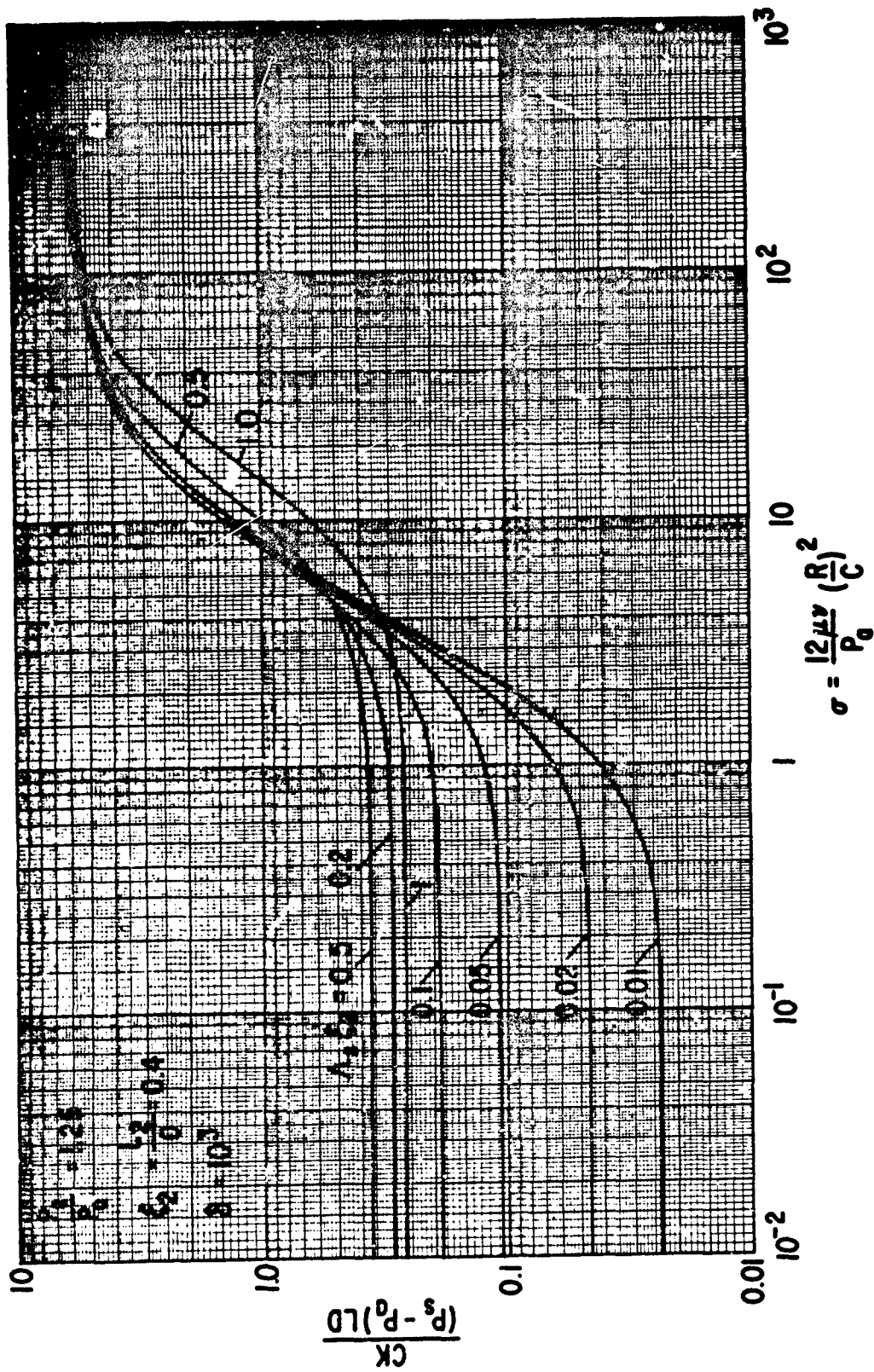


Figure 45. Hydrostatic Bearing, Compressible,  $\frac{P_s}{P_0} = 1.25$ , Stiffness

NET-5953

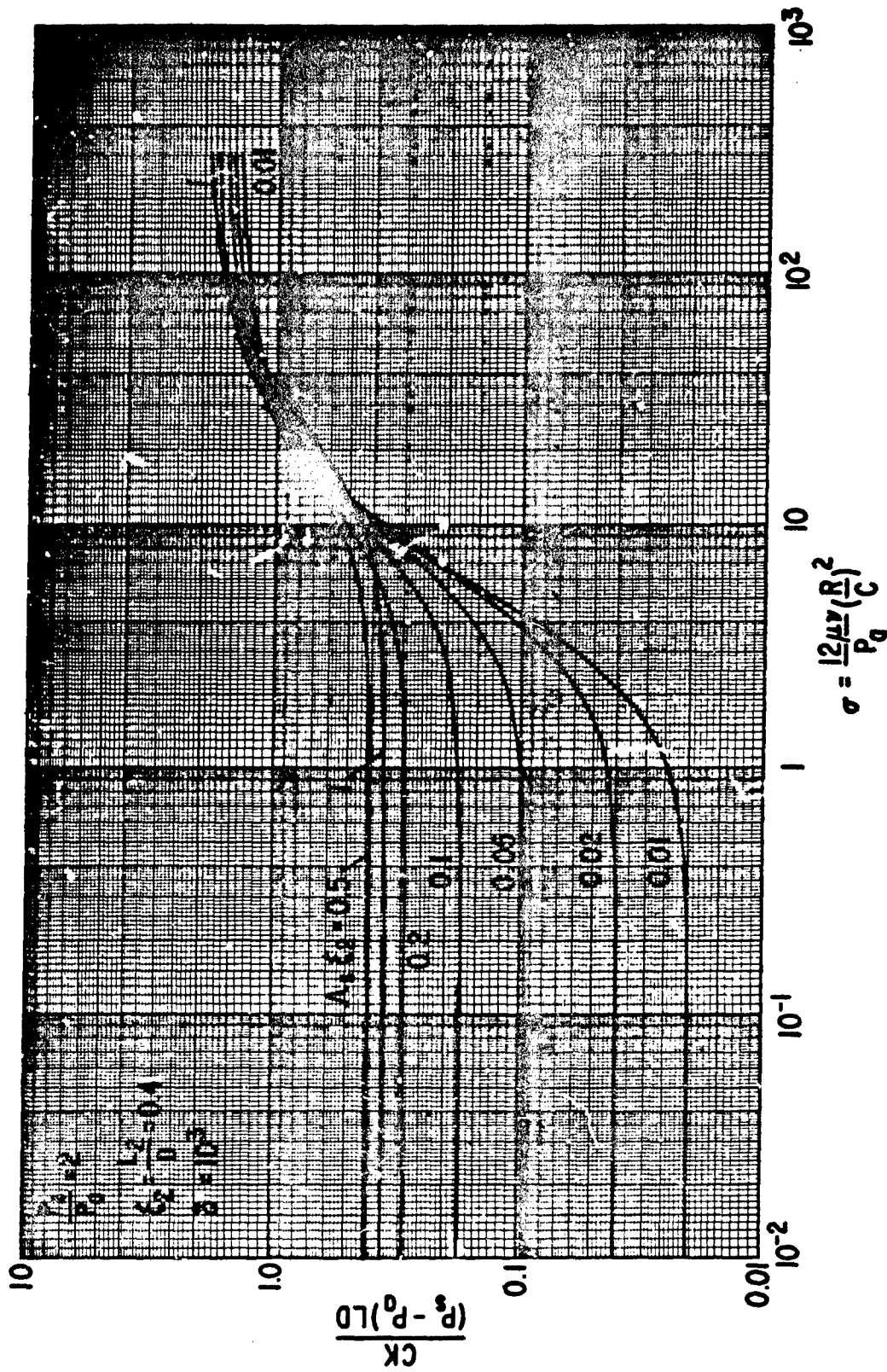


Figure 46. Hydrostatic Bearing, Compressible,  $\frac{P_s}{P_0} = 2$ , Stiffness

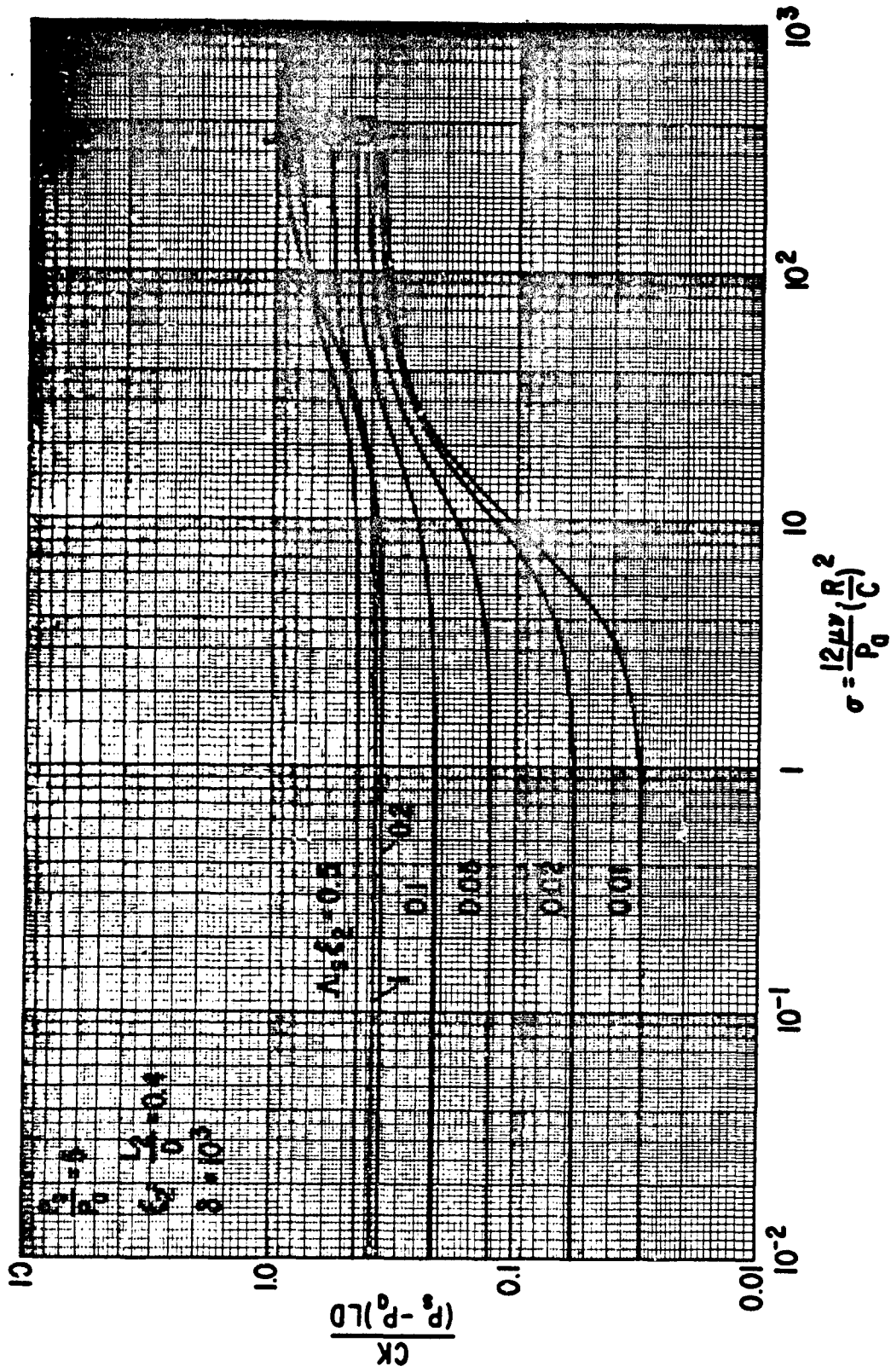


Figure 47. Hydrostatic Bearing, Compressible,  $\frac{P}{P_0} = 5$ , Stiffness

NET-5804

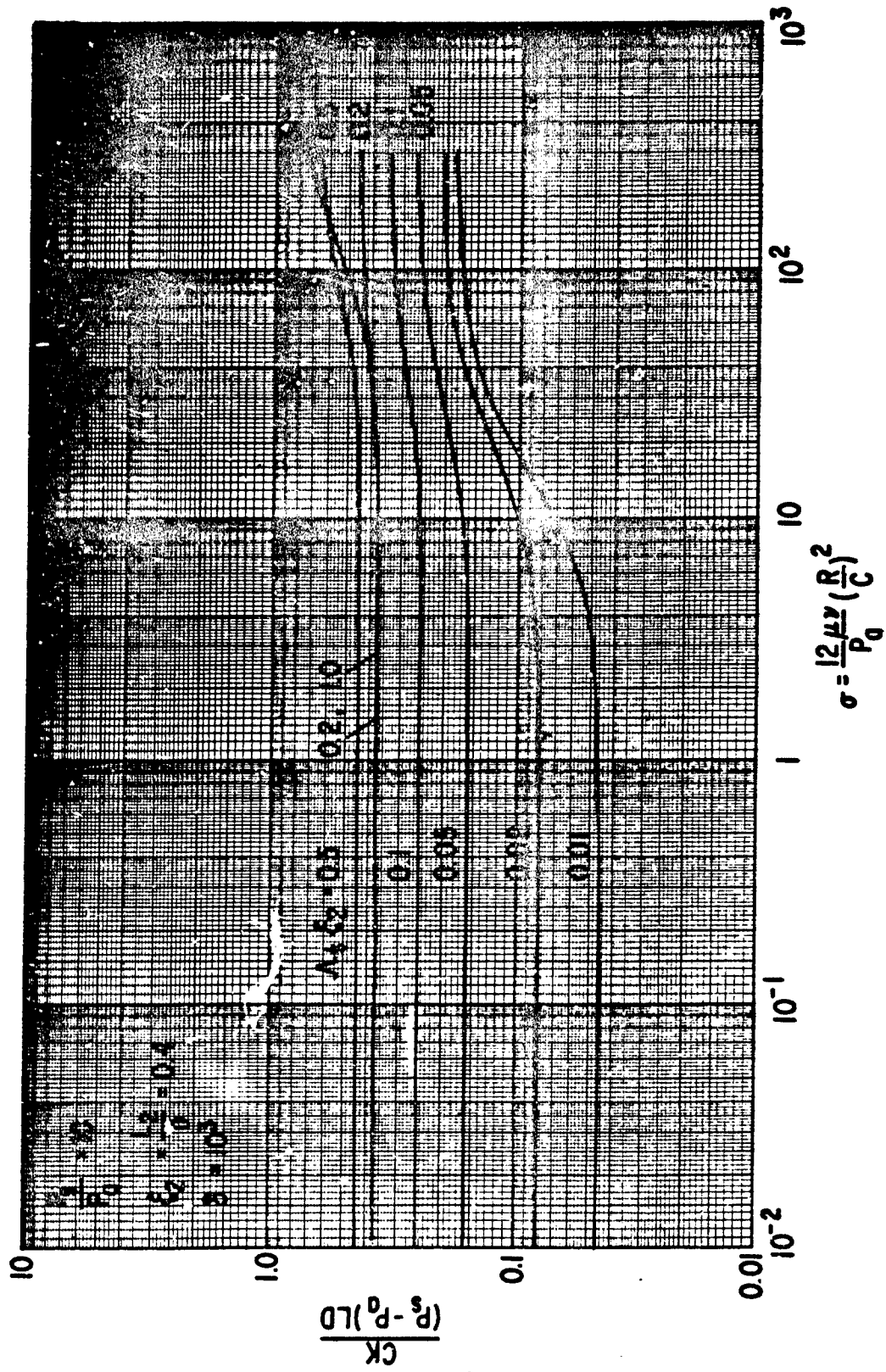


Figure 48. Hydrostatic Bearing, Compressible,  $\frac{P_s}{P_0} = 10$ , Stiffness

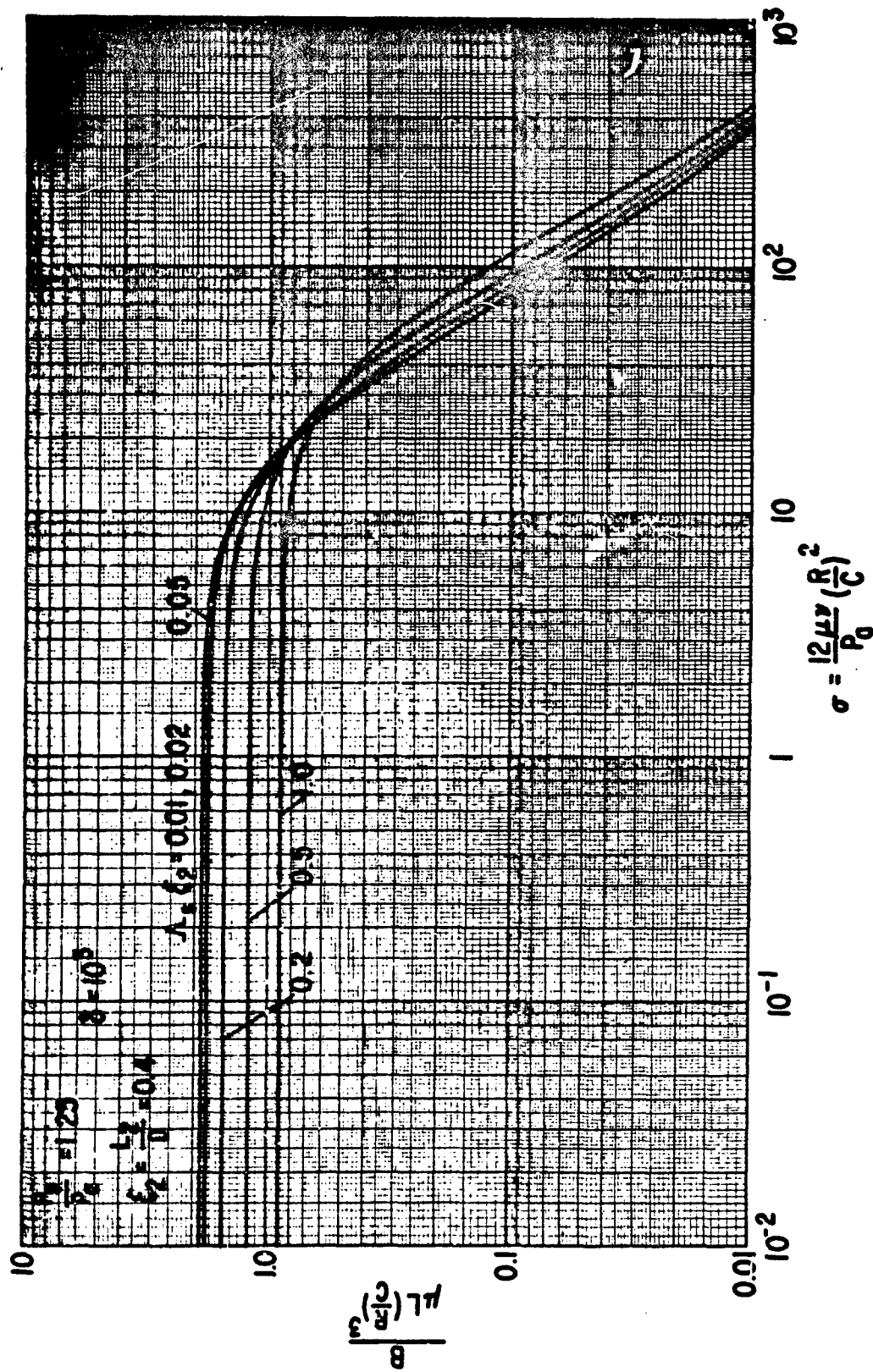


Figure 49. Hydrostatic Bearing, Compressible,  $\frac{P_a}{P_0} = 1.25$ , Damping

MIT-5056

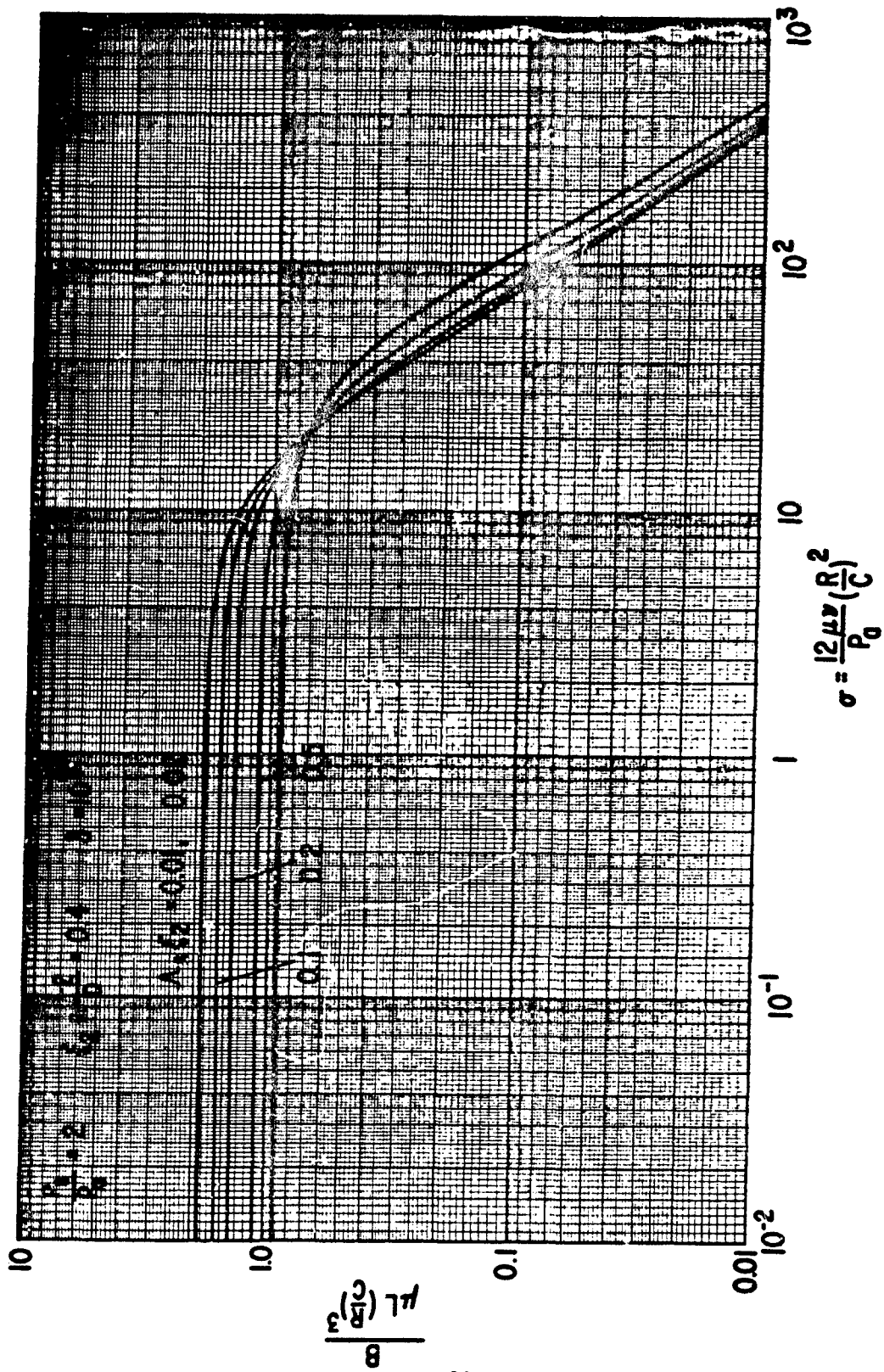


Figure 50. Hydrostatic Bearing, Compressible,  $\frac{P_a}{P_0} = 2$ , Damping

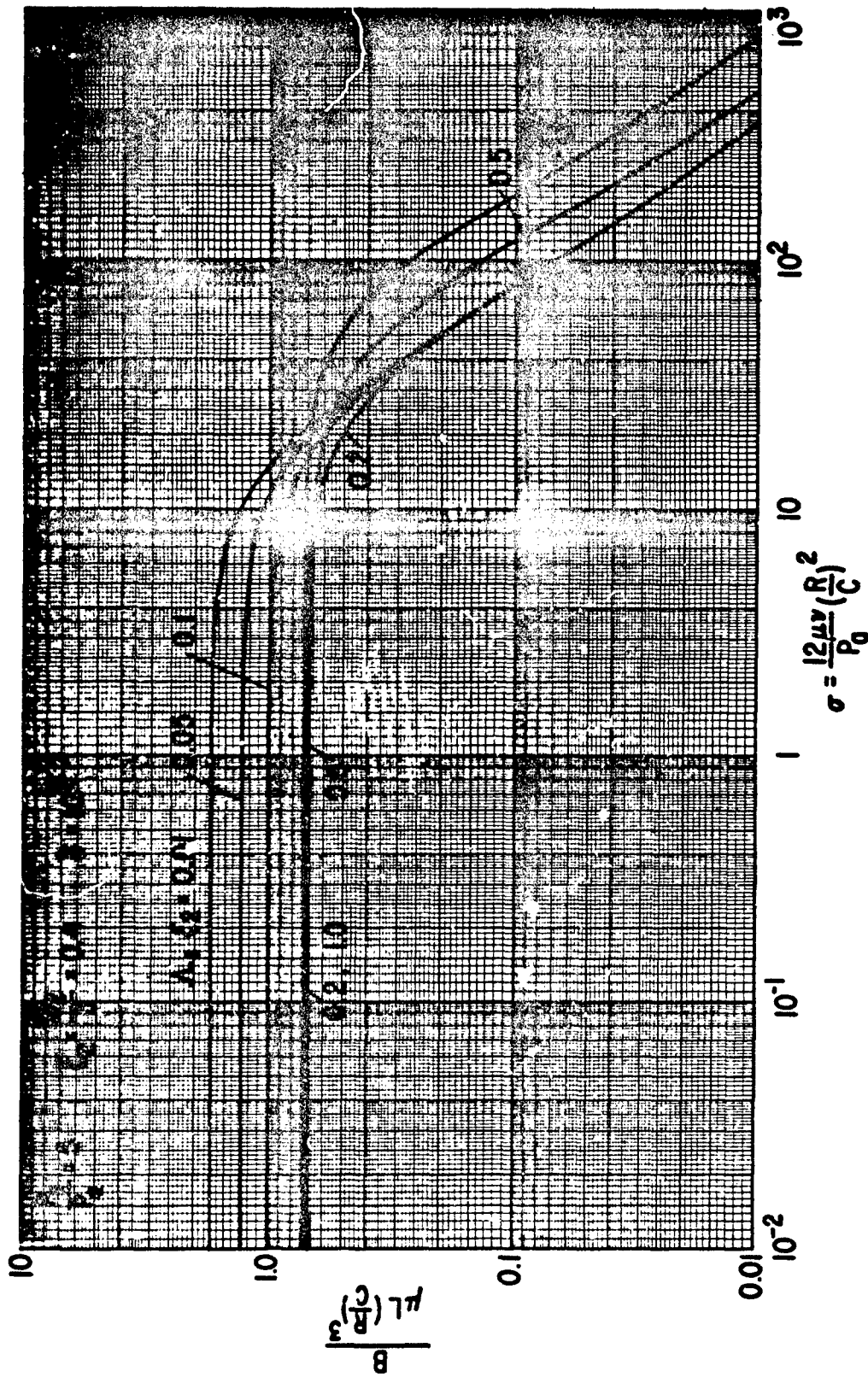


Figure 51. Hydrostatic Bearing, Compressible,  $\frac{P_a}{P_0} = 5$ , Damping

MEI-5058

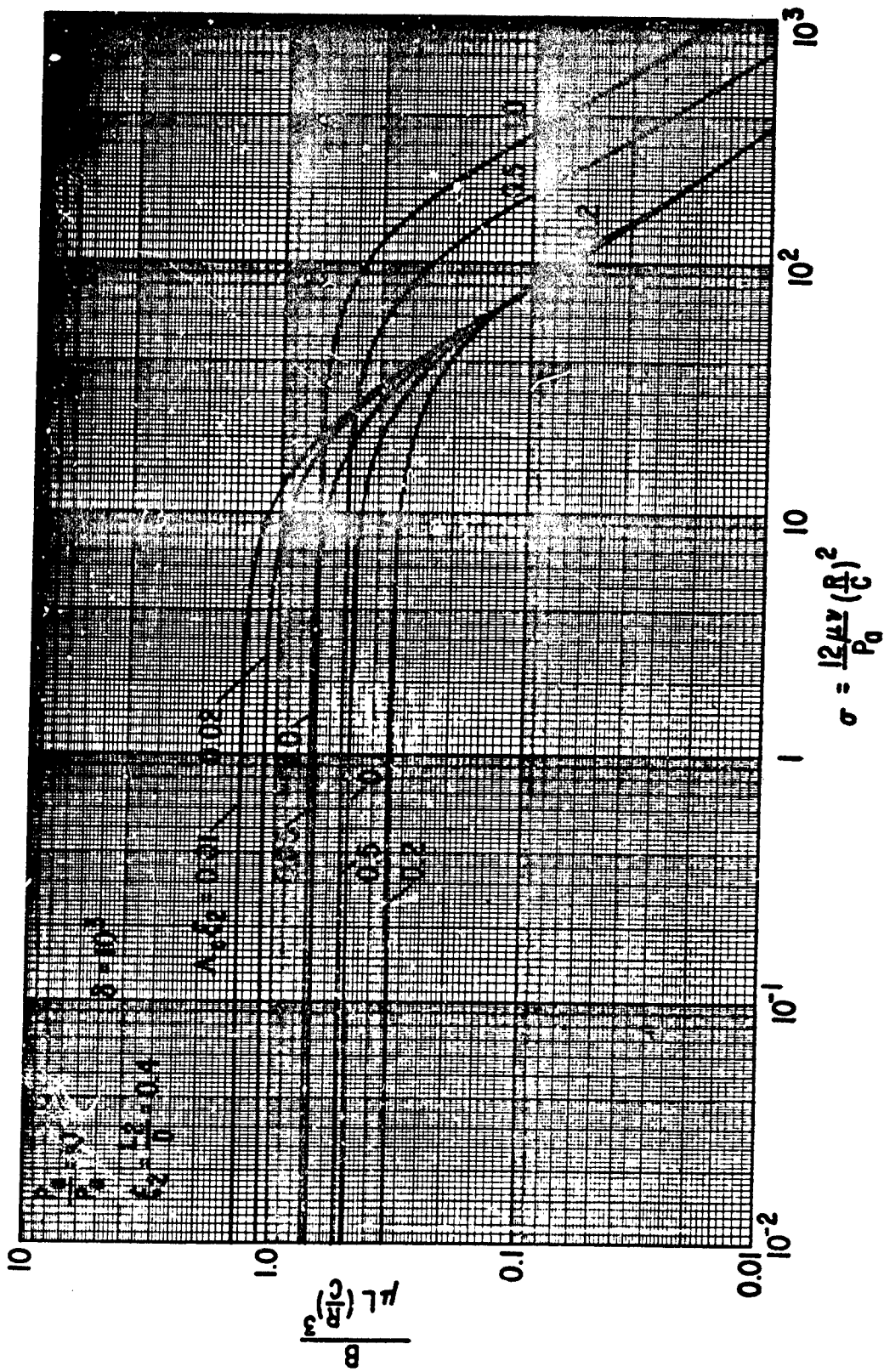


Figure 52. Hydrostatic Bearing, Compressible,  $\frac{P_a}{P_0} = 10$ , Damping

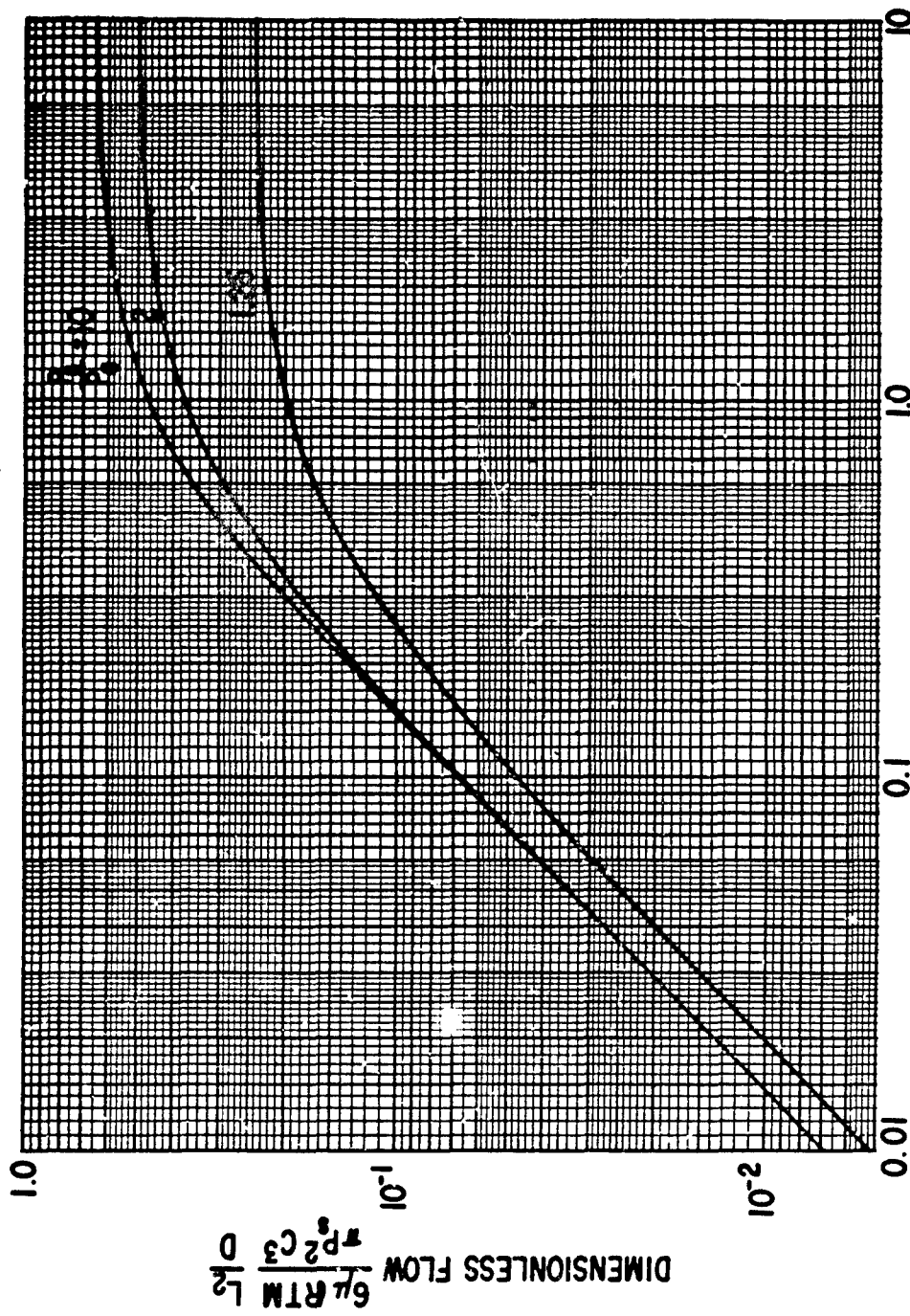


Figure 53. Hydrostatic Bearing, Compressible, Flow

RT-5060

APPENDIX I: The Static and Dynamic Performance of a Partial Arc Bearing with Turbulent Film

To calculate the load carrying capacity, the friction, the flow and the dynamic coefficients of a turbulent lubricant film it is necessary to solve Reynolds equation. This is done numerically as described in this appendix.

In a turbulent lubricant film Reynolds equation is given by (see reference 1):

$$\frac{\partial}{R \partial \theta} \left[ G_x \frac{\bar{h}^3}{12\mu} \frac{\partial \bar{P}}{R \partial \theta} \right] + \frac{\partial}{\partial z} \left[ G_z \frac{\bar{h}^3}{12\mu} \frac{\partial \bar{P}}{\partial z} \right] = \frac{1}{2} R \omega \frac{\partial \bar{h}}{R \partial \theta} + \frac{\partial \bar{h}}{\partial t} \quad (A-1)$$

where  $\bar{P}$  is the film pressure,  $\mu$  is the lubricant viscosity,  $R$  is the journal radius,  $\omega$  is the angular speed of the journal,  $\theta$  is the angular coordinate, (see fig. 54),  $z$  is the axial coordinate,  $t$  is time,  $G_x$  and  $G_z$  are turbulent flow coefficients and  $\bar{h}$  is the local film thickness:

$$\bar{h} = C + e \cdot \cos \theta \quad (A-2)$$

Here,  $C$  is the radial clearance (the difference between the radius of curvature of the bearing surface, and the radius of the journal, see fig. 54) and  $e$  is the eccentricity (the distance between the journal center and the center of curvature of the bearing).

Reynolds equation, eq. (A-1), is made dimensionless by setting:

$$\zeta = \frac{z}{R} \quad (A-3)$$

$$\tau = \omega t \quad (A-4)$$

$$h = \frac{\bar{h}}{C} = 1 + \epsilon \cos \theta \quad (A-5)$$

$$\epsilon = \frac{e}{C} \quad (A-6)$$

$$P = \frac{\bar{P}}{\mu \omega \left(\frac{R}{C}\right)^2} = \frac{1}{2\pi S} \frac{\bar{P}}{W/LD} \quad (A-7)$$

where  $W$  is the load carried by the bearing,  $L$  is the bearing length,  $D$  is the journal diameter and:

$$\text{Sommerfeld Number: } S = \frac{\mu N D L}{W} \left(\frac{R}{C}\right)^2 \quad (\text{A-8})$$

( $N$  is the journal speed in rps, i.e.  $\omega = 2\pi N$ )

Substituting eqs. (A-3) to (A-7) into eq. (A-1) yields Reynolds equation in dimensionless form:

$$\frac{d}{d\theta} \left[ G_x h^3 \frac{\partial P}{\partial \theta} \right] + \frac{d}{d\zeta} \left[ G_z h^3 \frac{\partial P}{\partial \zeta} \right] = 6 \frac{\partial h}{\partial \theta} + 12 \frac{\partial h}{\partial \zeta} \quad (\text{A-9})$$

The dimensionless turbulent flow coefficients  $G_x$  and  $G_z$  are functions of the local Reynolds number  $R_h$ :

$$R_h = h R_e \quad (\text{A-10})$$

where:

$$\text{Reynolds Number: } R_e = \frac{\rho R \omega C}{\mu} \quad (\text{A-11})$$

$\rho$  is the mass density of the lubricant.

The actual functional relationships between  $G_x$ ,  $G_z$  and  $R_h$  are given in reference 1. When comparing with ref. 1, however, it should be noted that  $G_x$  and  $G_z$  as used in the present analysis are larger than the values given in ref. 1 by a factor of 12 such that for laminar flow ( $R_h = R_e = 0$ ),  $G_x$  and  $G_z$  are equal to unity rather than 1/12 as in ref. 1.

From eq. (A-10) it is seen, that for a given Reynolds number  $R_e$ ,  $G_x$  and  $G_z$  are functions of  $\theta$  only (since they are functions of  $h$ ) and do not depend on the axial coordinate  $\zeta$ .

Before solving eq. (A-9) it is convenient to give it another form. Introduce the new variables:

$$G = \frac{G_x}{G_y} \quad (A-12)$$

$$H = h^{3/2} G_x^{1/2} \quad (A-13)$$

$$\psi = PH = Ph^{3/2} G_x^{1/2} \quad (A-14)$$

whereby eq. (A-9) can be written:

$$\frac{\partial^2 \psi}{\partial \theta^2} + G \frac{\partial^2 \psi}{\partial \tau^2} - \frac{1}{H} \frac{\partial^2 H}{\partial \theta^2} \psi = \frac{1}{H} \left[ 6 \frac{\partial h}{\partial \theta} + 12 \frac{\partial h}{\partial \tau} \right] \quad (A-15)$$

Assume that the journal operates under static conditions with an eccentricity ratio  $\epsilon$ , and an attitude angle  $\phi$ , where, in the present analysis, the attitude angle  $\phi$  is the angle from a fixed x-axis to the line connecting the center of the bearing with the center of the journal:

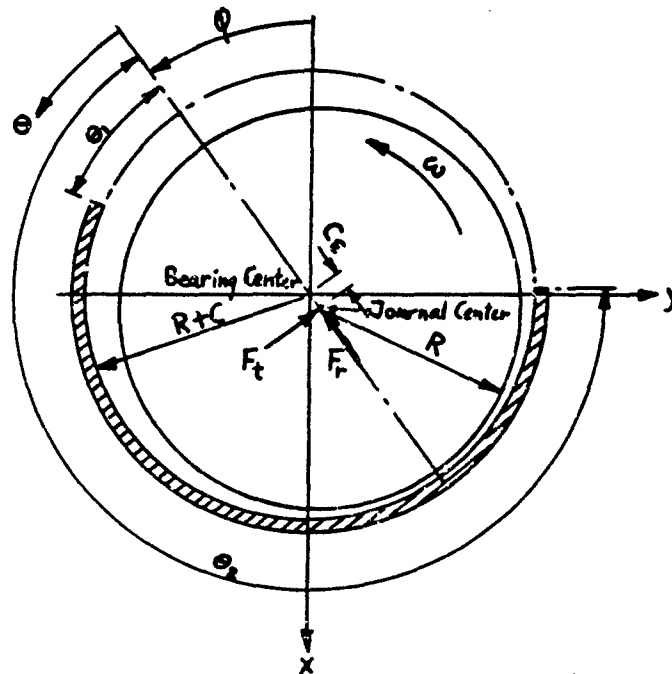


Figure 54: Geometry of Partial Arc Bearing

The static equilibrium position  $(\epsilon_0, \phi_0)$  is perturbed by giving the journal center a small amplitude motion with amplitudes  $(\epsilon_1, \phi_1)$  and corresponding velocities  $(\dot{\epsilon}_1, \dot{\phi}_1)$  where "dot" refers to  $d/dt$ . Hence, the instantaneous position of the journal center is defined by:

$$\epsilon = \epsilon_0 + \epsilon_1 \quad (A-16)$$

$$\phi = \phi_0 + \phi_1$$

where  $\epsilon_1 \ll \epsilon_0$  and  $\phi_1 \ll \phi_0$ . This motion causes similar perturbations in the film pressure and the film thickness such that:

$$\psi = \psi_0 + \epsilon_1 \psi_1 + \epsilon_0 \phi_1 \psi_2 + \dot{\epsilon}_1 \psi_3 + \epsilon_0 \dot{\phi}_1 \psi_4 \quad (A-17)$$

$$H = H_0 + \epsilon_1 H_1 + \epsilon_0 \phi_1 H_2 \quad (A-18)$$

$$G = G_0 + \epsilon_1 G_1 + \epsilon_0 \phi_1 G_2 \quad (A-19)$$

$$h = 1 + \epsilon_0 \cos \theta + \epsilon_1 \cos \theta + \epsilon_0 \phi_1 \sin \theta = h_0 + \epsilon_1 \cos \theta + \epsilon_0 \phi_1 \sin \theta \quad (A-20)$$

Substitution of eqs. (A-17) to (A-20) into eq. (A-15) yields 5 equations to determine the static pressure and its four perturbation components:

$$\frac{\partial^2 \psi_0}{\partial \theta^2} + G_0 \frac{\partial^2 \psi_0}{\partial \zeta^2} - \frac{1}{H_0} \frac{\partial^2 H_0}{\partial \theta^2} \psi_0 = \frac{6}{H_0} \frac{dh_0}{d\theta} = -\frac{6 \sin \theta}{H_0} \epsilon_0 \quad (A-21)$$

$$\frac{\partial^2 \psi_1}{\partial \theta^2} + G_0 \frac{\partial^2 \psi_1}{\partial \zeta^2} - \frac{1}{H_0} \frac{\partial^2 H_0}{\partial \theta^2} \psi_1 = \frac{1}{H_0} \left( \frac{\partial^2 H_1}{\partial \theta^2} - \frac{H_1}{H_0} \frac{\partial^2 H_0}{\partial \theta^2} \right) \psi_0 - G_1 \frac{\partial^2 \psi_0}{\partial \zeta^2} - \frac{6}{H_0} \left( \sin \theta + \frac{H_1}{H_0} \frac{dh_0}{d\theta} \right) \quad (A-22)$$

$$\frac{\partial^2 \psi_2}{\partial \theta^2} + G_0 \frac{\partial^2 \psi_2}{\partial \zeta^2} - \frac{1}{H_0} \frac{\partial^2 H_0}{\partial \theta^2} \psi_2 = \frac{1}{H_0} \left( \frac{\partial^2 H_2}{\partial \theta^2} - \frac{H_2}{H_0} \frac{\partial^2 H_0}{\partial \theta^2} \right) \psi_0 - G_2 \frac{\partial^2 \psi_0}{\partial \zeta^2} - \frac{6}{H_0} \left( -\cos \theta + \frac{H_2}{H_0} \frac{dh_0}{d\theta} \right) \quad (A-23)$$

$$\frac{\partial^2 \psi_3}{\partial \theta^2} + G_0 \frac{\partial^2 \psi_3}{\partial \zeta^2} - \frac{1}{H_0} \frac{\partial^2 H_0}{\partial \theta^2} \psi_3 = \frac{12 \cos \theta}{H_0} \quad (A-24)$$

$$\frac{\partial^2 \psi_4}{\partial \theta^2} + G_0 \frac{\partial^2 \psi_4}{\partial \xi^2} - \frac{1}{H_0} \frac{\partial^2 H_0}{\partial \theta^2} \psi_4 = \frac{12 \sin \theta}{H_0} \quad (\text{A-25})$$

Comparing eqs. (A-21) and (A-25), it is seen that:

$$\psi_0 = -\frac{1}{2} \epsilon_0 \psi_4 \quad (\text{A-26})$$

The boundary conditions are that the pressure is ambient (i.e. zero) along the periphery of the film. Hence, at the sides of the bearing,  $\bar{P} = 0$  or:

$$\xi = \pm \frac{L}{D} \quad (z = \pm \frac{L}{2}): \quad \psi = 0$$

Since there is symmetry with respect to  $\xi = 0$ , this condition can also be written:

$$\xi = \frac{L}{D}: \quad \psi = 0 \quad \therefore \psi_0 = \psi_1 = \psi_2 = \psi_3 = \psi_4 = 0 \quad (\text{A-27})$$

$$\xi = 0: \quad \frac{\partial \psi}{\partial \xi} = 0 \quad \therefore \frac{\partial \psi_0}{\partial \xi} = \frac{\partial \psi_1}{\partial \xi} = \frac{\partial \psi_2}{\partial \xi} = \frac{\partial \psi_3}{\partial \xi} = \frac{\partial \psi_4}{\partial \xi} = 0 \quad (\text{A-28})$$

If the film is complete over the entire bearing surface, the two remaining boundary conditions are that the pressure is zero at the leading edge and at the trailing edge of the bearing arc:

$$\left. \begin{array}{l} \theta = \theta_1 \\ \theta = \theta_2 \end{array} \right\}: \quad \psi = 0 \quad \therefore \psi_0 = \psi_1 = \psi_2 = \psi_3 = \psi_4 = 0 \quad (\text{A-29})$$

No film rupture

On the other hand, the film is frequently not complete. If any portion of the bearing arc is in the diverging part of the film (i.e.  $180 < \Theta < 360$ , see fig. A-1), Reynolds equation predicts subambient film pressures in this region. These subambient pressures cannot, in general, exist unless the bearing is submerged completely in its own lubricant. Instead, the film contracts such that it does not take up the full length of the bearing, and the pressure in the contracted film is zero. This is called film rupture. On the boundary between the complete film and the contracted film, the pressure is zero (i.e. eq. (A-29) is valid when  $\Theta_1$  and  $\Theta_2$  are adjusted to give the angular location of the boundary). In addition, a second condition is:

$$\frac{\partial \bar{P}}{\partial \Theta} = \frac{\partial \bar{P}}{\partial \zeta} = 0$$

or since  $\psi = 0$  on the boundary:

$$\frac{\partial \psi}{\partial \Theta} = \frac{\partial \psi}{\partial \zeta} = 0$$

Let a point on the boundary have the coordinates  $(\Theta, \zeta)$ , i.e.:

$$\text{on free boundary: } \psi(\Theta, \zeta) = 0 \quad \left. \frac{\partial \psi}{\partial \Theta} \right|_{\Theta, \zeta} = \left. \frac{\partial \psi}{\partial \zeta} \right|_{\Theta, \zeta} \quad (\text{A-30})$$

Under static conditions the boundary has the coordinates  $(\Theta_0, \zeta_0)$ . For small scale motion of the journal the boundary is perturbed such that:

$$\begin{aligned} \Theta &= \Theta_0 + \delta\Theta \\ \zeta &= \zeta_0 + \delta\zeta \end{aligned} \quad (\text{A-31})$$

where  $\delta\Theta$  and  $\delta\zeta$  are small quantities. This results in a similar perturbation of the pressure variable  $\psi$ :

$$\psi = \psi_0 + \delta\psi \quad (\text{A-32})$$

Expand  $\psi$  in a Taylor series from a point on the boundary:

$$\psi(\theta, \zeta) = \psi(\theta_0, \zeta_0) + \left. \frac{\partial \psi}{\partial \theta} \right|_0 \delta\theta + \left. \frac{\partial \psi}{\partial \zeta} \right|_0 \delta\zeta = 0$$

where terms of order  $\delta^2$  have been ignored. Introduce eq. (A-32) to get:

$$\psi(\theta, \zeta) = \psi_0(\theta_0, \zeta_0) + \delta\psi(\theta_0, \zeta_0) + \left. \frac{\partial \psi_0}{\partial \theta} \right|_0 \delta\theta + \left. \frac{\partial \psi_0}{\partial \zeta} \right|_0 \delta\zeta = 0 \quad (\text{A-33})$$

With  $\psi_0(\theta_0, \zeta_0) = \left. \frac{\partial \psi_0}{\partial \theta} \right|_0 = \left. \frac{\partial \psi_0}{\partial \zeta} \right|_0 = 0$  as the given boundary condition, this equation results in:

$$\delta\psi(\theta_0, \zeta_0) = 0 \quad (\text{A-34})$$

Comparing eq. (A-32) with eq. (A-17) it is seen that:

$$\delta\psi(\theta_0, \zeta_0) = \left[ \varepsilon_1 \psi_1 + \varepsilon_0 \phi_1 \psi_2 + \dot{\varepsilon}_1 \psi_3 + \varepsilon_0 \dot{\phi}_1 \psi_4 \right]_{\theta_0, \zeta_0}$$

Since  $\varepsilon_1$ ,  $\phi_1$ ,  $\dot{\varepsilon}_1$  and  $\dot{\phi}_1$  are independent variables, each of the four pressure perturbations must vanish independently on the same free boundary as obtained under static conditions. Hence, the complete boundary conditions at the free boundary becomes:

$$\left. \begin{array}{l} \text{on "zero order"} \\ \text{free boundary} \end{array} \right\} \psi_0 = \frac{\partial \psi_0}{\partial \theta} = \frac{\partial \psi_0}{\partial \zeta} = 0 \quad (\text{A-35})$$

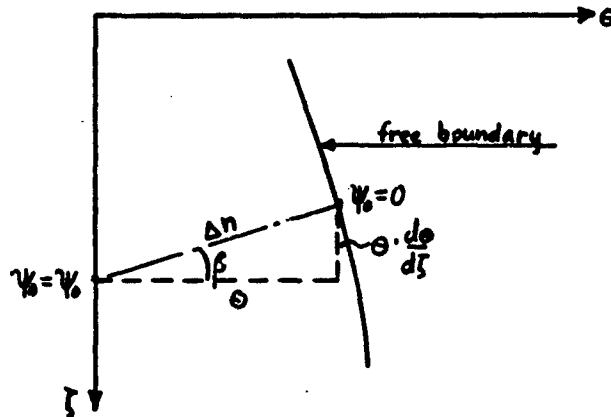
$$\psi_1 = \psi_2 = \psi_3 = \psi_4 = 0 \quad (\text{A-36})$$

Hence, the location of the free boundary is determined from the solution of  $\psi_0$  (i.e. the steady-state solution). Once the boundary has been established, the perturbations  $\psi_1$ ,  $\psi_2$ ,  $\psi_3$  and  $\psi_4$  are to be solved over the same domain such that they vanish along the periphery of the domain.

To determine the coordinates of the free boundary, substitution of eq. (A-35) into eq. (A-21) yields:

on free boundary: 
$$\frac{\partial^2 \psi_0}{\partial \theta^2} + G_0 \frac{\partial^2 \psi_0}{\partial \zeta^2} = \frac{6}{H_0} \frac{\partial h_0}{\partial \theta} \quad (\text{A-37})$$

Let the free boundary have the coordinates  $(\theta, \zeta)$  where  $\theta$  is considered a function of  $\zeta$ :



The inward directed normal to the boundary is  $n$ . Since all derivatives along the boundary are zero,  $\psi_0$  can be expanded in a Taylor series from a point on the boundary as:

$$\psi_0 \cong \frac{1}{2} \frac{\partial^2 \psi_0}{\partial n^2} (\Delta n)^2 \quad (\text{A-38})$$

From the above figure:

$$(\Delta n)^2 = \theta^2 \left[ 1 + \left( \frac{d\theta}{d\zeta} \right)^2 \right] = \theta^2 (1 + \tan^2 \beta) \quad (\text{A-39})$$

By a coordinate transformation,  $\frac{\partial^2 \psi_0}{\partial n^2}$  can be found from eq. (A-37) as:

$$\frac{\partial^2 \psi_0}{\partial n^2} [\cos^2 \beta + G_0 \sin^2 \beta] = \frac{\partial^2 \psi_0}{\partial \theta^2} + G_0 \frac{\partial^2 \psi_0}{\partial \zeta^2} = \frac{6}{H_0} \frac{\partial h_0}{\partial \theta} \quad (\text{A-40})$$

Combining eqs. (A-38) to (A-40) yields:

$$\frac{3}{H_0} \frac{\partial h_0}{\partial \theta} \frac{1 + \tan^2 \beta}{\cos^2 \beta + G_0 \sin^2 \beta} \theta^2 - \psi_0 = 0 \quad (\text{A-41})$$

or since  $\frac{1}{\cos^2 \beta} = 1 + \tan^2 \beta = 1 + \left(\frac{d\phi}{d\zeta}\right)^2$ :

$$\frac{3}{H_0} \frac{\partial h_0}{\partial \theta} \frac{[1 + \left(\frac{d\phi}{d\zeta}\right)^2]^2}{1 + G_0 \left(\frac{d\phi}{d\zeta}\right)^2} \theta^2 - \psi_0 = 0 \quad (\text{A-42})$$

This equation must be solved together with eq. (A-21) as described later.

Equations (A-21) to (A-25) are solved by finite difference methods. A finite difference grid is introduced with  $i$ -axis along the  $\zeta$ -direction and  $j$ -axis along the  $\theta$ -direction:

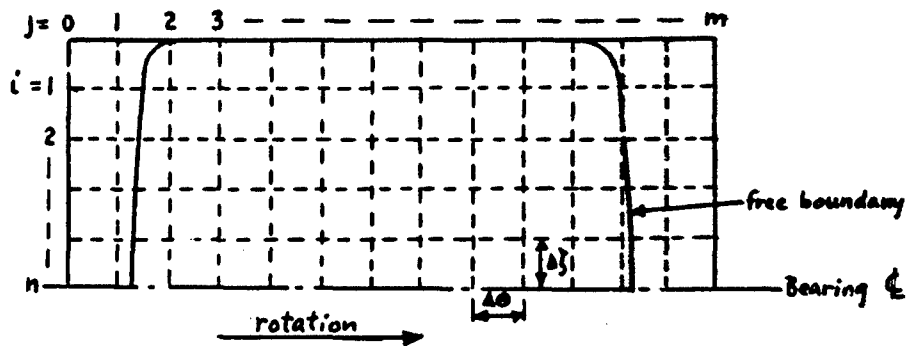


Figure 55: Finite Difference Grid

There are  $n$  increments in the  $\zeta$ -direction such that the length of an increment becomes:

$$\Delta \zeta = \frac{1}{n} \frac{L}{D} \quad (\text{A-43})$$

In the  $\theta$ -direction, the arc length of the bearing pad is subdivided into equal increments of length  $\Delta \theta$ .

In order to write eqs. (A-21) to (A-25) as finite difference equations, consider the grid point  $(i, j)$ :

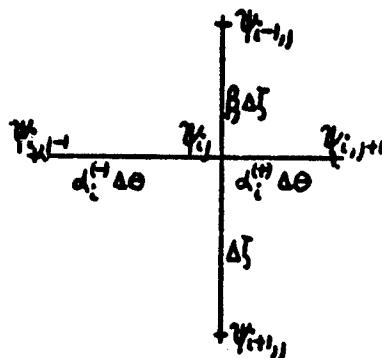


Figure 56: Finite Difference Grid Lines

Here,  $d_i^{(+)}$ ,  $d_i^{(-)}$  and  $\beta_j$  are introduced to take into account the location of the free boundary. Hence, for most points  $d_i^{(+)} = d_i^{(-)} = \beta_j = 1$ , and only for the  $j$ -grid lines closest to the boundaries do  $d_i^{(+)}$ ,  $d_i^{(-)}$  or  $\beta_j$  differ from 1.

Eqs. (A-21) to (A-25) can be written in the general form:

$$\frac{\partial^2 \psi}{\partial \theta^2} + G_0 \frac{\partial^2 \psi}{\partial \zeta^2} + f_1 \psi = f_2 + f_3 \psi_0 + f_4 \frac{\partial^2 \psi_0}{\partial \zeta^2} \quad (\text{A-44})$$

where:

$$f_1 = -\frac{1}{H_0} \frac{\partial^2 H_0}{\partial \theta^2} \quad (\text{A-45})$$

and where  $f_2$ ,  $f_3$  and  $f_4$  are only functions of  $\theta$  which can be determined by comparing eq. (A-44) with any one of eqs. (A-21) to (A-25). Thus,  $f_3 = f_4 = 0$  for  $\psi = \psi_0, \psi_3$  and  $\psi_4$ .

Referring to fig. 56. eq. (A-44) can be written in finite difference form as:

$$\begin{aligned} & \frac{2G_0}{\beta_j(1+\beta_j)\Delta\zeta^2} \psi_{i-1,j} + \left[ f_{1j} - \frac{2}{d_i^{(+)}d_i^{(-)}\Delta\theta^2} - \frac{2G_0}{\beta_j\Delta\zeta^2} \right] \psi_{i,j} + \frac{2G_0}{(1+\beta_j)\Delta\zeta^2} \psi_{i+1,j} \\ & + \frac{2}{d_i^{(+)}(d_i^{(+)}+d_i^{(-)})\Delta\theta^2} \psi_{i,j-1} + \frac{2}{d_i^{(+)}(d_i^{(+)}+d_i^{(-)})\Delta\theta^2} \psi_{i,j+1} = \\ & f_{2j} + \left[ f_{3j} - \frac{2}{\beta_j\Delta\zeta^2} f_{4j} \right] (\psi_0)_{i,j} + f_{4j} \frac{2}{(1+\beta_j)\Delta\zeta^2} \left[ \frac{1}{\beta_j} (\psi_0)_{i-1,j} + (\psi_0)_{i+1,j} \right] \end{aligned} \quad (\text{A-46})$$

Introduce the n-dimensional vector  $\phi_j$ :

$$\phi_j = \begin{Bmatrix} \psi_{1j} \\ \psi_{2j} \\ \vdots \\ \psi_{nj} \end{Bmatrix} \quad (\text{A-47})$$

whereby eq. (A-46) can be written as:

$$A_j \phi_j + B_j \phi_{j-1} + C_j \phi_{j+1} = F_j \quad (\text{A-48})$$

Here,  $F_j$  is an n-dimensional vector whose n elements are given by the right hand side of eq. (A-46),  $A_j$  is an nxn - matrix, and  $B_j$  and  $C_j$  are nxn - diagonal matrices. Noting that  $\psi_{0j} = 0$  and  $\psi_{n+1,j} = \psi_{n-1,j}$  from the given boundary conditions, the elements of the matrix  $A_j$  become (first index gives row number, second index gives column number):

$$\begin{aligned} (A_j)_{ii} &= f_{1j} - \frac{2}{d_i^{(+)} d_i^{(-)} \Delta \theta^2} - \frac{2G_{0j}}{\beta_j \Delta \xi^2} & \underline{1 \leq i \leq n} \\ (A_j)_{i,i-1} &= \frac{2G_{0j}}{\beta_j (1+\beta_j) \Delta \xi^2} & \underline{2 \leq i \leq n} \\ (A_j)_{n,n-1} &= \frac{2G_{0j}}{\beta_j \Delta \xi^2} & \underline{i=n} \\ (A_j)_{i,i+1} &= \frac{2G_{0j}}{(1+\beta_j) \Delta \xi^2} & \underline{1 \leq i \leq n-1} \end{aligned} \quad (\text{A-49})$$

All other elements are zero such that  $A_j$  is a tri-diagonal matrix. The elements of the  $B_j$  -matrix and  $C_j$  -matrix are:

$$\begin{aligned} (B_j)_{ii} &= \frac{2}{d_i^{(+)} (d_i^{(+)} + d_i^{(-)}) \Delta \theta^2} & \underline{1 \leq i \leq n} \\ (C_j)_{ii} &= \frac{2}{d_i^{(-)} (d_i^{(+)} + d_i^{(-)}) \Delta \theta^2} & \underline{1 \leq i \leq n} \end{aligned} \quad (\text{A-50})$$

All other elements are zero.

To solve eq. (A-48), define an nxn-matrix,  $D_j$ , and an n-dimensional vector  $E_j$ ,

such that:

$$\phi_{j-1} = D_{j-1} \phi_j + E_{j-1} \quad (\text{A-51})$$

Substitution of this expression into eq. (A-48), yields the following recurrence relationships:

$$D_j = -(A_j + B_j D_{j-1})^{-1} C_j = -G_j C_j \quad (\text{A-52})$$

$$E_j = (A_j + B_j D_j)^{-1} (F_j - B_j E_{j-1}) = G_j (F_j - B_j E_{j-1}) \quad (\text{A-53})$$

In figure 55, the points on the free boundary should be at  $j=0$  and  $j=m$ . Since  $\psi = 0$  on the boundary, the boundary condition becomes:

$$\phi_0 = \phi_m = 0 \quad (\text{A-54})$$

Hence, from eq. (A-51):

$$D_0 = E_0 = 0$$

after which eqs. (A-52) and (A-53) can be used to calculate  $D_j$  and  $E_j$  step by step, starting with  $j = 1$ , until  $j = m-1$ . Then eq. (A-51) is employed, letting  $j$  go from  $j = m$ , where  $\phi_m = 0$ , to  $j = 2$ .

In this way the solution for  $\psi$  has been obtained. It should be noted, that since  $A_j$ ,  $B_j$  and  $C_j$  are the same for all the  $\psi$ -equations (i.e. eq. (A-21) to (A-25)), then the  $D_j$ -matrices and the  $G_j$ -matrices are also the same. Thus,  $D_j$  and  $G_j$  can be stored in the first  $\psi$ -calculation and used unchanged in all the remaining  $\psi$ -calculations.

In order to avoid a singularity when  $E_0 = 0$ , it is most convenient to solve for  $\psi_4$  first from eq. (A-25). With  $\psi_0 = -\frac{1}{2} \epsilon_0 \psi_4$  from eq. (A-26), the equation to determine the free boundary, eq. (A-42), becomes:

$$\left(\frac{6 \sin \theta}{H_0}\right) \frac{[1 + (\frac{d\theta}{dz})^2]^{3/2}}{1 + G_0 (\frac{d\theta}{dz})^2} \theta^2 - (\psi_4)_{ij} = 0 \quad (A-55)$$

To solve this equation it is necessary to have a first estimate of the  $\psi_4$  distribution available. For this purposes eqs. (A-52) and (A-53) are used directly such that  $j=0$  corresponds to the leading edge of the bearing arc and  $j = n$  corresponds to the trailing edge of the arc. In the "back-sweep", employing eq. (A-51), any negative value in a  $\phi_j$ -vector is set equal to zero before computing the next  $\phi_j$ -vector. Based on the  $\psi_4$ -distribution determined in this way, eq. (A-55) is solved step by step, letting  $i$  go from  $i=n$  to  $i=1$ . At  $i=n$ ,  $\frac{d\theta}{dz} = 0$  such that eq. (A-55) is readily solved for the corresponding  $\theta$ -value. At subsequent  $i$ -values,  $\frac{d\theta}{dz}$  can be expressed in terms of  $\theta$  and the previous  $\theta$ -values, allowing the complete boundary to be established.

Once the free boundary is known,  $d_i^{(+)}$ ,  $d_i^{(-)}$  and  $\beta_j$  can be found for use in the finite difference equations (see fig. 55), a new  $\psi_4$ -distribution can be computed and the corresponding new boundary can be found. This process is repeated until the relative difference between two subsequent boundaries is smaller than some preassigned error limit. When the final boundary has been established, the solutions for  $\psi_1$ ,  $\psi_2$  and  $\psi_3$  are obtained simply by matrix multiplications.

The film forces have two components acting in the journal center: a radial component  $F_r$  directed towards the bearing center and a tangential component positive in the direction of rotation, (see fig. 54). These forces are obtained by integration of the film pressures  $\bar{P}$ :

$$\left. \begin{matrix} F_r \\ F_t \end{matrix} \right\} = 2 \int_0^{\frac{1}{2}} \int_{\theta_1}^{\theta_2} \bar{P} \begin{Bmatrix} -\cos \theta \\ \sin \theta \end{Bmatrix} R d\theta dz \quad (A-56)$$

or by substitution from eqs. (A-3), (A-7) and (A-8):

$$\left. \begin{aligned} f_r &= \frac{F_r}{SW} = \frac{F_r}{\mu NDL \left(\frac{B}{L}\right)^2} \\ f_t &= \frac{F_t}{SW} = \frac{F_t}{\mu NDL \left(\frac{B}{L}\right)^2} \end{aligned} \right\} = \frac{\pi}{L} \int_0^{\frac{L}{D}} \int_{\theta_1}^{\theta_2} P \begin{Bmatrix} -\cos\theta \\ \sin\theta \end{Bmatrix} d\theta d\xi \quad (\text{A-57})$$

Combining eqs. (A-14), (A-17) and (A-18):

$$P = \frac{\psi}{H} = \frac{\psi_0}{H_0} + \left[ \frac{\psi_1}{H_0} - \frac{H_1}{H_0} \frac{\psi_0}{H_0} \right] \epsilon_1 + \left[ \frac{\psi_2}{H_0} - \frac{H_2}{H_0} \frac{\psi_0}{H_0} \right] \epsilon_0 \phi_1 + \frac{\psi_3}{H_0} \dot{\epsilon}_1 + \frac{\psi_4}{H_0} \epsilon_0 \dot{\phi}_1 \quad (\text{A-58})$$

At the same time,  $f_r$  and  $f_t$  can be expanded as:

$$f_r = f_{r0} + \frac{\partial f_r}{\partial \epsilon} \epsilon_1 + \frac{\partial f_r}{\epsilon_0 \partial \phi} \epsilon_0 \phi_1 + \frac{\partial f_r}{\partial \dot{\epsilon}} \dot{\epsilon}_1 + \frac{\partial f_r}{\epsilon_0 \partial \dot{\phi}} \epsilon_0 \dot{\phi}_1 \quad (\text{A-59})$$

and similarly for  $f_t$ . Thus, substituting eq. (A-58) into eq. (A-57) and comparing with eq. (A-59) results in:

$$\left. \begin{aligned} \frac{\partial f_r}{\partial \epsilon} \\ \frac{\partial f_t}{\partial \epsilon} \end{aligned} \right\} = \frac{\pi}{L} \int_0^{\frac{L}{D}} \int_{\theta_1}^{\theta_2} \left[ \frac{\psi_1}{H_0} - \frac{H_1}{H_0} \frac{\psi_0}{H_0} \right] \begin{Bmatrix} -\cos\theta \\ \sin\theta \end{Bmatrix} d\theta d\xi \quad (\text{A-60})$$

$$\left. \begin{aligned} \frac{\partial f_r}{\epsilon_0 \partial \phi} \\ \frac{\partial f_t}{\epsilon_0 \partial \phi} \end{aligned} \right\} = \frac{\pi}{L} \int_0^{\frac{L}{D}} \int_{\theta_1}^{\theta_2} \left[ \frac{\psi_2}{H_0} - \frac{H_2}{H_0} \frac{\psi_0}{H_0} \right] \begin{Bmatrix} -\cos\theta \\ \sin\theta \end{Bmatrix} d\theta d\xi \quad (\text{A-61})$$

$$\left. \begin{array}{l} \frac{\partial f_r}{\partial \xi} \\ \frac{\partial f_t}{\partial \xi} \end{array} \right\} = \frac{\pi}{L} \int_0^{\frac{L}{D}} \int_0^{\theta_2} \frac{\psi_2}{H_0} \left\{ \begin{array}{l} -\cos \theta \\ \sin \theta \end{array} \right\} d\theta d\xi \quad (\text{A-62})$$

$$\left. \begin{array}{l} \frac{\partial f_r}{\epsilon_0 \partial \phi} \\ \frac{\partial f_t}{\epsilon_0 \partial \phi} \end{array} \right\} = \frac{\pi}{L} \int_0^{\frac{L}{D}} \int_0^{\theta_2} \frac{\psi_2}{H_0} \left\{ \begin{array}{l} -\cos \theta \\ \sin \theta \end{array} \right\} d\theta d\xi \quad (\text{A-63})$$

$$\left. \begin{array}{l} f_{r0} \\ f_{t0} \end{array} \right\} = -\frac{1}{2} \epsilon_0 \left\{ \begin{array}{l} \frac{\partial f_r}{\epsilon_0 \partial \phi} \\ \frac{\partial f_t}{\epsilon_0 \partial \phi} \end{array} \right\} \quad (\text{A-64})$$

For convenience in combining several bearing lobes and also to eliminate the changing polar coordinate system (i.e.  $\phi_0$  changes with applied static load), a fixed cartesian in x-y-coordinate system is introduced as shown in fig. 54. The following coordinate transformations are readily deduced:

$$-F_x = F_r \cos \phi_0 + F_t \sin \phi_0 \quad (\text{A-65})$$

$$-F_y = F_r \sin \phi_0 - F_t \cos \phi_0 \quad (\text{A-66})$$

$$\frac{x}{C} = \epsilon \cos \phi \quad (\text{A-67})$$

$$\frac{y}{c} = \epsilon \sin \varphi \quad (\text{A-68})$$

from which:

$$\frac{\partial \epsilon}{\partial x} = \frac{1}{c} \cos \varphi_0 \quad \frac{\partial \varphi}{\partial x} = -\frac{1}{c \epsilon_0} \sin \varphi_0 \quad (\text{A-69})$$

$$\frac{\partial \epsilon}{\partial y} = \frac{1}{c} \sin \varphi_0 \quad \frac{\partial \varphi}{\partial y} = \frac{1}{c \epsilon_0} \cos \varphi_0$$

Thus, from eqs. (A-65) and (A-66):

$$\frac{CK_{xx}}{SW} = -\frac{C \partial}{\partial x} \left( \frac{F_x}{SW} \right) = \left( \frac{\partial f_r}{\partial \epsilon} \cos \varphi_0 + \frac{\partial f_t}{\partial \epsilon} \sin \varphi_0 \right) \cos \varphi_0 - \left( \frac{\partial f_r}{\epsilon_0 \partial \varphi} \cos \varphi_0 + \frac{\partial f_t}{\epsilon_0 \partial \varphi} \sin \varphi_0 \right) \sin \varphi_0 \quad (\text{A-70})$$

$$\frac{CK_{xy}}{SW} = -\frac{C \partial}{\partial y} \left( \frac{F_x}{SW} \right) = \left( \frac{\partial f_r}{\partial \epsilon} \cos \varphi_0 + \frac{\partial f_t}{\partial \epsilon} \sin \varphi_0 \right) \sin \varphi_0 + \left( \frac{\partial f_r}{\epsilon_0 \partial \varphi} \cos \varphi_0 + \frac{\partial f_t}{\epsilon_0 \partial \varphi} \sin \varphi_0 \right) \cos \varphi_0 \quad (\text{A-71})$$

$$\frac{CK_{yx}}{SW} = -\frac{C \partial}{\partial x} \left( \frac{F_y}{SW} \right) = \left( \frac{\partial f_r}{\partial \epsilon} \sin \varphi_0 - \frac{\partial f_t}{\partial \epsilon} \cos \varphi_0 \right) \cos \varphi_0 - \left( \frac{\partial f_r}{\epsilon_0 \partial \varphi} \sin \varphi_0 - \frac{\partial f_t}{\epsilon_0 \partial \varphi} \cos \varphi_0 \right) \sin \varphi_0 \quad (\text{A-72})$$

$$\frac{CK_{yy}}{SW} = -\frac{C \partial}{\partial y} \left( \frac{F_y}{SW} \right) = \left( \frac{\partial f_r}{\partial \epsilon} \sin \varphi_0 - \frac{\partial f_t}{\partial \epsilon} \cos \varphi_0 \right) \sin \varphi_0 + \left( \frac{\partial f_r}{\epsilon_0 \partial \varphi} \sin \varphi_0 - \frac{\partial f_t}{\epsilon_0 \partial \varphi} \cos \varphi_0 \right) \cos \varphi_0 \quad (\text{A-73})$$

$$\frac{C \omega B_{xx}}{SW} = -\frac{C \partial}{\omega \partial \left( \frac{dx}{dt} \right)} \left( \frac{F_x}{SW} \right) = \left( \frac{\partial f_r}{\partial \epsilon} \cos \varphi_0 + \frac{\partial f_t}{\partial \epsilon} \sin \varphi_0 \right) \cos \varphi_0 - \left( \frac{\partial f_r}{\epsilon_0 \partial \varphi} \cos \varphi_0 + \frac{\partial f_t}{\epsilon_0 \partial \varphi} \sin \varphi_0 \right) \sin \varphi_0 \quad (\text{A-74})$$

$$\frac{C \omega B_{xy}}{SW} = -\frac{C \partial}{\omega \partial \left( \frac{dy}{dt} \right)} \left( \frac{F_x}{SW} \right) = \left( \frac{\partial f_r}{\partial \epsilon} \cos \varphi_0 + \frac{\partial f_t}{\partial \epsilon} \sin \varphi_0 \right) \sin \varphi_0 + \left( \frac{\partial f_r}{\epsilon_0 \partial \varphi} \cos \varphi_0 + \frac{\partial f_t}{\epsilon_0 \partial \varphi} \sin \varphi_0 \right) \cos \varphi_0 \quad (\text{A-75})$$

$$\frac{C\omega B_{yx}}{SW} = -\frac{C}{\omega} \frac{\partial}{\partial t} \left( \frac{F_y}{SW} \right) = \left( \frac{\partial f_r}{\partial \xi} \sin \phi_0 - \frac{\partial f_t}{\partial \xi} \cos \phi_0 \right) \cos \phi_0 - \left( \frac{\partial f_r}{\partial \phi} \sin \phi_0 - \frac{\partial f_t}{\partial \phi} \cos \phi_0 \right) \sin \phi_0 \quad (A-76)$$

$$\frac{C\omega B_{yy}}{SW} = -\frac{C}{\omega} \frac{\partial}{\partial t} \left( \frac{F_y}{SW} \right) = \left( \frac{\partial f_r}{\partial \xi} \sin \phi_0 - \frac{\partial f_t}{\partial \xi} \cos \phi_0 \right) \sin \phi_0 + \left( \frac{\partial f_r}{\partial \phi} \sin \phi_0 - \frac{\partial f_t}{\partial \phi} \cos \phi_0 \right) \cos \phi_0 \quad (A-77)$$

$$-\frac{F_{x0}}{SW} = f_{r0} \cos \phi_0 + f_{t0} \sin \phi_0 \quad (A-78)$$

$$-\frac{F_{y0}}{SW} = f_{r0} \sin \phi_0 - f_{t0} \cos \phi_0 \quad (A-79)$$

The forces acting on the journal can, therefore be written:

$$F_x = F_{x0} - K_{xx}x - B_{xx} \frac{dx}{dt} - K_{xy}y - B_{xy} \frac{dy}{dt} \quad (A-80)$$

$$F_y = F_{y0} - K_{yy}y - B_{yy} \frac{dy}{dt} - K_{yx}x - B_{yx} \frac{dx}{dt} \quad (A-81)$$

The static load on the bearing pad is W where:

$$W = \sqrt{F_{r0}^2 + F_{t0}^2} \quad (A-82)$$

or, with the definition of  $f_r$  and  $f_t$  from eq. (A-57):

$$S = \frac{1}{\sqrt{f_{r0}^2 + f_{t0}^2}} \quad (\text{A-83})$$

The friction force  $F_f$  acting on the journal is determined by integrating the shear stress over the wetted area of the journal. The shear stress is:

$$\bar{\tau} = \frac{1}{2} R_h C_f \frac{\mu R \omega}{h} + \frac{1}{2} \bar{h} \frac{\partial P}{R \partial \theta} \quad (\text{A-84})$$

where  $C_f$  is the turbulent friction coefficient. In laminar flow with  $R_e = 0$ ,  $\frac{1}{2} R_h C_f = 1$ . For details, see reference 1.

The total friction force then becomes:

$$F_f = 2 \int_0^{\frac{1}{2}} \int_{\theta_1}^{\theta_2} \bar{\tau} R d\theta dz$$

Introducing  $\bar{\tau}$  from eq. (A-84) and making the equation dimensionless by means of eqs. (A-3), (A-5), (A-7) and (A-8) results in:

$$\frac{R}{C} \frac{F_f}{SW} = \pi \int_{\theta_1}^{\theta_2} \frac{1}{2} R_h C_f \frac{1}{h} d\theta + \frac{1}{2} \frac{\pi}{D} \int_0^{\frac{1}{2}} \int_{\theta_1}^{\theta_2} h \frac{\partial P}{\partial \theta} d\theta d\xi \quad (\text{A-85})$$

where  $R \cdot F_f$  is the total friction torque. The last integral in this equation can be reduced as follows:

$$\int_{\theta_1}^{\theta_2} h \frac{\partial P}{\partial \theta} d\theta = \int_{\theta_1}^{\theta_2} h dP = hP \Big|_{\theta_1}^{\theta_2} - \int_{\theta_1}^{\theta_2} P \frac{dh}{d\theta} d\theta = \epsilon_0 \int_{\theta_1}^{\theta_2} P \sin \theta d\theta$$

whereby eq. (A-85) becomes:

$$\frac{R}{C} \frac{F_f}{5W} = \pi \int_{\theta_1}^{\theta_2} \frac{\frac{1}{2} R h C_f}{h} d\theta + \frac{\epsilon_0}{2} f_{t0} \quad (\text{A-86})$$

Turning next to the flow, the volume flow per inch in the circumferential direction is:

$$q_x = \frac{1}{2} R \omega \bar{h} - G_x \frac{\bar{h}^3}{12\mu} \frac{\partial \bar{P}}{R \partial \theta}$$

The volume flow per inch in the axial direction is:

$$q_z = -G_z \frac{\bar{h}^3}{12\mu} \frac{\partial \bar{P}}{\partial z}$$

The total flow is found by integration which, in dimensionless form becomes:

$$\left[ \frac{Q_x}{\text{NDLC}} \right]_{\text{lead.edge}} = \left[ \frac{\pi}{2} h - \frac{\pi}{12} G_x h^3 \frac{1}{\frac{L}{D}} \int_0^{\frac{b}{D}} \frac{\partial P}{\partial \theta} d\zeta \right]_{\theta=\theta_1} \quad (\text{A-87})$$

$$\left[ \frac{Q_x}{\text{NDLC}} \right]_{\text{trail.edge}} = \left[ \frac{\pi}{2} h - \frac{\pi}{12} G_x h^3 \frac{1}{\frac{L}{D}} \int_0^{\frac{b}{D}} \frac{\partial P}{\partial \theta} d\zeta \right]_{\theta=\theta_2} \quad (\text{A-88})$$

$$\left[ \frac{Q_z}{\text{NDLC}} \right]_{\text{sides}} = -\frac{\pi}{12} \frac{1}{\frac{L}{D}} \int_{\theta_1}^{\theta_2} G_z h^3 \left( \frac{\partial P}{\partial \zeta} \right)_{\zeta=\frac{1}{2}} d\theta \quad (\text{A-89})$$

where  $Q_z$  is the total side flow (i.e. for both sides of the bearing). For flow continuity:

$$(Q_x)_{\text{lead.edge}} = (Q_x)_{\text{trail.edge}} + (Q_z)_{\text{sides}} \quad (\text{A-90})$$

If there is film rupture at either the leading edge, at the trailing edge or at both edges, the integrals in eqs. (A-87) and/or (A-88) are zero, and the remaining term,  $\int \frac{1}{2} h$  must be integrated along the boundary.

Having described the calculation of the dynamic coefficients, the load carrying capacity, the friction force and the flow, it remains to determine the various functions in the basic eqs. (A-21) to (A-25). With:

$$h_0 = 1 + \epsilon_0 \cos \theta \quad (\text{A-91})$$

the derivatives of  $H_0$  become:

$$\frac{1}{H_0} \frac{\partial H_0}{\partial \theta} = \frac{1}{H_0} \frac{dH_0}{dh_0} \frac{dh_0}{d\theta} \quad (\text{A-92})$$

$$\frac{1}{H_0} \frac{\partial^2 H_0}{\partial \theta^2} = \frac{1}{H_0} \frac{dH_0}{dh_0} \frac{d^2 h_0}{d\theta^2} + \frac{1}{H_0} \frac{d^2 H_0}{dh_0^2} \left( \frac{dh_0}{d\theta} \right)^2 \quad (\text{A-93})$$

where (see eq. (A-13)):

$$H_0 = h_0^{3/2} G_x^{1/2} \quad (\text{A-94})$$

Expansion of  $H$  yields:

$$H = H_0 + \frac{dH_0}{dh_0} (h - h_0) = H_0 + \epsilon_1 \frac{dH_0}{dh_0} \cos \theta + \epsilon_0 \phi_1 \frac{dH_0}{dh_0} \sin \theta \quad (\text{A-95})$$

or, by comparison with eq. (A-18):

$$\frac{1}{H_0} H_1 = \frac{1}{H_0} \frac{dH_0}{dh_0} \cos \theta \quad (\text{A-96})$$

$$\frac{1}{H_0} H_2 = \frac{1}{H_0} \frac{dH_0}{dh_0} \sin \theta \quad (\text{A-97})$$

from which:

$$\frac{1}{H_0} \frac{\partial^3 H_1}{\partial \theta^3} = -\cos \theta \frac{1}{H_0} \frac{dH_0}{dh_0} + \left[ \frac{d^2 h_0}{d\theta^2} \cos \theta - 2 \frac{dh_0}{d\theta} \sin \theta \right] \frac{1}{H_0} \frac{d^2 H_0}{dh_0^2} + \left( \frac{dh_0}{d\theta} \right)^2 \cos \theta \frac{1}{H_0} \frac{d^3 H_0}{dh_0^3} \quad (\text{A-98})$$

$$\frac{1}{H_0} \frac{\partial^3 H_2}{\partial \theta^3} = -\sin \theta \frac{1}{H_0} \frac{dH_0}{dh_0} + \left[ \frac{d^2 h_0}{d\theta^2} \sin \theta + 2 \frac{dh_0}{d\theta} \cos \theta \right] \frac{1}{H_0} \frac{d^2 H_0}{dh_0^2} + \left( \frac{dh_0}{d\theta} \right)^2 \sin \theta \frac{1}{H_0} \frac{d^3 H_0}{dh_0^3} \quad (\text{A-99})$$

These equations contain the first three derivatives of  $H_0$  with respect to  $h_0$ .

The derivatives are found from Eq. (A-94):

$$\frac{1}{H_0} \frac{dH_0}{dh_0} = \frac{3}{2} \frac{1}{h_0} + \frac{1}{2} \frac{1}{G_x} \frac{dG_x}{dh_0} \quad (\text{A-100})$$

$$\frac{1}{H_0} \frac{d^2 H_0}{dh_0^2} = \frac{3}{4} \frac{1}{h_0^2} + \frac{3}{2} \frac{1}{h_0} \frac{1}{G_x} \frac{dG_x}{dh_0} - \frac{1}{4} \left( \frac{1}{G_x} \frac{dG_x}{dh_0} \right)^2 + \frac{1}{2} \frac{1}{G_x} \frac{d^2 G_x}{dh_0^2} \quad (\text{A-101})$$

$$\begin{aligned} \frac{1}{H_0} \frac{d^3 H_0}{dh_0^3} = & -\frac{3}{8} \frac{1}{h_0^3} + \frac{9}{8} \frac{1}{h_0^2} \frac{1}{G_x} \frac{dG_x}{dh_0} - \frac{9}{8} \frac{1}{h_0} \left( \frac{1}{G_x} \frac{dG_x}{dh_0} \right)^2 + \frac{3}{8} \left( \frac{1}{G_x} \frac{dG_x}{dh_0} \right)^3 \\ & - \frac{3}{4} \frac{1}{G_x} \frac{d^2 G_x}{dh_0^2} \frac{1}{G_x} \frac{d^2 G_x}{dh_0^2} + \frac{9}{4} \frac{1}{h_0} \frac{1}{G_x} \frac{d^2 G_x}{dh_0^2} + \frac{1}{2} \frac{1}{G_x} \frac{d^3 G_x}{dh_0^3} \end{aligned} \quad (\text{A-102})$$

where

$$\begin{aligned}\frac{1}{G_x} \frac{dG_x}{dh_0} &= R_e \left( \frac{1}{G_x} \frac{dG_x}{dR_h} \right) \\ \frac{1}{G_x} \frac{d^2G_x}{dh_0^2} &= R_e^2 \left( \frac{1}{G_x} \frac{d^2G_x}{dR_h^2} \right) \\ \frac{1}{G_x} \frac{d^3G_x}{dh_0^3} &= R_e^3 \left( \frac{1}{G_x} \frac{d^3G_x}{dR_h^3} \right)\end{aligned}\tag{A-103}$$

Since  $G_x$  is a given function of the local Reynolds number  $R_h$ , the three derivatives of  $G_x$  are known. For laminar flow, these derivatives are zero.

Similarly, eq. (A-12) can be expanded:

$$G = G_0 + \frac{dG_0}{dh_0} (h - h_0) = G_0 + \epsilon_1 \frac{dG_0}{dh_0} \cos\theta + \epsilon_0 \phi_1 \frac{dG_0}{dh_0} \sin\theta\tag{A-104}$$

where:

$$\epsilon_1 = \frac{u_1}{G_x}\tag{A-105}$$

Comparing eqs. (A-104) and (A-105):

$$G_1 = \frac{dG_0}{dh_0} \cos\theta = R_e \frac{d}{dR_h} \left( \frac{G_z}{G_x} \right) \cos\theta\tag{A-106}$$

$$G_2 = \frac{dG_0}{dh_0} \sin\theta = R_e \frac{d}{dR_h} \left( \frac{G_z}{G_x} \right) \sin\theta$$

In this way, all the coefficients in eqs. (A-24) to (A-25) can be evaluated and the equations can be solved as previously discussed.

**BLANK PAGE**

APPENDIX II: The Static and Dynamic Performance of the Three Lobe Bearing with Turbulent Film

The three lobe bearing is made up of three arcs:

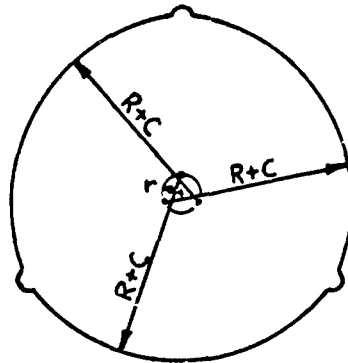


Figure 57: Three Lobe Bearing

The centers of curvature of the arcs do not coincide with the center of the bearing. Instead, the centers lie on a small circle with radius  $r$ . In this way the lobes are pre-loaded.

For the purpose of generality, assume that each lobe has its own pre-load radius  $r=r_p$ . Introduce a cartesian  $x$ - $y$  - coordinate system with origin in the bearing center and the  $x$ -axial in the direction of the applied static load:

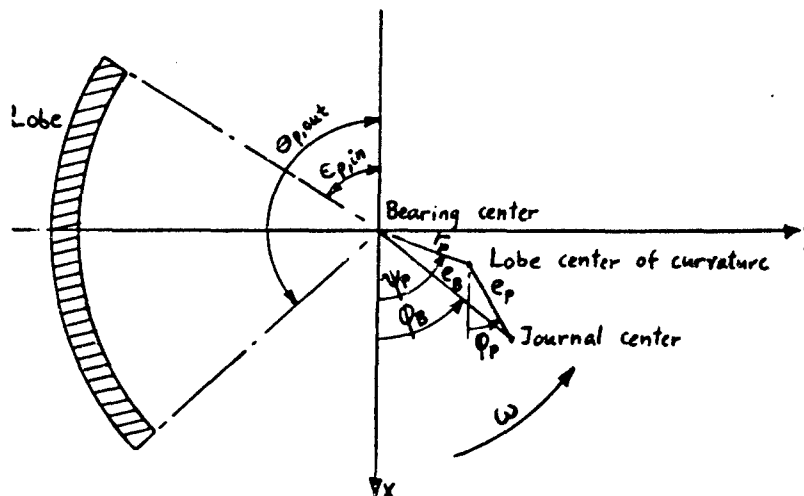


Figure 58: Geometry of Single Lobe

The journal radius is  $R$  and the lobes have the common radius of curvature:  $R+C$ , where  $C$  is the radial clearance. The center of the lobe is removed from the bearing center by a distance  $r_p$ , and the angle between the x-axis and the line connecting the two centers is  $\psi_p$ . The distance between the journal center and the lobe center is the lobe eccentricity  $e_p$ , and  $\phi_p$  is the angle between the x-axis and the line connecting the two centers. With respect to the bearing center, the journal center has the eccentricity  $e_B$  and the attitude angle  $\phi_B$ . From fig. 58.

$$e_B \cos \phi_B = e_p \cos \phi_p + r_p \cos \psi_p \quad (B-1)$$

$$e_B \sin \phi_B = e_p \sin \phi_p + r_p \sin \psi_p$$

Introduce the eccentricity ratios:

$$\epsilon_B = \frac{e_B}{C} \quad (B-2)$$

$$\epsilon_p = \frac{e_p}{C}$$

and the preload:

$$\delta_p = \frac{r_p}{C} \quad (B-3)$$

whereby eq. (B-1) becomes:

$$\epsilon_p \cos \phi_p = \epsilon_B \cos \phi_B - \delta_p \cos \psi_p \quad (B-4)$$

$$\epsilon_p \sin \phi_p = \epsilon_B \sin \phi_B - \delta_p \sin \psi_p$$

Hence:

$$\epsilon_p = \sqrt{(\epsilon_B \cos \phi_B - \delta_p \cos \psi_p)^2 + (\epsilon_B \sin \phi_B - \delta_p \sin \psi_p)^2} \quad (B-5)$$

$$\phi_p = \tan^{-1} \left[ \frac{E_B \sin \phi_B - \delta_p \sin \psi_p}{E_B \cos \phi_B - \delta_p \cos \psi_p} \right] \quad (\text{B-6})$$

Thus, for given coordinates of the journal center with respect to the bearing center, the corresponding lobe eccentricity ratio and attitude angle can be determined. The angles from the line of centers to the beginning and the end of the lobe become:

$$\theta_1 = \theta_{p,in} - \phi_p \quad (\text{B-7})$$

$$\theta_2 = \theta_{p,out} - \phi_p$$

Thereby all the data required for calculating the lobe are known. The calculation is described in Appendix I. Performing calculations for each of the  $n$  lobes making up the bearing, the properties of the composite bearing are obtained by a simple summation over the lobes:

$$-\frac{F_{x0}}{\mu NDL \left(\frac{R}{C}\right)^2} = \sum_1^n \left( -\frac{F_{x2}}{SW} \right)_p \quad (\text{B-8})$$

$$\frac{F_{y0}}{\mu NDL \left(\frac{R}{C}\right)^2} = \sum_1^n \left( \frac{F_{y0}}{SW} \right)_p \quad (\text{B-9})$$

$$\frac{R}{C} \frac{F_z}{\mu NDL \left(\frac{R}{C}\right)^2} = \sum_1^n \left( \frac{R}{C} \frac{F_z}{SW} \right)_p \quad (\text{B-10})$$

$$\frac{Q_z}{NDLC} = \sum_1^n \left( \frac{Q_z}{NDLC} \right)_p \quad (\text{B-11})$$

$$\frac{CK_{xx}}{\mu NDL \left(\frac{R}{C}\right)^2} = \sum_1^n \left(\frac{CK_{xx}}{SW}\right)_p \quad (B-12)$$

$$\frac{C\omega B_{xx}}{\mu NDL \left(\frac{R}{C}\right)^2} = \sum_1^n \left(\frac{C\omega B_{xx}}{SW}\right)_p \quad (B-13)$$

and similarly for the 6 remaining dynamic coefficients.

The total hydrodynamic bearing flow is the side flow  $Q_z$ . To this should be added, however, any "surplus" flow from the grooves between the lobes. To illustrate, the circumferential flow from lobe  $p$  into the groove separating lobe  $p$  and lobe  $(p+1)$ , is  $(Q_x)_{p, \text{trail edge}}$  (see Appendix I, eq. (A-88)). Similarly, the circumferential flow out of the groove is  $(Q_x)_{p+1, \text{lead edge}}$ . If  $(Q_x)_{p, \text{trail edge}}$  is greater than  $(Q_x)_{p+1, \text{lead edge}}$ , the difference should be added to  $Q_z$ . Otherwise, there is no surplus flow.

If in eqs. (B-8) to (B-13), the  $x$ -direction is considered to be the direction of the applied load  $W$ , then for static equilibrium:

$$F_{y_0} = 0 \quad (B-14)$$

$$-F_{x_0} = W \quad (B-15)$$

This condition is satisfied by performing the calculations with a fixed value of  $\epsilon_B \cos \phi_B$  and vary  $\epsilon_B \sin \phi_B$  until eq. (B-14) is fulfilled. Then, combining eqs. (B-15) and (B-8):

$$S = \frac{\mu NDL}{W} \left(\frac{R}{C}\right)^2 = \left(-\frac{F_{x_0}}{\mu NDL \left(\frac{R}{C}\right)^2}\right)^{-1} \quad (B-16)$$

where  $S$  is the Sommerfeld number for the bearing. Thereafter the bearing friction and the dynamic coefficients can be given in a different dimensionless form than in eqs. (B-10), (B-12) and (B-13):

$$\frac{R}{C} \frac{F_f}{W} = S \left( \frac{R}{C} \frac{F_f}{\mu NDL \left(\frac{R}{C}\right)^2} \right) \quad (\text{B-17})$$

$$\frac{CK_{xx}}{W} = S \left( \frac{CK_{xx}}{\mu NDL \left(\frac{R}{C}\right)^2} \right) \quad (\text{B-18})$$

$$\frac{C\omega B_{xx}}{W} = S \left( \frac{C\omega B_{xx}}{\mu NDL \left(\frac{R}{C}\right)^2} \right) \quad (\text{B-19})$$

and similarly for the 6 remaining coefficients. This latter form is to be preferred except when the bearing is unloaded in which case the original expressions are employed.

In order to express the stability properties of the bearing, a symmetrical, rigid rotor with a mass of  $2M$  is considered. The rotor is supported in two identical bearings. Assuming the translatory critical speed to be the lowest (corresponds approximately to requiring that the transverse radius of gyration of the rotor is less than half the bearing span which is normally the case), the motions of the two journals in their bearings will be in phase and be the same. Hence, the mass of the rotor can be divided in two equal parts, each of mass  $M$ , and lumped at the journals. Hence, the equations of motion for a journal become:

$$M \frac{d^2x}{dt^2} = -K_{xx}x - B_{xx} \frac{dx}{dt} - K_{xy}y - B_{xy} \frac{dy}{dt} \quad (\text{B-20})$$

$$M \frac{d^2y}{dt^2} = -K_{yx}x - B_{yx} \frac{dx}{dt} - K_{yy}y - B_{yy} \frac{dy}{dt}$$

At the threshold of instability,  $x$  and  $y$  are pure harmonic motions with frequency  $\nu$ , i.e.:

$$x = x_c \cos(\nu t) - x_s \sin(\nu t) = (x_c + ix_s)e^{i\nu t} \quad (\text{B-21})$$

and similarly for  $y$  where:

$$i = \sqrt{-1} \quad (\text{B-22})$$

Hence, eq. (B-20) can be written:

$$\begin{Bmatrix} (K_{xx} - M\nu^2 + i\nu B_{xx}) & (K_{xy} + i\nu B_{xy}) \\ (K_{yx} + i\nu B_{yx}) & (K_{yy} - M\nu^2 + i\nu B_{yy}) \end{Bmatrix} \begin{Bmatrix} x \\ y \end{Bmatrix} = 0 \quad (\text{B-23})$$

These two equations only have a non-trivial solution when the determinant is zero. Equating the real part and the imaginary part of the determinant to zero results in:

$$M\nu^2 = \frac{K_{xx} B_{yy} + K_{yy} B_{xx} - K_{xy} B_{yx} - K_{yx} B_{xy}}{B_{xx} + B_{yy}} \quad (\text{B-24})$$

$$\nu^2 = \frac{(K_{xx} - M\nu^2)(K_{yy} - M\nu^2) - K_{xy} K_{yx}}{B_{xx} B_{yy} - B_{xy} B_{yx}} \quad (\text{B-25})$$

Computing eq. (B-24) first,  $M\nu^2$  can be substituted into eq. (B-25) whereby the instability frequency  $\nu$  is determined. Thereafter the corresponding journal mass  $M$  is readily obtained.

The results are most conveniently represented in dimensionless form. For this

purpose, eqs. (B-24) and (B-25) are written:

$$4\pi^2 \frac{CMN}{\mu DL \left(\frac{B}{L}\right)^2} \left(\frac{\nu}{\omega}\right)^2 = \frac{\frac{CK_{xx}}{SW} \cdot \frac{C\omega B_{yy}}{SW} + \frac{CK_{yy}}{SW} \frac{C\omega B_{xx}}{SW} - \frac{CK_{xy}}{SW} \frac{C\omega B_{yx}}{SW} - \frac{CK_{yx}}{SW} \frac{C\omega B_{xy}}{SW}}{\frac{C\omega B_{xx}}{SW} + \frac{C\omega B_{yy}}{SW}} \quad (B-26)$$

$$\left(\frac{\nu}{\omega}\right)^2 = \frac{\left[\frac{CK_{xx}}{SW} - 4\pi^2 \frac{CMN}{\mu DL \left(\frac{B}{L}\right)^2} \left(\frac{\nu}{\omega}\right)^2\right] \left[\frac{CK_{yy}}{SW} - 4\pi^2 \frac{CMN}{\mu DL \left(\frac{B}{L}\right)^2} \left(\frac{\nu}{\omega}\right)^2\right] - \frac{CK_{xy}}{SW} \frac{CK_{yx}}{SW}}{\frac{C\omega B_{xx}}{SW} \frac{C\omega B_{yy}}{SW} - \frac{C\omega B_{xy}}{SW} \frac{C\omega B_{yx}}{SW}} \quad (B-27)$$

where the 8 bearing coefficients are in dimensionless form as defined by equations (B-12) and (B-13).

The ratio  $\frac{\nu}{\omega}$  between the instability frequency and the rotational speed is known as the frequency ratio. Under most conditions,  $\frac{\nu}{\omega} \cong \frac{1}{2}$ . The instability mass can either be expressed in the form given by eq. (B-26) or in the form:

$$\frac{CM\omega^2}{W} = 4\pi^2 S \frac{CMN}{\mu DL \left(\frac{B}{L}\right)^2} \quad (B-28)$$

**BLANK PAGE**

APPENDIX III: The Stiffness and the Damping of a Hydrostatic Bearing with an Incompressible Lubricant

In the hydrodynamic-hydrostatic ring bearing where the lubricant is a liquid (incompressible), the outer bearing is a purely hydrostatic bearing. This appendix describes the analysis for calculating the flow, the stiffness and the damping of a hydrostatic bearing.

The basic equation governing the flow through the bearing film is Reynolds equation in which there is no contribution from journal rotation:

$$\frac{\partial}{R \partial \theta} \left[ \frac{\bar{h}^3}{12\mu} \frac{\partial \bar{P}}{R \partial \theta} \right] + \frac{\partial}{\partial z} \left[ \frac{\bar{h}^3}{12\mu} \frac{\partial \bar{P}}{\partial z} \right] = \frac{\partial \bar{h}}{\partial t} \quad (C-1)$$

Here,  $\bar{P}$  is the film pressure,  $\mu$  is the lubricant viscosity,  $t$  is time,  $R$  is journal radius (outer radius of ring),  $\theta$  is the angular coordinate,  $z$  is the axial coordinate and  $\bar{h}$  is the film thickness:

$$\bar{h} = C + e \cos \theta \quad (C-2)$$

where  $C$  is the radial clearance and  $e$  is the eccentricity between the bearing center and the journal center.

To make Reynolds equation dimensionless, set:

$$P = \frac{P_0}{P_0} \quad (C-3)$$

$$h = \frac{\bar{h}}{C} \quad (C-4)$$

$$z = \frac{z}{R} \quad (C-5)$$

$$\tau = \nu t \quad (C-6)$$

Thereby eq. (C-1) becomes:

$$\frac{d}{d\theta} \left( h^3 \frac{dP}{d\theta} \right) + \frac{d}{d\xi} \left( h^3 \frac{dP}{d\xi} \right) = \sigma \frac{dh}{d\tau} \quad (C-7)$$

where:

$$\sigma = \frac{12\mu\nu}{P_s} \left( \frac{R}{C} \right)^2 \quad (C-8)$$

$P_s$  is the supply pressure of the lubricant to the bearing and  $\nu$  is the frequency of the motion of the journal.

The flow is supplied to the bearing through restricted feeder holes. The flow restriction may either be accomplished by an orifice or by a thin tube, the latter method denoted as the laminar restrictor. In the case of an orifice the mass flow through the feeder hole is given by:

$$\text{Orifice Restrictor} \quad M_B = C_D \pi a^2 \frac{\sqrt{\rho (P_s - \bar{P}'_c)}}{\sqrt{1 + \left( \frac{a}{h} \right)^2}} \quad (C-9)$$

where  $M_B$  is the mass flow in lbs.sec/inch,  $C_D$  is a discharge coefficient,  $a$  is the radius of the orifice,  $\rho$  is the mass density of the lubricant,  $\bar{P}'_c$  is the pressure downstream of the feeder hole at the inlet to the bearing film,  $h$  is the dimensionless film thickness at the feeder hole and  $\delta$  is the inherent compensation factor:

$$\delta = \frac{a^2}{dC}$$

$d$  is the diameter of the feeding hole. Thus eq. (C-9) assumes a pressure drop both through the orifice and through the "curtain" area between the rim of the feeder hole and the journal surface. When  $\delta \cong 0$ , the flow restriction takes place only in the orifice whereas  $\delta \rightarrow \infty$  means that the curtain area dominates as the restricting mechanism.

It is also possible to restrict the flow by simply relying on the feeder hole itself to provide the restriction. The viscous drag in the hole causes a drop in pressure as the flow passes through. The relationship is given by:

$$\text{Laminar Restrictor} \quad M_B = \frac{\pi \rho a^4}{8 \mu l} (P_s - \bar{P}'_c) \quad (C-10)$$

where  $l$  is the length of the feeder hole,  $a$  is the radius of the feeder hole and the other symbols are defined above.

The two restrictor equations can be written in dimensionless form as:

$$\frac{3 \mu n M_B}{\pi \rho C^3 P_s} \lambda \xi_2 = \Lambda_s m \quad (C-11)$$

where:

$$\Lambda_s = \begin{cases} \frac{3 \mu C_D n a^2}{C^3 \sqrt{\rho P_s} \sqrt{1 + \delta^2}} \lambda \xi_2 & \text{Orifice Restrictor} \\ \frac{3}{8} \frac{n a^4}{C^3 l} \lambda \xi_2 & \text{Laminar Restrictor} \end{cases} \quad (C-12)$$

$$m = \begin{cases} \frac{\sqrt{1-P_c'}}{\sqrt{(1+(\frac{\delta}{h})^2)/(1+\delta^2)}} & \text{Orifice Restrictor} \\ (1-P_c') & \text{Laminar Restrictor} \end{cases} \quad (C-13)$$

Here,  $P_c' = \bar{P}_c'/P_s$  which defines the pressure ratio across the feeder hole. The symbols  $\lambda$  and  $\xi_2$  will be defined later.

$\lambda_s$  is known as the restrictor coefficient and it is the governing parameter for the performance of the hydrostatic bearing. It defines the ratio between the flow resistance of the bearing film and the flow resistance of the feeder holes.

To calculate the bearing performance, Reynolds equation, eq. (C-7), must be solved together with the feeder hole flow equation, eq. (C-11). The present solution will be based on the fact that the journal in a hydrostatic bearing normally operates close to its concentric position. This means that the journal center eccentricity  $e$  is small compared to the radial clearance  $C$ , or in terms of the eccentricity ratio  $\epsilon$  :

$$\epsilon = \frac{e}{C} \quad (C-14)$$

$\epsilon$  is much smaller than 1 (in practice the solution is a valid approximation for  $\epsilon$ - values as large as 0.4 to 0.5). Thus, the dimensionless pressure can be written as:

$$P = P_0 + \epsilon P_1 + \dot{\epsilon} P_2 \quad (C-15)$$

where:

$$\dot{\epsilon} = \frac{d\epsilon}{d\tau} = \frac{1}{C\nu} \frac{de}{dt} \quad (C-16)$$

The dimensionless film thickness is found from eqs. (C-2) and (C-4) as:

$$h = 1 + \epsilon \cos \theta \quad (C-17)$$

Substitute eqs. (C-15) and (C-17) into eq. (C-7) and collect terms according to the perturbation variables:

$$\frac{\partial^2 P_0}{\partial \theta^2} + \frac{\partial^2 P_0}{\partial \xi^2} = 0 \quad (C-18)$$

$$\frac{\partial^2 P_1}{\partial \theta^2} + \frac{\partial^2 P_1}{\partial \xi^2} = 3 \sin \theta \frac{\partial P_0}{\partial \theta} \quad (C-19)$$

$$\frac{\partial^2 P_2}{\partial \theta^2} + \frac{\partial^2 P_2}{\partial \xi^2} = \sigma \cos \theta \quad (C-20)$$

Consider first eq. (C-18) which gives the solution for the pressure in the film when the journal is concentric in the bearing. Under that condition each feeder hole has the same flow and in the analysis it is only necessary to consider an axial strip belonging to one feeder hole:

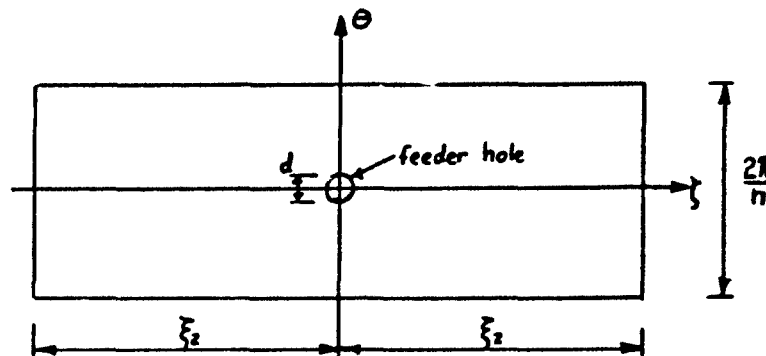


Figure 59: Axial Strip

The strip extends over the length  $L_z$  of the bearing and its width is  $2\pi R/n$ . Hence, the ranges of the coordinates are:

$$-\frac{L_2}{2} \leq z \leq \frac{L_2}{2}$$

$$-\frac{\pi R}{n} \leq R\theta \leq \frac{\pi R}{n}$$

or dimensionless:

$$-\xi_2 \leq \zeta \leq \xi_2$$

$$-\frac{\pi}{n} \leq \theta \leq \frac{\pi}{n}$$
(C-21)

where:

$$\xi_2 = \frac{L_2}{D}$$
(C-22)

and  $D = 2R$  is the diameter of the bearing.

The boundary conditions are that the pressure is ambient, (i.e. it is zero) at the ends of the bearing and there is no flow across the sides of the strip:

$$\text{for } \zeta = \pm \xi_2: \quad P_0 = 0$$
(C-23)

$$\text{for } \theta = \pm \frac{\pi}{n}: \quad \frac{\partial P_0}{\partial \theta} = 0$$

The solution of eq. (C-18) is then the solution of the potential equation for a rectangle with a source in the center. If the source strength in  $\bar{C}$ , the solution becomes:

$$P_0 = \frac{1}{2} \bar{C} \sum_{k=-\infty}^{\infty} (-1)^k \log \left[ \frac{\cosh(n\xi_2(2k+1)) - 1}{\cosh((\xi_2 + 2k\xi_2)n) - \cos(n\theta)} \right]$$
(C-24)

(see reference 2). To determine the source strength, the flow out of the strip which, of course, is the same as the flow  $M_{B0}$  through the feeder hole, can be computed:

$$M_{B0} = 4 \int_0^{\frac{\pi}{2}} \rho \frac{C^3}{12\mu} \left( -\frac{\partial \bar{P}_0}{\partial z} \right)_{z=\frac{t}{2}} R d\theta$$

or:

$$\frac{3\mu M_{B0}}{\rho C^3 P_s} = - \int_0^{\frac{\pi}{2}} \left( \frac{\partial P_0}{\partial \xi} \right)_{\xi=\xi_2} d\theta = \frac{1}{2} \bar{C} \sum_{k=-\infty}^{\infty} (-1)^k \int_0^{\pi} \frac{\sinh((\xi+2k\xi_2)n) d(n\theta)}{\cosh((\xi+2k\xi_2)n) - \cos n\theta} = \frac{\pi}{2} \bar{C} \quad (C-25)$$

Hence:

$$\frac{1}{2} \bar{C} = \frac{3\mu M_{B0}}{\pi \rho C^3 P_s} \quad (C-26)$$

The pressure  $P'_{oc}$  at which the flow enters the film, is taken at a point on the rim of the feeder hole with the coordinates  $\xi=0, \theta=d/D$  where  $d$  is the feeder hole diameter. Thus, from eq. (C-24):

$$P'_{oc} = \frac{1}{2} \bar{C} n \lambda \xi_2 = \frac{3\mu n M_{B0}}{\pi \rho C^3 P_s} \lambda \xi_2 \quad (C-27)$$

where:

$$\lambda = \frac{1}{n\xi_2} \sum_{k=-\infty}^{\infty} (-1)^k \log \left[ \frac{\cosh(n\xi_2(2k+1)) - 1}{\cosh(2kn\xi_2) - \cos(n\frac{d}{D})} \right] \quad (C-28)$$

Single Plane Admission

Since  $\frac{d}{D} \ll 1$ , eq. (C-28) can be written with good approximation as:

$$\lambda \cong \frac{1}{n\xi_2} \log \left[ \frac{\cosh(n\xi_2) - 1}{1 - \cos(n\frac{d}{\xi_1})} \right] \cong 1 + \frac{2}{n\xi_2} \log \left( \frac{D}{nd} \right) \quad (C-29)$$

Single Plane Admission

If there are two admission planes, there are two feeder holes per axial strip and fig. 59 is modified to:

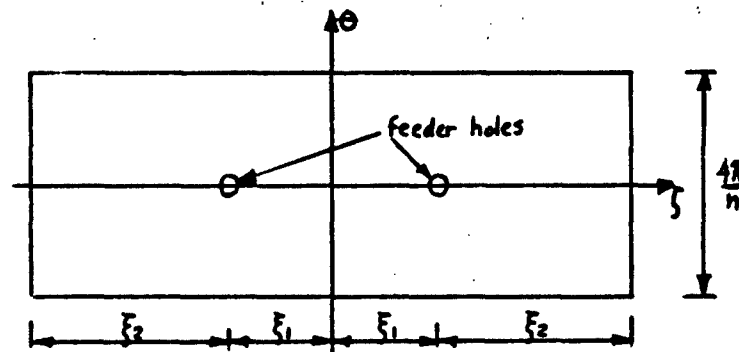


Figure 60: Axial Strip

With a total of  $n$  feeder holes, there are  $1/2n$  holes per admission plane. The length between admission planes is  $L_1$ , and the total bearing length is:  $L = L_1 + L_2$  such that  $L_2$  becomes the combined length outside the admission planes. The ranges of the dimensionless coordinates for the strip are:

$$-(\xi_1 + \xi_2) \leq \xi \leq (\xi_1 + \xi_2) \quad (C-30)$$

$$-\frac{2\pi}{n} \leq \theta \leq \frac{2\pi}{n}$$

where:

$$\xi_1 = \frac{L_1}{D} \quad (C-31)$$

The solution for the pressure distribution is found from the method of sources and sinks to be:

$$P_0 = \bar{C} \sum_{k=-\infty}^{\infty} (-1)^k \log \left[ \frac{[\cosh(\frac{n}{2}(\xi_2 + 2k(\xi_1 + \xi_2))) - 1] [\cosh(\frac{n}{2}(\xi_2 + 2\xi_1 + 2k(\xi_1 + \xi_2))) - 1]}{[\cosh(\frac{n}{2}(\xi_1 + 2k(\xi_1 + \xi_2))) - \cos(\theta)] [\cosh(\frac{n}{2}(\xi_1 + 2\xi_1 + 2k(\xi_1 + \xi_2))) - \cos(\theta)]} \right] \quad (C-32)$$

Defining the pressure,  $P'_{oc}$  downstream of the feeder hole to be the pressure at:  $(\xi = \xi_1, \theta = \frac{nd}{2D})$ , eq. (C-27) can be employed with:

$$\lambda = \frac{1}{h\xi_2} \sum_{k=-\infty}^{\infty} (-1)^k \log \left[ \frac{[\cosh(\frac{n}{2}(\xi_2 + 2k(\xi_1 + \xi_2))) - 1] [\cosh(\frac{n}{2}(\xi_2 + 2\xi_1 + 2k(\xi_1 + \xi_2))) - 1]}{[\cosh(nk(\xi_1 + \xi_2)) - \cos(\frac{nd}{2D})] [\cosh(n(\xi_1 + k(\xi_1 + \xi_2))) - \cos(\frac{nd}{2D})]} \right] \quad (C-33)$$

#### Double Plane Admission

In practice,  $\frac{nd}{2D} \ll 1$  whereby an approximate expression for  $\lambda$  becomes:

$$\lambda \cong \frac{1}{h\xi_2} \log \left[ \frac{[\cosh(\frac{n}{2}\xi_2) - 1] [\cos(\frac{n}{2}(\xi_2 + 2\xi_1)) - 1]}{[1 - \cos(\frac{nd}{2D})] [\cosh(n\xi_1) - \cos(\frac{nd}{2D})]} \right] \cong 1 + \frac{2}{h\xi_2} \log \left( \frac{2D}{nd} \right) \quad (C-34)$$

The perturbation of the film pressure defined by eq. (C-15) causes a similar perturbation in the flow. From eq. (C-13):

$$m = m_0 + \epsilon \left[ \left( \frac{dm}{dP'_c} \right) P'_c + \left( \frac{dm}{dh} \right) \cos \theta \right] + \epsilon' \left( \frac{dm}{dP'_x} \right) P'_x \quad (C-35)$$

$$m_0 = \begin{cases} \sqrt{1 - P'_{oc}} & \text{Orifice Restrictor} \\ 1 - P'_{oc} & \text{Laminar Restrictor} \end{cases} \quad (C-36)$$

$$\left(\frac{dm}{dP'_c}\right)_0 = \begin{cases} -\frac{1}{2m_0} & \text{Orifice Restrictor} \\ -1 & \text{Laminar Restrictor} \end{cases} \quad (C-37)$$

$$\left(\frac{dm}{dh}\right)_0 = \begin{cases} \frac{\delta^2}{1+\delta^2} m_0 & \text{Orifice Restrictor} \\ 0 & \text{Laminar Restrictor} \end{cases} \quad (C-38)$$

Define:

$$\psi = -\frac{\Lambda_2}{\xi_2} \left(\frac{dm}{dP'_c}\right)_0 \quad (C-39)$$

whereby eq. (C-35) can be written:

$$m = m_0 + \epsilon \left[ \left(\frac{dm}{dh}\right)_0 \cos\theta - \frac{\xi_2}{\Lambda_3} \psi P'_{1c} \right] - \epsilon \frac{\xi_2}{\Lambda_3} \psi P'_{2c} \quad (C-40)$$

In solving eqs. (C-18) to (C-20), only for the first equation is an exact solution readily obtained as shown by eqs. (C-24) and (C-32). To solve the two remaining equations it is necessary to perturb the source strength. In the present analysis this will be done by an approximate method.

Assume that there are infinitely many feeder holes. Thereby, the feeder holes form a continuous line feed from which the flow is purely axial. The mass flow per inch of circumference becomes:

$$\frac{\rho h^3}{12\mu} \left[ \frac{d\bar{P}}{dz} - \frac{d\bar{P}}{dz_2} \right]_{z=\frac{1}{2}L_1} = \frac{\frac{1}{2}nM_0}{2\pi R} \quad (C-41)$$

where  $z_2 = z - 1/2 L_1$ . In dimensionless form:

$$\left[ \frac{dP}{d\xi} - \frac{dP}{d\xi_2} \right]_{\xi=\xi_1} = \frac{3\mu n M_0}{\pi \rho P_0 C^3} \frac{1}{h^3} = \frac{\Lambda_5}{\lambda \xi_2} \frac{m}{h^3} \quad (C-42)$$

where:

$$\xi_2 = \frac{z_2}{R} = \xi - \xi_1 \quad (C-43)$$

Substitute from eqs. (C-15), (C-17) and (C-40) into eq. (C-42) to get:

$$\left[ \frac{dP_1}{d\xi} - \frac{dP_0}{d\xi_2} \right]_{\xi=\xi_1} = q \quad (C-44)$$

$$\left[ \frac{dP_1}{d\xi} - \frac{dP_1}{d\xi_2} \right]_{\xi=\xi_1} = -3q \frac{1+\frac{3}{2}\delta^2}{1+\delta^2} \cos\theta - \psi \frac{1}{\lambda} P_{1c}' \quad (C-45)$$

$$\left[ \frac{\partial P_2}{\partial \xi} - \frac{\partial P_2}{\partial \xi_2} \right]_{\xi=\xi_1} = -\psi \frac{1}{\lambda} P_{2c}' \quad (C-46)$$

where:

$$q = \frac{\lambda_s m_0}{\lambda \xi_2} = \frac{3\mu n M_{Bo}}{\pi \rho C^3 P_3} \quad (C-47)$$

and  $\delta$  is defined to be zero for the laminar restrictor. Making use of eqs. (C-47) and (C-37), eq. (C-39) becomes:

$$\psi = \begin{cases} \frac{\lambda_s^2}{2q\lambda\xi_2} & \text{Orifice Restrictor} \\ \frac{\lambda_s}{\xi_2} & \text{Laminar Restrictor} \end{cases} \quad (C-48)$$

With the assumption of a line feed instead of discrete feeder holes, there is no variation circumferentially in the pressure when the journal is concentric in the bearing. Therefore:

$$\frac{\partial P_0}{\partial \theta} = 0 \quad (C-49)$$

Hence, the solution for  $P_0$  can be found directly from eqs. (C-18) and (C-44) as:

$$P_0 = \begin{cases} q(\xi_2 - \xi_2) & 0 \leq \xi_2 \leq \xi_2 \quad (\text{or: } \xi_1 \leq \xi \leq (\xi_1 + \xi_2)) \\ q\xi_2 & 0 \leq \xi \leq \xi_1 \end{cases} \quad (C-50)$$

The pressure at the line feed is:

$$P_{oc} = qF_2 = \frac{\Lambda_s m_o}{\lambda} \quad (C-51)$$

Comparing eqs. (C-51) and (C-27):

$$P'_{oc} = \Lambda_s m_o = \lambda P_{oc} \quad (C-52)$$

which gives the actual pressure downstream of the feeder holes in terms of the approximate line feed pressure. Inserting eq.(C-52) into eq. (C-27), the feeder hole downstream pressure is found to be:

$$P'_{oc} = \begin{cases} \frac{1}{2} \Lambda_s [-\Lambda_s + \sqrt{\Lambda_s^2 + 4}] & \text{Orifice Restrictor} \\ \frac{\Lambda_s}{1 + \Lambda_s} & \text{Laminar Restrictor} \end{cases} \quad (C-53)$$

Then:

$$q = \frac{1}{\lambda F_2} P'_{oc} \quad (C-54)$$

Thus, the exact solution for  $P_o$ , eq. (C-24) or eq. (C-32) can be replaced by the approximate solution of eq. (C-50). The total flow is the same in the two cases which means that only in the immediate neighborhood of the feeder holes is there any significant difference between the two solutions. This localized effect can be ignored in computing the load carrying capacity of the bearing.

Turning to the solution of the perturbed pressures, it is again assumed that the feeder holes can be represented by a line feed but with a correction introduced for the pressure downstream of the feeder holes to insure a correct flow. Actually, this correction factor must be determined from a perturbation of the source strength in eqs. (C-24) and (C-32). However, in the present analysis it shall be assumed that the same correction factor as derived for  $P_0$ , namely  $\lambda$ , also applies to the perturbed pressure. In other words, it is assumed that:

$$P'_{1c} = \lambda P_{1c} \quad (C-55)$$

$$P'_{2c} = \lambda P_{2c}$$

The solutions are taken in the form:

$$P_1 = H_1 \cos \theta \quad (C-56)$$

$$P_2 = \delta H_2 \cos \theta$$

where  $H_1$  and  $H_2$  are functions of  $\xi$  only. Thereby eqs. (C-19), (C-20), (C-45) and (C-46) become:

$$\frac{d^2 H_1}{d\xi^2} - H_1 = 0 \quad (C-57)$$

$$\frac{d^2 H_2}{d\xi^2} - H_2 = 1 \quad (C-58)$$

$$\left[ \frac{dH_1}{d\xi} - \frac{dH_2}{d\xi} \right]_{\xi=\xi_0} = -3q \frac{1+\frac{3}{2}\delta^2}{1+\delta^2} - \psi H_{1c} \quad (C-59)$$

$$\left[ \frac{dH_1}{d\xi} - \frac{dH_2}{d\xi_2} \right]_{\xi=\xi_1} = -\psi H_{2c} \quad (\text{C-60})$$

where eqs. (C-59) and (C-60) serve as boundary conditions to eqs. (C-57) and (C-58). The other boundary conditions are:

$$\text{at } \xi=0: \quad \frac{dH_1}{d\xi} = \frac{dH_2}{d\xi} = 0 \quad (\text{C-61})$$

$$\text{at } \xi_2 = \xi_2 \quad (\xi = \xi_1 + \xi_2): \quad H_1 = H_2 = 0 \quad (\text{C-62})$$

The solutions are obtained directly as:

$$H_1 = \begin{cases} H_{1c} \frac{\cosh \xi}{\cosh \xi_1} & 0 \leq \xi \leq \xi_1 - \\ H_{1c} \frac{\sinh(\xi_2 - \xi_2)}{\sinh \xi_2} & 0 \leq \xi_2 \leq \xi_2 - \end{cases} \quad (\text{C-63})$$

$$H_2 = \begin{cases} (H_{2c} + 1) \frac{\cosh \xi}{\cosh \xi_1} - 1 & 0 \leq \xi \leq \xi_1 - \\ (H_{2c} + 1) \frac{\sinh(\xi_2 - \xi_2)}{\sinh \xi_2} + \frac{\sinh \xi_2}{\sinh \xi_2} - 1 & 0 \leq \xi_2 \leq \xi_2 - \end{cases} \quad (\text{C-64})$$

where:

$$H_{1c} = \frac{-3q \frac{1+\xi^2}{1+\delta^2} \sinh \xi_2}{\cosh \xi_2 + [\psi + \tanh \xi_1] \sinh \xi_2} \quad (C-65)$$

$$H_{2c} + 1 = \frac{\psi \sinh \xi_2 + 1}{\cosh \xi_2 + [\psi + \tanh \xi_1] \sinh \xi_2} \quad (C-66)$$

The force  $F$  exerted on the journal by the film is found by integrating the pressure  $\bar{P}$  in the film:

$$F = - \int_{-\frac{1}{2}}^{\frac{1}{2}} \int_0^{2\pi} \bar{P} \cos \theta R d\theta dz \quad (C-67)$$

Making use of eqs. (C-3), (C-5), (C-22), (C-31) and (C-15), eq. (C-67) becomes:

$$F = -2R^2 P_3 \int_0^{(\xi_1 + \xi_2)} \int_0^{2\pi} (P_0 + \epsilon P_1 + \dot{\epsilon} P_2) \cos \theta d\theta d\xi \quad (C-68)$$

With  $P_0$  given by eq. (C-50), it is seen that  $P_0$ , of course, gives no contribution to the force, i.e.  $F_0 = 0$ . Substituting for  $P_1$  and  $P_2$  from eq. (C-56) yields:

$$F = -2\pi R^2 P_3 \int_0^{(\xi_1 + \xi_2)} (\epsilon H_1 + \dot{\epsilon} H_2) d\xi \quad (C-69)$$

Since the solution has been linearized, the force can be expressed in terms of a spring coefficient K and a damping coefficient B:

$$F = Ke + B \frac{de}{dt} = CKe + C\gamma B \dot{e} \quad (C-70)$$

where  $e$  is the displacement (the eccentricity) of the journal center, see eqs. (C-14) and (C-16). Comparing eqs. (C-69) and (C-70):

$$CK = -2\pi R^2 P_s \int_0^{\xi_1 + \xi_2} H_1 d\xi \quad (C-71)$$

$$C\gamma B = -2\pi R^2 P_s \alpha \int_0^{\xi_1 + \xi_2} H_2 d\xi \quad (C-72)$$

In dimensionless form:

$$\frac{CK}{(L_1 + L_2) D P_s} = - \frac{\pi/2}{\xi_1 + \xi_2} \int_0^{\xi_1 + \xi_2} H_1 d\xi \quad (C-73)$$

$$\frac{CB}{\mu(L_1 + L_2) D \left(\frac{R}{c}\right)^2} = - \frac{6\pi}{\xi_1 + \xi_2} \int_0^{\xi_1 + \xi_2} H_2 d\xi \quad (C-74)$$

With substitution from eqs. (C-63) and (C-65), eq. (C-73) yields:

$$\frac{1+\delta^2}{1+\frac{2}{3}\delta^2} \frac{CK}{(L_1+L_2)DP_s} \lambda = \frac{3\pi}{2(\xi_1+\xi_2)} \frac{q\lambda}{\cosh\xi_2 + [\psi + i \tanh\xi_1] \sinh\xi_2} [\cosh\xi_2 - 1 + \sinh\xi_2 \tanh\xi_1] \quad (C-75)$$

In this form, the dimensionless stiffness is a function of three parameters only:  $\Lambda_s$ ,  $\xi_1$  and  $\xi_2$ . The factor:  $q\lambda\xi_2$  depends on  $\Lambda_s$  only (see eqs. (C-53) and (C-54) and the parameter  $\psi\xi_2$ , therefore, is also a function of  $\Lambda_s$  only (see eq. (C-48)).

With substitution from eqs. (C-64) and (C-66), eq. (C-74) yields:

$$\frac{CB}{\mu(L_1+L_2)D\left(\frac{R}{C}\right)^2} = 6\pi \left[ 1 - \frac{1}{\xi_1+\xi_2} \frac{\sinh\xi_2 + \cosh\xi_2 \tanh\xi_1 + \psi(2\cosh\xi_2 - 2 + \sinh\xi_2 \tanh\xi_1)}{\cosh\xi_2 + (\psi + \tanh\xi_1) \sinh\xi_2} \right] \quad (C-76)$$

The dimensionless damping is a function of three parameters only:  $\Lambda_s$ ,  $\xi_1$  and  $\xi_2$ .

The total volume flow to the bearing,  $Q$  inch<sup>3</sup>/sec, can be defined in dimensionless form from eq. (C-47) as:

$$\frac{3\mu Q}{\pi P_s C^3} \lambda \xi_2 = q\lambda \xi_2 = P'_{oc} \quad (C-77)$$

which depends only on  $\Lambda_3$  and is independent of  $\xi_1$  and  $\xi_2$ .

Eqs. (C-75) to (C-77) are used to calculate the design charts for the stiffness, the damping and the flow for a hydrostatic journal bearing with an incompressible lubricant.

**BLANK PAGE**

APPENDIX IV: The Stability of the Hydrodynamic - Hydrostatic Ring Bearing with an Incompressible Lubricant

In the hydrodynamic-hydrostatic ring bearing there is a ring between the journal and the bearing. The ring is prevented from rotating but is otherwise free to move. The inner diameter of the ring is  $D$  and the outer diameter is  $D_o$ . The radial clearance of the inner film is  $C$  and that of the outer film is  $C_o$ . The bearing length is  $L$ .

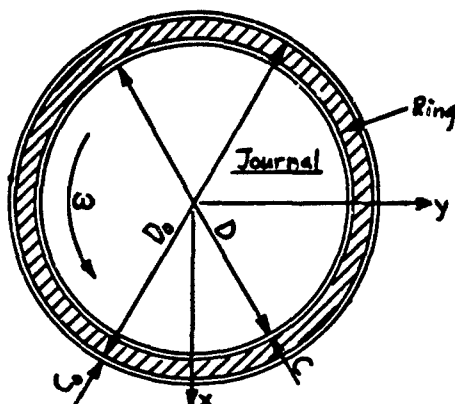


Figure 61: Hydrodynamic-Hydrostatic Ring Bearing

As shown in Appendix I, the dynamic forces of the inner film can be expressed in terms of 8 coefficients:  $K_{xx}$ ,  $K_{xy}$ ,  $K_{yx}$ ,  $K_{yy}$ ,  $B_{xx}$ ,  $B_{xy}$ ,  $B_{yx}$  and  $B_{yy}$ . The outer film, on the other hand, requires only two coefficients, a spring coefficient  $K_o$  and a damping coefficient  $B_o$ , as given in Appendix III.

In calculating the stability properties of this bearing, the rotor is assumed to be rigid and symmetrical with a mass of  $2M$ . As discussed in connection with eq. (B-20) in Appendix II, the rotor mass can be lumped at the journals whereby each journal is assigned a mass of  $M$ .

Then the equations of motion become:

$$M \frac{d^2x}{dt^2} = -K_{xx}(x-x_o) - B_{xx} \frac{d(x-x_o)}{dt} - K_{xy}(y-y_o) - B_{xy} \frac{d(y-y_o)}{dt} = -K_o x_o - B_o \frac{dx_o}{dt}$$

$$M \frac{d^2y}{dt^2} = -K_{yx}(x-x_o) - B_{yx} \frac{d(x-x_o)}{dt} - K_{yy}(y-y_o) - B_{yy} \frac{d(y-y_o)}{dt} = -K_o y_o - B_o \frac{dy_o}{dt} \quad (D-1)$$

where  $x$  and  $y$  are the amplitudes of the journal center, and  $x_0$  and  $y_0$  are the amplitudes of the center of the ring. In these equations, the mass of the ring itself has been ignored because it is small compared to the journal mass. Eq. (D-1) is made dimensionless by setting:

$$\bar{x} = \frac{x}{C} \qquad \bar{y} = \frac{y}{C} \qquad (D-2)$$

$$\bar{x}_0 = \frac{x_0}{C} \qquad \bar{y}_0 = \frac{y_0}{C} \qquad (D-3)$$

$$\tau = \omega t \qquad (D-4)$$

$$\bar{k}_0 = \frac{CK_0}{\mu NDL \left(\frac{R}{C}\right)^2} = \left(\frac{C}{C_0}\right) \frac{P_2 LD_0}{SW} \frac{C_0 K_0}{P_3 LD_0} \qquad (D-5)$$

$$\bar{b}_0 = \frac{C\omega B_0}{\mu NDL \left(\frac{R}{C}\right)^2} = 2\pi \left(\frac{C}{C_0}\right)^3 \left(\frac{D_0}{D}\right)^3 \frac{C_0 B_0}{\mu LD_0 \left(\frac{R_0}{C_0}\right)^2} \qquad (D-6)$$

$$\bar{m} = \frac{C\omega^2 M}{SW} = 4\pi^2 \frac{CNM}{\mu DL \left(\frac{R}{C}\right)^2} \qquad (D-7)$$

$$\bar{k}_{xx} = \frac{CK_{xx}}{SW} = \frac{CK_{xx}}{\mu DL \left(\frac{R}{C}\right)^2} \qquad (D-8)$$

$$\bar{B}_{xx} = \frac{C\omega B_{xx}}{SW} = \frac{C\omega B_{xx}}{\mu NDL \left(\frac{\omega}{2}\right)^2} \quad (D-9)$$

and similarly for  $\bar{K}_{xy}$ ,  $\bar{K}_{yx}$ ,  $\bar{K}_{yy}$ ,  $\bar{B}_{xy}$ ,  $\bar{B}_{yx}$  and  $\bar{B}_{yy}$ . Here,  $\omega$  is the angular speed of the journal and  $S$  is the Sommerfeld number. Thereby eq. (D-1) becomes:

$$\bar{M}\ddot{\bar{x}} = -\bar{K}_{xx}(\bar{x}-\bar{x}_0) - \bar{B}_{xx}(\dot{\bar{x}}-\dot{\bar{x}}_0) - \bar{K}_{xy}(\bar{y}-\bar{y}_0) - \bar{B}_{xy}(\dot{\bar{y}}-\dot{\bar{y}}_0) = -\bar{K}_0\bar{x}_0 - \bar{B}_0\dot{\bar{x}}_0 \quad (D-10)$$

$$\bar{M}\ddot{\bar{y}} = -\bar{K}_{yx}(\bar{x}-\bar{x}_0) - \bar{B}_{yx}(\dot{\bar{x}}-\dot{\bar{x}}_0) - \bar{K}_{yy}(\bar{y}-\bar{y}_0) - \bar{B}_{yy}(\dot{\bar{y}}-\dot{\bar{y}}_0) = -\bar{K}_0\bar{y}_0 - \bar{B}_0\dot{\bar{y}}_0$$

where "dot" refers to  $\frac{d}{dt}$ .

At the threshold of instability, the motion is purely harmonic with frequency  $\gamma$  such that:

$$\bar{x} = \bar{x}_c \cos(\gamma t) - \bar{x}_s \sin(\gamma t) = \text{Re} \{ (\bar{x}_c + i\bar{x}_s) e^{i\gamma t} \} \quad (D-11)$$

and similarly for  $\bar{y}$ ,  $\bar{x}_0$  and  $\bar{y}_0$ , where:

$$\gamma = \frac{\nu}{\omega} \quad (D-12)$$

Then eq. (D-10) can be written as:

$$\bar{M}\gamma^2 \bar{x} = (\bar{K}_{xx} + i\gamma \bar{B}_{xx})(\bar{x}-\bar{x}_0) + (\bar{K}_{xy} + i\gamma \bar{B}_{xy})(\bar{y}-\bar{y}_0) = (\bar{K}_0 + i\gamma \bar{B}_0)\bar{x}_0 \quad (D-13)$$

$$\bar{M}\gamma^2 \bar{y} = (\bar{K}_{yx} + i\gamma \bar{B}_{yx})(\bar{x}-\bar{x}_0) + (\bar{K}_{yy} + i\gamma \bar{B}_{yy})(\bar{y}-\bar{y}_0) = (\bar{K}_0 + i\gamma \bar{B}_0)\bar{y}_0$$

Solve for  $\bar{x}_0$  and  $\bar{y}_0$ :

$$\bar{x}_0 = \frac{\bar{M}_y^2}{\bar{K}_0 + i\gamma \bar{B}_0} \bar{x}$$

(D-14)

$$\bar{y}_0 = \frac{\bar{M}_y^2}{\bar{K}_0 + i\gamma \bar{B}_0} \bar{y}$$

and substitute into eq. (D-13) to get:

$$\left\{ \begin{array}{cc} \left( \bar{K}_{xx} - \frac{(\bar{K}_0 + i\gamma \bar{B}_0) \bar{M}_y^2}{\bar{K}_0 - \bar{M}_y^2 + i\gamma \bar{B}_0} + i\gamma \bar{B}_{xx} \right) & (\bar{K}_{xy} + i\gamma \bar{B}_{xy}) \\ (\bar{K}_{yx} + i\gamma \bar{B}_{yx}) & \left( \bar{K}_{yy} - \frac{(\bar{K}_0 + i\gamma \bar{B}_0) \bar{M}_y^2}{\bar{K}_0 - \bar{M}_y^2 + i\gamma \bar{B}_0} + i\gamma \bar{B}_{yy} \right) \end{array} \right\} \begin{Bmatrix} \bar{x} \\ \bar{y} \end{Bmatrix} = 0 \quad (D-15)$$

At the threshold of instability, the determinant of the coefficient matrix vanishes. For convenience, introduce the abbreviations:

$$E = \frac{(\bar{K}_0 + i\gamma \bar{B}_0) \bar{M}_y^2}{\bar{K}_0 - \bar{M}_y^2 + i\gamma \bar{B}_0} \quad (D-16)$$

$$Z_{xx} = \bar{K}_{xx} + i\gamma \bar{B}_{xx} \quad (\text{similarly for } Z_{xy}, Z_{yx}, Z_{yy}) \quad (D-17)$$

With this notation, the determinant of eq. (D-15) can be equated to zero to give:

$$E^2 - (Z_{xx} + Z_{yy})E + (Z_{xx}Z_{yy} - Z_{xy}Z_{yx}) = 0 \quad (D-18)$$

with the solution:

$$E = \frac{1}{2}(Z_{xx} + Z_{yy}) \pm \sqrt{\frac{1}{4}(Z_{xx} - Z_{yy})^2 + Z_{xy}Z_{yx}} \quad (D-19)$$

where only the root with the minus sign in front of the square root is of interest when studying stability. Set:

$$G = \text{Re} \left\{ \frac{1}{2}(Z_{xx} - Z_{yy})^2 + Z_{xy}Z_{yx} \right\} = \frac{1}{4}(\bar{K}_{xx} - \bar{K}_{yy})^2 + \bar{K}_{xy}\bar{K}_{yx} - \frac{1}{4}\gamma^2(\bar{B}_{xx} - \bar{B}_{yy}) - \gamma^2\bar{B}_{xy}\bar{B}_{yx} \quad (D-20)$$

$$H = \frac{1}{2} \text{Im} \left\{ \frac{1}{4}(Z_{xx} - Z_{yy})^2 + Z_{xy}Z_{yx} \right\} = \gamma \left[ \frac{1}{4}(\bar{K}_{xx} - \bar{K}_{yy})(\bar{B}_{xx} - \bar{B}_{yy}) + \frac{1}{2}(\bar{K}_{xy}\bar{B}_{yx} + \bar{K}_{yx}\bar{B}_{xy}) \right] \quad (D-21)$$

whereby eq. (D-19) becomes:

$$E = \frac{1}{2}(Z_{xx} + Z_{yy}) - \left\{ \sqrt{\frac{1}{4}(G + \sqrt{G^2 + 4H^2})} + i \sqrt{\frac{1}{4}(-G + \sqrt{G^2 + 4H^2})} \right\} \quad (D-22)$$

Set:

$$E = \bar{K}_0 + i\gamma\bar{B}_0 \quad (D-23)$$

where:

$$\bar{K}_0 = \frac{1}{2}(\bar{K}_{xx} + \bar{K}_{yy}) - \sqrt{\frac{1}{4}(G + \sqrt{G^2 + 4H^2})} \quad (D-24)$$

$$\gamma\bar{B}_0 = \frac{1}{2}\gamma(\bar{B}_{xx} + \bar{B}_{yy}) + \sqrt{\frac{1}{4}(-G + \sqrt{G^2 + 4H^2})} \quad (D-25)$$

Combining eqs. (D-16) and (D-23) yields:

$$\bar{K}_0 = \bar{M}\gamma^2 \left[ 1 + \bar{M}\gamma^2 \frac{\bar{K}_0 - \bar{M}\gamma^2}{(\bar{K}_0 - \bar{M}\gamma^2)^2 + (\gamma\bar{B}_0)^2} \right] \quad (D-26)$$

$$\gamma\bar{B}_0 = -(\bar{M}\gamma^2)^2 \frac{\gamma\bar{B}_0}{(\bar{K}_0 - \bar{M}\gamma^2)^2 + (\gamma\bar{B}_0)^2} \quad (D-27)$$

Eliminate  $\bar{M}\gamma^2 / [(\bar{K}_0 - \bar{M}\gamma^2)^2 + (\gamma\bar{B}_0)^2]$  between the two equations to get:

$$\bar{M}\gamma^2 = \frac{\bar{K}_0\gamma\bar{B}_0 + \bar{K}_0\gamma\bar{B}_0}{\gamma\bar{B}_0 + \gamma\bar{B}_0} \quad (D-28)$$

Substitute for  $\bar{M}\gamma^2$  into eq. (D-27) to obtain an equation which contains  $\gamma$  as the only unknown:

$$\gamma\bar{B}_0 [\bar{K}_0^2 + (\gamma\bar{B}_0)^2] + \gamma\bar{B}_0 [\bar{K}_0^2 + (\gamma\bar{B}_0)^2] = 0 \quad (D-29)$$

Since  $\bar{K}_0$  and  $\gamma\bar{B}_0$ , as seen from eqs. (D-24) and (D-25), are rather complicated functions of  $\gamma$ , eq. (D-29) is a higher order polynomial in  $\gamma$  which cannot be solved in closed form. Instead, the solution is found numerically. Once the roots for  $\gamma$  have been obtained, the corresponding dimensionless journal mass  $\bar{M}$  is found from eq. (D-28).

If  $\bar{M}$  is plotted as a function of  $\bar{B}_0$  for a fixed value of  $\bar{K}_0$ , it is found that under certain circumstances the rotor is inherently stable, i.e.  $\bar{M} \rightarrow \infty$ . When  $\bar{M} \rightarrow \infty, \gamma \rightarrow 0$  such that eqs. (D-24) and (D-25) yield:

$$\bar{K}_0 \rightarrow \frac{1}{2}(\bar{K}_{xx} + \bar{K}_{yy}) \quad (D-30)$$

$$\gamma\bar{B}_0 \rightarrow -\sqrt{-\left[\frac{1}{4}(\bar{K}_{xx} - \bar{K}_{yy})^2 + \bar{K}_{xy}\bar{K}_{yx}\right]}$$

where  $(\frac{1}{4}(\bar{K}_{xx} - \bar{K}_{yy})^2 + \bar{K}_{xy}\bar{K}_{yx}) < 0$  which holds true except at large eccentricity ratios. Solve eq. (D-29) for  $\gamma \bar{B}_0 / \gamma \bar{B}_0$ :

$$\frac{\gamma \bar{B}_0}{\gamma \bar{B}_0} = -\frac{1}{2} \frac{\bar{K}_0^2 + \gamma \bar{B}_0^2}{\gamma \bar{B}_0^2} + \sqrt{\frac{1}{4} \left( \frac{\bar{K}_0^2 + \gamma \bar{B}_0^2}{\gamma \bar{B}_0^2} \right)^2 - \frac{\bar{K}_0^2}{(\gamma \bar{B}_0)^2}} \quad (D-31)$$

For a given value of  $\bar{K}_0$  and with  $\bar{K}_0$  and  $\gamma \bar{B}_0$  defined by eq. (D-30), this equation allows calculation  $\gamma \bar{B}_0 / \gamma \bar{B}_0$  for  $\gamma = 0$ .

Noting that:

$$\gamma^2 = \left( \frac{\gamma \bar{B}_0}{\gamma \bar{B}_0} \right)^2 \frac{(\gamma \bar{B}_0)^2}{\bar{B}_0^2}$$

eq. (D-28) yields:

$$\bar{M} = \frac{1}{\gamma^2} \frac{\bar{K}_0 \left( \frac{\gamma \bar{B}_0}{\gamma \bar{B}_0} \right) + \bar{K}_0^2}{1 + \left( \frac{\gamma \bar{B}_0}{\gamma \bar{B}_0} \right)} = \frac{\bar{K}_0 + \frac{\gamma \bar{B}_0}{\gamma \bar{B}_0} \bar{K}_0}{(\gamma \bar{B}_0)^2 \left( \frac{\gamma \bar{B}_0}{\gamma \bar{B}_0} \right)^2 \left[ 1 + \frac{\gamma \bar{B}_0}{\gamma \bar{B}_0} \right]} \bar{B}_0^2 \quad (D-32)$$

Corresponding to the two roots for  $\gamma \bar{B}_0 / \gamma \bar{B}_0$  from eq. (D-31), eq. (D-32) yields two possible values for  $\bar{M}$ . The rotor is stable between these two values.

**BLANK PAGE**

**APPENDIX V: THE STIFFNESS AND THE DAMPING OF A HYBRID JOURNAL BEARING WITH A COMPRESSIBLE LUBRICANT**

In the hybrid-hydrostatic ring bearing which is gas lubricated, the outer bearing is purely hydrostatic whereas the inner bearing, supplied with pressurized gas from the outer bearing, is a hybrid bearing. This appendix describes the analysis for calculating the load carrying capacity, the flow, the stiffness and the damping of the hybrid journal bearing but the analysis applies equally well to the hydrostatic bearing.

For a compressible lubricant under isothermal conditions, Reynolds equation becomes:

$$\frac{\partial}{\partial \theta} \left[ \frac{\bar{h}^3}{12\mu} \bar{P} \frac{\partial \bar{P}}{\partial \theta} \right] + \frac{\partial}{\partial z} \left[ \frac{\bar{h}^3}{12\mu} \bar{P} \frac{\partial \bar{P}}{\partial z} \right] = \frac{1}{2} R\omega \frac{\partial(\bar{P}\bar{h})}{\partial \theta} + \frac{\partial(\bar{P}\bar{h})}{\partial t} \quad (E-1)$$

where the symbols are defined in connection with eq. (A-1), Appendix I. The equation is made dimensionless by setting:

$$\bar{\theta} = \frac{\theta}{R} \quad (E-2)$$

$$\bar{t} = \nu t \quad (E-3)$$

$$\bar{h} = \frac{h}{C} = 1 + \epsilon \cos \theta \quad (E-4)$$

$$\bar{\epsilon} = \frac{\epsilon}{C} \quad (E-5)$$

$$\bar{P} = \frac{P}{P_0} \quad (E-6)$$

whereby eq. (E-1) can be written in dimensionless form as:

$$\frac{d}{d\theta} \left[ h \frac{d(P_h)^2}{d\theta} - 2 \frac{dh}{d\theta} (P_h)^2 \right] + \frac{d}{d\zeta} \left[ h \frac{d(P_h)^2}{d\zeta} \right] = 2\Lambda \frac{d(P_h)}{d\theta} + 4\gamma\Lambda \frac{d(P_h)}{d\tau} \quad (E-7)$$

where:

$$\text{Compressibility Number:} \quad \Lambda = \frac{6\mu\omega}{P_a} \left( \frac{R}{C} \right)^2 \quad (E-8)$$

$$\text{Frequency Ratio:} \quad \gamma = \frac{\nu}{\omega} \quad (E-9)$$

In the purely hydrostatic bearing,  $\omega = 0$  which means that  $\Lambda = 0$ . In that case:

$$\text{Squeeze Number:} \quad \sigma = 2\gamma\Lambda = \frac{12\mu\nu}{P_a} \left( \frac{R}{C} \right)^2 \quad (E-10)$$

Eq. (E-7) is non-linear. It shall be solved under the assumption that the eccentricity ratio  $\epsilon$  is small whereby the pressure variable can be expanded in a perturbation:

$$P_h = P_0 + \epsilon P_1 \quad (E-11)$$

In making use of eq. (E-11) it shall be assumed that the pressure,  $P_0$ , which is the film pressure when the journal is concentric in the bearing, does not depend

on  $\Theta$  (i.e.  $\partial P_0 / \partial \Theta = 0$ ) . This assumption implies that the flow to the bearing is considered to be supplied by a line feed rather than discrete feeding holes. A correction factor will be added later to adjust the flow.

With this assumption, eqs. (E-11) and (E-4) can be substituted into eq. (E-7) whereby two equations are obtained. The first equation is simply:

$$\frac{\partial^2 P_0^2}{\partial \zeta^2} = 0 \quad (E-12)$$

In deriving the second equation it should be noted that eq. (E-4) is based on  $\Theta$  being measured from the line connecting the bearing center with the journal center. The angle between this line and the static load line is the attitude angle  $\phi$  . Therefore:

$$\frac{\partial(P_h)}{\partial \tau} = - \frac{\partial(P_h)}{\partial \Theta} \frac{d\phi}{d\tau} + \frac{\partial(P_h)}{\partial \tau} \Big|_{\Theta \text{ constant}} \quad (E-13)$$

Thereby the second perturbation equation becomes:

$$\frac{\partial^2(\epsilon P_0 P_1)}{\partial \Theta^2} + \frac{\partial^2(\epsilon P_0 P_1)}{\partial \zeta^2} - \frac{\Lambda}{P_0} (1 - 2\gamma \phi) \frac{\partial(\epsilon P_0 P_1)}{\partial \Theta} - 2\gamma \frac{\Lambda}{P_0} \frac{\partial(\epsilon P_0 P_1)}{\partial \tau} = -\epsilon \cos \Theta P_0^2 \quad (E-14)$$

Under static conditions, the journal center operates at an eccentricity ratio  $\epsilon_0$  and an attitude angle  $\phi_0$  . Letting the journal center perform a harmonic small amplitude motion (  $\epsilon_1 e^{i\omega t}$  ,  $\phi_1 e^{i\omega t}$  ) with frequency  $\omega$  around this equilibrium position, the journal center coordinates become:

$$\epsilon = \epsilon_0 + \epsilon_1 e^{i\tau} \quad (E-15)$$

$$\phi = \phi_0 + \phi_1 e^{i\tau}$$

The corresponding changes in the pressure variable can be expressed by:

$$\varepsilon P_0 P_1 = \varepsilon_0 q_0 + \varepsilon_1 e^{i\tau} q_1 + \varepsilon_2 e^{i\tau} q_2 \quad (\text{E-16})$$

Set:

$$q_0 = \text{Re} \{ G_0(\zeta) e^{j\omega} \} \quad (\text{E-17})$$

$$q_1 = \text{Re} \{ e^{i\tau} \text{Re} \{ G_1(\zeta) e^{j\omega} \} \} \quad (\text{E-18})$$

$$q_2 = \text{Re} \{ e^{i\tau} \text{Re} \{ G_2(\zeta) e^{j\omega} \} \} \quad (\text{E-19})$$

where:  $i = \sqrt{-1}$  and  $j = \sqrt{-1}$  With these definitions, eq. (E-14) gives rise to 3 equations:

$$\frac{d^2 G_0}{d\zeta^2} - \left(1 + j \frac{\Lambda}{P_0}\right) G_0 = -P_0^2 \quad (\text{E-20})$$

$$\frac{d^2 G_1}{d\zeta^2} - \left(1 + j \frac{\Lambda}{P_0} + i 2\gamma \frac{\Lambda}{P_0}\right) G_1 = -P_0^2 \quad (\text{E-21})$$

$$\frac{d^2 G_2}{d\zeta^2} - \left(1 + j \frac{\Lambda}{P_0} + i 2\gamma \frac{\Lambda}{P_0}\right) G_2 = -i j 2\gamma \frac{\Lambda}{P_0} G_0 \quad (\text{E-22})$$

The length of the bearing is  $L$ . There are two admission planes separated by the distance  $L_1$ , and the combined length outside the admission planes is  $L_2 = L - L_1$ . Since there is symmetry with respect to the centerplane of the bearing, the dimensionless axial coordinate ranges from  $\zeta = 0$  to  $\zeta = (\zeta_1 + \zeta_2)$

where:

$$\xi_1 = \frac{L_1}{D} \quad (E-23)$$

$$\xi_2 = \frac{L_2}{D}$$

It is convenient to introduce an additional axial coordinate:

$$\zeta_2 = \zeta - \xi_1$$

so that  $0 \leq \zeta_2 \leq \xi_2$ .

At the end of the bearing the pressure is ambient and equal to  $P_a$ , i.e.  
 $P = \bar{P}/P_a = 1$  at  $\zeta_2 = \xi_2$  which means:

$$\zeta_2 = \xi_2 : \begin{cases} P_0 = G_0 = G_1 = 1 \\ G_2 = 0 \end{cases} \quad (E-24)$$

At the centerplane of the bearing,  $\partial P / \partial \zeta = 0$  whereby:

$$\zeta = 0 : \frac{\partial P_0}{\partial \zeta} = \frac{dG_0}{d\zeta} = \frac{dG_1}{d\zeta} = \frac{dG_2}{d\zeta} = 0 \quad (E-25)$$

There are  $\frac{1}{2}n$  feeder holes per admission plane. The mass flow through a hole is  $M_B$ . Thus, when the admission plane is represented by a line feed, the flow per inch is  $n M_B / 4\pi R$ . Hence, the boundary condition at the admission plane becomes:

$$\zeta = \xi_1, \zeta_2 = 0 : \frac{6\mu RT}{\pi P_a^2 C^3} n M_B = h \left[ \left( \frac{d(P_h)}{d\zeta} \right)_{\zeta=\xi_1} - \left( \frac{d(P_h)}{d\zeta_2} \right)_{\zeta_2=0} \right] \quad (E-26)$$

where  $R$  is the gas constant and  $T$  is the total temperature. Expand the right hand side by means of eqs. (E-11), (E-16) and (E-4):

$$\begin{aligned} \frac{6\mu RT}{\pi P_a^2 C^3} n M_B &= (1 + \epsilon \cos \theta) \left( \frac{d}{d\bar{s}} - \frac{d}{d\bar{s}_2} \right)_c [P_o^2 + 2\epsilon P_o P_1] = \left( \frac{d}{d\bar{s}} - \frac{d}{d\bar{s}_2} \right)_c [P_o^2 + 2(\epsilon P_o P_1 + \frac{1}{2} \epsilon P_o^2 \cos \theta)] \\ &= \left( \frac{d}{d\bar{s}} - \frac{d}{d\bar{s}_2} \right) [P_o^2 + 2\epsilon_o (q_o + \frac{1}{2} P_o^2 \cos \theta) + 2\epsilon_o e^{i\tau} (q_1 + \frac{1}{2} P_o^2 \cos \theta) + 2\epsilon_o \phi_1 e^{i\tau} q_2] \quad (E-27) \end{aligned}$$

where subscript  $c$  refers to the condition at the admission plane.

Next, the left hand side of eq. (E-27) must be expanded. Let the volume of a feeder hole be represented by  $V_c$  and let the flow into the feeder hole be  $M_c$ . The pressure in the feeder hole is  $\bar{P}'_c$ . Then a flow balance for the feeder hole volume can be set up:

$$M_B = M_c - \frac{d(V_c \bar{\rho}'_c)}{dt} \quad (E-28)$$

where  $\bar{\rho}'_c = \bar{P}'_c / RT$  is the mass density of the gas in the feeder hole. To make eq. (E-28) dimensionless, set:

$$\frac{M_c \sqrt{RT}}{\pi a^2 P_s} = \frac{m}{\sqrt{1 + \left(\frac{d}{h}\right)^2}} \quad (E-29)$$

where  $\delta$  is the inherent compensation factor:

$$\delta = \frac{a^2}{dC} \quad (E-30)$$

Here,  $P_s$  is the supply pressure,  $a$  is the radius of the orifice and  $d$  is the diameter of the feeding hole. The dimensionless orifice flow  $m$  is given by the standard equation:

$$m = \begin{cases} C_D \sqrt{\frac{2k}{k+1}} \left(\frac{2}{k+1}\right)^{\frac{1}{k-1}} & \frac{P'_c}{P_s} \leq \left(\frac{2}{k+1}\right)^{\frac{k}{k-1}} \\ C_D \sqrt{\frac{2k}{k-1}} \left(\frac{P'_c}{P_s}\right)^{\frac{1}{k}} \sqrt{1 - \left(\frac{P'_c}{P_s}\right)^{\frac{k-1}{k}}} & \left(\frac{2}{k+1}\right)^{\frac{k}{k-1}} \leq \frac{P'_c}{P_s} \leq 1 \end{cases} \quad (\text{E-31})$$

where  $C_D$  is the vena contracta coefficient. Actually,  $C_D$  is a function of the pressure ratio  $\frac{P'_c}{P_s}$ .

The dimensionless form of eq. (E-28) becomes:

$$\frac{6\mu RT}{\pi P_a^2 C^3} n M_0 = \Lambda_s V^2 \frac{\sqrt{1+\delta^2}}{\sqrt{1+(\frac{\delta}{h})^2}} m - 4\gamma \Lambda \frac{n V_c}{\pi D L C} (\xi_1 + \xi_2) \frac{dP'_c}{dT} \quad (\text{E-32})$$

where:

$$\text{Restrictor Coefficient: } \Lambda_s = \frac{6\mu n a^2 \sqrt{RT}}{P_s C^3 \sqrt{1+\delta^2}} \quad (\text{E-33})$$

$$\text{Pressure Ratio: } V = \frac{P_s}{P_a} \quad (\text{E-34})$$

$$P'_c = \frac{P'_c}{P_a} \quad (\text{E-35})$$

The restrictor coefficient,  $\Lambda_s$ , is, together with  $\Lambda$ , the governing performance parameter. It gives the ratio between the flow resistance of the bearing film and the flow resistance of the feeder hole restrictor.

From eqs. (E-11) and (E-16):

$$\begin{aligned}
 p'_z &= \frac{(Ph)_z}{h} = (1 - \epsilon \cos \theta) (P_{oc} + \epsilon P_{ic}) = P_{oc} + \frac{1}{P_{oc}} [(\epsilon P_o P_i)_c - \epsilon P_{oc}^2 \cos \theta] \\
 &= P_{oc} + \frac{1}{P_{oc}} [\epsilon_o (q_{oc} - P_{oc}^2 \cos \theta) + \epsilon_i e^{i\tau} (q_{ic} - P_{oc}^2 \cos \theta) + \epsilon_o \phi_i e^{i\tau} q_{2c}] \quad (E-36)
 \end{aligned}$$

On this basis and making use of eq. (E-13), it is found that:

$$\frac{dp'_z}{dt} = \frac{i}{P_{oc}} [\epsilon_i e^{i\tau} (q'_{ic} - P_{oc}'^2 \cos \theta) + \epsilon_o \phi_i e^{i\tau} (q'_{2c} - (\frac{dq_o}{d\theta})'_c - P_{oc}'^2 \sin \theta)] \quad (E-37)$$

Furthermore,  $m$  must also be expanded:

$$m = m_o + \left( \frac{dm}{d(\frac{P_c}{h})} \right)_o \frac{1}{V} (P'_c - P'_{oc}) = m_o + \left( \frac{dm}{d(\frac{P_c}{h})} \right)_o \frac{1}{V P_{oc}'} [\epsilon_o (q'_{oc} - P_{oc}'^2 \cos \theta) + \epsilon_i e^{i\tau} (q'_{ic} - P_{oc}'^2 \cos \theta) + \epsilon_o \phi_i e^{i\tau} q'_{2c}] \quad (E-38)$$

where:

$$m_o = m \left( \frac{P_{oc}}{V} \right) \quad (E-39)$$

Introduce the abbreviations:

$$q = \Lambda_s V^2 m_o \quad (E-40)$$

$$\psi'_0 = -\frac{\Lambda_c V}{2P'_{oc}} \left( \frac{dm}{d\left(\frac{P'}{P_s}\right)} \right)_0 \quad (E-41)$$

$$\psi'_1 = \frac{nV_c}{\pi DLC} \frac{f_1 + f_2}{P'_{oc}} \quad (E-42)$$

Eqs. (E-37) to (E-42) are substituted into eq. (E-32) which is then compared to eq. (E-27). Collecting terms according to  $\epsilon_0$ ,  $\epsilon$ , and  $\phi$ , four equations are obtained

$$\left( \frac{\partial P'_0}{\partial \xi_c} \right)_c = -q + \left( \frac{\partial P'_0}{\partial \xi_c} \right)_c \quad (E-43)$$

$$\left( \frac{\partial q_0}{\partial \xi_c} \right)_c = \frac{q}{2(1+\delta^2)} \cos\theta + \psi'_0 (q'_{oc} - P'^2_{oc} \cos\theta) + \left( \frac{\partial q_0}{\partial \xi_c} \right)_c \quad (E-44)$$

$$\left( \frac{\partial q_1}{\partial \xi_c} \right)_c = \frac{q}{2(1+\delta^2)} \cos\theta + (\psi'_0 + i2\gamma\Lambda\psi'_1) (q'_{oc} - P'^2_{oc} \cos\theta) + \left( \frac{\partial q_1}{\partial \xi_c} \right)_c \quad (E-45)$$

$$\left( \frac{\partial q_2}{\partial \xi_c} \right)_c = (\psi'_0 + i2\gamma\Lambda\psi'_1) q'_{oc} - i2\gamma\Lambda\psi'_1 \left( \left( \frac{\partial q_0}{\partial \theta} \right)_c + P'^2_{oc} \sin\theta \right) + \left( \frac{\partial q_2}{\partial \xi_c} \right)_c \quad (E-46)$$

In these equations, the primed quantities refer to the actual conditions at the feeder holes whereas the unprimed quantities derive from the solution based on the line feed assumption. Thus, it is necessary to establish a relationship between the two conditions in order to apply the equations. This is done by the same method as employed in Appendix III. In other words, consider the case where the journal is concentric in the bearing ( $\epsilon = 0$ ). Because of symmetry, it is then only necessary to consider an axial strip:

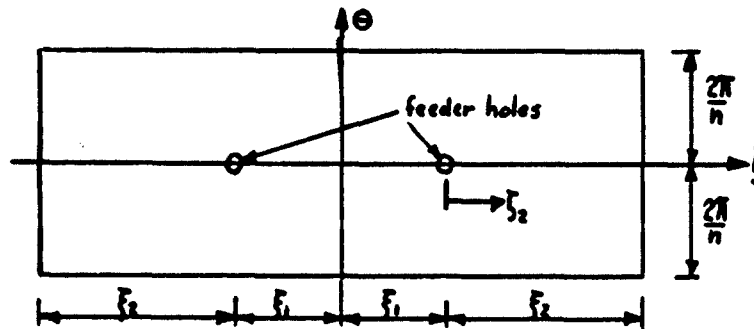


Figure 62: Axial Strip

The solution for the gas film pressure,  $P'_o$ , can be obtained from the method of sources and sinks as:

$$P'_o{}^{1/2} = 1 + \frac{6\mu RT}{\pi P_a^2 C^3} M_{B0} \sum_{k=-\infty}^{\infty} (-1)^k \log \left[ \frac{[\cosh(\frac{\theta}{2}(\xi_2 + 2k(\xi_1 + \xi_2))) - 1] [\cosh(\frac{\theta}{2}(\xi_2 + 2\xi_1 + 2k(\xi_1 + \xi_2))) - 1]}{[\cosh(\frac{\theta}{2}(\xi_2 + 2k(\xi_1 + \xi_2))) - \cos(\frac{\theta}{2})] [\cosh(\frac{\theta}{2}(\xi_1 + \xi_2 + 2k(\xi_1 + \xi_2))) - \cos(\frac{\theta}{2})]} \right] \quad (E-47)$$

If there is only one admission plane ( $\xi_1 = 0$ ) with  $n$  feeder holes, the solution becomes (see reference 2):

$$P'_o{}^{1/2} = 1 + \frac{6\mu RT}{\pi P_a^2 C^3} M_{B0} \sum_{k=-\infty}^{\infty} (-1)^k \log \left[ \frac{\cosh(n\xi_2(2k+1)) - 1}{\cosh(n(\xi_2 + 2k\xi_2)) - \cos(n\theta)} \right] \quad (E-48)$$

In these two equations,  $M_B$  is the mass flow from one feeder hole (concentric journal). The pressure,  $P'_{oc}$ , downstream of the feeder hole is defined as the pressure on the rim of the feeder hole where  $\xi_2 = 0$  (i.e.  $\xi = \xi_1$ ) and  $\theta = d/D$  ( $d$  = feeder hole diameter,  $D$  = journal diameter). Since  $d \ll D$  the dominant term in the series in eqs. (E-47) and (E-48) is the one where  $k = 0$ , which is the only term that needs to be considered. Define:

Double Plane Admission

$$\lambda = \frac{1}{n\xi_2} \sum_{k=-\infty}^{\infty} (-1)^k \log \left[ \frac{[\cosh(\frac{\eta}{2}(\xi_2 + 2k(\xi_1 + \xi_2)) - 1)] [\cosh(\frac{\eta}{2}(\xi_2 + 2\xi_1 + 2k(\xi_1 + \xi_2)) - 1)]}{[\cosh(nk(\xi_1 + \xi_2)) - \cos(\frac{\eta}{2} \frac{D}{B})] [\cosh(n(\xi_1 + k(\xi_1 + \xi_2)) - \cos(\frac{\eta}{2} \frac{D}{B}))]} \right] \quad (E-49)$$

$$\cong \frac{1}{n\xi_2} \log \left[ \frac{[\cosh(\frac{\eta}{2}\xi_2) - 1] [\cosh(\frac{\eta}{2}(\xi_2 + 2\xi_1)) - 1]}{[1 - \cos(\frac{\eta}{2} \frac{D}{B})] [\cosh(n\xi_1) - \cos(\frac{\eta}{2} \frac{D}{B})]} \right] \cong 1 + \frac{2}{n\xi_2} \log \left( \frac{2D}{nd} \right)$$

Single Plane Admission

$$\lambda = \frac{1}{n\xi_2} \sum_{k=-\infty}^{\infty} (-1)^k \log \left[ \frac{\cosh(n\xi_2(2k+1)) - 1}{\cosh(2nk\xi_2) - \cos(n \frac{D}{B})} \right] \cong \frac{1}{n\xi_2} \log \left[ \frac{\cosh(n\xi_2) - 1}{1 - \cos(n \frac{D}{B})} \right] \cong 1 + \frac{2}{n\xi_2} \log \left( \frac{D}{nd} \right) \quad (E-50)$$

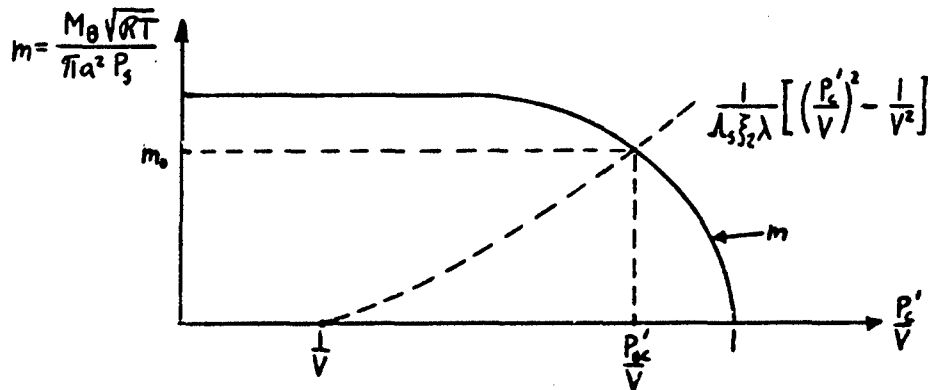
Then the downstream feeder hole pressure becomes:

$$P'_{oc}{}^2 = 1 + \frac{6\mu RT n M_{B0}}{\pi P_a^2 C^3} \lambda \xi_2 = 1 + \lambda_5 V^2 m_0 \xi_2 \lambda = 1 + q \xi_2 \lambda \quad (E-51)$$

Now,  $m_0$  is a function of  $\frac{P'_{oc}}{V}$  (see Eqs. (E-31) and (E-39)). From Eq. (E-51):

$$\frac{1}{\lambda_5 \xi_2 \lambda} \left[ \left( \frac{P'_{oc}}{V} \right)^2 - \frac{1}{V^2} \right] = m_0 = m \left( \frac{P'_{oc}}{V} \right) \quad (E-52)$$

This equation can be solved graphically:



Knowing  $\frac{P'_{oc}}{V}$ ,  $q$  can be calculated directly from Eq. (E-51). In addition, the slope  $\left(\frac{dm}{d\left(\frac{P'}{V}\right)}\right)_0$  of  $m$  at  $\frac{P'_{oc}}{V}$  can be computed whereby  $\psi'_0$  is given through Eq. (E-41).

The corresponding line feed solution can be determined from solving Eq. (E-12) with boundary conditions specified by Eqs. (E-24), (E-25) and (E-43):

$$\underline{0 \leq \xi \leq \xi_1} \quad P_0^2 = 1 + q\xi_2 \quad (E-53)$$

$$\underline{0 \leq \xi_2 \leq \xi_1} \quad P_0^2 = 1 + q(\xi_2 - \xi_1)$$

from which

$$P_{oc}^2 = 1 + q\xi_2 \quad (E-54)$$

A comparison between Eqs. (E-54) and (E-51) yields:

$$\frac{P_{oc}^{\prime 2} - 1}{P_{oc}^2 - 1} = \lambda \quad (E-55)$$

This establishes the relationship between the actual feeder hole downstream pressure and the one obtained from the line feed solution, based on a concentric journal. When the journal is eccentric, the flow from the feeder holes is no longer confined to the axial strip shown in Fig. 62 and, furthermore, the source strength changes. However, to get an approximate solution, consider a rectangular strip as in Fig. 62 with a uniform film thickness. In that case, the ratio:

$$\lambda = \frac{P_c^{\prime 2} - 1}{P_c^2 - 1} \quad (E-56)$$

stays constant, independent of the film thickness. Assuming that this relationship is valid even under dynamic conditions, Eq. (E-36) can be used to expand Eq. (56):

$$\lambda = \frac{P_{oc}^{\prime 2} - 1 + 2\epsilon((P_0 P_1)_c' - P_{oc}^{\prime 2} \cos\theta)}{P_{oc}^2 - 1 + 2\epsilon((P_0 P_1)_c - P_{oc}^2 \cos\theta)} = \frac{1}{P_{oc}^2 - 1} \left[ P_{oc}^{\prime 2} - 1 + 2\epsilon((P_0 P_1)_c' - P_{oc}^{\prime 2} \cos\theta) \right] \left[ 1 - \frac{2\epsilon}{P_{oc}^2 - 1} ((P_0 P_1)_c - P_{oc}^2 \cos\theta) \right]$$

from which

$$\frac{P_{oc}'^2 - 1}{P_{oc}^2 - 1} = \lambda$$

$$(\epsilon P_o P_i)_c' - \epsilon P_{oc}'^2 \cos \theta = \lambda [(\epsilon P_o P_i)_c - \epsilon P_{oc}^2 \cos \theta]$$

The first equation checks with Eq. (E-55). The second equation can be expanded further by means of Eqs. (E-15) and (E-17) to yield:

$$g_{oc}' - P_{oc}'^2 \cos \theta = \lambda [g_{oc} - P_{oc}^2 \cos \theta] \quad (E-57)$$

$$g_{ic}' - P_{oc}'^2 \cos \theta = \lambda [g_{ic} - P_{oc}^2 \cos \theta] \quad (E-58)$$

$$g_{ic}' = \lambda g_{ic} \quad (E-59)$$

Define the parameters:

$$\psi_o = \lambda \psi_o' = - \frac{\lambda \Lambda_s V}{2 P_{oc}'} \left( \frac{dm}{d(\frac{P_o'}{P_s})} \right) \quad (E-60)$$

$$\psi_i = \lambda \psi_i' = \frac{n V_c}{\pi D L C} \frac{\lambda (\xi_1 + \xi_2)}{P_{oc}'} \quad (E-61)$$

Thus, Eqs. (E-57) to (E-61) can be substituted into Eqs. (E-44) to (E-46).

Noting that:

$$P_{oc}^2 \cos \theta = \operatorname{Re} \{ P_{oc}^2 e^{j\theta} \}$$

$$P_{oc}^2 \sin \theta = \operatorname{Re} \{ -j P_{oc}^2 e^{j\theta} \}$$

and making use of Eqs. (E-17) to (E-19), the resulting equations become:

$$\left( \frac{dG_o}{d\xi_2} \right)_c = \frac{q}{2(1+\delta^2)} + \psi_o (G_{oc} - P_{oc}^2) + \left( \frac{dG_o}{d\xi} \right)_c \quad (E-62)$$

$$\left( \frac{dG_i}{d\xi_2} \right)_c = \frac{q}{2(1+\delta^2)} + (\psi_o + i 2\gamma \lambda \psi_i) (G_{ic} - P_{oc}^2) + \left( \frac{dG_i}{d\xi} \right)_c \quad (E-63)$$

(E-64)

$$\left(\frac{dG_2}{d\xi}\right)_c = (\psi_0 + i\gamma_1 \Lambda \psi_1) G_{2c} - i\gamma_1 \Lambda \psi_1 (G_{oc} - P_{oc}^2) + \left(\frac{dG_2}{d\xi}\right)_c$$

These equations together with Eqs. (E-24) and (E-25) are the boundary conditions for Eqs. (E-20) to (E-22).

It is seen directly that:

$$G_2 = j(G_0 - G_1) \quad (E-65)$$

It remains to determine the solutions for  $G_0$  and  $G_1$ .

$P_0$  is constant between the feeding planes, i.e. in the range  $0 \leq \xi \leq \xi_1$ , as given by the first of Eqs. (E-53). Under these circumstances,  $G_0$  and  $G_1$  have closed form solutions:

$$G_0 = \frac{P_{oc}^2}{1+j\frac{\Lambda}{P_{oc}}} + \left[ G_{oc} - \frac{P_{oc}^2}{1+j\frac{\Lambda}{P_{oc}}} \right] \frac{\cosh(\alpha_0 + j\beta_0)\xi}{\cosh(\alpha_0 + j\beta_0)\xi_1} \quad (E-66)$$

$$G_1 = \frac{P_{oc}^2}{1+j\frac{\Lambda}{P_{oc}} + i\gamma_1 \frac{\Lambda}{P_{oc}}} + \left[ G_{1c} - \frac{P_{oc}^2}{1+j\frac{\Lambda}{P_{oc}} + i\gamma_1 \frac{\Lambda}{P_{oc}}} \right] \frac{\cosh(\alpha + j\beta + i(\alpha_1 + j\beta_1))\xi}{\cosh(\alpha + j\beta + i(\alpha_1 + j\beta_1))\xi_1} \quad (E-67)$$

where:

$$\alpha_0 + j\beta_0 = \sqrt{1+j\frac{\Lambda}{P_{oc}}} \quad (E-68)$$

$$\alpha + j\beta + i(\alpha_1 + j\beta_1) = \sqrt{1+j\frac{\Lambda}{P_{oc}} + i\gamma_1 \frac{\Lambda}{P_{oc}}} \quad (E-69)$$

$$\alpha_0 = \left[ \frac{1}{2} \left( 1 + \sqrt{1 + \frac{\Lambda^2}{P_{oc}^2}} \right) \right]^{1/2} \quad (E-70)$$

$$\beta_0 = \left[ \frac{1}{2} \left( -1 + \sqrt{1 + \frac{\Lambda^2}{P_{oc}^2}} \right) \right]^{1/2} \quad (E-71)$$

$$\alpha = \left\{ \frac{1}{4} \left[ \alpha_1 + 1 + \sqrt{(\alpha_1 + 1)^2 + \left( \alpha_2 + \frac{\Lambda}{P_{oc}} \right)^2} \right] \right\}^{1/2} \quad (E-72)$$

$$\beta = \left\{ \frac{1}{2} \left[ -x_1 - 1 + \sqrt{(x_1 + 1)^2 + \left(x_2 + \frac{\Lambda}{P_\alpha}\right)^2} \right] \right\}^{1/2} \quad (\text{E-73})$$

$$\alpha_1 = \left\{ \frac{1}{2} \left[ x_1 - 1 + \sqrt{(x_1 - 1)^2 + \left(x_2 - \frac{\Lambda}{P_\alpha}\right)^2} \right] \right\}^{1/2} \quad (\text{E-74})$$

$$\beta_1 = \left\{ \frac{1}{2} \left[ -x_1 + 1 + \sqrt{(x_1 - 1)^2 + \left(x_2 - \frac{\Lambda}{P_\alpha}\right)^2} \right] \right\}^{1/2} \quad (\text{E-75})$$

$$x_1 = \left\{ \frac{1}{2} \left[ 1 - \left(\frac{\Lambda}{P_\alpha}\right)^2 + \left(2\gamma \frac{\Lambda}{P_\alpha}\right)^2 + \sqrt{\left(1 - \left(\frac{\Lambda}{P_\alpha}\right)^2 + \left(2\gamma \frac{\Lambda}{P_\alpha}\right)^2\right)^2 + 4\left(\frac{\Lambda}{P_\alpha}\right)^2} \right] \right\} \quad (\text{E-76})$$

$$x_2 = \left\{ \frac{1}{2} \left[ -\left(1 - \left(\frac{\Lambda}{P_\alpha}\right)^2 + \left(2\gamma \frac{\Lambda}{P_\alpha}\right)^2\right) + \sqrt{\left(1 - \left(\frac{\Lambda}{P_\alpha}\right)^2 + \left(2\gamma \frac{\Lambda}{P_\alpha}\right)^2\right)^2 + 4\left(\frac{\Lambda}{P_\alpha}\right)^2} \right] \right\}^{1/2} \quad (\text{E-77})$$

Hence:

$$\left(\frac{dG_0}{d\xi}\right)_c = \left[ G_{0c} - \frac{P_{0c}^2}{1 + j \frac{\Lambda}{P_{0c}}} \right] (\alpha_0 + j\beta_0) \tanh(\alpha_0 + j\beta_0) \xi_1 \quad (\text{E-78})$$

$$\left(\frac{dG_1}{d\xi}\right)_c = \left[ G_{1c} - \frac{P_{1c}^2}{1 + j \frac{\Lambda}{P_{1c}} + i2\gamma \frac{\Lambda}{P_{1c}}} \right] (\alpha_1 + j\beta_1 + i(2\gamma \frac{\Lambda}{P_{1c}})) \tanh(\alpha_1 + j\beta_1 + i(2\gamma \frac{\Lambda}{P_{1c}})) \xi_1 \quad (\text{E-79})$$

These expressions can be substituted into Eqs (E-62) and (E-63) to eliminate the two derivatives.

Eqs. (E-20) and (E-21) are solved by numerical integration. They have the general form:

$$\frac{d^2 G}{d\xi^2} - EG = F \quad (\text{E-80})$$

where:

$$E = \begin{cases} 1 + j \frac{\Lambda}{P_0} & \text{for } G = G_0 \\ 1 + j \frac{\Lambda}{P_0} + i2\gamma \frac{\Lambda}{P_0} & \text{for } G = G_1 \end{cases} \quad (\text{E-81})$$

$$F = -P_0^2 = -(1 + \gamma(\xi_2 - \xi_1)) \quad (\text{E-82})$$

The boundary conditions are:

$$\xi_2 = \xi_2 \quad G = 1 \quad (E-83)$$

$$\xi_2 = 0 \quad \frac{dG}{d\xi_2} = a + b G_c \quad (E-84)$$

where:

$$a = \begin{cases} \frac{q}{2(1+\delta^2)} - \left[ \psi_0 + \frac{(\alpha_0 + j\beta_0) \tanh(\alpha_0 + j\beta_0) \xi_1}{1 + j \frac{\Lambda}{P_{0c}}} \right] (1 + q \xi_2) & G = G_0 \\ \frac{q}{2(1+\delta^2)} - \left[ \psi_0 + i 2\gamma \frac{\Lambda}{P_{0c}} + \frac{(\alpha_0 + j\beta_0) \tanh(\alpha_0 + j\beta_0) \xi_1}{1 + j \frac{\Lambda}{P_{0c}} + i 2\gamma \frac{\Lambda}{P_{0c}}} \right] (1 + q \xi_2) & G = G_1 \end{cases} \quad (E-85)$$

$$b = \begin{cases} \psi_0 + (\alpha_0 + j\beta_0) \tanh(\alpha_0 + j\beta_0) \xi_1 & G = G_0 \\ \psi_0 + i 2\gamma \frac{\Lambda}{P_{0c}} + (\alpha_0 + j\beta_0) \tanh(\alpha_0 + j\beta_0) \xi_1 & G = G_1 \end{cases} \quad (E-86)$$

Integrate Eq. (E-80) twice to get:

$$G = \int_0^{\xi_2} (\xi_2 - \xi_2') (EG + F) d\xi_2' + a \xi_2 + (b \xi_2 + 1) G_c \quad (E-87)$$

Subdivide the length of integration into  $m$  increments of length  $\Delta \xi = \xi_2/m$  and write Eq. (E-87) in finite difference form:

$$G_{n+1} = G_n + (\Delta \xi)^2 \left[ \frac{1}{2} H_0 + H_1 + \dots + H_n \right] + \Delta \xi (a + b G_c) \quad 0 \leq n \leq m-1 \quad (E-88)$$

where  $H = EG + F$ . Setting:

$$G = t_c + j t_s + i(u_c + j u_s) + [v_c + j v_s + i(w_c + j w_s)] G_c \quad (E-89)$$

eq. (E-88) can be used to calculate  $G_n$  step by step, keeping  $G_c$  as an unknown constant ( $G_0 = G_c$ ). At  $\xi_2 = \xi_2$ ,  $G_m = 1$  from which  $G_c$  can be computed. Thereafter,  $G$  can be determined at each point by back substitution.

The force acting on the journal is found by integration of the film pressure.

The force has a radial component  $F_r$  and a tangential component  $F_t$  :

$$\left. \begin{array}{l} F_r \\ F_t \end{array} \right\} = 2 \int_0^L \int_0^{2\pi} \bar{P} \begin{Bmatrix} -\cos\theta \\ \sin\theta \end{Bmatrix} R d\theta dz = 2R^2 P_a \int_0^{(R_1+R_2)2\pi} \int_0^{2\pi} P \begin{Bmatrix} -\cos\theta \\ \sin\theta \end{Bmatrix} d\theta d\zeta \quad (E-90)$$

or, in dimensionless form, making use of Eqs. (E-16), (E-4) and (E-15):

$$\left. \begin{array}{l} f_r = \frac{F_r}{P_a LD} \\ f_t = \frac{F_t}{P_a LD} \end{array} \right\} = \frac{1}{2(\zeta_1 + \zeta_2)} \int_0^{(R_1+R_2)2\pi} \int_0^{2\pi} \frac{P_0 + \epsilon_0 \frac{q_0}{P_0} + \epsilon_1 e^{i\tau} \left[ \frac{q_1}{P_0} - \frac{\cos\theta}{1 + \epsilon_0 \cos\theta} (P_0 + \epsilon_0 \frac{q_0}{P_0}) \right] + \epsilon_0 \rho_1 e^{i\tau} \frac{q_2}{P_0}}{1 + \epsilon_0 \cos\theta} \begin{Bmatrix} -\cos\theta \\ \sin\theta \end{Bmatrix} d\theta d\zeta \quad (E-91)$$

The following integrals can be derived:

$$\int_0^{2\pi} \frac{d\theta}{1 + \epsilon_0 \cos\theta} = \frac{2\pi}{\eta} \quad (E-92)$$

$$\int_0^{2\pi} \frac{\cos\theta d\theta}{1 + \epsilon_0 \cos\theta} = -\frac{2\pi\epsilon_0}{\eta(1+\eta)} \quad (E-93)$$

$$\int_0^{2\pi} \frac{\sin\theta d\theta}{1 + \epsilon_0 \cos\theta} = 0 \quad (E-94)$$

$$\int_0^{2\pi} \frac{\cos^2\theta d\theta}{1 + \epsilon_0 \cos\theta} = \frac{2\pi}{\eta(1+\eta)} \quad (E-95)$$

$$\int_0^{2\pi} \frac{\sin^2\theta d\theta}{1 + \epsilon_0 \cos\theta} = \frac{2\pi}{(1+\eta)} \quad (E-96)$$

$$\int_0^{2\pi} \frac{\cos\theta \sin\theta d\theta}{1 + \epsilon_0 \cos\theta} = 0 \quad (E-97)$$

$$\int_0^{2\pi} \frac{d\theta}{(1 + \epsilon_0 \cos\theta)^2} = \frac{2\pi}{\eta^3} \quad (E-98)$$

$$\int_0^{2\pi} \frac{\cos\theta d\theta}{(1 + \epsilon_0 \cos\theta)^2} = -\frac{2\pi\epsilon_0}{\eta^3} \quad (E-99)$$

$$\int_0^{2\pi} \frac{\sin \theta d\theta}{(1 + \epsilon_0 \cos \theta)^2} = 0 \quad (\text{E-100})$$

$$\int_0^{2\pi} \frac{\cos^2 \theta d\theta}{(1 + \epsilon_0 \cos \theta)^2} = \frac{2\pi}{\eta^3(1+\eta)} (1 + \eta - \eta^2) \quad (\text{E-101})$$

$$\int_0^{2\pi} \frac{\sin^2 \theta d\theta}{(1 + \epsilon_0 \cos \theta)^2} = \frac{2\pi}{\eta(1+\eta)} \quad (\text{E-102})$$

$$\int_0^{2\pi} \frac{\cos \theta \sin \theta d\theta}{(1 + \epsilon_0 \cos \theta)^2} = 0 \quad (\text{E-103})$$

$$\int_0^{2\pi} \frac{\cos^3 \theta d\theta}{(1 + \epsilon_0 \cos \theta)^2} = -\frac{2\pi}{\epsilon_0 \eta^3(1+\eta)} (1-\eta)(1+2\eta) \quad (\text{E-104})$$

$$\int_0^{2\pi} \frac{\cos^2 \theta \sin \theta d\theta}{(1 + \epsilon_0 \cos \theta)^2} = 0 \quad (\text{E-105})$$

$$\int_0^{2\pi} \frac{\cos \theta \sin^2 \theta d\theta}{(1 + \epsilon_0 \cos \theta)^2} = -\frac{2\pi(1-\eta)}{\epsilon_0 \eta(1+\eta)} \quad (\text{E-106})$$

where:

$$\eta = \sqrt{1 - \epsilon_0^2} \quad (\text{E-107})$$

From Eqs. (E-17) and (E-18):

$$g_0 = \operatorname{Re}_e \{ G_0 \} \cos \theta - \operatorname{Im}_i \{ G_0 \} \sin \theta \quad (\text{E-108})$$

$$g_1 = \operatorname{Re}_e \{ [ \operatorname{Re}_e \{ G_1 \} \cos \theta - \operatorname{Im}_i \{ G_1 \} \sin \theta ] e^{i\tau} \}$$

Thus, the integrals in Eq. (E-91) can be computed as:

$$f_r = \frac{2\epsilon_0}{\eta(1+\eta)} H_{0r} + \epsilon_1 e^{i\tau} \left[ \frac{2(1-\eta)(2\eta+1)}{\eta^3(1+\eta)} H_{0r} + \frac{2}{\eta(1+\eta)} (H_{1r} + iJ_{1r}) \right] + \epsilon_0 \phi_1 e^{i\tau} \frac{2}{\eta(1+\eta)} [-H_{0j} + H_{1j} + iJ_{1j}] \quad (\text{E-109})$$

$$f_t = \frac{2\varepsilon_0}{H\eta} H_{0j} + \varepsilon_0 e^{i\tau} \left[ \frac{2(1-\eta)}{\eta(H\eta)} H_{0j} + \frac{2}{H\eta} (H_{1j} + iJ_{1j}) \right] - \varepsilon_0 \rho_1 e^{i\tau} \frac{2}{H\eta} [-H_{0r} + H_{1r} + iJ_{1r}] \quad (\text{E-110})$$

where:

$$H_{0r} = \frac{\pi}{2(\xi_1 + \xi_2)} \int_0^{\xi_1 + \xi_2} \left( P_0 - \frac{\operatorname{Re}\{G_0\}}{P_0} \right) d\xi \quad (\text{E-111})$$

$$H_{0j} = -\frac{\pi}{2(\xi_1 + \xi_2)} \int_0^{\xi_1 + \xi_2} \frac{\operatorname{Im}\{G_0\}}{P_0} d\xi \quad (\text{E-112})$$

$$H_{1r} + jH_{1j} + i(J_{1r} + jJ_{1j}) = \frac{\pi}{2(\xi_1 + \xi_2)} \int_0^{\xi_1 + \xi_2} \left( P_0 - \frac{G_0}{P_0} \right) d\xi \quad (\text{E-113})$$

With substitution from Eqs. (E-53), (E-66) and (E-57) these integrals become:

$$H_{0r} + jH_{0j} = \frac{\pi}{2(\xi_1 + \xi_2)} \left\{ \xi_1 \sqrt{1+q\xi_2} + \frac{2}{3q} [(1+q\xi_2)^{3/2} - 1] - \xi_1 \frac{\sqrt{1+q\xi_2}}{1+j\frac{k}{P_{oc}}} - \left[ \frac{G_{0c}}{P_{oc}} - \frac{\sqrt{1+q\xi_2}}{1+j\frac{k}{P_{oc}}} \right] \frac{\tanh(k_0 + j\beta)\xi_1}{d_0 + j\beta_0} - \int_0^{\xi_2} \frac{G_0}{\sqrt{1+q(\xi_2 - \xi_1)}} d\xi_2 \right\} \quad (\text{E-114})$$

$$H_{1r} + jH_{1j} + i(J_{1r} + jJ_{1j}) = \frac{\pi}{2(\xi_1 + \xi_2)} \left\{ \xi_1 \sqrt{1+q\xi_2} + \frac{2}{3q} [(1+q\xi_2)^{3/2} - 1] - \xi_1 \frac{\sqrt{1+q\xi_2}}{1+j\frac{k}{P_{oc}} + i\gamma\frac{k}{P_{oc}}} - \left[ \frac{G_{1c}}{P_{oc}} - \frac{\sqrt{1+q\xi_2}}{1+j\frac{k}{P_{oc}} + i\gamma\frac{k}{P_{oc}}} \right] \frac{\tanh(k + j\beta + i(d_1 + j\beta_1))\xi_1}{d_1 + j\beta_1 + i(a_1 + j\beta_1)} - \int_0^{\xi_2} \frac{G_1}{\sqrt{1+q(\xi_2 - \xi_1)}} d\xi_2 \right\} \quad (\text{E-115})$$

where  $P_{oc}$  is given by:

$$P_{oc} = \sqrt{1+q\xi_2} \quad (\text{E-116})$$

The two integrals on the right hand side are evaluated by numerical integration from the previously determined values of  $G_0$  and  $G_1$ .

When the static load on the bearing is  $W$ , the total force components acting on the journal in the radial and tangential directions are:

$$\begin{aligned} \text{Radial direction (opposite } \mathbf{e}_r): \quad F_r^* &= F_r - W \cos \varphi \\ \text{Tangential direction (opposite to } \mathbf{e}_\theta): \quad F_t^* &= F_t + W \sin \varphi \end{aligned} \quad (\text{E-117})$$

With  $\varphi$  given by Eq. (E-15), these components can be written in dimensionless form as:

$$f_r^* = f_r - \frac{W}{P_a L D} \cos \varphi = f_r - \frac{W}{P_a L D} (\cos \varphi_0 - \varphi_1 e^{i\tau} \sin \varphi_0) \quad (\text{E-118})$$

$$f_t^* = -f_t + \frac{W}{P_a L D} \sin \varphi = -f_t + \frac{W}{P_a L D} (\sin \varphi_0 + \varphi_1 e^{i\tau} \cos \varphi_0)$$

Set:

$$f_{r0} = \frac{2\varepsilon_0}{\eta(1+\eta)} H_{0r} \quad (\text{E-119})$$

$$f_{t0} = \frac{2\varepsilon_0}{1+\eta} H_{0j} \quad (\text{E-120})$$

$$f_r^* = f_r - \frac{W}{P_a L D} \cos \varphi = (\bar{K}_{rr} + i\bar{J}_{rr}) \varepsilon_1 e^{i\tau} + (\bar{K}_{rr} + i\bar{J}_{rr}) \varepsilon_0 \varphi_1 e^{i\tau} \quad (\text{E-121})$$

$$f_t^* = -f_t + \frac{W}{P_a L D} \sin \varphi = (\bar{K}_{tr} + i\bar{J}_{tr}) \varepsilon_1 e^{i\tau} + (\bar{K}_{tr} + i\bar{J}_{tr}) \varepsilon_0 \varphi_1 e^{i\tau} \quad (\text{E-122})$$

Then:

$$\frac{W}{P_a L D} \cos \varphi_0 = f_{r0} \quad (\text{E-123})$$

$$\frac{W}{P_a L D} \sin \varphi_0 = f_{t0} \quad (\text{E-124})$$

$$\frac{W}{P_a L D} = \sqrt{f_{r0}^2 + f_{t0}^2} \quad (\text{E-125})$$

$$\varphi_0 = \tan^{-1} \left( \frac{f_{t0}}{f_{r0}} \right) \quad (\text{E-126})$$

$$Z_{rr} = \bar{K}_{rr} + i\bar{J}_{rr} = \frac{2(1-\eta)(2\eta+1)}{\eta^2(1+\eta)} H_{0r} + \frac{2}{\eta(1+\eta)} (H_{1r} + iJ_{1r}) \quad (\text{E-127})$$

$$Z_{re} = \bar{K}_{re} + i\gamma \bar{B}_{re} = -\frac{2(1-\eta)}{\eta(1+\eta)} H_{0j} + \frac{2}{\eta(1+\eta)} (H_{1j} + iJ_{1j}) \quad (\text{E-128})$$

$$Z_{tr} = \bar{K}_{tr} + i\gamma \bar{B}_{tr} = -\frac{2(1-\eta)}{\eta(1+\eta)} H_{0j} - \frac{2}{1+\eta} (H_{1j} + iJ_{1j}) \quad (\text{E-129})$$

$$Z_{te} = \bar{K}_{te} + i\gamma \bar{B}_{te} = \frac{2(1-\eta)}{\eta(1+\eta)} H_{0r} + \frac{2}{1+\eta} (H_{1r} + iJ_{1r}) \quad (\text{E-130})$$

Here,  $\bar{K}_{rr}, \bar{B}_{rr}, \bar{K}_{re}, \bar{B}_{re}$  etc. are the dimensionless spring and damping coefficients:

$$\begin{aligned} \bar{K}_{rr} &= \frac{\partial f_r^*}{\partial \varepsilon} = \frac{CK_{rr}}{P_a LD} \\ \bar{B}_{rr} &= \frac{\partial f_r^*}{\gamma \partial \dot{\varepsilon}} = \frac{C\omega B_{rr}}{P_a LD} \\ \bar{K}_{re} &= \frac{\partial f_r^*}{\varepsilon_0 \partial \varphi} = \frac{CK_{re}}{P_a LD} \\ \bar{B}_{re} &= \frac{\partial f_r^*}{\gamma \varepsilon_0 \partial \dot{\varphi}} = \frac{C\omega B_{re}}{P_a LD} \end{aligned} \quad (\text{E-131})$$

and analogously for the four remaining coefficients. If it is desired, the coefficients can readily be expressed in an x-y-coordinate system with the x-axis in the direction of the static load  $W$  as in the preceding appendices. This is done by making use of Eqs. (A-70) to (A-77), Appendix I where  $SW$  is replaced by  $P_a LD$ ,  $f_r$  by  $f_r^*$  and  $(-f_c)$  by  $f_c^*$ .

For the purely hydrostatic bearing,  $\Lambda = 0$  but such that  $2\gamma\Lambda = \delta$  where  $\delta$  is the squeeze number (see Eq. (E-10)). In that case  $H_{0j} = H_{1j} = J_{1j} = 0$  and  $\beta_0 = \beta = \beta_1 = 0$  which considerably simplifies the calculations. Furthermore, for the hydrostatic bearing, the static load increases almost proportional with displacement and, therefore,  $\eta$  should be set equal to 1 in the above equations. In total, then, for a hydrostatic bearing:

#### Purely Hydrostatic Bearing

$$\begin{aligned} \frac{W}{P_a LD} &= f_{r0} = \varepsilon_0 H_{0r} \\ f_{t0} &= 0 \quad \varphi_0 = 0 \end{aligned} \quad (\text{E-132})$$

$$\bar{K}_{rr} + i\gamma \bar{B}_{rr} = \bar{K}_{tt} + i\gamma \bar{B}_{tt} = H_{tr} + iJ_{tr} \quad (\text{E-133})$$

$$\bar{K}_{rt} + i\gamma \bar{B}_{rt} = \bar{K}_{tr} + i\gamma \bar{B}_{tr} = 0$$

Thus, for a purely hydrostatic bearing there is only one spring coefficient and one damping coefficient which shall be denoted as  $K_0$  and  $B_0$ . It is convenient to express these coefficients and the load carrying capacity in the dimensionless form:

$$\frac{W}{(P_s - P_a)LD} = \frac{1}{V-1} \frac{W}{P_a LD} \quad (\text{E-134})$$

$$\frac{CK_0}{(P_s - P_a)LD} = \frac{1}{V-1} \bar{K}_{rr} \quad (\text{E-135})$$

$$\frac{B_0}{\mu L \left(\frac{R}{L}\right)^3} = \frac{24}{\sigma} \gamma \bar{B}_{rr} \quad (\text{E-136})$$

APPENDIX VI: THE STABILITY OF THE HYBRID-HYDROSTATIC RING BEARING WITH A COMPRESSIBLE LUBRICANT

The analysis of the stability of the hybrid-hydrostatic ring bearing is almost identical to the analysis of the hydrodynamic-hydrostatic ring bearing given in Appendix IV. Therefore, the present appendix will only describe the differences between the two analyses and otherwise refer to Appendix IV.

The equations of motion are given by Eqs. (D-1) where  $K_{xx}, B_{xx}, K_{xy}$  and so on are the dynamic coefficients of the inner film, and  $K_o$  and  $B_o$  are the coefficients of the outer film. They are determined from the analysis in Appendix V (note: instead of  $K_{xx}, B_{xx}, K_{xy}$ , etc can be used  $K_{rr}, B_{rr}, K_{rt}$ , etc. or the latter set of coefficients can be transformed to the first set of coefficients as discussed in Appendix V). Eq. (D-1) is made dimensionless by setting:

$$\bar{K}_o = \frac{CK_o}{P_a LD} = \left(\frac{C}{C_o}\right) \left(\frac{D_o}{D}\right) \left(\frac{P_s}{P_a} - 1\right) \frac{C_o K_o}{(P_s - P_a) L D_o} \quad (F-1)$$

$$\gamma \bar{B}_o = \frac{C_o B_o}{P_a LD} = \left(\frac{C}{C_o}\right) \left(\frac{D_o}{D}\right) \frac{\epsilon_o}{24} \frac{B_o}{\mu L \left(\frac{R_o}{C_o}\right)^3} \quad (F-2)$$

$$\bar{M} = \frac{C \omega^2 M}{P_a LD} \quad (F-3)$$

$$\bar{K}_{xx} = \frac{CK_{xx}}{P_a LD} \quad (F-4)$$

$$\bar{B}_{xx} = \frac{C \omega B_{xx}}{P_a LD} \quad (F-5)$$

and similarly for  $\bar{K}_{xy}, \bar{K}_{yx}, \bar{K}_{yy}, \bar{B}_{xy}, \bar{B}_{yx}$  and  $\bar{B}_{yy}$ . The symbols are defined in Appendix IV and Appendix E.

The stability analysis is performed for fixed values of the compressibility number  $\Lambda$  and the static eccentricity ratio  $\epsilon_o$  (i.e. for a constant static load  $W$  and a given speed  $\omega$ ). Hence, the dynamic coefficients are only functions of the frequency ratio  $\gamma = \frac{\omega}{\omega_c}$ . Then the analysis given in

Appendix *N* can be used directly as long as it is remembered, that whereas the dynamic coefficients in Appendix D are independent of  $\gamma$  because the lubricant is incompressible, they now depend implicitly on  $\gamma$ . The equations, however, are the same in the two cases.

APPENDIX VII: Computer Program - The Static and Dynamic Performance of a Lobed Bearing with Turbulent Film

This appendix describes the computer program PN0375: "The Static and Dynamic Performance of a Lobed Bearing with Turbulent Film" and gives the detailed instructions for using the program. The program is based on the analyses contained in Appendices I and II. It calculates the Sommerfeld number, the flow, the coefficient of friction, the 8 dynamic bearing coefficients and the critical journal mass, for a journal bearing with up to 12 lobes whose lubricant film may be turbulent. Film rupture is included.

COMPUTER INPUT

An input data form is given in back of this appendix for quick reference when preparing the computer input. In the following, the more detailed instructions are given.

Card 1 (15)

This card contains one value:

NRET which gives the number of film Reynolds numbers in the table of turbulent flow coefficients ( $1 \leq NRET \leq 250$ )

Table of Turbulent Flow Coefficients (4E15.7)

In a bearing film with fully developed turbulence where the Couette flow is the dominating flow component, the effect of turbulence on the lubrication action can be accounted for by means of two coefficients,  $G_v$  and  $G_g$ . These coefficients modify the Poiseuille flow (the pressure induced flow) and they are functions of the film Reynolds number  $R_h$ :

$$R_h = \frac{\rho R \omega h}{\mu} = h R_e$$

where  $h$  is the local film thickness, normalized with respect to the radial clearance  $C$ , and  $R_e$  is the Reynolds number for the bearing.  $G_x$  and  $G_z$  are given in reference 1 and can also be found in the table in the input data for the sample calculation later in this appendix. It should be noted, that the values used for  $G_x$  and  $G_z$  in the present program are twelve times the values found in reference 1. By doing this,  $G_x$  and  $G_z$  are equal to 1 when  $R_h = 0$  (ie. for laminar flow).

For use in the calculation of the dynamic performance of the bearing it is necessary to specify the first three derivatives of  $G_x$  with respect to  $R_h$ . Also, the first derivative of  $\frac{G_z}{G_x}$  is required. Finally, to determine the friction loss of the bearing, the coefficient of friction,  $C_f$  must be given. In the table,  $C_f$  is specified by giving the product  $\frac{1}{8} R_h C_f$  which is equal to 1 for  $R_h = 0$ . In total, then, there are 7 quantities for each film Reynolds number. They are given on two cards:

First Card (4E15.7)

1.  $R_h = \frac{\rho \omega R \bar{h}}{\mu} = h R_e$ , the film Reynolds number. The first value in the table should preferably be 0. In any case, the table must span over the range:  $(1-\epsilon_p) R_e \leq R_h \leq (1+\epsilon_p) R_e$  where  $R_e$  is the input value of the bearing Reynolds number (see later input list) and  $\epsilon_p$  is the maximum eccentricity ratio for any lobe in the particular calculation. Since the largest possible value of  $\epsilon_p$  is 1, it is safest to let the range of  $R_h$  be:  $0 \leq R_h \leq 2 R_e$ .

To use the table, the program employs linear interpretation. The local dimensionless film thickness  $h$  is computed from which the film Reynolds number is determined as  $R_h = h R_e$  where  $R_e$  is given in the input. Then the table is scanned, starting with the first table value of  $R_h$ , until  $(R_h)_{Table} \geq (R_h)_{Calculated}$ . Assume this to be at the  $k$ 'th table value (ie.  $(R_h)_{Table} = (R_h)_k$ ). The proper value of  $G_x$  is then computed as:

$$G_x = \frac{(R_h)_k - (R_h)_{Calc.}}{(R_h)_k - (R_h)_{k-1}} (G_x)_{k-1} + \frac{(R_h)_{Calc.} - (R_h)_{k-1}}{(R_h)_k - (R_h)_{k-1}} (G_x)_k$$

and similarly for the remaining 6 quantities. If  $(R_h)_{\text{calcul.}}$  is greater than the last value in the table, the program sets  $(R_h)_{\text{calcul.}} = (R_h)_{\text{last value}}$ . If  $(R_h)_{\text{calcul.}}$  is smaller than the first value in the table, the program will be in error.

2.  $\frac{1}{8} R_h C_f$ , the dimensionless friction factor. For  $R_h=0$  (laminar flow),  $\frac{1}{8} R_h C_f = 1$ .
3.  $G_x$ , the dimensionless Poiseuille flow coefficient for the circumferential direction. For  $R_h=0$  (laminar flow),  $G_x = 1$ .
4.  $\frac{1}{G_x} \frac{dG_x}{dR_h}$ , dimensionless. This is the first derivative of  $G_x$  divided by  $G_x$ . For  $R_h=0$  (laminar flow),  $\frac{1}{G_x} \frac{dG_x}{dR_h} = 0$ .

Second Card(4E15.7)

1.  $\frac{1}{G_x} \frac{d^2 G_x}{dR_h^2}$ , dimensionless. This is the second derivative of  $G_x$  divided by  $G_x$ . For  $R_h=0$  (laminar flow),  $\frac{1}{G_x} \frac{d^2 G_x}{dR_h^2} = 0$ .
2.  $\frac{1}{G_x} \frac{d^3 G_x}{dR_h^3}$ , dimensionless. This is the third derivative of  $G_x$  divided by  $G_x$ . For  $R_h=0$  (laminar flow),  $\frac{1}{G_x} \frac{d^3 G_x}{dR_h^3} = 0$ .
3.  $\frac{G_z}{G_x}$ , dimensionless. This is the ratio between the Poiseuille flow coefficient,  $G_z$ , for flow in the axial direction, and  $G_x$ . For  $R_h=0$  (laminar flow),  $\frac{G_z}{G_x} = 1$ .
4.  $\frac{d}{dR_h} \left( \frac{G_z}{G_x} \right)$ , dimensionless. This is the first derivative of  $\frac{G_z}{G_x}$ . For  $R_h=0$  (laminar flow),  $\frac{d}{dR_h} \left( \frac{G_z}{G_x} \right) = 0$ .

In total the table contains NRET entry values of  $R_h$  arranged in sequence, starting with the smallest value. Thus, the table consists of 2 NRET cards. There can be a maximum of 250 entry values.

Card (72H)

This card is used as a title card, identifying the calculation. Any descriptive text can be given in columns 2 to 72. If a 1 is punched in Column 1, the output listing will start on a new page for each case.

Control Card (1215)

This card controls the input and the output. It has 12 values:

1. M. This is the number of finite difference increments in the circumferential direction per lobe, see Fig. 55, Appendix I. When the lobe arc is  $(\theta_{out} - \theta_{in})$ , degrees, the circumferential increment is:

$$\Delta\theta = \frac{(\theta_{out} - \theta_{in})}{M} \text{ degrees}$$

It is suggested to let  $\Delta\theta$  be 10 to 15 degrees, depending on the eccentricity ratio (the larger the eccentricity ratio, the smaller should  $\Delta\theta$  be). The largest allowable value of M is 36. Also, M must be larger than or equal to 3.

2. N. This is the number of finite difference increments in the axial direction on half of the bearing length (see Fig. 55, Appendix I). If the increment is  $\Delta Z$  and the bearing length is L, then:

$$\Delta Z = \frac{L/2}{N}$$

In dimensionless form as used by the program:

$$\Delta\bar{z} = \frac{1}{R} \Delta Z = \frac{L/D}{N}$$

N should be chosen such that  $\Delta\bar{z}$  is approximately the same as  $\Delta\theta$  when  $\Delta\theta$  is measured in radians. However, since there are pressure gradients in the circumferential direction which are considerably larger than the axial pressure gradients,  $\Delta\bar{z}$  can be made somewhat larger than  $\Delta\theta$ . Furthermore, it is of great importance to keep N as small as possible since the calculation time is roughly proportional to  $N^2$  or  $N^3$ .

Usual values for N are 5 to 7, depending, of course, on the L/D- ratio.  
The allowable range of N is:  $3 \leq N \leq 13$ .

3. NLD Specifies the number of L/D-values in the designated input list (L/D is the length-to-diameter ratio of the bearing). The allowable range is:  $1 \leq NLD \leq 20$ .

4. NRE Specifies the number of bearing Reynolds numbers  $R_e$  in the designated input list. The allowable range is:  $1 \leq NRE \leq 30$ .

5. NPAD Specifies the number of bearing lobes. The allowable range is:  $1 \leq NPAD \leq 12$ .

6. NECA Specifies the number of  $\epsilon_B \cos \phi_B$  values in the designated input list. ( $\epsilon_B$  is the bearing eccentricity ratio,  $\phi_B$  is the bearing attitude angle) The allowable range is:  $1 \leq NECA \leq 20$ .

7. NAB Specifies the maximum allowable number of calculations to be performed in determining that bearing attitude angle for which the horizontal force  $F_y$  is zero. A detailed discussion is given later in connection with the input list for  $\epsilon_B \cos \phi_B$  and  $\epsilon_B \sin \phi_B$ . NAB should be greater than NAT (the number of  $\epsilon_B \sin \phi_B$ -values in designated input list).

8. NRP The program provides for the case of film rupture where no sub-ambient film pressures are permitted. In the regions where the pressure otherwise would have been less than ambient, the film contracts such that the pressure in the contracted film becomes ambient. The boundary separating the full film and the contracted portion is determined by iterations as discussed later in connection with the convergence limit for the rupture calculation. NRP specifies the maximum allowable number of such iterations to be performed. A usual value for NRP is 5 to 7. If it is not desired to include the effect of rupture, set  $NRP = -1$ .

9. NPW In most cases, only the final results of the calculations for the composite bearing are of interest. Then NPW is set equal to zero. On occasions, however, it may be desired to get the results for each bearing lobe before they are combined into the composite bearing. In that case, set NPW=1 or NPW = -1. If NPW = -1, the results will include the pressure distribution. If NPW = 1, the pressure distribution will be omitted from the output.

10. NRW Under certain conditions the calculations of the boundary between the complete film and the contracted film does not readily converge. In that case it may be desired to explore the matter in more detail. If NRW = 1, the output lists the "error" (the relative difference between two successive calculations) for each rupture iteration of each lobe. If NRW = -1, the output gives, in addition to the "error", the coordinates of the rupture boundary for each iteration. If NRW = -2, the output gives, in addition to the output for NRW = -1, the finite difference coefficients  $\alpha_i^{(+)}$ ,  $\alpha_i^{(-)}$  and  $\beta_j$  (see Fig. 56, Appendix I) for each iteration..

When the calculations experience difficulties, the "error" does not converge smoothly. It will normally be found that the reason is that the rupture boundary intersects a  $f$ -gridline (see Fig. 55, Appendix I). Thus, the trouble can frequently be eliminated by changing the gridline spacing (ie. change M, item 1, control card).

Only under unusual circumstances is it of interest to explore the rupture boundary calculations. By setting NRW = 0, the output will not include any results of these calculations. Hence, the normal value of NRW is zero.

11. NPUN As discussed in connection with Item 7, the program may perform several calculations in order to determine the attitude angle for which the horizontal force is zero. If it is desired to get the results from each calculation, set NPUN = -1 or NPUN = -2. In the latter case, the

results for the composite bearing are punched on cards after each attitude angle calculation but only if there is no more than 1 lobe. No punched card output is given if NPUN = -1. If it is desired to get the final results only after the correct attitude angle has been determined, set NPUN = 0 or NPUN = 1. In the latter case, the output is also punched on cards for bearings with 1 lobe only. This is omitted when NPUN = 0.

Thus, the usual value of NPUN is zero (or 1, if punched card output is also desired).

12. INP When INP = 0, a new set of input data follows the present set of data. The new set of data starts with the text card (Card (72H)). The table of turbulent flow coefficients should not be repeated and can only be given with the first set of input. If INP = 1, the present set of data is the last or only set.

Card (1P5E14.6)

This card contains two values:

1. CVLA This is the convergence limit for the bearing attitude angle  $\phi_B$ . After each complete bearing calculation, the total horizontal force  $F_{y_0}$  and the total vertical force  $F_{x_0}$  are computed by a summation over all bearing lobes, see eqs. (B-8) and (B-9), Appendix II. The correct attitude angle is the one for which  $F_{y_0} = 0$ . This condition is accepted to be satisfied by the program when:

$$\left| \frac{F_{y_0}}{F_{x_0}} \right| \leq \text{CVLA}$$

or when the total number of attitude angle calculations exceeds NAB (Item 7, control card).

The attitude angle is  $\phi_B$ . If the deviation between the attitude angle for which  $F_{y_0} = 0$ , and the calculated attitude angle is called  $\Delta\phi_B$ , then:

$$\Delta \phi_B = \tan^{-1} \left( \frac{F_{y0}}{F_{x0}} \right)$$

When  $F_{y0}$  is small this is equivalent to:

$$\Delta \phi_B \cong \frac{F_{y0}}{F_{x0}}$$

Hence, the given convergence criteria corresponds to requiring:

$$|\Delta \phi_B|, \text{ radians} < \text{CVLA}$$

or

$$|\Delta \phi_B|, \text{ degrees} < 57.3 \cdot \text{CVLA}$$

If it is desired to obtain the attitude angle within 0.01 degrees, then set  $\text{CVLA} \cong 1.7 \cdot 10^{-4}$ . A typical value for CVLA is  $10^{-4}$ .

2. CVLR This is the convergence limit for the calculation of the rupture boundary for each bearing lobe. The program calculates the angular coordinates of the boundary for each  $i$  gridline (see fig. 55, Appendix I) let these coordinates be  $\theta_i, i=1,2, \dots, n$ . After the  $k$ 'th rupture iteration, the program tests the convergence of the calculations by:

$$\frac{\sum |\theta_i^{(k)} - \theta_i^{(k-1)}|}{\sum |\theta_i^{(k-1)}|} \leq \text{CVLR}$$

When this condition is satisfied or when the total number of iterations is equal to NRP (Item 8, control card), i.e. when  $k = \text{NRP}$ , the program assumes that the calculations have converged. A typical value for CVLR is  $10^{-5}$ .

When NRP = -1, set CVLR = 100.

List of Bearing Length-to-Diameter Ratios (1P5E14.6)

This list gives the input values of the length-to-diameter ratio,  $L/D$ , where  $L$  is the bearing length and  $D$  is the journal diameter. In total there are NLD values (Item 3, control card), maximum 20.

### List of Bearing Reynolds Numbers (1P5E14.6)

This list gives the input values for the bearing Reynolds number:

$$R_e = \frac{\rho R \omega C}{\mu}$$

where  $\rho$  = mass density of lubricant,  $\text{lbs}\cdot\text{sec}^2/\text{inch}^4$ ,  $\mu$  = viscosity of lubricant,  $\text{lbs}\cdot\text{sec}/\text{inch}^2$ ,  $\omega$  = angular speed of journal, radians/sec,  $R$  = journal radius, inch, and  $C$  = radial clearance of lobes, inch. When  $R_e = 0$ , the film is laminar. In total, there are NRE values of  $R_e$  (item 4, control card), maximum 30.

### Data for Journal Center Position

Referring to fig. 58, Appendix II, the coordinates of the journal center with respect to the bearing center can be expressed by means of the eccentricity ratio  $\epsilon_0$  and the attitude angle  $\phi_0$ .  $\epsilon_0$  is the ratio between the journal center eccentricity,  $e_0$ , and the machined radial clearance,  $C$ , of the lobes:

$$\epsilon_0 = \frac{e_0}{C}$$

The attitude angle,  $\phi_0$ , is the angle between the static load line (the x-axis) and the line connecting the bearing center and the journal center, measured in the direction of journal rotation. The corresponding coordinates in the x-y-coordinate system are:  $\epsilon_0 \cos \phi_0$  and  $\epsilon_0 \sin \phi_0$ .

A given bearing calculation is performed for a fixed value of  $\epsilon_0 \cos \phi_0$ . With this value fixed,  $\epsilon_0 \sin \phi_0$  is varied over a range in specified increments to determine when the horizontal force  $F_{y_0}$  becomes zero. For each value of  $\epsilon_0 \sin \phi_0$ , the program calculates the static horizontal force  $F_{y_0}$ . When  $F_{y_0}$  changes sign,  $F_{y_0}$  is calculated at the midpoint of the last  $\epsilon_0 \sin \phi_0$ -interval and quadratic interpolation is employed to obtain the first "guess" of the value of  $\epsilon_0 \sin \phi_0$  for which  $F_{y_0}$  should be zero. If the corresponding value of  $F_{y_0}$  is not sufficiently small, as tested by means of the convergence criteria explained above, the latest obtained value of  $F_{y_0}$  is used together with the two closest previously obtained values to calculate a new value of  $\epsilon_0 \sin \phi_0$  by quadratic interpolation. This procedure is repeated until either the convergence criteria is satisfied or the total number of calculations exceeds the

allowable limit NAB (Item 7, control card).

In total, there are NECA values of  $\epsilon_b \cos \phi_b$  (Item 6, control card), maximum 20. The card specifying  $\epsilon_b \cos \phi_b$ , contains two items:

Card (1PE14.6, 15)

1.  $\epsilon_b \cos \phi_b$ . It can have any value as long as the corresponding eccentricity ratios,  $\epsilon_p$ , for any of the bearing lobes do not equal or exceed 1, see eq. (B-5), Appendix II.
2. NAT If  $NAT \geq 1$ , the program determines the attitude angle for which the horizontal force is zero. Then NAT gives the number of values of  $\epsilon_b \sin \phi_b$  in the following input list. Item 7, control card: NAB should be greater than NAT to allow for several interpolations in determining  $\phi_b$  (suggested value:  $NAB = NAT + 3$ ).

If  $NAT \leq -1$ , no interpolation is performed to determine when the horizontal force is zero. The program calculates the bearing for each specified value of  $\epsilon_b \sin \phi_b$  and gives the results of each calculation (set NPUN = -1 or -2, item 11, control card). The absolute value of NAT,  $|NAT|$ , specifies the number of values of  $\epsilon_b \sin \phi_b$  in the following input list. Item 7, control card: NAB should be set eq. to  $|NAT|$ .

Note: NAT cannot be zero. The maximum value of NAT (or  $|NAT|$ ) is 25.

This card is followed by:

List of  $\epsilon_b \sin \phi_b$  Values (1P5E14.6)

This list gives the input values of  $\epsilon_b \sin \phi_b$  for the above specified  $\epsilon_b \cos \phi_b$  value. In total there are NAT values, maximum 25.  $\epsilon_b \sin \phi_b$  may have any value as long as the eccentricity ratio,  $\epsilon_p$ , of any bearing lobe does not equal or exceed 1, see eq. (B-5), Appendix II.

If it is desired to calculate the bearing with a concentric journal, set  $\epsilon_B \cos \varphi_B = 0$  and give only one value of  $\epsilon_B \sin \varphi_B$ , namely  $\epsilon_B \sin \varphi_B = 0$ . Furthermore, set NAT = 1 and NAB = 0.

In the case where  $\epsilon_B \cos \varphi_B = 0$  and the journal is not concentric in the bearing, no value of  $\epsilon_B \sin \varphi_B$  should be zero.

If it is desired to calculate the attitude angle for which the horizontal force is zero (i.e. NAT is positive), the  $\epsilon_B \sin \varphi_B$  values should be listed in sequence, starting with the lowest value (it may be zero when  $\epsilon_B \cos \varphi_B \neq 0$ ). The range of  $\epsilon_B \sin \varphi_B$  should be large enough that it includes the point where  $F_{y_0} = 0$ . Otherwise, the program cannot obtain a solution.

The preceding input, namely the card with  $\epsilon_B \cos \varphi_B$  and the list of  $\epsilon_B \sin \varphi_B$  values, must be repeated together NECA times (Item 6, control card).

#### Bearing Geometry Data (1P5E14.6)

The bearing is made up of NPAD lobes (Item 5, control card). The geometry of the lobe is specified by giving the angles from the static load line (the x-axis) to the leading edge and the trailing edge of the lobe, and by giving the coordinates of the center of curvature of the lobe relative to the bearing center and the static load line, see figure 56, Appendix II. The input consists of NPAD cards, maximum 12, and on each card are four values:

1.  $\Theta_{p,in}$ , degrees. This is the angle from the load line (the negative x-axis) to the leading edge of the lobe, measured in the direction of journal rotation (see fig. 58, Appendix II). The value for  $\Theta_{p,in}$  should be such that:  $0 \leq \Theta_{p,in} \leq 360$ .  $\Theta_{p,in}$  must be smaller than  $\Theta_{p,out}$ .
2.  $\Theta_{p,out}$ , degrees. This is the angle from the load line (the negative x-axis) to the trailing edge of the lobe, measured in the direction of journal rotation (see Fig. 58, Appendix II). The value for  $\Theta_{p,out}$  should lie in

range:  $\theta_{p,in} < \theta_{p,out} \leq 360 + \theta_{p,in}$  ( $\theta_{p,out} > 0$ ).

3.  $\delta_p$ . This is the preload of the lobe:

$$\delta_p = \frac{r_p}{C}$$

where  $r_p$  is the distance between the bearing center and the center of curvature of the lobe.  $C$  is the machined radial clearance of the lobe (i.e. the difference between the lobe radius of curvature and the journal radius.  $C$  is the same for all lobes). For a cylindrical bearing,  $\delta_p = 0$ . For the elliptical bearing or a three-lobe bearing,  $\delta_p$  is the same for all lobes and equal to the preload of the bearing in which case  $\delta_p < 1$ .

4.  $\psi_p$  degrees. This is the angle from the static load line (the positive x-axis) to the line connecting the bearing center and the center of curvature of the lobe, measured in the direction of journal rotation (see Fig. 58, Appendix II). For a cylindrical bearing, set  $\psi_p = 0$ . In the elliptical bearing or the three-lobe bearing, set  $\psi_p = \frac{1}{2}(\theta_{p,out} + \theta_{p,in})$ .

#### COMPUTER OUTPUT

The output first repeats the input data for checking purposes (the table of turbulent flow coefficients is not included). Then follow the results of the calculations. Because of the several output format options, a complete sequential description of the output will not be given. Instead, the output for the normal type of calculation will be described where only the final results for the composite bearing are given. The final results are in five lines where the items are identified by the titles:

L/D is the specified length - to-diameter ratio of the bearing.

REYN.NO. is the specified bearing Reynolds number  $R_e$ .

ECC\* $\cos(\text{ATT})$  is the specified fixed value of  $\epsilon_0 \cos \varphi_0$ .

ECC\* $\sin(\text{ATT})$  is the final value of  $\epsilon_0 \sin \varphi_0$ .

ECC.RATIO is the bearing eccentricity ratio  $\epsilon_0 = \sqrt{(\epsilon_0 \cos \varphi_0)^2 + (\epsilon_0 \sin \varphi_0)^2}$

ATT, ANGLE is the bearing attitude angle  $\varphi_0 = \tan^{-1}(\epsilon_0 \sin \varphi_0 / \epsilon_0 \cos \varphi_0)$ , degrees.

1/S is the inverse Sommerfeld number for the bearing:  $\frac{1}{S} = \frac{W}{\mu N D L (\epsilon)^2}$

$F\text{-}Y/S*W$  is the residual dimensionless horizontal force:  $F_{y0}/\mu NDL(\xi)^2$ , eq. (B-9)

$1/S*(R/C*F/W)$  is the friction factor:  $\frac{R}{C} \frac{F_z}{SW} = \frac{R}{C} \frac{F_z}{\mu NDL(\xi)^2}$ , eq. (B-10)

$(Q\text{-}Z/NDLC)\text{SIDE}$  is the dimensionless flow out of both bearing sides:  $Q_z/NDLC$ , see eq.

$(Q/NDLC)\text{TOTAL}$  is the total dimensionless flow consumption of the bearing:  $Q/NDLC$

For a lobed bearing with NPAD lobes, the total flow is:

$$Q = \sum_{p=1}^{NPAD} \left[ (Q_z)_p + \left\{ \begin{array}{l} (Q_x)_{p, \text{trail. edge}} - (Q_x)_{p, \text{lead. edge}} \text{ when positive} \\ 0 \text{ (when above quantity is negative)} \end{array} \right\} \right]$$

(see remarks following eq. (B-13), Appendix II)

When NPAD = 1:  $Q = Q_z + (Q_x)_{\text{trail. edge}}$

$(Q\text{-}X/NDLC)\text{CIRC}$  is the dimensionless total flow into the bearing lobes from the grooves:

$$\sum_{p=1}^{NPAD} \left( \frac{Q_x}{NDLC} \right)_{p, \text{lead. edge}}$$

$F\text{-}X/S*W$  is the dimensionless vertical bearing reaction:  $-F_{x0}/\mu NDL(\xi)^2$ , eq. (B-8). When  $F_{y0} = 0$ , this is equal to  $1/S$ , see eq. (B-16)

$CMN/MUJDL(R/C)2$  is the dimensionless critical journal mass at the threshold of instability:  $\frac{CMN}{\mu NDL(\xi)^2}$ , calculated from eqs. (B-26) and (B-27).

$FREQ/W$  is the frequency ratio:  $\gamma = \frac{\omega}{\omega_c}$ , at the threshold of instability.

$(FREQ/W)**2$  is the square of the instability frequency ratio:  $\gamma^2 = \left(\frac{\omega}{\omega_c}\right)^2$ , calculated from eqs. (B-27). When  $\gamma^2$  is negative, there is no instability threshold.

$CKXX/SW$  is the dimensionless bearing spring coefficient for the x-direction:

$$\frac{CK_{xx}}{SW} = \frac{CK_{xx}}{\mu NDL(\xi)^2}, \text{ see eq (B-12)}$$

$CKXY/SW$  is the dimensionless bearing cross-coupling spring coefficient for the

x-direction:  $\frac{CK_{xy}}{SW} = \frac{CK_{xy}}{\mu NDL(\xi)^2}$

$CKYX/SW$  is the dimensionless bearing cross-coupling spring coefficient for the

y-direction:  $\frac{CK_{yx}}{SW} = \frac{CK_{yx}}{\mu NDL(\xi)^2}$

$CKYY/SW$  is the dimensionless bearing spring coefficient for the y-direction:

$$\frac{CK_{yy}}{SW} = \frac{CK_{yy}}{\mu NDL(\xi)^2}$$

$CWEXX/SW$  is the dimensionless bearing damping for the x-direction:

$$\frac{C\omega B_{xx}}{SW} = \frac{C\omega B_{xx}}{\mu NDL(\xi)^2}, \text{ see eq. (B-13).}$$

CWBXY/SW is the dimensionless bearing cross-coupling damping for the x-direction:

$$\frac{C_{\omega B_{xy}}}{SW} = \frac{C_{\omega B_{xy}}}{\mu NDL (\frac{R}{C})^2}$$

CWBXY/SW is the dimensionless bearing cross-coupling damping for the y-direction:

$$\frac{C_{\omega B_{yx}}}{SW} = \frac{C_{\omega B_{yx}}}{\mu NDL (\frac{R}{C})^2}$$

CWBY/SW is the dimensionless bearing damping for the y-direction:

$$\frac{C_{\omega B_{yy}}}{SW} = \frac{C_{\omega B_{yy}}}{\mu NDL (\frac{R}{C})^2}$$

SOMMERFELD NO is the Sommerfeld number:  $S = \frac{\mu NDL}{W} \left(\frac{R}{C}\right)^2$

F-X/W is a second form of the dimensionless vertical bearing reaction:  $-F_{x0}/W$   
(= 1 when  $F_{y0} = 0$ )

F-Y/W is a second form of the dimensionless residual horizontal force:  $F_{y0}/W$

(R/C)\*(F/W) is the most usual form of the friction factor:  $\frac{R}{C} \frac{F}{W}$ , see eq. (B-17)

CW\*\*2/W is a second form of the dimensionless critical journal mass:  $\frac{CM\omega^2}{W}$

see eq. (B-28)

CKXX/W is a second form of the dimensionless bearing spring coefficient in the

x-direction:  $\frac{CK_{xx}}{W}$ , see eq. (B-18)

$$\frac{CK_{xy}}{W} = \frac{CK_{xy}}{W}$$

$$\frac{CK_{yx}}{W} = \frac{CK_{yx}}{W}$$

$$\frac{CK_{yy}}{W} = \frac{CK_{yy}}{W}$$

CWBXX/W is a second form of the dimensionless bearing damping in the x-direction:

$$\frac{C_{\omega B_{xx}}}{W}, \text{ see eq. (B-19)}$$

$$\frac{C_{\omega B_{xy}}}{W} = \frac{C_{\omega B_{xy}}}{W}$$

$$\frac{C_{\omega B_{yx}}}{W} = \frac{C_{\omega B_{yx}}}{W}$$

$$\frac{C_{\omega B_{yy}}}{W} = \frac{C_{\omega B_{yy}}}{W}$$

The nomenclature is:

$B_{xx}, B_{xy}, B_{yx}, B_{yy}$

Damping coefficients for the bearing, lbs sec/inch

C

The machined radial clearance of the lobes, inch

D

The journal diameter, inch

$e_B$

The eccentricity between the journal center and the bearing center, inch

$F_{x0}$

The static bearing reaction in the x-direction, lbs.

$F_{y0}$

The static bearing reaction in the y-direction, lbs.

$F_f$

The friction force, lbs (the friction torque =  $RF_f$ )

$K_{xx}, K_{xy}, K_{yx}, K_{yy}$	Spring coefficients for the bearing, lbs/inch
L	The bearing length, inch
M	The critical mass of the journal at the threshold of instability, lb
N	The rotor speed, rps
Q	The total hydrodynamic bearing flow, cub.inch/sec
$Q_x$	The hydrodynamic flow in the circumferential direction, cub.inch/sec
$Q_z$	The hydrodynamic flow out of both bearing sides, cub.inch/sec
R	The journal radius, inch
$R_e$	The Reynolds number for the bearing: $R_e = \frac{\rho R \omega C}{\mu}$ dimensionless
S	The Sommerfeld number for the bearing: $S = \frac{\mu N D L}{W} \left(\frac{R}{C}\right)^2$ dimensionless
W	The static bearing load, lbs
$\gamma$	The instability frequency ratio: $\gamma = \frac{\omega}{\omega_c}$ , dimensionless
$\epsilon_0$	The eccentricity ratio for the bearing, $\epsilon_0 = e_0/C$ dimensionless
$\mu$	The lubricant viscosity, lbs.sec/inch <sup>2</sup>
$\nu$	The frequency at the threshold of instability, radians/sec
$\rho$	The mass density of the lubricant, lbs.sec <sup>2</sup> /inch <sup>4</sup>
$\phi_0$	The attitude angle for the bearing. It is the angle from the X-axis to the line connecting the bearing center and the journal center, measured in the direction of journal rotation, degrees.
$\omega$	The angular speed of the journal, radians/sec.

When it is desired to obtain the data for the individual lobes in addition to the composite bearing results,  $NPW \neq 0$  in the input (Item 9, control card). Then there will be output for each lobe for each attitude angle iteration. Each set of output is identified by the title: BEARING PAD NO., followed by the number of the particular lobe (the lobes are numbered consecutively in the

sequence as given in the input). The results are identified by titles:

SOMMERFELD NO is the Sommerfeld number for the lobe,  $S_p = \frac{\mu NDL}{W_p} \left( \frac{R}{C} \right)^2$

ECC. RATIO is the lobe eccentricity ratio  $\epsilon_p$ , see eq. (B-5)

ATT. ANGLE is the lobe attitude angle  $\phi_p$ , see eq. (B-6), degrees.

CALC. ATT. ANG is the angle:  $\tan^{-1}(f_{to}/f_{ro})$ , see Appendix I, eqs (A-64), (A-78) and (A-79)

F-R/S\*W is the dimensionless radial static force component for the lobe:  $f_{ro} = \frac{F_{ro}}{S_p W_p}$

F-T/S\*W is the dimensionless tangential static force component for the lobe:  $f_{to} = \frac{F_{to}}{S_p W_p}$

1/S\*(R/C\*F/W) is the dimensionless friction factor for the lobe:  $\frac{R}{C} \frac{F_{\epsilon,p}}{S_p W_p} = \frac{R}{C} \frac{F_{\epsilon,p}}{\mu NDL \left( \frac{R}{C} \right)^2}$

(Q-X/NDLC)IN is the dimensionless flow into the lobe across the leading edge:  $\left( \frac{Q_x}{NDLC} \right)_{lead}$

(Q-X/NDLC)OUT is the dimensionless flow out of the lobe across the trailing edge:  $\left( \frac{Q_x}{NDLC} \right)_{tr}$

(Q-Z/NDLC)SIDE is the dimensionless flow out of the lobe across both sides of the lobe:  $\frac{Q_z}{NDLC}$

F-X/S\*W is the dimensionless x-component of the static force on the lobe:

$$- \frac{F_{xo}}{S_p W_p}, \text{ see eq (A-78)}$$

F-Y/S\*W is the dimensionless y-component of the static force on the lobe:

$$- \frac{F_{yo}}{S_p W_p}, \text{ see eq. (A-79)}$$

DFR/SDE is the dimensionless radial stiffness:  $\frac{\partial f_r}{\partial \epsilon}$ , see eqs. (A-59) and (A-60)

DFT/SDE is the dimensionless tangential cross-coupling stiffness:  $\frac{\partial f_t}{\partial \epsilon}$ , see eq. (A-60)

DFR/SDA is the dimensionless radial cross-coupling stiffness:  $\frac{\partial f_r}{\epsilon_0 \partial \phi}$ , see eqs. (A-59) and A-61)

DFT/SDA is the dimensionless tangential stiffness:  $\frac{\partial f_t}{\epsilon_0 \partial \phi}$ , see eq. (A-61)

DFR/SDEDT is the dimensionless radial damping:  $\frac{\partial f_r}{\partial \dot{\epsilon}}$ , see eqs. (A-59) and (A-62)

DFT/SDEDT is the dimensionless tangential damping:  $\frac{\partial f_t}{\partial \dot{\epsilon}}$ , see eqs. (A-62)

DFR/SDADT is the dimensionless radial cross-coupling damping:  $\frac{\partial f_r}{\epsilon_0 \partial \dot{\phi}}$ , see eqs. (A-59 and (A-63)

DFT/SDADT is the dimensionless tangential damping:  $\frac{\delta_t}{\epsilon_{00} \omega}$ , see eq. (A-63)

CKXX/SW is the dimensionless stiffness, x-direction:  $\frac{CK_{xx}}{S_p W_p}$ , see eq. (A-70)

CKXY/SW =  $\frac{CK_{xy}}{S_p W_p}$ , eq. (A-71)

CKYX/SW =  $\frac{CK_{yx}}{S_p W_p}$ , eq. (A-72)

CKYY/SW =  $\frac{CK_{yy}}{S_p W_p}$ , eq. (A-73)

CWBXX/SW =  $\frac{C_{wBxx}}{S_p W_p}$ , eq. (A-74)

CWBXY/SW =  $\frac{C_{wBxy}}{S_p W_p}$ , eq. (A-75)

CWBYX/SW =  $\frac{C_{wByx}}{S_p W_p}$ , eq. (A-76)

CWBYY/SW =  $\frac{C_{wByy}}{S_p W_p}$ , eq. (A-77)

CMN/MUDL(R/C)2 is the dimensionless critical journal mass for the lobe:  $\frac{CM_p N}{\mu DL (\frac{R}{C})^2}$

CMW\*\*2/W is another form of the dimensionless critical journal mass:  $CM_p \omega^2 / W_p$

FREQ/W is the instability frequency ratio for the lobe:  $\gamma_p = \omega_p / \omega$

(FREQ/W)\*\*2 is the square of the instability frequency ratio for the lobe:  $\gamma_p^2$ .

If  $\gamma_p^2$  is negative, there is no instability threshold for the lobe.

In addition to these data, the output for a lobe also includes the results from the last rupture boundary calculation. First is a line giving the number of iterations and the final error (the left hand side of the equation given in the discussion of the input data for CVLR). This is followed by a 5 column list, giving the coordinates of the rupture boundary. The five columns are identified by titles:

I is the i-index for the gridline (see fig. 55, Appendix I).

BEGIN, INDEX gives the j-coordinate (see fig. 55.) of the rupture boundary at the leading edge. If j=1, leading edge rupture does not occur.

END INDEX gives the j-coordinate (see fig. 55.) of the rupture boundary at the trailing edge. If j = M + 1 (item 1, control card in input), trailing edge rupture does not occur.

BEGIN, ANGLE gives the angular coordinate in degrees of the rupture boundary at the leading edge. The angle is measured from the line connecting the bearing center and the journal center.

END ANGLE gives the angular coordinate in degrees of the rupture boundary at the trailing edge. The angle is measured in the same way as for the leading edge angle. When  $NRW \leq -1$  (item 10, control card in input), the above data are repeated for each rupture calculation.

When  $NPW = -1$ , the output includes the pressure distribution for each lobe. It is identified in the output by the title: PRESSURE DISTRIBUTION. The dimensionless pressure  $P = \bar{P} / \mu \omega (\frac{R}{C})^2 = \frac{1}{2NS_p} \frac{\bar{P}}{W/LD}$  (see eq. (A-7)), where  $\bar{P}$  is the actual pressure in psi, is listed starting at the leading edge of the lobe (i.e. at  $j = 0$  in figure 55). The first value in each line is at  $i = 1$  and the last value is at the centerline ( $i = N$ ), see fig. 55.

When  $NPUN = 1$  or  $-2$  (item 11, control card in input), punched card output will be given. The first card is given at the start of a calculation for a new value of the L/D-ratio or new value of the Reynolds number (it is only given if  $NPAD = 1$ ). The card contains four values:

Card (4E13.5)

1. L/D
2. The lobe arc, degrees (  $\theta_{p,out} - \theta_{p,in}$  )
3. The relative angular location of the center of pressure (  $(180^\circ - \theta_{p,in}) / (\theta_{p,out} - \theta_{p,in})$  )
4. The Reynolds number  $R_e$

This card is followed by the results of the composite bearing for each value of  $\epsilon_B \cos \phi_B$  (and if  $NPUN = -2$ , also for each value of  $\epsilon_B \sin \phi_B$  ), there will be two cards:

Card (5E13.5)

1.  $\epsilon_B \cos \phi_B$
2.  $1/S = W / \mu NDL (\frac{R}{C})^2$ , the inverse Sommerfeld number
3. The friction factor:  $\frac{R}{C} \frac{F_f}{SW} = \frac{R}{C} \frac{F_f}{\mu NDL (R/C)^2}$
4. The dimensionless flow across the leading edge:  $\frac{Q_L}{NDLC}$
5. The bearing eccentricity ratio  $\epsilon_B$ .

Card (SE13.5)

1. The dimensionless radial stiffness for an inertialess tilting pad:

$$\frac{C}{SW} \left[ K_{xx} - \operatorname{Re} \left\{ \frac{(K_{xy} + i\omega B_{xy})(K_{yx} + i\omega B_{yx})}{K_{yy} + i\omega B_{yy}} \right\} \right]$$

2. The dimensionless radial damping for an inertialess tilting pad:

$$\frac{C}{SW} \left[ \omega B_{xx} - \operatorname{Im} \left\{ \frac{(K_{xy} + i\omega B_{xy})(K_{yx} + i\omega B_{yx})}{K_{yy} + i\omega B_{yy}} \right\} \right]$$

3. The dimensionless stiffness for the y-direction:  $\frac{CK_{yy}}{SW}$
4. The dimensionless damping for the y-direction:  $\frac{C\omega B_{yy}}{SW}$
5. The attitude angle  $\phi_B$ , degrees

INPUT FORM FOR COMPUTER PROGRAM  
PN0375: THE STATIC AND DYNAMIC PERFORMANCE OF A  
LOBED BEARING WITH TURBULENT FILM

Card 1 (15)

NRET = Number of film Reynolds numbers in table for turbulent flow coefficients

Table of Turbulent Flow Coefficients(4E15.7)

For each Reynolds number, give two cards with four values per card.

First Card:

1.  $R_h = \rho R \omega \bar{h} / \mu$ , the film Reynolds number (dimensionless)
2.  $\frac{1}{2} C_f R_h$ , the friction factor (dimensionless). For  $R_h = 0$ ,  $\frac{1}{2} C_f R_h = 1$
3.  $G_x$ , the turbulent flow coefficient for the circumferential direction (dimensionless). For  $R_h = 0$ ,  $G_x = 1$
4.  $\frac{1}{G_x} \frac{dG_x}{dR_h}$ , the first derivative of  $G_x$  divided by  $G_x$  (dimensionless) For  $R_h = 0$ ,  $\frac{dG_x}{dR_h} = 0$

Second Card:

1.  $\frac{1}{G_x} \frac{d^2 G_x}{dR_h^2}$ , the second derivative of  $G_x$  divided by  $G_x$  (dimensionless). For  $R_h = 0$ ,  $\frac{d^2 G_x}{dR_h^2} = 0$
2.  $\frac{1}{G_x} \frac{d^3 G_x}{dR_h^3}$ , the third derivative of  $G_x$  divided by  $G_x$  (dimensionless). For  $R_h = 0$ ,  $\frac{d^3 G_x}{dR_h^3} = 0$
3.  $\frac{G_x}{G_z}$ , where  $G_z$  is the turbulent flow coefficient for the axial direction (dimensionless). For  $R_h = 0$ ,  $\frac{G_x}{G_z} = 1$
4.  $\frac{1}{R_h} \left( \frac{G_x}{G_z} \right)$ , the first derivative of  $\frac{G_x}{G_z}$  (dimensionless). It is zero for  $R_h = 0$ .

Card (72))

Text

Control Card (1215)

1. M = Number of finite difference increments in the circumferential direction per lobe ( $3 \leq M \leq 36$ )
2. N = Number of finite difference increments in the axial direction on half the bearing length ( $3 \leq N \leq 13$ )
3. NLD = Number of L/D-ratios in input list ( $1 \leq NLD \leq 20$ )
4. NRE = Number of bearing Reynolds numbers,  $Re$ , in input list ( $1 \leq NRE \leq 30$ )
5. NPAD = Number of lobes ( $1 \leq NPAD \leq 12$ )
6. NECA = Number of  $\epsilon_B \cos \varphi_B$  - values in input list ( $1 \leq NECA \leq 20$ )
7. NAB = Maximum allowable number of attitude angle iterations.
8. NRP; If  $NRP \geq 1$ : Maximum allowable number of iterations to determine rupture boundary.  
If  $NRP = 0$ : Film rupture tables place, but there are no iterations.  
If  $NRP = -1$ : No film rupture, and no iterations.
9. NPW; If  $NPW = 0$ : Only the composite bearing results are given, not the results for the individual lobes.  
If  $NPW = 1$ : The results for the individual pads and the composite bearing are given, but not the pressure distribution.  
If  $NPW = -1$ : Same as for  $NPW = 1$ , but with pressure distribution.
10. NRW; If  $NRW = 0$ : No results are given from the rupture boundary iteration.  
If  $NRW = 1$ : The convergence error for each rupture boundary iteration is given.  
If  $NRW = -1$ : Same as for  $NRW = 1$ , but output also includes the coordinates of the rupture boundary for each iteration.  
If  $NRW = -2$ : Diagnostic for rupture boundary calculation.
11. NPUN; If  $NPUN = 0$ : The composite bearing results are only given after the final attitude angle calculation, no cards are punched.  
If  $NPUN = 1$ : Same as  $NPUN = 0$ , but the results are also punched on cards.  
If  $NPUN = -1$ : The composite bearing results are given after each attitude angle calculation, no cards are punched.

If NPUN = -2: Same as NPUN = -1, but the results are also punched on cards.

12. INP; If INP = 0: More input data follows the present set of data, starting with the text card.

If INP = 1: This is the last set of input data.

Card (1P5E14.6)

1. CVLA = Convergence limit for attitude angle calculation.
2. CVLR = Convergence limit for rupture boundary iteration.

List of L/D-Ratios (1P5E14.6)

Give NLD-values of the length-to-diameter ratio, L/D, 5 values per card.

List of Bearing Reynolds Numbers (1P5E14.6)

Give NRE-values of the bearing Reynolds number,  $R_e$ , 5 values per card.

Data for Journal Center Position

The following two input items, namely the card with  $\epsilon_0 \cos \varphi_0$  and the list of  $\epsilon_0 \sin \varphi_0$ , must be repeated together NECA times (Item 6, control card).

Card (1PE14.6, I5)

1.  $\epsilon_0 \cos \varphi_0$
2. NAT; If NAT  $\geq 1$ : Number of  $\epsilon_0 \sin \varphi_0$ -values in input list which follows. The program iterates on the attitude angle to make horizontal force zero ( $1 \leq \text{NAT} \leq 25$ )

If NAT  $\leq -1$ : The absolute value of NAT gives the number of  $\epsilon_0 \sin \varphi_0$  values in input list which follows ( $1 \leq |\text{NAT}| \leq 25$ ). No attitude angle iteration takes place. Set NAB = |NAT|, Item 7, control card.

List of  $\epsilon_B \sin \varphi_B$  Values (1P5E14.6)

Give |NAT| -values of  $\epsilon_B \sin \varphi_B$ , 5 values per card.

Bearing Geometry Data (1P5E14.6)

Give NPAD cards (Item 5, control card). Each card contains 4 values:

1.  $\Theta_{in}$ , degrees. The angle from the load line to the leading edge of the lobe
2.  $\Theta_{out}$ , degrees. The angle from the load line to the trailing edge of the lobe
3.  $d_p = \frac{r_p}{c}$ . The lobe preload ( $0 \leq d_p \leq 1$ ), dimensionless.
4.  $\psi_p$ . Preload angle, degrees.

```

SSETUP A(6)   DISK,PUNCH
STBJOB      MAP,ALTIO ,NOGO
SIOFTC MAIPRO DECK
C           MECHANICAL TECHNOLOGY INC., J. LUND, 5-25-67
C           PNO375 - PARTIAL ARC OR LOBED BRG, TURBULENT
DIMENSION D(37,13,13),G(37,13,13),B(37,13),E(37,13),F(37,13),
1P(37,13),ALFAP(37,13),ALFAM(37,13),H32(37),THA(37),AG1(37),
2AG4(37),CS(37),SS(37),BT(37),KI(37),JSX(13),JEX(13),SX(13),EX(13),
3THS(13),THE(13)
COMMON D,G,B,E,F,P,ALFAP,ALFAM,H32,THA,AG1,AG4,CS,SS,BT,KI,JSX,
1JEX,SX,EX,THS,THE,DX,DZ,CSII,ALPH
DIMENSION RH(250),CFR(250),GXC(250),GX1(250),GX2(250),GX3(250),
1GX4(250),GX5(250),ALDS(20),REYN(30),ECAST(20),NATS(20),THN(12),
2THT(12),PRLD(12),PRAN(12),ESAS(25),AG2(37),AG3(37),AF1(37),
3AF2(37),AF3(37),AF4(37),AF5(37),AF6(37),AF7(37),AF8(37),AF9(37),
4CFP(12),C(13),FXP(12),FYP(12),QZT(12),QXL(12),QKT(12),
5SXXP(12),SXYP(12),SYXP(12),SYYP(12),BXXP(12),BXYP(12),BYXP(12),
6BYYP(12),X(3),Y(3),HMN(12),[HM(12)
DIMENSION ESAST(20,25),A(13,13),AK(13,13),GK(13,1)
DO 10 I=1,12
10 IHM(I)=I
READ(5,98) NRET
DO 11 I=1,NRET
READ(5,99) RH(I),CFR(I),GXC(I),GX1(I)
11 READ(5,99) GX2(I),GX3(I),GX4(I),GX5(I)
NPUN1=I
12 READ(5,100)
READ(5,101) M,N,NLD,NRE,NPAD,NECA,NAB,NRP,NPW,NRW,NPUN,INP
READ(5,102) CVLA,CVLR
WRITE(6,100)
WRITE(6,104)
WRITE(6,105)M,N,NLD,NRE,NPAD,NECA,NAB,NRP,NPW,NRW,NPUN,INP
WRITE(6,106)
WRITE(6,102)CVLA,CVLR
WRITE(6,107)
READ(5,102) (ALDS(I),I=1,NLD)
WRITE(6,102)(ALDS(I),I=1,NLD)
READ(5,102) (REYN(I),I=1,NRE)
WRITE(6,108)
WRITE(6,102)(REYN(I),I=1,NRE)
WRITE(6,109)
DO 13 I=1,NECA
READ(5,103) ECAST(I),NATS(I)
J1=ABS(NATS(I))
READ(5,102) (ESAST(I,J),J=1,J1)
WRITE(6,110)ECAST(I),NATS(I)
WRITE(6,111)
13 WRITE(6,102)(ESAST(I,J),J=1,J1)
WRITE(6,112)
WRITE(6,113)
DO 14 I=1,NPAD
READ(5,102) THN(I),THT(I),PRLD(I),PRAN(I)
14 WRITE(6,102)THN(I),THT(I),PRLD(I),PRAN(I)
M3=M+1
M1=M-1
M2=M-2
NC=N+1
HM=M
NLD1=1
20 ALD=ALDSTNLD1
C2=N
OZ=ALD/C2

```

	DELX3=1.0/DZ/DZ	63
	DZ2=DELX3+DELX3	64
	SPD2=1.0471976/C2	65
	SPD3=0.021816616/C2	66
	SPD4=0.78539816/C2	67
	SPD5=0.043633231/ALD*C2/ALD	68
	SPD6=0.17453293/C2	69
	NRE1=1	70
21	RE=REYN(NRE1)	71
	NEC1=1	72
22	ECA=ECAST(NEC1)	73
	NAT=NATS(NEC1)	74
	IF(NAT) 23,24,24	75
23	NAB1=-NAT	76
	J1=NAB1	77
	GO TO 25	78
24	NAB1=NAB	79
	J1=NAT	80
25	CC 26 J=1,J1	81
26	ESAS(J)=ESAST(NEC1,J)	82
	ESA=ESAS(1)	83
	NA=1	84
	NA1=0	85
	NA2=1	86
32	IPD=1	87
34	DX=(THT(IPD)-THN(IPD))/HM*0.017453293	88
	DELY3=1.0/DX/DX	89
	DX2=DELY3+DELY3	90
	SPD=SPD6*DX	91
	IF(NA-1) 30,27,30	92
27	IF(NPUN) 28,30,29	93
28	IF(NPUN+1) 29,30,30	94
29	C1=THT(IPD)-THN(IPD)	95
	C2=(180.0-THN(IPD))/C1	96
	WRITE(10,114)ALD,C1,C2,RE,NPUN1	
	NPUN1=NPUN1+1	98
30	C1=0.017453293*PRAN(IPD)	99
	C2=SIN(C1)	100
	C1=COS(C1)	101
	C1=ECA-C1*PRLD(IPD)	102
	C2=ESA-C2*PRLD(IPC)	103
	ECC=SQRT(C1*C1+C2*C2)	104
	IF(1.0-ECC) 15,15,18	105
15	WRITE(6,140)IPD	106
	IF(NA-NAB1) 16,17,17	107
16	NA=NA+1	108
	GO TO 443	109
17	WRITE(6,134)	110
	GO TO 485	111
18	ATP=TANV(C1,C2)	112
	C1=ATP+180.0	113
	KRB=1	114
	KRE=1	115
	KBE=1	116
	C2=THN(IPD)	117
	C3=C2+360.0	118
	C4=THT(IPD)	119
	C5=C4-360.0	120
35	IF(C1-360.0) 37,36,36	121
36	C1=C1-360.0	122
	GO TO 35	123
37	IF(ATP-C4) 39,38,38	124

38	IF(C1-C4) 37,43,43	125
39	IF(ATP-C2) 40,40,44	126
40	IF(ATP-C5) 44,41,41	127
41	IF(C2-C1) 45,42,42	128
42	IF(C1-C5) 45,43,43	129
43	KRE=-1	130
	GO TO 49	131
44	MFB=0	132
	MBE=0	133
45	IF(C1-C4) 46,49,49	134
46	IF(C1-C2) 47,47,48	135
47	IF(C1-C5) 48,49,49	136
48	KRE=0	137
	KBE=0	138
49	O13=0.0	139
	CS11=C2-ATP	140
	ALPH=C4-C2	141
	C3=0.017453293*CS11	142
	DO 60 J=1,M8	143
	C1=COS(C3)	144
	C2=SIN(C3)	145
	CS(J)=C1	146
	SS(J)=C2	147
	THA(J)=C3	148
	C4=ECC*C1	149
	C5=ECC*C2	150
	C6=1.0+C4	151
	C7=C5*C5	152
	C8=SQRT(C6)	153
	C9=C6*C8	154
	IF(RE) 50,50,51	155
50	D1=1.0	156
	D2=1.0	157
	D3=0.0	158
	D4=0.0	159
	D5=0.0	160
	D6=0.0	161
	D7=1.0	162
	D12=1.0	163
	GO TO 56	164
51	C8=RE*C6	165
	DO 55 K=1,NRET	166
	IF(D8-RH(K)) 52,52,53	167
52	D9=RH(K)-RH(K-1)	168
	D6=(RH(K)-D8)/D9	169
	D7=(D8-RH(K-1))/D9	170
	D1=D6*GXC(K-1)+D7*GXC(K)	171
	D12=D6*CFR(K-1)+D7*CFR(K)	172
	D14=D6*GX4(K-1)+D7*GX4(K)	173
	C2=SQRT(D1)	174
	D3=RE*(D6*GX1(K-1)+D7*GX1(K))	175
	D4=RE*(D6*GX2(K-1)+D7*GX2(K))	176
	D5=RE*(D6*GX3(K-1)+D7*GX3(K))	177
	D6=RE*(D6*GX5(K-1)+D7*GX5(K))	178
	D7=D14	179
	GO TO 56	180
53	IF(NRET-K) 54,54,55	181
54	D8=RH(K)	182
	GO TO 52	183
55	CONTINUE	184
56	D11=C9*D2	185
	M32(J)=D11	186

D10=1.0/(C6*C6)	187
D8=1.5/C6+0.5*D3	188
D9=3.75*D10+(1.5/C6-0.25*D3)*D3+0.5*D4	189
D10=-0.375/C6*D10+0.375*D3*(3.0*D10-04+D3*(D3-3.0/C6))	190
1+2.25/C6*D4+0.5*D5	191
AG1(J)=D7	192
AG2(J)=C1*D6*D11	193
AG3(J)=C2*D6*D11	194
D4=C1*D8	195
D5=C2*D8	196
D6=C7*D9-C4*D8	197
AG4(J)=D1	198
AF1(J)=(-C1*D8+(2.0*C5*C2-C4*C1)*D9+C7*C1*D10-D4*D6)*D11	199
AF2(J)=(D4*C5-C2)/D11*6.0	200
AF3(J)=12.0/D11*C1	201
AF4(J)=-D4	202
AF5(J)=-D6	203
AF6(J)=-6.0/D11*C2	204
AF7(J)=(-C2*D8-(2.0*C5*C1+C4*C2)*D9+C7*C2*D10-D5*D6)*D11	205
AF8(J)=(D5*C5+C1)/D11*6.0	206
AF9(J)=-D5	207
D14=D12/C6*DX	208
IF(J-1) 67,67,57	209
67 HLE=C6	210
GO TO 58	211
57 IF(MB-J) 68,68,59	212
69 HTE=C6	213
58 D14=0.5*D14	214
59 D13=D13+D14	215
60 C3=C3+DX	216
IF(KRE) 70,69,70	217
69 HMN(IPD)=1.0-ECC	218
GO TO 73	219
70 IF(HLE-HTE) 72,72,71	220
71 HMN(IPD)=HTE	221
GO TO 73	222
72 HMN(IPD)=HLE	223
73 C5=MB	224
DO 63 J=1,MB	225
BT(J)=1.0	226
NI(J)=1	227
DO 62 I=1,N	228
JSX(I)=2	229
JEX(I)=M	230
SX(I)=1.0	231
EX(I)=C5	232
TMS(I)=CSII	233
THE(I)=CSII+ALPH	234
ALFAM(J,I)=1.0	235
62 ALFAP(J,I)=1.0	236
63 CONTINUE	237
JS=1	238
JF=MB	239
JSI=2	240
JFI=MB-1	241
NIT=0	242
ERR=1.0	243
IF(NPW) 65,64,65	244
64 IF(NRW) 65,66,65	245
65 WRITE(6,116)IPD	246
66 IF(KBE) 423,301,301	247
301 DO 303 I=1,N	248

DO 302 K=1,N	249
C(JS,I,K)=0.0	250
302 G(JS,I,K)=0.0	251
G(JS,I,I)=1.0	252
GK(I,I)=0.0	253
DO 303 J=1,MB	254
P(J,I)=0.0	255
E(J,I)=0.0	256
303 F(J,I)=0.0	257
DO 326 J=JS1,JF1	258
C1=AF5(J)	259
C2=AE6(J)	260
C3=AG1(J)	261
C4=C3+DELX3	262
DO 305 I=1,N	263
P(J,I)=0.0	264
DO 304 K=1,N	265
304 A(I,K)=0.0	266
B(J,I)=0.0	267
C(I)=0.0	268
305 F(J,I)=0.0	269
KJ=KI(J)	270
KJ1=KJ-1	271
BT1=1.0	272
IF(KJ1) 306,327,311	273
306 DO 310 I=1,N	274
A(I,I)=C1-DELY3-DELY3-C4-C4	275
B(J,I)=DELY3	276
C(I)=DELY3	277
F(J,I)=C2	278
IF(N-I) 307,307,308	279
307 A(I,I-1)=C4+C4	280
GO TO 310	281
308 A(I,I+1)=C4	282
IF(I-1) 310,310,309	283
309 A(I,I-1)=C4	284
310 CONTINUE	285
GO TO 320	286
311 BT1=BT(J)	287
DO 312 I=1,KJ1	288
312 A(I,I)=1.0	289
327 DO 319 I=KJ,N	290
C5=ALFAP(J,I)	291
C9=ALFAM(J,I)	292
D1=C5+C9	293
O1=DX2/D1	294
D2=D1/C5	295
D1=D1/C9	296
C7=DX2/C5/C9	297
F(J,I)=C2	298
IF(I-KJ1) 313,313,314	299
313 C6=C1-C9-D22/BT1*C3	300
C8=D22/(1.0+BT1)*C3	301
C7=C8/BT1	302
GO TO 315	303
314 C6=C1-C9-D22*C3	304
C8=DELX3*C3	305
C7=C8	306
315 A(I,I)=C6	307
IF(N-I) 317,317,316	308
316 A(I,I-1)=C7	309
A(I,I+1)=C8	310

	GO TO 318	311
317	A(I,I-1)=C7+C8	312
318	B(J,I)=D1	313
	C(I)=U2	314
319	CONTINUE	315
320	DO 322 I=1,N	316
	DO 321 K=1,N	317
321	AK(I,K)=A(I,K)+B(J,I)*D(J-1,I,K)	318
322	CONTINUE	319
	CALL MATINV(AK,N,GK,J,DET,ID)	320
	GO TO (324,323),ID	321
323	WRITE(6,139)IPD	322
	GO TO 425	323
324	DO 325 I=1,N	324
	DO 325 K=1,N	325
	C5=AK(I,K)	326
	G(J,I,K)=C5	327
325	D(J,I,K)=-C5*C(K)	328
326	CONTINUE	329
	CALL PRESS(JS1,JF1,N,NRP)	330
	IF(NRW) 341,344,344	331
341	WRITE(6,117)NIT	332
	WRITE(6,118)	333
	DO 342 I=1,N	334
342	WRITE(6,119)I,SX(I),EX(I),THS(I),THE(I)	335
	IF(NRW+1) 343,344,344	336
343	WRITE(6,120)	337
344	DO 347 J=JS,JF	338
	C3=H32(J)	339
	DO 345 I=1,N	340
	C4=E(J,I)/C3	341
	E(J,I)=C4	342
345	P(J,I)=C4*ECC	343
	IF(NRW+1) 346,347,347	344
346	WRITE(6,121)(P(J,I),I=1,N)	345
347	CONTINUE	346
	CALL SIMP(N,FR,FT)	347
	FR=SPD*FR	348
	FT=SPD*FT	349
	BRDA=-FR-FR	350
	BTDA=-FT-FT	351
	FR=ECC*FR	352
	FT=ECC*FT	353
	SMFV=SQRT(FR*FR+FT*FT)	354
	IF(SMFV) 423,423,349	
349	SMF=1.0/SMFV	
	ATT=TANV(FR,FT)	356
	CFP(IPD)=3.1415927*D13+C.5*ECC*FT	357
	C1=0.017453293*ATP	358
	CATP=COS(C1)	359
	SATP=SIN(C1)	360
	FXP(IPD)=FR*CATP+FT*SATP	361
	FYP(IPD)=FT*CATP-FR*SATP	362
	IF(KRB) 351,362,351	363
351	IF((N/2)*2-N) 352,353,353	364
352	QXS=16.0*P(2,N)-4.0*P(3,N)	365
	J1=N-2	366
	GO TO 354	367
353	QXS=2.0*P(3,N)-8.0*P(2,N)	368
	J1=N-1	369
354	DO 355 I=1,J1,2	370
355	QXS=QXS+32.0*P(2,I)-8.0*P(3,I)+16.0*P(2,I+1)-4.0*P(3,I+1)	371

	$GXS=1.5707963*(1.0+ECC*CS(1))-SPD3*QXS/OX*(H32(1)**2)$	372
396	IF(KRE) 357,367,357	373
397	IF((N/2)*2-N) 358,359,359	374
398	$CXE=16.0*P(M,N)-4.0*P(M1,N)$	375
	J1=N-2	376
	GO TO 360	377
399	$CXE=2.0*P(M1,N)-8.0*P(M,N)$	378
	J1=N-1	379
340	CO 361 I=1,J1,2	380
361	$CXE=QXE+32.0*P(M,I)-8.0*P(M1,I)+16.0*P(M,I)-4.0*P(M1,I)$	381
	$QXE=1.5707763*(1.0+ECC*CS(MB))+SPD3*QXE/OX*(H32(MB)**2)$	382
	GO TO 372	383
362	CXS=0.0	384
	CO 366 I=1,N	385
	$C1=THE(I)/57.29578$	386
	$C1=1.0+ECC*COS(C1)$	387
	IF(I-2) 363,366,364	388
363	$C1=4.0*C1$	389
	GO TO 366	390
364	IF(N-I) 366,366,365	391
365	$C1=C1+C1$	392
366	$QXS=QXS+C1$	393
	$QXS=SPD4*QXS$	394
	GO TO 356	395
367	QXE=0.0	396
	DO 371 I=1,N	397
	$C1=1.0+ECC*COS(THI(I)/57.29578)$	398
	IF(I-2) 368,371,369	399
368	$C1=4.0*C1$	400
	GO TO 371	401
369	IF(N-I) 371,371,370	402
370	$C1=C1+C1$	403
371	$QXE=QXE+C1$	404
	$QXE=SPD4*QXE$	405
372	$QZ2=AG1(M)*(H32(M)**2)*(16.0*P(M,1)-4.0*P(M,2))$	406
	J1=2	407
	IF((M/2)*2-M) 373,374,374	408
373	$QZ2=QZ2+3.0*AG1(2)*(H32(2)**2)*(4.0*P(2,1)-P(2,2))$	409
	$1-0.25*AG1(3)*(H32(3)**2)*(4.0*P(3,1)-P(3,2))$	410
	J1=3	411
374	DO 375 J=J1,M2,2	412
375	$QZ2=QZ2+4.0*AG1(J)*(H32(J)**2)*(4.0*P(J,1)-P(J,2))$	413
	$1+2.0*AG1(J+1)*(H32(J+1)**2)*(4.0*P(J+1,1)-P(J+1,2))$	414
	$QZT(IPD)=SPD5*OX*QZ2$	415
	$QXL(IPD)=QXS$	416
	$QXT(IPD)=QXE$	417
	ERR=0.0	418
	IF(NRP) 387,387,380	419
380	IF(KBE) 387,381,387	420
381	ERR=ECC	421
	CALL RUPT(M,N,KRB,KRE,NRW,JS,JF,JS1,JF1,ERR)	422
	NIT=NIT+1	423
	IF(NRW) 382,383,382	424
382	WRITE(6,122)NIT,ERR	425
	J1=1	426
383	IF(NRW) 384,385,385	427
384	WRITE(6,124)	428
	WRITE(6,123)SMF,ECC,ATP,ATT,FR,FT	429
	WRITE(6,125)	430
	WRITE(6,123)CFP(IPD),QXS,QXE,QZT(IPD),FXP(IPD),FYP(IPD)	431
	IF(J1) 388,388,385	432
385	IF(CVLR-ERR) 386,387,387	433

386	IF(NRP=NIT) 387,301,301	434
387	J1=0	435
	IF(NPW) 384,392,384	436
388	WRITE(6,122)NIT,ERR	437
	WRITE(6,118)	438
	DO 389 I=1,N	439
389	WRITE(6,119)I,SX(I),EX(I),THS(I),THE(I)	440
	IF(NPW) 390,392,392	441
390	WRITE(6,120)	442
	DO 391 J=1,MB	443
391	WRITE(6,121)(P(J,I),I=1,N)	444
392	DO 393 J=1,MB	445
	DO 393 I=1,N	446
	E(J,I)=0.0	447
393	F(J,I)=0.0	448
	DO 402 J=JS1,JF1	449
	C1=AF1(J)	450
	C2=AF2(J)	451
	C3=-AG2(J)	452
	NJ=KI(J)	453
	IF(KJ) 394,394,395	454
394	NJ=1	455
395	DO 401 I=KJ,N	456
	C4=P(J,I)	457
	IF(I=KJ) 396,396,397	458
396	C5=0.0	459
	GO TO 398	460
397	C5=P(J,I-1)	461
398	IF(N=I) 399,399,400	462
399	C6=C5	463
	GO TO 401	464
400	C6=P(J,I+1)	465
401	F(J,I)=C1*C4+C2+C3*DELX3*(C5+C6-C4-C4)	466
402	CONTINUE	467
	CALL PRESS(JS1,JF1,N,-1)	468
	DO 404 J=JS,JF	469
	C1=H32(J)	470
	C2=AF4(J)	471
	DO 403 I=1,N	472
403	E(J,I)=E(J,I)/C1+C2*P(J,I)	473
404	CONTINUE	474
	CALL SIMP(N,C1,C2)	475
	DRDE=SPD*C1	476
	DTDE=SPD*C2	477
	DO 413 J=JS1,JF1	478
	C1=AF7(J)	479
	C2=AF8(J)	480
	C3=-AG3(J)	481
	NJ=KI(J)	482
	IF(KJ) 405,405,406	483
405	KJ=1	484
406	DO 412 I=KJ,N	485
	C4=P(J,I)	486
	IF(I=KJ) 407,407,408	487
407	C5=0.0	488
	GO TO 409	489
408	C5=P(J,I-1)	490
409	IF(N=I) 410,410,411	491
410	C6=C5	492
	GO TO 412	493
411	C6=P(J,I+1)	494
412	F(J,I)=C1*C4+C2+C3*DELX3*(C5+C6-C4-C4)	495

413	CONTINUE	496
	CALL PRESS(JS1,JF1,N,-1)	497
	DO 415 J=JS,JF	498
	C1=M32(J)	499
	C2=AF9(J)	500
	DO 414 I=1,N	501
414	E(J,I)=E(J,I)/C1+C2*P(J,I)	502
415	CONTINUE	503
	CALL SIMP(N,C1,C2)	504
	DRDA=SPD*C1	505
	DTDA=SPD*C2	506
	DO 419 J=JS1,JF1	507
	C1=AF3(J)	508
	NJ=K1(J)	509
	IF(KJ) 416,416,417	510
416	NJ=1	511
417	DO 418 I=KJ,N	512
418	F(J,I)=C1	513
419	CONTINUE	514
	CALL PRESS(JS1,JF1,N,-1)	515
	DO 421 J=JS,JF	516
	C1=M32(J)	517
	DO 420 I=1,N	518
420	E(J,I)=E(J,I)/C1	519
421	CONTINUE	520
	CALL SIMP(N,C1,C2)	521
	BRDE=SPD*C1	522
	BTDE=SPD*C2	523
	C1=DRDE*CATP+DTDE*SATP	524
	C2=DRDA*CATP+DTDA*SATP	525
	SXXP(IPD)=C1*CATP-C2*SATP	526
	SXYP(IPD)=C1*SATP+C2*CATP	527
	C1=DRDE*SATP-DTDE*CATP	528
	C2=DRDA*SATP-DTDA*CATP	529
	SYXP(IPD)=C1*CATP-C2*SATP	530
	SYYP(IPD)=C1*SATP+C2*CATP	531
	C1=BRDE*CATP+BTDE*SATP	532
	C2=BRDA*CATP+BTDA*SATP	533
	BXXP(IPD)=C1*CATP-C2*SATP	534
	BXYP(IPD)=C1*SATP+C2*CATP	535
	C1=BRDE*SATP-BTDE*CATP	536
	C2=BRDA*SATP-BTDA*CATP	537
	BYXP(IPD)=C1*CATP-C2*SATP	538
	BYYP(IPD)=C1*SATP+C2*CATP	539
	C1=(SXXP(IPD)*BYYP(IPD)+SYYP(IPD)*BXXP(IPD)-	540
	SXYP(IPD)*BXYP(IPD))/(BXXP(IPD)+BYYP(IPD))	541
	C2=((SXXP(IPD)-C1)*(SYYP(IPD)-C1)-SXYP(IPD)*SYXP(IPD))/	542
	1(BXXP(IPD)*BYYP(IPD)-BXYP(IPD)*BYXP(IPD))	543
	C1=C2/C1	544
	C3=SQRT(ABS(C2))	545
	C4=SMF*C1	546
	C1=C1/39.478418	547
	IF(NPW) 422,425,422	548
422	WRITE(6,126)	549
	WRITE(6,123)DRDE,DTDE,DRDA,DTDA,BRDE,BTDE,BRDA,BTDA	550
	WRITE(6,127)	551
	WRITE(6,123)SXXP(IPD),SXYP(IPD),SYXP(IPD),SYYP(IPD),BXXP(IPD),	552
	1BXYP(IPD),BYXP(IPD),BYYP(IPD)	553
	WRITE(6,128)	554
	WRITE(6,123)C1,C4,C3,C2	555
	GO TO 425	556
423	CFP(IPD)=3.1415927*O13	557

	QXL(IPD)=1.5707963*(1.0+ECC*CS(1))	558
	QXT(IPD)=QXL(IPD)	559
	QZT(IPD)=0.0	560
	FXP(IPD)=0.0	561
	FYP(IPD)=0.0	562
	SXXP(IPD)=0.0	563
	SKYP(IPD)=0.0	564
	SYXP(IPD)=0.0	565
	SYYP(IPD)=0.0	566
	BXXP(IPD)=0.0	567
	BXYP(IPD)=0.0	568
	BYXP(IPD)=0.0	569
	BYYP(IPD)=0.0	570
	IF(NPW) 424,425,424	571
424	WRITE(6,129)	572
	WRITE(6,130)	573
	WRITE(6,123)CFP(IPD),QXL(IPD)	574
425	IPD=IPD+1	575
	IF(NPAD-IPD) 426,34,34	576
426	FXB=0.0	577
	FYB=0.0	578
	SXXB=0.0	579
	SXB=0.0	580
	SXB=0.0	581
	SXB=0.0	582
	BXXB=0.0	583
	BXB=0.0	584
	BXB=0.0	585
	BXB=0.0	586
	RCFW=0.0	587
	QXLB=0.0	588
	QZTB=0.0	589
	QBT=0.0	590
	DO 432 I=1,NPAC	591
	IF(NPAD-I) 427,427,428	592
427	C1=QXT(I)-QXL(I)	593
	GO TO 429	594
428	C1=QXT(I)-QXL(I+1)	595
429	IF(C1) 430,430,431	596
430	C1=0.0	597
431	QBT=QBT+C1	598
	QXLB=QXLB+QXL(I)	599
	QZTB=QZTB+QZT(I)	600
	RCFW=RCFW+CFP(I)	1
	FXB=FXB+FXP(I)	2
	FYB=FYB+FYP(I)	3
	SXXB=SXXB+SXXP(I)	4
	SXB=SXB+SKYP(I)	5
	SXB=SXB+SYXP(I)	6
	SXB=SXB+SYYP(I)	7
	BXXB=BXXB+BXXP(I)	8
	BXB=BXB+BXP(I)	9
	BXB=BXB+BYXP(I)	10
432	BXB=BXB+BYYP(I)	11
	QBT=QBT+QZTB	12
	IF(NPAD-I) 436,436,437	13
436	QBT=QZTB+QXT(I)	14
437	SMFV=SQRT(FXB*FXB+FYB*FYB)	15
	IF(NPW) 435,433,435	16
433	IF(NAT) 435,435,434	17
434	IF(NPUN) 435,440,440	18
435	WRITE(6,132)NA	19

WRITE(6,131)ESA,FYB	20
WRITE(6,133)	21
WRITE(6,123)FXB,RCFW,QZTB,QBT,QXLR,SMFV	22
WRITE(6,127)	23
WRITE(6,123)SXZH,SKYB,SYXB,SYVB,RXXB,BXYB,BYXB,YYB	24
440 IF(NA-NAB) 442,441,441	25
441 WRITE(6,134)	26
GO TO 475	27
442 NA=NA+1	28
IF(NAT) 443,441,444	29
443 ESA=ESAS(NA)	30
GO TO 32	31
444 IF(FXB) 446,445,447	32
445 FXB=1.0	33
446 IF(NA1) 447,452,447	34
447 IF(CVLA-ARS(FYB/FXB)) 448,475,475	35
448 IF(NA1) 455,449,454	36
449 IF(NA2) 451,451,450	37
450 NA2=0	38
GO TO 452	39
451 IF(FYB*X(1)) 453,475,452	40
452 X(1)=FYB	41
Y(1)=ESA	42
GO TO 443	43
453 NA1=1	44
X(3)=FYB	45
Y(3)=ESA	46
ESA=(Y(1)+ESA)/2.0	47
GO TO 32	48
454 NA1=-1	49
X(2)=FYB	50
Y(2)=ESA	51
GO TO 465	52
455 IF(ESA-Y(2)) 461,456,456	53
456 IF(X(2)*X(3)) 457,457,458	54
457 X(1)=X(2)	55
X(2)=FYB	56
Y(1)=Y(2)	57
Y(2)=ESA	58
GO TO 465	59
458 IF(FYB*X(1)) 459,459,460	60
459 X(3)=FYB	61
Y(3)=ESA	62
GO TO 465	63
460 X(2)=FYB	64
Y(2)=ESA	65
GO TO 465	66
461 IF(X(1)*X(2)) 462,462,463	67
462 X(3)=X(2)	68
X(2)=FYB	69
Y(3)=Y(2)	70
Y(2)=ESA	71
GO TO 465	72
463 IF(FYB*X(3)) 464,464,460	73
464 X(1)=FYB	74
Y(1)=ESA	75
465 C1=Y(2)-Y(1)	76
C2=Y(3)-Y(2)	77
C3=Y(3)-Y(1)	78
C4=(X(3)-X(2))/(C2*C3)	79
C5=(X(1)-X(2))/(C1*C3)	80
C3=C4+C5	81

	C4=C1*C4-C2*C5	82
	C5=X(2)	83
	IF(C3) 467,466,467	84
466	C6=-C5/C4	85
	GO TO 470	86
467	C6=0,5*C4/C3	87
	C7=SQRT(ABS(C6+C6-C5/C3))	88
	IF(C6) 468,469,469	89
468	C7=-C7	90
469	C6=C7-C6	91
470	ESA=Y(2)+C6	92
	GO TO 32	93
475	ECC=SQRT(ECA*ECA+ESA*ESA)	94
	ATT=TANV(ECA,ESA)	95
	IF(NPAD=1) 476,476,477	96
476	QRT=QZT(1)+QXT(1)	97
477	C1=(SXXB*BYYB+SYXB*BXXB-SXYB*BYXB-SYXB*BYXB)/(BXXB*BYYB)	98
	C2=((SXXB-C1)*(SYXB-C1)-SXYB*SYXB)/(BXXB*BYYB-BXYB*BYXB)	99
	C1=C1/C2	100
	C3=SQRT(ABS(C2))	101
	C5=C1/3,478,418	102
	WRITE(6,135)	103
	WRITE(6,123)ALD,RE,ECA,ESA,ECC,ATT,SMFV,FYB	104
	WRITE(6,136)	105
	WRITE(6,123)RCFW,QZTB,QBT,QXLB,FXB,C5,C3,C2	106
	WRITE(6,127)	107
	WRITE(6,123)SXXB,SXYB,SYXB,SYXB,BXXB,BXYB,BYXB,BYYB	108
	IF(SMFV) 479,479,478	109
478	SMF=1,0/SMFV	110
	RCFWS=SMF*RCFW	111
	FXBS=SMF*FXB	112
	FYBS=SMF*FYB	113
	C1=SMF*C1	114
	SXXS=SMF*SXXB	115
	SXYS=SMF*SXYB	116
	SYXS=SMF*SYXB	117
	SYYS=SMF*SYXB	118
	BXXS=SMF*BXXB	119
	BXYS=SMF*BXYB	120
	BYXS=SMF*BYXB	121
	BYYS=SMF*BYXB	122
	WRITE(6,137)	123
	WRITE(6,123)SMF,FXBS,FYBS,RCFWS,C1	124
	WRITE(6,138)	125
	WRITE(6,123)SXXS,SXYS,SYXS,SYYS,BXXS,BXYS,BYXS,YYYS	126
479	WRITE(6,141)	127
	WRITE(6,143)(IHM(I),I=1,NPAD)	128
	WRITE(6,142)(HMN(I),I=1,NPAD)	129
	IF(NPUN) 480,485,481	130
480	IF(NPUN+1) 481,485,485	131
481	C6=SXYB*SYXB-BXYB*BYXB	132
	C7=SXYB*BYXB+SYXB*BXYB	133
	C8=SYXB*SYXB+BYYB*BYXB	134
	C9=BXXB-(SYXB*C7-BYYB*C6)/C8	135
	C8=SXXB-(SYXB*C6+BYYB*C7)/C8	136
	WRITE(10,115)ECA,SMFV,RCFW,QXLB,ECC,NPUN1	
	NPUN1=NPUN1+1	138
	WRITE(10,115)C8,C9,SYXB,BYYB,ATT,NPUN1	
	NPUN1=NPUN1+1	140
	IF(NPUN=1) 485,485,482	141
482	WRITE(10,114)SXXB,SXYB,SYXB,SYXB	
	NPUN1=NPUN1+1	143

```

WRITE(10,114) BXXB,BXYB,BYXB,BYYB
NPUN1=NPUN1+1
485 NEC1=NEC1+1
IF(NECA-NEC1) 486,22,22
486 NRE1=NRE1+1
IF(NRE-NRE1) 487,21,21
487 NLD1=NLD1+1
IF(NLD-NLD1) 488,20,20
488 IF(INP) 489,12,489
489 STOP
98 FORMAT(15)
99 FORMAT(4E15,7)
100 FORMAT(72H
1
101 FORMAT(1215)
102 FORMAT(1P5E14,6)
103 FORMAT(1PE14,6,15)
104 FORMAT(1H0,117HCIRC.DIV AX.DIV NO.L/D NO.REYN NO.PAD N
10.E*CO5A NO.A-IT NO.RUP.IT PAD.DATA RUPT.DATA ATT.A.DATA INPUT
1)
105 FORMAT(16,11110)
106 FORMAT(1H0,27HCONV.LIM.ATT.A CONV.LIM.RUP)
107 FORMAT(1H0,10HL/D RATIOS)
108 FORMAT(1H0,16HREYNOLDS NUMBERS)
109 FORMAT(1H0,17HECC*COS(ATT) DATA)
110 FORMAT(1H0,13HECC*COS(ATT)=1PE13,6,14H NO.E*SIN(A)=13)
111 FORMAT(2)H LIST OF ECC*SIN(ATT)
112 FORMAT(1H0,21HBEARING GEOMETRY DATA)
113 FORMAT(55H INLET ANGLE OUTLET ANGLE PRELOAD ANGLE PRLD-X)
114 FORMAT(4E13,5,128)
115 FORMAT(5E13,5,115)
116 FORMAT(1H1,15HBEARING PAD NO.,12)
117 FORMAT(///1H0,21HRUPTURE ITERATION NO.,12)
118 FORMAT(1H0,60H I BEGIN INDEX END INDEX BEGIN ANGLE E
IND ANGLE)
119 FORMAT(13,1P4E15,7)
120 FORMAT(1H0,21HPRESSURE DISTRIBUTION)
121 FORMAT(1PE12,4,1P5E11,4)
122 FORMAT(22H RUPTURE ITERATION NO.12,9H ERROR=1PE13,6)
123 FORMAT(1P8E15,7)
124 FORMAT(1H0,86HSOMMERFELD NO ECC.RATIO ATT.ANGLE CALC.AT
IT.ANG. F-R/S*W F-T/S*W)
125 FORMAT(1H0,86H 1/S*(R/C*F/W) (Q-X/NDLC)IN (Q-X/NDLC)OUT (Q-Z/NO
ILC)SIDE F-X/S*W F-Y/S*W)
126 FORMAT(1H0,12H DFR/SDE,8X,7HDFT/SDE,8X,7HDFR/SDA,8X,7HDFT/SDA,7
1X,9HDFR/SDEDT,6X,9HDFT/SDEDT,6X,9HDFR/SDADT,6X,9HDFT/SDADT)
127 FORMAT(1H0,4X,7HCKXX/SW,8X,7HCKXY/SW,8X,7HCKYX/SW,8X,7HCKYY/SW,7X,
18HCWBXX/SW,7X,8HCWBXY/SW,7X,8HCWBXY/SW,7X,8HCWBYY/SW)
128 FORMAT(1H0,58HCMN/MUCL(R/C)2 CMW**2/W FREQ/W (FREQ
1/W)**2)
129 FORMAT(1H0,15HPAD IS UNLOADED)
130 FORMAT(1H0,28H 1/S*(R/C*F/W) (Q-X/NDLC)IN)
131 FORMAT(1H0,13HECC*SIN(ATT)=1PE13,6,17H HORIZ.FORCE/SW=1PE13,6)
132 FORMAT(///1H0,33HBEARING RESULTS,ATT.ANGLE IT.NO.,12)
133 FORMAT(1H0,4X,7HF-X/S*W,5X,12H1/S(R/C*F/W),2X,14H(Q-Z/NDLC)SIDE,2X
1,13H(Q/NDLC)TOTAL,1X,14H(Q-X/NDLC)CIRC,7X,3H1/S)
134 FORMAT(1H0,40HNUMBER OF ATT.ANGLE ITERATIONS TOO LARGE)
135 FORMAT(///1H0,6X,3HL/D,9X,98HREYN.NO. ECC*COS(ATT) ECC*SIN(A
ITT) ECC.RATIO ATT.ANGLE 1/S F-Y/S*W)
136 FORMAT(1H0,116H 1/S*(R/C*F/W) (Q-Z/NDLC)SIDE (Q/NDLC)TOTAL Q-X/NO
ILC)CIRC F-X/S*W CMN/MUCL(R/C)2 FREQ/W (FREQ/W**2)
137 FORMAT(1H0,72H SOMMERFELD NO F-X/W F-Y/W (R/C

```

```

1)*(F/W)      CMW**2/W)
138 FORMAT(1H0,5X,6HCKXX/W,9X,6HCKXY/W,9X,6HCKYX/W,9X,6HCKYY/W,8X,7HCV
1BXX/W,8X,7HCWBXY/W,8X,7HCWBYX/W,8X,7HCWBY/W)
139 FORMAT(1H0,26HPMATRIX IS SINGULAR,PAD NO.,I2)
140 FORMAT(1H0,41HECCENTRICITY RATIO GREATER THAN 1,PAD NO.,I2)
141 FORMAT(1H0,34HMINIMUM FILM THICKNESS FOR PAD NO.)
142 FORMAT(1P10E12,4)
143 FORMAT(17,9I12)
END
SIBFTC SURPT  DECK
SUBROUTINE RUPT(M,N,KRB,KRE,MP,JS,JF,JS1,JF1,ERR)
DIMENSION D(37,13,13),G(37,13,13),B(37,13),E(37,13),F(37,13),
1P(37,13),ALFAP(37,13),ALFAM(37,13),H32(37),THA(37),AG1(37),
2AG4(37),CS(37),SS(37),BT(37),KI(37),JSX(13),JEX(13),SX(13),EX(13),
3THS(13),THE(13)
COMMON D,G,B,E,F,P,ALFAP,ALFAM,H32,THA,AG1,AG4,CS,SS,BT,KI,JSX,
1JEX,SX,EX,THS,THE,DX,DZ,CSII,ALPH
M=M
N=N
KRB=KRB
KRE=KRE
MP=MP
JS=JS
JF=JF
JF1=JF1
JS1=JS1
ECC=ERR
N1=N-1
MB=M+1
NC=N+1
N2=NC+2
SER1=1.0
SER2=0.0
SER3=1.0
SER4=0.0
DR=0.1*DX
JS=1
JS1=2
JF=MB
JF1=M
DO 502 J=1,MB
BT(J)=1.0
MI(J)=0
DO 501 I=1,N
ALFAM(J,I)=1.0
501 ALFAP(J,I)=1.0
502 CONTINUE
C1=MB
DO 503 I=1,N
THS(I)=CSII
THE(I)=CSII+ALPH
JSX(I)=2
503 JEX(I)=M
DO 542 I=1,N
J1=NC-I
K7=I-1
C1=K7
Y4=C1*DZ
K7=0
IF(J1-N1) 509,508,507
507 K5=1
GO TO 510

```

```

211
212
213
2
3
4
5
6
7
8
9
10
11
12
13
14
15
16
17
18
19
20
21
22
23
24
25
26
27
28
29
30
31
32
34
33
35
36
37
38
39
40
41
42
43
44
45
46
47
48
49
50
51
52
53

```

508	K5=-1	54
	GO TO 510	55
509	N5=0	56
510	DO 591 J=2,N	57
	PR= P(J,J1)	58
	IF(PR) 511,511,515	59
511	IF(K7) 591,591,512	60
512	K7=0	61
	IF(KRE) 591,513,591	62
513	X4=1.0	63
	TMC=TMA(J-1)	64
	P2= P(J-1,J1)/3.0	65
	GX1=AG4(J-1)	66
	GX2=AG4(J)	67
	GZ1=AG1(J-1)	68
	GZ2=AG1(J)	69
	X2=X2E	70
	X3=X3E	71
	Z2=Z2E	72
	Z3=Z3E	73
	Y2=Y2E	74
	N2=K2E	75
	K3=K3E	76
	KX=J-1	77
	NJ=KX	78
	JP=KX	79
	MX1=L	80
	NX2=0	81
	VI=MB-KX	82
	GO TO 525	83
515	IF(K7) 591,516,591	84
516	N7=1	85
	IF(KRB) 591,517,591	86
517	IF(J-2) 591,518,520	87
518	NRB=L	88
	DO 519 K=1,N	89
	ALFAM(J,K)=1.0	90
	SX(K)=1.0	91
	TMS(K)=C911	92
519	JSX(K)=2	93
	SER2=0.0	94
	SER1=1.0	95
	BT(J)=1.0	96
	GO TO 591	97
520	X4=-1.0	98
	TMC=YMA(J)	99
	GX1=AG4(J)	100
	GX2=AG4(J-1)	101
	GZ1=AG1(J)	102
	GZ2=AG1(J-1)	103
	P2=PR/3.0	104
	X2=X2B	105
	X3=X3B	106
	Z2=Z2B	107
	Z3=Z3B	108
	Y2=Y2B	109
	N2=K2B	110
	K3=K3B	111
	KX=MS-J	112
	NJ=J	113
	JP=KJ	114
	KX1=-1	115

KX2=0	116
Y1=J-1	117
525 KJ(KJ)=1	118
GX2=(GX2-GX1)/DX	119
GZ2=(GZ2-GZ1)/DX	120
IF(K5) 527,528,526	121
526 K2=KX	122
V1=DX*Y1	123
GO TO 534	124
527 K3=K2	125
GO TO 530	126
528 KQ=K3-KX	127
IF(KQ) 530,530,529	128
529 C2=KQ	129
C2=C2*DX	130
Z3=Z3+C2	131
X3=X3+C2	132
530 Y1=X2	133
IF(Z2-X2) 531,532,532	134
531 Y1=Z2	135
532 NQ=K2-KX	136
IF(KQ) 534,534,533	137
533 C2=KQ	138
C2=C2*DX	139
Z2=Z2+C2	140
X2=X2+C2	141
Y1=Y1+C2	142
534 C6=0.0	143
C9=(Y2+DZ-Y4)/DR	144
C3=-P2	145
K4=0	146
535 C6=C6+DR	147
536 C7=C6*C9*Y4	148
IF(K5) 538,539,537	149
537 C7=0.0	150
C9=0.0	151
GO TO 545	152
538 C9=(X2-C6)/C7*2.0	153
GO TO 545	154
539 D2=X3-X2	155
D1=X3-C6	156
IF(D1) 540,540,541	157
540 C9=0.0	158
GO TO 545	159
541 IF(D2) 542,542,543	160
542 C9=D1/C7*2.0	161
GO TO 545	162
543 C9=D1/D2	163
IF(C9-1.0) 540,540,544	164
544 C9=ALOG(ABS(C9))/ALOG(ABS(C7/Y2))*D1/C7	165
545 C8=THC+X4*C6	166
U3=COS(C8)	167
D4=-ECC*SIN(C8)	168
D5=1.0+ECC*D3	169
D1=GZ1+C6*GZ2	170
D2=GX1+C6*GX2	171
D6=D5*D5*D5	172
C5=(1.0+C9*C9)*C6	173
C5=(C5/D2)*(C5/D6)*(D4/(1.0+D1+C9*C9))-P2	174
C7=C6*C9*Y4	175
IF(K4) 556,546,550	176
546 C1=C3	177

	C3=C5	
	IF(C1+C5) 549,556,547	178
547	IF(C6-Y1) 535,548,548	179
548	C6=Y1	180
	C7=Y4	181
	C8=THC+X4+C6	182
	KX2=1	183
	GO TO 557	184
549	K4=1	185
	C9=C6-0.5*DR	186
	GO TO 536	187
550	K4=-1	188
	D3=(C1+C3-C5-C5)/DR*2.0/DR	189
	D4=(C3-C1)/DR	190
	IF(D3) 552,551,552	191
551	D5=-C5/D4	192
	GO TO 555	193
552	D6=D4/D3*0.5	194
	D7=SQR(A8S(D6**2-C5/D3))	195
	IF(D6) 553,554,554	196
553	D5=-D6-D7	197
	GO TO 555	198
554	D5=-D6+D7	199
555	C6=C6+D5	200
	GO TO 536	201
556	IF(C6-Y1) 557,558,548	202
557	K4=0	203
	Y1=C7	204
	THC=C8	205
	IF(K5) 559,560,558	206
558	Z1=C6	207
	Y1=0.0	208
	GO TO 561	209
559	D3=Y1*Y1	210
	D3=(C6-Z1)/D3	211
	D4=0.0	212
	Z1=D3*D2*D2+Z2	213
	GO TO 561	214
560	D5=Y1-Y4+DZ	215
	D6=Y4-DZ	216
	D7=(Z3-Z2)/D6	217
	D8=(C6-Z2)/D5	218
	D4=D5+D6	219
	D3=(D7+D8)/D4	220
	D4=(D8*D6-D7*D5)/D4	221
	Z1=DZ*(D3*D2+D4)+Z2	222
561	IF(Z1-DX) 565,565,562	223
562	KI(KJ)=0	224
	JP=KJ	225
563	KX=KX+1	226
	JP=JP+KX1	227
	Z1=Z1-DX	228
	Z2=Z2-DX	229
	C6=C6-DX	230
	IF(Z1) 564,564,563	231
564	Z1=Z1+DX	232
	Z2=Z2+DX	233
	C6=C6+DX	234
	KX=KX-1	235
	JP=JP-KX1	236
565	IF(K5) 566,566,580	237
566	IF(Z1-Z2) 568,567,567	238
		239

567	Z1=Z2	240
	GO TO 580	241
568	IF(Z2-DX) 580,569,570	242
569	KQ=JP+KX1	243
	KI(KQ)=J1+1	244
	BT(KQ)=1.0	245
	GO TO 580	246
570	KQ=KX+1	247
	JQ=JP	248
	DO 579 L=KQ,K2	249
	JQ=JQ+KX1	250
	IF(KX1) 571,572,572	251
571	IF(JQ=1) 579,579,573	252
572	IF(JQ-MM) 573,579,579	253
573	KI(JQ)=J1+1	254
	D5=L-KX	255
	C5=Z2-D5*DX	256
	IF(D3) 575,574,575	257
574	D5=-D5/D4	258
	GO TO 576	259
575	C6=D4/D3*0.5	260
	C5=-D6+SQRT(ABS(D6**2-D5/D3))	261
	D5=-D6+SQRT(ABS(D6**2-D5/D3))	262
576	D5=D5/D2	263
	IF(D5-1.0) 578,578,577	264
577	D5=1.0	265
578	BT(JQ)=D5	266
579	CONTINUE	267
580	D5=Z1/DX	268
	IF(K7) 586,581,586	269
581	IF(K5) 585,585,582	270
582	IF(KX2) 583,584,583	271
583	KRE=1	272
	JF=MH	273
	JF1=M	274
	GO TO 591	275
584	JF1=JP	276
	JF=JP+1	277
	K3E=KX	278
	X3E=Z1	279
	Z3E=Z1	280
585	Y2E=Y1	281
	X2E=C6	282
	Z2E=Z1	283
	K2E=KX	284
	THE(J1)=57.29578*THC	285
	ALFAP(JP,J1)=D5	286
	D6=JP	287
	D6=D6+D5	288
	SER3=SER3+ABS(EX(J1))	289
	SER4=SER4+ABS(EX(J1)-D6)	290
	EX(J1)=D6	291
	JEX(J1)=JP	292
	GO TO 591	293
586	IF(K5) 590,590,587	294
587	IF(KX2) 588,589,588	295
588	KRB=1	296
	JS=1	297
	JS1=2	298
	GO TO 591	299
589	JS1=JP	300
	JS=JP-1	301

K7B=KX	302
X7B=Z1	303
Z7B=Z1	304
590 Y2B=Y1	305
X2B=C6	306
Z2B=Z1	307
K2B=KX	308
THS(J1)=57.2957H*THC	309
ALFAM(JP,J1)=D5	310
D6=JP	311
D6=D6-D5	312
SER1=SER1+ANS(SX(J1))	313
SER2=SER2+A3S(SX(J1)-D6)	314
SX(J1)=D6	315
JSX(J1)=JP	316
591 CONTINUE	317
592 CONTINUE	318
ERR=SER2/SER1+SER4/SER3	319
IF(MP+1) 593,596,596	320
593 WRITE(6,599)	321
WRITE(6,597)((ALFAP(J,I),I=1,N),J=1,MB)	322
WRITE(6,597)((ALFAM(J,I),I=1,N),J=1,MB)	323
WRITE(6,597)(BT(J),J=1,MB)	324
WRITE(6,598)(KI(J),J=1,MB)	325
596 RETURN	326
597 FORMAT(1PE12.4,1P9E11.4)	327
598 FORMAT(20I5)	328
599 FORMAT(1H0,32HRUPTURE DIAGN.=ALFAP,ALFAM,BT,KI)	330
END	
*IBFTC SUPRES DECK	
SUBROUTINE PRESS(J1T,J2T,NCT,NZT)	2
DIMENSION D(37,13,13),G(37,13,13),B(37,13),E(37,13),F(37,13),	3
IP(37,13),ALFAP(37,13),ALFAM(37,13),H32(37),THA(37),AG1(37),	4
ZAG4(37),CS(37),SS(37),BT(37),KI(37),JSX(13),JEX(13),SX(13),EX(13),	5
THS(13),THE(13)	6
COMMON D,G,B,E,F,P,ALFAP,ALFAM,H32,THA,AG1,AG4,CS,SS,BT,KI,JSX,	7
IJEX,SX,EX,THS,THE,DX,DZ,CSII,ALPH	8
J1=J1T	9
J2=J2T	10
NC=NCT	11
NZ=NZT	12
DO 503 J=J1,J2	13
DO 502 I=1,NC	14
C3=0.0	15
DO 501 K=1,NC	16
501 C3=C3+(F(J,K)-B(J,K)*E(J-1,K))*G(J,I,K)	17
502 E(J,I)=C3	18
503 CONTINUE	19
DO 508 J=J1,J2	20
J3=J1+J2-J	21
DO 507 I=1,NC	22
C3=E(J3,I)	23
DO 504 K=1,NC	24
504 C3=C3+D(J3,I,K)*E(J3+1,K)	25
IF(NZ) 507,505,505	26
505 IF(C3) 506,506,507	27
506 C3=J.0	28
507 E(J3,I)=C3	29
508 CONTINUE	30
RETURN	31
END	32
*IBFTC SURSIM DECK	

SUBROUTINE SIMP(NCT,FRT,FTT)	2
DIMENSION D(37,13,13),G(37,13,13),B(37,13),E(37,13),F(37,13),	3
IP(37,13),ALFAP(37,13),ALFAM(37,13),H32(37),THA(37),AG1(37),	4
2AG4(37),CS(37),SS(37),BT(37),KI(37),JSX(13),JEX(13),SX(13),EX(13),	5
3THS(13),THE(13)	6
COMMON D,G,B,E,F,P,ALFAP,ALFAM,H32,THA,AG1,AG4,CS,SS,BT,KI,JSX,	7
1JEX,SX,EX,THS,THE,DX,DZ,CSII,ALPH	8
DIMENSION SR(13),ST(13)	9
NC=NCT	10
DO 710 I=1,NC	11
JS=JSX(I)	12
JE=JEX(I)	13
AS=ALFAM(JS,I)	14
AE=ALFAP(JS,I)	15
KX=JE-JS	16
J2=JE-1	17
C1=E(JS,I)	18
C2=(1.0-AE)*E(JE,I)	19
C3=C2*CS(JE)	20
C4=C2*SS(JE)	21
IF((KX/2)*2-KX) 704,703,703	22
703 C1=(1.0+AS)*C1	23
C3=C3-C1*CS(JS)	24
C4=C4+C1*SS(JS)	25
J1=JS+1	26
GO TO 708	27
704 C5=(1.0+AS)*(3.0-AS)/4.0	28
IF(AS=0.0) 705,705,706	29
705 C6=0.0	30
C5=C5/3.0*4.0	31
GO TO 707	32
706 C6=1.0+AS	33
C6=C6/AS*C6/2.0	34
C6=C6*C6	35
707 C5=(1.0+C5)*E(JS+1,I)	36
C6=C6*C1	37
C3=C3-C6*CS(JS)-C5*CS(JS+1)	38
C4=C4+C6*SS(JS)+C5*SS(JS+1)	39
J1=JS+2	40
708 DO 709 J=J1,J2,2	41
C3=C3-4.0*E(J,I)*CS(J)-2.0*E(J+1,I)*CS(J+1)	42
709 C4=C4+4.0*E(J,I)*SS(J)+2.0*E(J+1,I)*SS(J+1)	43
SR(I)=C3	44
710 ST(I)=C4	45
C1=SR(NC)	46
C2=ST(NC)	47
IF((NC/2)*2-NC) 711,712,712	48
711 J1=NC-2	49
FR=4.0*C1	50
FT=4.0*C2	51
GO TO 713	52
712 J1=NC-1	53
FR=-2.0*C1	54
FT=-2.0*C2	55
713 DO 714 I=1,J1,2	56
FR=FR+8.0*SR(I)+4.0*SR(I+1)	57
714 FT=FT+8.0*ST(I)+4.0*ST(I+1)	58
FRT=FR	59
FTT=FT	60
RETURN	61
END	62
SIOPTC MAINVR DECK	

C	MATRIX INVERSION WITH ACCOMPANYING SOLUTION OF LINEAR EQUATIONS	2
C	NOVEMBER 1692 S GOOD DAVID TAYLOR MODEL BASIN AM MAT1	3
C		4
	SUBROUTINE MATINVA(N1,B,M1,DETERM,IO)	5
C		6
C	GENERAL FORM OF DIMENSION STATEMENT	7
C		8
	DIMENSION A(13,13),B(13,1)	9
	DIMENSION INDEX(13,3)	10
	EQUIVALENCE (IROW,JROW), (ICOLUJ,COLUJ), (AMAX, T, SWAP)	11
C		12
C	INITIALIZATION	13
C		14
	M=N1	15
	N=N1	16
	DO 8 I=1,N	17
	K1=1	18
	K2=1	19
	DO 6 J=1,N	20
	IF(A(I,J)) 3,4,3	21
3	K1=0	22
4	IF(A(J,I)) 5,6,5	23
5	K2=0	24
6	CONTINUE	25
	IF(K1+K2) 8,8,7	26
7	ID=2	27
	DETERM=0.0	28
	GO TO 740	29
8	CONTINUE	30
10	DETERM=1.0	31
15	DO 20 J=1,N	32
20	INDEX(J,3) = 0	33
30	DO 550 I=1,N	34
C		35
C	SEARCH FOR PIVOT ELEMENT	36
C		37
	40 AMAX=0.0	38
45	DO 105 J=1,N	39
	IF(INDEX(J,3)-1) 60, 105, 60	40
60	DO 100 K=1,N	41
	IF(INDEX(K,3)-1) 80, 100, 715	42
80	IF(AMAX-ABS(A(J,K))) 85,100,100	43
85	IROW=J	44
90	ICOLUJ=K	45
	AMAX=ABS(A(J,K))	46
100	CONTINUE	47
105	CONTINUE	48
	INDEX(ICOLUJ,3) = INDEX(ICOLUJ,3) +1	49
260	INDEX(I,1)=IROW	50
270	INDEX(I,2)=ICOLUJ	51
C		52
C	INTERCHANGE ROWS TO PUT PIVOT ELEMENT ON DIAGONAL	53
C		54
	130 IF (IROW-ICOLUJ) 140, 310, 140	55
	140 DETERM=-DETERM	56
	150 DO 200 L=1,N	57
	160 SWAP=A(IROW,L)	58
	170 A(IROW,L)=A(ICOLUJ,L)	59
	200 A(ICOLUJ,L)=SWAP	60
	IF(M) 310, 310, 210	61
	210 DO 250 L=1, M	62
	220 SWAP=B(IROW,L)	63

230	R(IROW,L)=B(ICOLUM,L)	64
250	B(ICOLUM,L)=SWAP	65
C		66
C	DIVIDE PIVOT ROW BY PIVOT ELEMENT	67
C		68
310	PIVOT =A(ICOLUM,ICOLUM)	69
	DETERM=DETERM*PIVOT	70
330	A(ICOLUM,ICOLUM)=1.0	71
340	DO 350 L=1,N	72
350	A(ICOLUM,L)=A(ICOLUM,L)/PIVOT	73
355	IF(M) 380, 380, 360	74
360	DO 370 L=1,M	75
370	B(ICOLUM,L)=B(ICOLUM,L)/PIVOT	76
C		77
C	REDUCE NON-PIVOT ROWS	78
C		79
380	DO 550 LI=1,N	80
390	IF(LI-ICOLUM) 400, 550, 400	81
400	T=A(LI,ICOLUM)	82
420	A(LI,ICOLUM)=0.0	83
430	DO 450 L=1,N	84
450	A(LI,L)=A(LI,L)-A(ICOLUM,L)*T	85
455	IF(M) 550, 550, 460	86
460	DO 500 L=1,M	87
500	B(LI,L)=B(LI,L)-B(ICOLUM,L)*T	88
550	CONTINUE	89
C		90
C	INTERCHANGE COLUMNS	91
C		92
600	DO 710 I=1,N	93
610	L=N+I-I	94
620	IF (INDEX(L,1)-INDEX(L,2)) 630, 710, 630	95
630	JROW=INDEX(L,1)	96
640	JCOLUM=INDEX(L,2)	97
650	DO 705 K=1,N	98
660	SWAP=A(K,JROW)	99
670	A(K,JROW)=A(K,JCOLUM)	100
700	A(K,JCOLUM)=SWAP	101
705	CONTINUE	102
710	CONTINUE	103
	DO 730 K = 1,N	104
	IF(INDEX(K,3) -1) 715,720,715	105
715	ID =2	106
	GO TO 740	107
720	CONTINUE	108
730	CONTINUE	109
	ID=1	110
740	RETURN	111
C		112
C	LAST CARD OF PROGRAM	112
	END	113
SIBFTC	ARCROU DECK	
C	ARCTAN ROUTINE, TANV GREATER OR EQUAL ZERO, LESS THAN 360.	2
	FUNCTION TANV(CSS,SNN)	3
	CS=CSS	4
	SN=SNN	5
	IF(CS) 57,50,54	6
50	IF(SN) 53,51,52	7
51	TANV=0.0	8
	GO TO 61	9
52	TANV=90.0	10
	GO TO 61	11
53	TANV=270.0	12

	GO TO 61	13
54	IF(SN) 56,55,55	14
55	A=0.0	15
	B=57.29578	16
	GO TO 60	17
56	A=360.0	18
	B=-57.29578	19
	SN=-SN	20
	GO TO 60	21
57	CS=-CS	22
	A=180.0	23
	IF(SN) 59,58,58	24
58	B=-57.29578	25
	GO TO 60	26
59	B=57.29578	27
	SN=-SN	28
60	TANV=A+B*ATAN(SN/CS)	29
61	RETURN	30
	END	31
SIGMAP	UNIT-P 8,DECK	
	ENTRY 0,UNIO.	
0,UNIO.	PZE UNIT10	
UNIT10	FILE ,A(6),READY,LIST,INOUT,BCD,BLK=14	
	END	

THREE LOBE BEARING, M=0.5

15	6	2	4	3	1	10	8	0	0	0	0
0.0001			0.0001								
0.5			1.0								
0.0			2000.0			10000.0				30000.0	
0.02			10								
0.0			0.05			0.1			0.15		0.2
0.25			0.3			0.35			0.4		0.45
10.0			110.0			0.5			60.0		
130.0			230.0			0.5			180.0		
250.0			350.0			0.5			300.0		

THREE LOBE BEARING, M=0.5  
 CIRC.DIV AX.DIV NO.L/D NO.REYN NO.PAD NO.ECCOSA NO.A-IT NO.RUP.IT PAD.DATA RUST.DATA ATT.A.DATA INPUT  
 15 6 2 4 3 1 10 0 0 0 0 0 0 0 0 0 0 0 0 0 0

CONV.LIM.ATT.A CONV.LIM.RUP  
 1.00000E-04 1.00000E-04  
 L/D RATIOS  
 5.00000E-01 1.00000E 00  
 REYNOLDS NUMBERS  
 0. 2.00000E 03 1.00000E 04 3.00000E 04

ECC\*COSS(ATT) DATA  
 ECC\*COSS(ATT)= 2.00000E-02 NO.ESIM(A)= 10  
 LIST OF ECC\*COSS(ATT)  
 0. 5.00000E-02 1.00000E-01 1.50000E-01 2.00000E-01  
 2.50000E-01 3.00000E-01 3.50000E-01 4.00000E-01 4.50000E-01

BEARING GEOMETRY DATA  
 INLET ANGLE OUTLET ANGLE PRELOAD ANGLE PRLD-X  
 1.00000E 01 1.10000E 02 5.00000E-01 6.00000E 01  
 1.30000E 02 2.30000E 02 5.00000E-01 1.00000E 02  
 2.50000E 02 3.50000E 02 5.00000E-01 3.00000E 02

L/D	REYN.NO.	ECC*COSS(ATT)	ECC*COSS(ATT)	ECC.RATIO	ATT.ANGLE	1/S	F-Y/S*W
5.00000E-01	0.	2.00000E-02	3.00000E-02	3.6306683E-02	5.6573987E 01	3.1983130E-01	-2.8861625E-06
1/S*(R/C*F/W)	(Q/NDLC)SIDE	(Q/NDLC)TOTAL	(Q-X/NDLC)CIRC	F-X/S*W	CMN/NUDL(R/C)2	FREQ/M	(FREQ/M)*02
2.980959E 01	3.8527824E-01	3.8327824E-01	2.8271798E 00	3.1983130E-01	5.5090043E-01	4.8104757E-01	2.3140676E-01
CKXX/SM	CKYY/SM	CKYY/SM	CKYY/SM	CKXX/SM	CKYY/SM	CKXX/SM	CKYY/SM
5.5947423E 00	6.8068700E 00	-7.1739856E 00	4.5513619E 00	1.5227733E 01	-4.5704956E-01	-4.1995123E-01	1.3793705E 01
SOMMERFELD NO	F-X/W	F-Y/W	(R/C)*(F/W)	CMN*02/W			
3.1266475E 00	1.000000E 00	-6.5226949E-06	9.3203356E 01	6.8000447E 01			
CKXX/W	CKYY/W	CKYY/W	CKYY/W	CKXX/W	CKYY/W	CKXX/W	CKYY/W
1.7492787E 01	2.1282683E 01	-2.2430524E 01	1.4230504E 01	4.7611753E 01	-1.4290329E 00	-1.3130395E 00	4.3126054E 01

MINIMUM FILM THICKNESS FOR PAD NO.  
 1  
 2  
 3  
 5.1624E-01 4.7912E-01 4.8274E-01

L/D	REYN.NO.	ECC*COSS(ATT)	ECC*COSS(ATT)	ECC.RATIO	ATT.ANGLE	1/S	F-Y/S*W
5.00000E-01	2.00000E 03	2.00000E-02	3.2770688E-02	3.6391632E-02	3.8404215E 01	4.4820513E-01	-1.1928929E-07
1/S*(R/C*F/W)	(Q/NDLC)SIDE	(Q/NDLC)TOTAL	(Q-X/NDLC)CIRC	F-X/S*W	CMN/NUDL(R/C)2	FREQ/M	(FREQ/M)*02

SOMMERFELD NO F-X/M F-Y/M (R/C)\*(P/M) CHXX/M CKYY/M CBYX/M CBYV/M  
 2.9314212E-00 8.9999999E-01 -2.4597837E-07 1.3324638 02 3.3324638 01  
 CKXX/M CKYY/M CBYX/M CBYV/M  
 1.2439686E 01 2.0712738E 01 -2.1715473E 91 1.2609208 01 4.5572998 61 -1.2157892E 00 -1.1130386E 00 4.1536459E 01  
 MINIMUM FILM THICKNESS FOR PAD NO.  
 1 2 3  
 5.3838E-01 4.7897E-01 4.8053E-01

L/D MEYM.NO. ECC=00S(ATT) ECC=SIN(ATT) ATT.ANGLB. F-Y/S=H  
 5.6000000E-01 1.0000000E 04 2.0000000E-02 3.2997570E-02 3.8954846E-02 5.8779727E 01 9.4516373E-01 1.6355901E-05  
 1/3\*(R/C\*F/M) (0-Z/NDLC)SIDE (0/NDLC)TOTAL (0-X/NDLC)GIRG F-X/S=H CHN/NUDL(R/C)2 FREQ/M (FREQ/M)\*0.8  
 1.9486673E-02 4.5269322E-01 4.9269322E-01 2.8991302E 00 0.4546324E-01 -1.3959189E 00 4.9889540E-01 2.4897837E-01  
 CKXX/SW CKYY/SW CBYX/SW CBYV/SW  
 1.3509874E 01 2.0086497E 01 -2.9820897E 01 1.1264417E 01 4.3349007E 01 -0.4515945E-01 -0.0984800E-01 3.9931128E 01  
 SOMMERFELD NO F-X/M F-Y/M (R/C)\*(P/M) CHXX/M CBYX/M CBYV/M  
 1.0588177E 00 9.9899999E-01 1.7389559E-05 1.4380533E 02 5.4132357E 01  
 CKXX/M CKYY/M CBYX/M CBYV/M  
 1.4293686E 01 2.1251870E 01 -2.2028079E 01 1.1917953E 01 4.9864017E 01 -0.9525171E-01 -0.5683355E-01 4.2247833E 01  
 MINIMUM FILM THICKNESS FOR PAD NO.  
 1 2 3  
 5.3858E-01 4.7895E-01 4.8032E-01

L/D MEYM.NO. ECC=00S(ATT) ECC=SIN(ATT) ATT.ANGLB. F-Y/S=H  
 5.6000000E-01 3.0000000E 04 2.0000000E-02 3.2670393E-02 3.8246380E-02 5.3471320E 01 1.8922900E 00 -4.9769708E-06  
 1/3\*(R/C\*F/M) (0-Z/NDLC)SIDE (0/NDLC)TOTAL (0-X/NDLC)GIRG F-X/S=H CHN/NUDL(R/C)2 FREQ/M (FREQ/M)\*0.8  
 3.4536464E 02 4.6528737E-01 4.6528737E-01 2.8997768E 00 1.8922900E 00 2.5673522E 00 4.9199498E-01 2.4285087E-01  
 CKXX/SW CKYY/SW CBYX/SW CBYV/SW  
 2.6866761E 01 4.1285703E 01 -4.2651574E 01 2.2488966E 01 8.0487424E 01 -1.5825709E 00 -1.5823866E 00 8.2823237E 01  
 SOMMERFELD NO F-X/M F-Y/M (R/C)\*(P/M) CHXX/M CBYX/M CBYV/M  
 5.9846023E-01 9.9999999E-01 -2.6301402E-06 1.8751148E 02 5.3562088E 01  
 CKXX/M CKYY/M CBYX/M CBYV/M  
 1.4166307E 01 2.1817852E 01 -2.2539661E 01 1.1884524E 01 4.0762084E 01 -8.3632579E-03 -7.9394853E-01 4.3344962E 01  
 MINIMUM FILM THICKNESS FOR PAD NO.  
 1 2 3  
 5.3823E-01 4.7898E-01 4.8068E-01

L/D MEYM.NO. ECC=00S(ATT) ECC=SIN(ATT) ATT.ANGLB. F-Y/S=H  
 1.0000000E 00 0. 2.0000000E-02 3.5310706E-02 4.0581349E-02 6.472764E 01 6.3667449E-01 -1.2665987E-07  
 1/3\*(R/C\*F/M) (0-Z/NDLC)SIDE (0/NDLC)TOTAL (0-X/NDLC)GIRG F-X/S=H CHN/NUDL(R/C)2 FREQ/M (FREQ/M)\*0.8  
 1.0000000E 00 0. 2.0000000E-02 3.5310706E-02 4.0581349E-02 6.472764E 01 6.3667449E-01 -1.2665987E-07

1/S\*(R/C\*F/W) (U-Z/NDLC)SIDE (O/NDLC)TOTAL (O-X/NDLC)CIRC F-X/S\*W CMN/MUDL(R/C)2 FREQ/M (FREQ/M)\*002  
 2.0917620E 01 1.5769897E-01 1.9769897E-01 2.6799314E 00 6.3667450E-01 9.3495510E-01 4.7401897E-01 2.2468643E-01  
 CKXX/SM CKYY/SM  
 9.1730096E 00 1.3382049E 01 -1.3286647E 01 7.3947384E 00 3.0214236E 01 -6.2815594E-01 -5.4996440E-01 2.8059344E 01  
 SOMMERFELD NO F-X/W F-Y/W (R/C)\*(F/W) CMW\*02/W  
 1.5706613E 00 1.0000000E 00 -1.9893978E-07 4.7021861E 01 5.7973973E 01  
 CKXX/M CKYY/M  
 1.4721823E 01 2.1018601E 01 -2.0888823E 01 1.1141430E 01 4.7456331E 01 -9.8662023E-01 -8.6371357E-01 4.9938435E 01

MINIMUM FILM THICKNESS FOR PAD NO.

1  
 2  
 3  
 5.4054E-01 4.7888E-01 4.7824E-01

L/D MEYN.NO. ECC\*COS(ATT) ECC\*SIN(ATT) ECC.RATIO ATT.ANGLE 1/S F-Y/S\*W  
 1.0000000E 00 2.0000000E 03 2.0000000E-02 3.9799411E-02 4.4542037E-02 6.3319557E 01 9.9694223E-01 -3.7252903E-07  
 1/S\*(R/C\*F/W) (U-Z/NDLC)SIDE (O/NDLC)TOTAL (O-X/NDLC)CIRC F-X/S\*W CMN/MUDL(R/C)2 FREQ/M (FREQ/M)\*002  
 5.5658815E 01 2.2422257E-01 2.2422257E-01 2.7054791E 00 9.9694224E-01 1.1718127E 00 4.8130690E-01 2.3165633E-01  
 CKXX/SM CKYY/SM  
 1.2227727E 01 1.9782748E 01 -1.9279074E 01 9.4737666E 00 4.3763401E 01 -8.8758790E-01 -7.6365053E-01 3.7450740E 01  
 SOMMERFELD NO F-X/W F-Y/W (R/C)\*(F/W) CMW\*02/W  
 1.0030621E 00 9.9999999E-01 -3.7367163E-07 5.5639558E 01 4.6403240E 01  
 CKXX/M CKYY/M  
 1.2260216E 01 1.9843424E 01 -1.9336206E 01 9.5628238E 00 4.3897629E 01 -8.9031032E-01 -7.6599275E-01 3.7565606E 01

MINIMUM FILM THICKNESS FOR PAD NO.

1  
 2  
 3  
 5.4444E-01 4.7848E-01 4.7421E-01

L/D MEYN.NO. ECC\*COS(ATT) ECC\*SIN(ATT) ECC.RATIO ATT.ANGLE 1/S F-Y/S\*W  
 1.0000000E 00 1.0000000E 04 2.0000000E-02 4.3197331E-02 4.7602619E-02 6.5156261E 01 2.4491436E 00 6.5945109E-07  
 1/S\*(R/C\*F/W) (U-Z/NDLC)SIDE (O/NDLC)TOTAL (O-X/NDLC)CIRC F-X/S\*W CMN/MUDL(R/C)2 FREQ/M (FREQ/M)\*002  
 1.5460118E 02 2.5431949E-01 2.5431949E-01 2.7290307E 00 2.4491436E 00 2.4248497E 00 4.8688555E-01 2.3697964E-01  
 CKXX/SM CKYY/SM  
 2.5958587E 01 4.0647465E 01 -4.4780384E 01 1.9999999E 01 1.0149782E 02 -1.8569430E 00 -1.5438963E 00 8.6589950E 01  
 SOMMERFELD NO F-X/W F-Y/W (R/C)\*(F/W) CMW\*02/W  
 4.0830599E-01 1.0000000E 00 2.6770627E-07 6.3124580E 01 3.9073905E 01  
 CKXX/M CKYY/M  
 1.0595780E 01 1.9046439E 01 -1.8284099E 01 8.1411143E 00 4.144168E 01 -7.5901755E-01 -5.3038293E-01 3.5122371E 01

MINIMUM FILM THICKNESS FOR PAD NO.

1  
 2  
 3  
 5.4719E-01 4.7821E-01 4.7116E-01

NUMBER OF ATT.ANGLE ITERATIONS TOO LARGE

L/D	KEYN.NO.	ECC*COS(ATT)	ECC*IN(ATT)	ECC.RATIO	ATT.ANGLE	1/S	F-Y/SM
1.000000E 00	3.000000E 04	2.000000E-02	4.4219224E-02	4.89318 2E-02	6.5653142E 01	5.2634884E 00	1.4278293E-03
1/S*(R/C*F/M)	(0-Z/NDLC)SIDE	(0/NDLC)TOTAL	(0-X/NDLC)DIRC	F-X/SM	CHN/MUDL(R/C)2	FREQ/M	(FREQ/M)**2
3.4654565E 02	2.6612027E-01	2.6612027E-01	2.7380186E 00	5.2634882E 00	4.9555744E 00	4.8837462E-01	2.3859977E-01
C*XX/SM	C*XY/SM	C*YY/SM	C*ZZ/SM	C*XX/SM	C*XY/SM	C*YY/SM	C*ZZ/SM
5.3318948E 01	9.9080295E 01	-9.4669126E 01	4.1235990E 01	2.1955204E 02	-3.6445442E 00	-2.9632985E 00	1.8760455E 02
SCHMERFELD NO	F-X/M	F-Y/M	(R/C)*(F/M)	CMH**2/M			
1.4998807E-01	9.999994E-01	2.7127052E-04	6.5459539E 01	3.7168945E 01			
C*XX/M	C*XY/M	C*YY/M	C*ZZ/M	C*XX/M	C*XY/M	C*YY/M	C*ZZ/M
1.0129968E 01	1.8820274E 01	-1.7984004E 01	7.8447694E 00	4.0762441E 01	-6.9242830E-01	-5.6299137E-01	3.4692885E 01

MINIMUM FILM THICKNESS FOR PAD NO.

1 4.827E-01  
 2 4.7812E-01  
 3 4.7024E-01

**BLANK PAGE**

APPENDIX VIII: Computer Program - The Performance and Stability of a Hybrid Journal Bearing with Flexible, Damped Support

This appendix describes the computer program PN0144: "The Performance and Stability of a Hybrid Journal Bearing with Flexible, Damped Support." It gives the detailed instructions for using the program, for preparing the input data and a listing of the Fortran instructions is also given. The analysis for the program is contained in Appendices V and VI. The program calculates the load carrying capacity, the flow, the 8 dynamic coefficients and the critical journal mass at the onset of instability. The program applies to a purely hydrostatic, a purely hydrodynamic or a hybrid bearing with a compressible lubricant. The bearing is cylindrical with a single row of feeder holes in the center plane of the bearing, and the support for the bearing has flexibility, damping and mass.

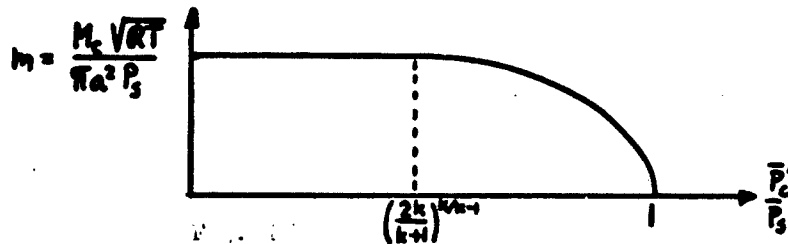
The analysis assumes that the bearing operates with a small eccentricity ratio

COMPUTER INPUT

An input data form is given in the back of this appendix for quick reference when preparing the computer input. In the following, the more detailed instructions are given.

Table of Vena Contracta Coefficients (5E14.6)

This table consists of 5 cards with a total of 25 values of the vena contracta coefficient  $C_D$  for the feeder hole restrictor.  $C_D$  is defined through eq. (E-31), Appendix V. The program assumes  $C_D = 1$  when the feeder hole is choked, and for unchoked conditions,  $C_D$  is specified by the present input list. The dimensionless flow through the restrictor is a function of the pressure ratio across the restrictor:



where  $M_c$  is the mass flow, lbs.sec/inch,  $RT$  is the product of the gas constant and the total temperature, inch<sup>2</sup>/sec<sup>2</sup>,  $a$  is the orifice radius, inch,  $P_s$  is the supply pressure, psia,  $P_c'$  is the pressure downstream of the orifice, psia, and  $k$  is the ratio of specific heats ( $k=1.4$  for air).

The vena contracts coefficient  $C_D$  is the ratio between the actual flow (made dimensionless) and the ideal isentropic flow such that  $C_D \leq 1$  (in general,  $0.6 \leq C_D \leq 1$ ). The 25 input values of  $C_D$  are taken at those pressure ratios which result from subdividing the range  $\left(\frac{2k}{k+1}\right)^{k/(k-1)} \leq \frac{P_c'}{P_s} \leq 1$  into 25 equal parts. The first value of  $C_D$  applies to the first pressure ratio after  $\frac{P_c'}{P_s} = \left(\frac{2k}{k+1}\right)^{k/(k-1)}$ , and the last value of  $C_D$  is taken at  $\frac{P_c'}{P_s} = 1$ .

Card (5E14.6)

This card contains one item, the ratio of specific heats,  $k$ . For air,  $k = 1.4$ .

Card (72H)

Any descriptive text may be given to identify the calculation.

Card (815)

This card is the "control" card which describes the subsequent input data. The card has 8 values:

1. NVL gives the number of pressure ratios,  $P_s/P_a$ , in the designated list. The maximum value of NVL is 25. For a purely hydrodynamic bearing, set NVL = 0 (then NLB  $\neq$  0).

2. NLSL gives the number of restrictor coefficients,  $\lambda$ , in the designated list. The maximum value of NLSL is 25. For a purely hydrodynamic bearing, set NLSL=0 (when NLSL = 0, NVL must be zero).

3. NLB gives the number of compressibility numbers,  $\lambda$ , in the designated list. The maximum value is 25. For a purely hydrostatic bearing, set NLB = 0 (then NLV  $\neq$  0).

4. NEP gives the number of eccentricity ratios,  $\epsilon$ , in the designated list. The maximum value is 25 (NEP  $\neq$  0).

5. MNS gives the number of values in the list of frequency ratios (when NLB=0, the list contains values of the squeeze number instead of the frequency ratio). The maximum value of MNS is 95 (MNS  $\neq$  0).

6. MT. As described in Appendix E, the program calculates the pressure in the gas film by numerical integration. To this end, the length between the admission plane and the end of the bearing is subdivided into increments. MT specifies the number of subdivisions. MT should be large for high values of  $\lambda$  and/or high values of the squeeze number  $\delta$ . A typical value for MT is 10 to 15 for moderate  $\lambda$  or  $\delta$  values (say up to  $\lambda \cong 5$  and  $\delta \cong 5$ ). The maximum value for MT is 30.

7. INT. If INT = 0, the bearing is rigidly supported and no input data can be given for the three support parameters. If INT = 1, the bearing is flexibly supported.

8. INP. If INP = 0, the program returns to read in more input after completion of the calculations for the present set of input data. A new set of input data starts with the identification card (i.e. with the card (72H)). The table of vena contracta coefficients and the card with the ratio of specific heats are not to be repeated.

If  $IMP = 1$ , the present set of input data is the last set.

Card (SE14.6)

This card contains 4 values:

1.  $L/D$ , the ratio between the total bearing length and the journal diameter.
2.  $\lambda$ , the source correction factor.  $\lambda$  is given by eq. (E-50), Appendix V, or in approximate form:

$$\lambda \cong 1 + \frac{2}{n \cdot f} \cdot \log_e \left( \frac{D}{nd} \right)$$

where  $n$  is the number of feeder holes,  $d$  is the feeder hole diameter (not the orifice diameter),  $D$  is the journal diameter and  $L$  is the total bearing length. Typically,  $\lambda = 1.3$  to  $1.5$ .

3.  $\delta$ , the inherent compensation factor. Even when the feeder holes are provided with orifices, an additional flow restriction normally occurs where the gas leaves the feeder hole and enters the bearing film:

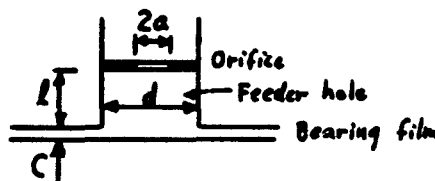


Figure 63: Feeding Hole

The orifice area is  $\pi a^2$  where  $a$  is the orifice radius. The "curtain" area at the rim of the feeder hole has the area  $\pi d C$  where  $d$  is the feeder hole diameter and  $C$  is the radial bearing clearance. The ratio between the two areas is called the inherent compensation factor:

$$\delta = \frac{a^2}{dC}$$

When there is no orifice,  $\delta = \infty$  and the bearing is called inherently compensated (for the inherently compensated bearing, set  $\delta = 1000$  or some other large value in the input). If the bearing is purely orifice restricted, set  $\delta = 0$ .

4.  $nV_c/\pi DLC$ , the ratio between the combined volume of all feeder holes and the volume of the gas film. Here,  $D$  is the journal diameter,  $L$  is the total bearing length,  $C$  is the radial bearing clearance,  $n$  is the number of feeder holes and  $V_c$  is the "capacitative" volume of one feeder hole. The effect of a feeder hole volume is to introduce a time lag between a change in the downstream feeder hole pressure and the corresponding change in the flow through the hole, see eq. (E-28), Appendix V. This time lag tends to reduce the damping capacity of the bearing and, in this way, adversely affects the stability margin. At present, there is no method to determine what this "capacitative" volume is, but it is suggested to set  $V_c$  equal to the volume of the feeder hole below the orifice, i.e. set  $V_c = \frac{\pi}{4} d^2 l$  in fig. 63 where  $l$  is the length of the feeder hole below the orifice. For an inherently compensated bearing in which there are no orifices,  $V_c$  may be set equal to zero. However, it must be remembered that  $V_c$ , properly interpreted, gives a measure of the time lag between pressure change and flow change. If there are other factors than the feeder hole volume which contributes to such a time lag, their effect must be reflected in the value for  $V_c$  according to eq. (E-28).

List of Supply Pressure Ratios (5E14.6)

This list consists of up to five cards with values of the ratio between the supply pressure  $P_s$ , psia, and the ambient pressure  $P_a$ , psia. In total, there are NVL values (item 1, control card), maximum 25 values. In the analysis in Appendix V, the pressure ratio is denoted by the symbol  $V$ . The ratio must be greater than 1. If NVL = 0, the list is omitted in the input and the bearing is purely hydrodynamic.

List of Restrictor Coefficients (5E14.6)

This list consists of up to five cards, giving the values of the restrictor coefficient  $\Lambda_s$ :

$$\Lambda_s = \frac{6\mu n a^2 \sqrt{RT}}{P_s C^3 \sqrt{1+\delta^2}}$$

where  $\mu$  is the viscosity of the gas, lbs.sec/inch,  $RT$  is the product of the gas constant and the total temperature, inch<sup>2</sup>/sec<sup>2</sup>,  $P_s$  is the supply

pressure, psia,  $C$  is the radial clearance, inch,  $n$  is the number of feeder holes,  $a$  is the orifice radius, inch, and  $\phi$  is the inherent compensation factor. In the inherently compensated bearing where there is no orifice, the restrictor coefficient becomes:

Inherently Compensated Bearing: 
$$\Lambda_s = \frac{b \mu n d \sqrt{RT}}{P_s C^2}$$

where  $d$  is the feeder hole diameter, inch.

In the purely hydrodynamic bearing, where  $NVL = 0$  and, therefore,  $NLSL = 0$ , this list is omitted. For  $NLSL \neq 0$ , give a total of  $NLSL$  values of  $\Lambda_s$ , maximum 25.

List of Compressibility Numbers (5E14.6)

This list consists of up to five cards, giving a total of  $NLB$  values of the compressibility number  $\Lambda$  (see item 3, control card).  $\Lambda$  is defined as:

$$\Lambda = \frac{\phi \mu \omega}{P_a} \left( \frac{R}{C} \right)^2$$

where  $\mu$  is the viscosity of the gas, lbs.sec/inch<sup>2</sup>,  $P_a$  is the ambient pressure, psia,  $\omega$  is the angular speed of the journal, radians/sec,  $R$  is the journal radius, inch and  $C$  is the radial clearance, inch. A maximum of 25 values can be given.

For the purely hydrostatic bearing, set  $NLB = 0$  and omit this list.

List of Eccentricity Ratios (5E14.6)

This list consists of up to five cards, giving a total of  $NEP$  values of the eccentricity ratio  $\epsilon$  (see item 4, control card).  $\epsilon$  is defined as:

$$\epsilon = e/C$$

where  $e$  is the distance between the journal center position and the bearing center, inch, and  $C$  is the radial clearance, inch.  $\epsilon$  cannot be zero and the input list cannot be omitted. A maximum of 25 values can be given.

List of Frequency Ratios or Squeeze Numbers (5E14.6)

This list consists of up to 19 cards, giving a total of  $MNS$  values (item 5,

control card). A maximum of 95 values can be given.

In the hybrid bearing or the purely hydrodynamic bearing ( $NLB \neq 0$ , item 3, control card), the list gives values of the frequency ratio  $\gamma$  :

$$\gamma = \frac{\nu}{\omega}$$

where  $\nu$  is the frequency for the journal center motion, radians/sec, and  $\omega$  is the angular speed of the roter, radians/sec.  $\gamma$  cannot be zero. The input values of  $\gamma$  are used by the program in searching for the threshold of instability. For each value of  $\gamma$ , the program calculates the left hand side of eq. (D-29), Appendix IV (as modified per Appendix VI), which represents the overall effective damping of the gas film and the bearing support. The threshold of instability occurs at those values of  $\gamma$  for which the effective damping is zero. The program uses the values of  $\gamma$  in the same sequence as given in the input. Thus, the input list should start with a small value of  $\gamma$  (say,  $\gamma = 0.0001$ ) and thereafter, give successively larger values of  $\gamma$  with the last value of  $\gamma \cong 0.51$ . Whenever the effective damping changes sign as the program goes through the  $\gamma$  list, the program interpolates to determine accurately the  $\gamma$  values at which the damping is zero.

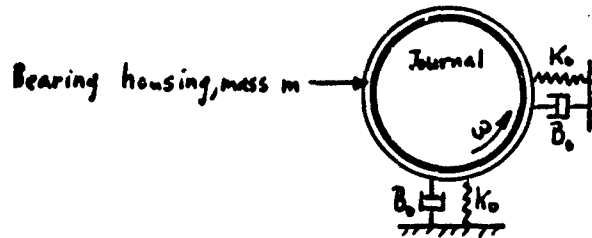
The very first value of  $\gamma$  is not used in the stability calculation and, therefore, can be any value. It is used as that value for which the program output gives the 8 dynamic coefficients. Thus, it is suggested to set the first value of  $\gamma$  equal to 1.

For the purely hydrostatic bearing ( $NLB = 0$ ), this input list gives values of the squeeze number  $\delta$  :

$$\delta = \frac{12\mu\nu}{P_a} \left(\frac{R}{C}\right)^2$$

where the symbols have been defined previously. The input is prepared in the same way as described above except that, whereas the range of interest for  $\gamma$  is known to be from 0 to 0.5, the range for  $\delta$  is not known in advance. It is suggested to let  $\delta$  go from a small value (say 0.001) to approximately 100. It should be noted, however, that the program is basically a hybrid bearing program and it is not very efficient in calculating a purely hydrostatic bearing although the answers are correct.

If INT = 0 (item 7, control card), the bearing is rigidly supported and the last input data is the preceding list of frequency ratios (or squeeze numbers). If INT = 1, the bearing is flexibly mounted and it is necessary to specify the support parameters. Schematically, the bearing and its support can be shown as:



### Card (815)

This card is the "control" card for the support parameters. It contains 3 items:

1. NK gives the number of values of the dimensionless support stiffness in the designated list ( $1 \leq NK \leq 25$ ).
2. NM gives the number of values of the dimensionless bearing boundary mass in the designated list ( $1 \leq NM \leq 25$ ).
3. ND gives the number of values of the dimensionless support damping in the designated list ( $ND \leq 25$ ). If  $ND = 0$ , the support is undamped and no input can be given for the support damping.

### List of Support Stiffness Values (5E14.6)

This list consists of up to five cards, giving a total of NK values of the dimensionless support stiffness:

$$\bar{K}_0 = \frac{CK_0}{P_a LD}$$

where  $K_0$  is the support spring coefficient, lbs/inch, C is the radial bearing clearance, inch, L is the bearing length, inch, D is the journal diameter, inch, and  $P_a$  is the ambient pressure, psia. There can be a maximum of 25 values.

List of Support Mass Values (5E14.6)

This list consists of up to five cards, giving a total of NM values of the dimensionless bearing housing mass:

$$\bar{m} = \frac{Cm\omega^2}{P_a L D}$$

where m is the bearing housing mass, lbs.sec<sup>2</sup>/inch,  $\omega$  is the angular speed of the journal, radians/sec, and the other symbols are defined above. There can be a maximum of 25 values. The mass may be zero if desired.

List of Support Damping Values (5E14.6)

If ND = 0, this list is omitted and the support has no damping. Otherwise, the list consists of up to five cards, giving a total of ND values of the dimensionless support damping:

$$\bar{B}_0 = \frac{B_0}{\mu L \left(\frac{R}{Z}\right)^3}$$

where  $B_0$  is the support damping coefficient, lbs.sec/inch, and the other symbols are defined above.

The support damping has a strong influence on the stability of a flexible mounted bearing. Properly chosen, the damping may vastly improve the stability limit of the bearing or even remove the tendency for instability all together. To determine which damping to provide, a whole range of damping values should be tried (say, from  $10^{-3}$  to 10). At the same time, the support stiffness should be considerably smaller than the bearing stiffness (of the order of one half or less of the bearing stiffness).

COMPUTER OUTPUT

The first page of output is a repetition of the input for checking purposes. Therefore, follow the output for each case. The output values are identified by text as follows:

L/D: the L/D-ratio

PR.RATIO: the supply pressure ratio  $V = P_3/P_2$

LAMBDA-S: the restrictor coefficient  $\Lambda_s$

LAMBDA: the compressibility number  $\Lambda$

ECCENTR: the eccentricity ratio  $\epsilon$

LAMBDA-T:  $\Lambda_s V$

Q: the dimensionless flow  $q = \frac{6\mu RT \bar{M}}{\sqrt{P_2} C^3}$  where  $\bar{M}$  is the total mass flow to the bearing, lbs.sec/inch, and the other symbols have been defined previously. Thus, knowing  $q$ , the bearings gas consumption can be determined.

M-O: the dimensionless orifice flow  $m_o = q/\Lambda_s V^2$  which is given by the right hand side of eq. (E-31), Appendix V.

PSI:  $\psi_o$ , the dimensionless rate of change of flow with changing downstream pressure (defined by eq. (E-60), Appendix V).

ORIF. PR. RATIO: the pressure ratio  $\bar{P}_c'/P_3$  across the feeder hole ( $\bar{P}_c'$  is the pressure downstream of the feeder hole).

W/PALD:  $W/P_2 LD$ , the dimensionless bearing load where  $W$  is the bearing load, lbs.

W/DPLD:  $W/(P_3 - P_2) LD$

ATT. ANG: the attitude angle  $\phi$ , degrees.

FR/PALD:  $f_r = F_r/P_2 LD$ , the dimensionless radial component of the bearing reaction, eq. (E-119), Appendix V.

FT/PALD:  $\bar{f}_t = F_t/P_aLD$ , the dimensionless tangential component of the bearing reaction, eq. (E-120), Appendix V.

CKKX/PALD:  $\bar{K}_{rr} = CK_{rr}/P_aLD$ , the dimensionless radial spring coefficient, eq. (E-131), Appendix V.

CWCX/PALD:  $\bar{B}_{rr} = C\omega B_{rr}/P_aLD$ , the dimensionless radial damping, eq. (E-131), Appendix V.

CKKY/PALD:  $\bar{K}_{rt} = CK_{rt}/P_aLD$ , the dimensionless radial cross-coupling spring coefficient, eq. (E-131), Appendix V.

CWCY/PALD:  $\bar{B}_{rt} = C\omega B_{rt}/P_aLD$ , the dimensionless radial cross-coupling damping, eq. (E-131) Appendix V.

CKYX/PALD:  $\bar{K}_{tr} = CK_{tr}/P_aLD$ , the dimensionless tangential cross-coupling spring coefficient.

CWCYX/PALD:  $\bar{B}_{tr} = C\omega B_{tr}/P_aLD$ , the dimensionless tangential spring coefficient.

CWCYY/PALD:  $\bar{B}_{tt} = C\omega B_{tt}/P_aLD$ , the dimensionless tangential damping.

EFF. STIFF-1: the major dimensionless, effective stiffness  $\bar{K}_g$  (eq. (D-24), Appendix IV, with plus in front of the square root instead of minus.

EFF. STIFF-2: the minor dimensionless, effective stiffness  $\bar{K}_g$ , eq. (D-24), Appendix IV,

EFF. DAMP-1: the major dimensionless, effective damping  $\gamma \bar{B}_g$  (eq. (D-25), Appendix IV, with plus in front of the square root instead of minus.

EFF. DAMP-2: the minor dimensionless, effective damping  $\gamma \bar{B}_g$ , eq. (D-25) Appendix IV.

FREQ/W:  $\gamma = \frac{\omega}{\omega_c}$ , the frequency ratio.

(S\*GAM)2:  $M\gamma^2 = (\bar{K}_0 \gamma \bar{B}_0 + \bar{K}_0 \gamma \bar{B}_0) / (\gamma \bar{B}_0 + (1+\bar{m}) \gamma \bar{B}_0)$ , see eq. (D-28), Appendix IV.

CG2/PALD:  $\bar{M} = CM\omega^2/P_a LD$ , the dimensionless journal mass.

CG2/DPLD:  $CM\omega^2/(P_s - P_a) LD$ , dimensionless expression for the journal mass.

MFA/MU2L(R/C)5:  $MP_a/\mu^2 L (\frac{R}{C})^5$ , dimensionless expression for the journal mass.

ERROR: the left hand side of eq. (D-29), Appendix IV.

PEDEST. STIFFN.:  $\bar{K}_0 = CK_0/P_a LD$ , the dimensionless support stiffness.

PEDEST. DAMPING:  $\bar{B}_0 = B_0/\mu L (\frac{R}{C})^3$ , the dimensionless support damping.

EFF. STIFFNESS: the minor dimensionless, effective stiffness  $\bar{K}_0$ , eq. (D-24), Appendix IV.

EFF. DAMPING: the negative of the minor dimensionless, effective damping  $\gamma \bar{B}_0$ , eq. (D-25), Appendix IV.

In each combination of  $\frac{L}{D}$ ,  $V$ ,  $\Lambda_s$ ,  $\Lambda$ ,  $\epsilon$ , there is a separate output which begins by specifying the appropriate values of  $\frac{L}{D}$ ,  $V$ ,  $\Lambda_s$ ,  $\Lambda$  and  $\epsilon$ , and then gives the corresponding bearing flow, the load carrying capacity, the attitude angle, the 8 dynamic coefficients and the four effective coefficients as identified by the labels explained above. The dynamic and the effective coefficients are calculated for the first frequency ratio given in the input data. Thereafter, follow the result of the stability calculation for a rigid support where eqs. (D-28) and (D-29) (S\*GAM)2 and ERROR) are listed for the specified values of the frequency ratio. The threshold of instability occurs when the "error" is zero and the program determines this by interpolation. For the threshold value of the frequency

ratio, the dimensionless journal mass is given in three different forms, identified by the labels explained above.

When the bearing is flexibly supported, the preceding results are followed by the calculations of the stability of the flexibly supported bearing. First, the dimensionless support stiffness is given together with the corresponding threshold value of the dimensionless journal mass for an undamped support. Thereafter, for each specified value of the dimensionless support damping is a 6 column list with the results of the calculations. The first column gives the frequency ratio  $\gamma$ , the second column gives  $\bar{M}\gamma^2$ , the third column gives the dimensionless minor effective bearing stiffness, the fourth column gives the dimensionless minor effective bearing damping and the sixth column gives the "ERROR". When an instability threshold is found, the corresponding dimensionless journal mass is given in three different forms in columns 3, 4, and 5.

For any given support damping, there may be up to three instability thresholds. At a threshold, the "error" must be very small (in theory it should be zero). This condition should be used to "weed out" a false root which frequently occurs. At such a false root,  $\bar{M}\gamma^2$  goes to plus-minus infinity on either side of the frequency ratio value and the corresponding dimensionless journal mass will tend to be very large (in theory, it is infinite). The solution should be ignored. It should be noted, however, that there are proper solutions where the dimensionless journal mass also is very large which must not be ignored.

#### SAMPLE CALCULATION

In back of this Appendix is shown the input for calculating the stability of a flexible supported bearing ( $L/D = 1$ ,  $\epsilon = 0.02$ ,  $\mathcal{A}_y = 0.7$ ,  $\lambda = 1.5$ ,  $\delta = 1000$ , 4 values of  $P_s/P_a$ , 7 values of  $\mathcal{A}$ , 3 values of support stiffness and 15 values of support damping). Also shown are the first couple of pages of output. The results are most conveniently plotted on logarithmic paper with the support damping as abscissa and the dimensionless journal mass as ordinate for fixed values of the supply pressure ratio and the support stiffness. The

compressibility number is used as a parameter. A typical plot is shown in figure 27. From such a plot it can be determined what support damping to provide to improve the stability limit of the bearing. A more detailed discussion is given in the body of the report.

INPUT FORM FOR COMPUTER PROGRAM  
PN0144: THE PERFORMANCE AND STABILITY OF A HYBRID JOURNAL  
BEARING WITH FLEXIBLE, DAMPED SUPPORT

Table of Vena Contracta Coefficients (5E14.6)

Give 25 values of the orifice vena contracta coefficient  $C_D$

Card (5E14.6)

k, the ratio of specific heats

Card (72H)

Text

Card (8I5)

1. NVL            Number of  $P_3/P_a$  -values in input ( $NVL \leq 25$ ). If  $NVL = 0$ , the bearing is purely hydrodynamic ( $NLB \neq 0$ ).
2. NLSL          Number of  $\lambda_3$  - values in input ( $NLSL \leq 25$ ). When  $NLSL = 0$ , NVL must be zero.
3. NLB           Number of  $\lambda$  -values in input ( $NLB \leq 25$ ). If  $NLB = 0$ , the bearing is purely hydrostatic ( $NVL \neq 0$ ).
4. NEP           Number of  $\epsilon$  -values in input ( $NEP \leq 25$ ).
5. MNS           If  $NLB \neq 0$ , MNS gives number of  $\delta$  -values in input. If  $NLB = 0$ , MNS gives number of  $\sigma$  -values in input ( $MNS \leq 95$ ).
6. MT            Number of finite difference increments ( $MT \leq 30$ ).

7. DMT                    0: Bearing support is rigid. 1: Bearing support is flexible.

8. IMP                    0: More input follows. 1: Last set of input.

Card (5E14.6)

1. L/D, the length-to-diameter ratio.
2.  $\lambda$ , the source correction factor (see eq. (E-50), Appendix V).
3.  $\delta = a^2/dC$ , the inherent compensation factor.
4.  $nV_c/\pi DLC$ , the feeder hold volume ratio.

List of Supply Pressure Ratios (5E14.6)

Give NVL values of  $V = P_s/P_a$ . Omit the list when NVL = 0.

List of Restrictor Coefficients (5E14.6)

Give NLSL values of  $\mathcal{A}_s$ . Omit the list when NVL = 0 (and, hence, NLSL = 0).

List of Compressibility Numbers (5E14.6)

Give NLB values of  $\mathcal{A}$ . Omit the list when NLB = 0.

List of Eccentricity Ratios (5E14.6)

Give NEP values of  $\epsilon$  ( $\epsilon \neq 0$ )

List of Frequency Ratios or Squeeze Numbers

If NLB  $\neq 0$  (hybrid or hydrodynamic bearing), give MNS values of the frequency ratio  $\mathcal{Z}$ .

If  $NLB = 0$  (hydrostatic bearing), give MNS values of the squeeze number  $\phi$  .

Note: If  $INT = 0$ , omit the following input data.

Card (815)

1. NK                    Number of support stiffness values in input ( $1 \leq NK \leq 25$ )
2. Ni                    Number of support mass values in input ( $1 \leq Ni \leq 25$ )
3. ND                    Number of support damping values in input ( $ND \leq 25$ )

List of Support Stiffness Values (5E14.6)

Give NK values of the dimensionless support stiffness.

List of Support Mass Values (5E14.6)

Give Ni values of the dimensionless support mass (may be zero).

List of Support Damping Values (5E14.6)

Give ND values of the dimensionless support damping. Omit the list when  $ND = 0$ .

SJOB 0.20,70000 66-217 CHASMAN APFL

SIBJOB MTI

STRPTC MTI

\*O ())))))))) ())))))))) (ZZZZZZZZZZZZZ)

C MECHANICAL TECHNOLOGY INC. JORGEN W. LUND 6-22-1966  
C PNC144 HYBRID JOURNAL BEARING STABILITY WITH FLEX-DAMPED SUPPORT  
DIMENSION TFR(31),TFE(31),VFR(31),VFE(31),EPSL(25),FRR(31),FJR(31)  
DIMENSION FJE(31),VCF(26),BSIG(25)  
DIMENSION FF(95),EF(95),PDKL(25),PDL(25),PJML(25)  
DIMENSION VLST(99),FLSL(99),FLBL(99), GST(99),PZ2(

199),PZN(99)

Y1=0.0

READ(5,301)(VCF(I),I=2,26)

READ(5,301)ADC

VCF(1)=1.0

WRITE(6,310)

WRITE(6,810)(VCF(I),I=2,26)

WRITE(6,315)

13 READ(5,300)

READ(5,302)NVL,NLSL,NLB,NEP,MNS,MT,INT,INP

READ(5,301)FLD,PRC,CMP,FDVL

WRITE(6,300)

WRITE(6,303)

WRITE(6,304)NVL,NLSL,NLB,NEP,MNS,MT,INP

WRITE(6,309)

WRITE(6,810) PRC,CMP,FDVL,ADC

IF(NVL) 15,14,15

14 VLST(1)=2.0

FLSL(1)=0.0

GO TO 20

15 WRITE(6,305)

READ(5,301)(VLST(I),I=1,NVL)

WRITE(6,810)(VLST(I),I=1,NVL)

WRITE(6,306)

READ(5,301)(FLSL(I),I=1,NLSL)

WRITE(6,810)(FLSL(I),I=1,NLSL)

IF(NLB) 20,19,20

19 FLBL(1)=1.0

GO TO 22

20 WRITE(6,307)

READ(5,301)(FLBL(I),I=1,NLB)

WRITE(6,810)(FLBL(I),I=1,NLB)

22 WRITE(6,316)

READ(5,301)(EPSL(I),I=1,NEP)

WRITE(6,810)(EPSL(I),I=1,NEP)

WRITE(6,308)

READ(5,301)(BSIG(I),I=1,MNS)

WRITE(6,810)(BSIG(I),I=1,MNS)

IF(INT) 24,29,24

24 READ(5,302)NK,NM,ND

READ(5,301)(PDKL(I),I=1,NK)

READ(5,301)(PDML(I),I=1,NM)

IF(ND) 29,29,27

27 READ(5,301)(PDL(I),I=1,ND)

29 EX6=2.0/(ADC+1.0)

EX1=1.0/(ADC-1.0)

EX7=(EX6\*\*EX1)\*SQRT(EX6\*ADC)

EX4=2.0\*EX1

EX1=ADC\*EX1

CRP=EX6\*\*EX1

C1=SQRT(2.0\*EX1)

```

EX6=1.0/EX5
EX7=1.0/ADC
DIT=(1.0-CRP)/50.0
CX=CRP
DO 51 I=1,50
CX=CX+DIT
C5=CX**EX1
51 QST(I)=C1*C5*SQRT (1.0-CX/C5)
C1=1.0+CMP*CMP
CMP=0.5/C1
C1=MT
DLT=FLD/C1
DL2=DLT*DLT
DL2H=0.5*DL2
SFAC=1.5707963/C1
MT1=MT+1
DO 285 NV=1,NVL
V=VLST(NV)
VMW=V-1.0
V2=V*V
DO 284 NLS=1,NLSL
FLAS=FLSL(NLS)
FLAT=FLAS*V
C1=FLAT*V*FLD*PRC
CX=SQRT (1.0+C1*EX7)/V
IF (CRP-CX) 152,151,151
151 Q=FLAT*V*EX7
SLP=0.0
PZ=V*CX
VC=1.0
DVC=0.0
GO TO 200
152 C2=V*CRP
C2=C2*C2-1.0-C1*EX7
C4=DIT+DIT
CX=CRP+C4
KS=0
L=2
M=2
154 VC=VCF(M)
155 C5=CX*CX*V2-1.0-C1*VC*QST(L)
IF (KS) 161,158,161
158 C6=C5*C2
IF (C6) 160,160,159
159 L=L+2
M=M+1
C2=C5
CX=CX+C4
IF (L-50) 154,154,284
160 KS=1
C7=C5
L=L-1
C5=VCF(M-1)
DVC=(VC-C5)/C4
VC=(VC+C5)/2.0
CX=CX-DIT
GO TO 155
161 C1=C4*C4
C1=2.0*(C2+C7-2.0*C5)/C1
C3=(C7-C2)/C4
IF (C1) 163,162,163

```

```

162 C6=-C5/C3
GO TO 166
163 C4=0.5*C3/C1
C6=SQRT (C4*C4-C5/C1)
IF (C4) 164,165,165
164 C6=-C6
165 C6=C6-C4
166 CX=CX+C6
167 PZ=V*CX
Q=(PZ*PZ-1.0)/FLD/PRC
VC=VC+C6*DVC
C4=VC*FLAT*V
C4=Q/C4
C5=-DVC/VC
C6=CX**EX1
SL1=VC/2.0*FLAT/PZ*(C5*C4+EX4*C6/C4*(EX6-C6/CX))
200 PZSQ=1.0+Q*FLD
PSC=PZ
PZ=SQRT(PZSQ)
C4=SL1*FLD*PRC
C4=(PRC+C4)/(1.0+C4)
FDV1=C4*FDVL/PSC*FLD*DLT
SLP=C4*SL1
BCZ=(CMP*Q-SLP*PZSQ)*DI T
BCZ1=DLT*SLP
IF(NVL) 192,191,192
191 FLWZ=0.0
SPZ=1.5707963
GO TO 193
192 FLWZ=Q/(FLAT*V)
SPZ=(PZSQ*PZ-1.0)/FLD*1.0471976/Q
193 PZ2(1)=PZSQ
C1=1.0+Q*FLD
C2=Q*DLT
PZN(1)=PZ
DO 201 I=2,MT1
C1=C1-C2
PZ2(I)=C1
201 PZN(I)=SQRT (C1)
DO 283 NL=1,NLB
FLA=FLBL(NL)
IF (NLB) 198,197,198
197 FLA=0.0
FLX=1.0
GO TO 199
198 FLX=2.0*FLA
FLA2=FLA*FLA
199 FLFZ=FLA/PZ
PR=-DL2H*PZSQ
PE=0.0
RR=DL2H
RE=DL2H*FLFZ
TFR(1)=0.0
TFE(1)=0.0
VFR(1)=1.0
VFE(1)=0.0
C1=0.0
C2=0.0
C3=0.5/PZ
C4=0.0
DO 205 I=2,MT1

```

```

TFR(I)=TFR(I-1)+PR+BCZ
TFE(I)=TFE(I-1)+PE
VFR(I)=VFR(I-1)+RR+BCZ1
VFE(I)=VFE(I-1)+RE
C5=PZN(I)
IF (I-MT1) 203,202,202
202 C5=2.0*C5
C6=1.0-TFR(I)
C7=TFE(I)
C8=VFR(I)
C9=VFE(I)
GO TO 204
203 C6=FLA/C5
PR=PR+DL2*(TFR(I)-C6*TFE(I)-C5*C5)
PE=PE+DL2*(TFE(I)+C6*TFR(I))
RR=RR+DL2*(VFR(I)-C6*VFE(I))
RE=RE+DL2*(VFE(I)+C6*VFR(I))
204 C1=C1+TFR(I)/C5
C2=C2+TFE(I)/C5
C3=C3+VFR(I)/C5
205 C4=C4+VFE(I)/C5
C5=C8*C8+C9*C9
HZR=(C6*C8-C7*C9)/C5
HZE=(-C6*C9-C7*C8)/C5
SFZR=SFACT*(C1+C3*HZR-C4*HZE)
SFZE=SFACT*(C2+C3*HZE+C4*HZR)
DO 206 I=1,MT1
TFR(I)=(TFR(I)+HZR*VFR(I)-HZE*VFE(I))/PZN(I)
206 TFE(I)=(TFE(I)+HZE*VFR(I)+HZR*VFE(I))/PZN(I)
FRSW=SPZ-SFZR
FTSW=-SFZE
DO 282 NE=1,NEP
EPS=EPSL(NE)
MC=MNS
GAM=0.0
EP2=EPS*EPS
E7=1.0-EP2
C1=SQRT (E7)
C2=1.0+C1
E1=2.0/C2
E2=E1-C1
E3=E1/C1
E4=E3*EPS
E5=E4*EPS/C2
E6=2.0/(C1*E7)-E3
E7=E4*EPS/E7+E5/C1
FRS=E4*FRSW
FTS=E2*FTSW
WPLD=SQRT (FRS*FRS+FTS*FTS)
WDPLD=WPLD/VMW
IF (FRS) 230,226,230
226 IF (FTS) 227,228,229
227 ANGZ=-90.0
GO TO 232
228 ANGZ=0.0
GO TO 232
229 ANGZ=90.0
GO TO 232
230 ANGZ=FTS/FRS
ANGZ=57.295780*ATAN (ANGZ)
IF (FRS) 231,232,232

```

```

231 ANGZ=ANGZ+180.0
232 WRITE(6,311)
WRITE(6,810)FLD,V,FLAS,FLA,EPS
WRITE(6,312)
WRITE(6,810)FLAT,Q,FLWZ,SLP,CX
WRITE(6,313)
WRITE(6,810)WPLD,WDPLD,ANGZ,FRS,FTS
FRS=FRS/EPS
FTS=FTS/EPS
MS=2
KC=0
LC=0
KK=0
DO 281 NS=1,MNS
SIG=BSIG(NS)
SIG2=SIG*SIG
IF(NS-2) 250,550,250
550 WRITE(6,318)
250 KS=0
SIG2=SIG*SIG
AS=BCZ
FDV2=FLX*SIG*FDV1
AS1=FDV2*PZSQ
BS=1.0
DO 251 I=1,MT1
FRR(I)=-PZ2(I)
FJR(I)=0.0
251 FJE(I)=0.0
252 PR=DL2H*FRR(1)
PE=0.0
QR=DL2H*FJR(1)
QE=DL2H*FJE(1)
RR=DL2H
RE=DL2H*FLFZ
SR=DL2H*FLX/PZ*SIG
SE=0.0
TR=0.0
TE=0.0
UR=0.0
UE=0.0
VE=0.0
WR=0.0
WE=0.0
VR=1.0
C1=0.0
C2=0.0
C3=0.0
C4=0.0
C6=0.0
C7=0.0
C8=0.0
C5=0.5/PZ
DO 256 I=2,MT1
TR=TR+PR+AS
TE=TE+PE
UR=UR+QR-AS1
UE=UE+QE
VR=VR+RR+BCZ1
VE=VE+RE
WR=WR+SR+FDV2
WE=WE+SE

```

```

A1=PZN(I)
IF (I-MT1) 254,253,253
253 A1=2.0
GO TO 255
254 A2=FLA/A1
A3=FLX/A1*SIG
PR=PR+DL2*(TR-A2*TE-A3*UR+FRR(I))
PE=PE+DL2*(TE+A2*TR-A3*UE)
QR=QR+DL2*(UR-A2*UE+A3*TR+FJR(I))
QE=QE+DL2*(UE+A2*UR+A3*TE+FJE(I))
RR=RR+DL2*(VR-A2*VE-A3*WR)
RE=RE+DL2*(VE+A2*VR-A3*WE)
SR=SR+DL2*(WR-A2*WE+A3*VR)
SE=SE+DL2*(WE+A2*WR+A3*VE)
255 C1=C1+TR/A1
C2=C2+TE/A1
C3=C3+UR/A1
C4=C4+UE/A1
C5=C5+VR/A1
C6=C6+VE/A1
C7=C7+WR/A1
256 C8=C8+WE/A1
TR=BS-TR
A1=TR*VR+TE*VE-UR*WR+UE*WC
A2=TR*VE-TE*VR-UR*WE-UE*WR
A3=-TR*WR-TE*WE-UR*VR+UE*VE
A4=-TR*WE+TE*WR-UR*VE-UE*VR
A5=VR*VR-VE*VE+WR*WR-WE*WE
A6=2.0*(VR*VE+WR*WE)
A7=A5*A5+A6*A6
HZR=(A1*A5+A2*A6)/A7
HZE=(A2*A5-A1*A6)/A7
HZJR=(A3*A5+A4*A6)/A7
HZJE=(A4*A5-A3*A6)/A7
IF(INP) 401,402,402
401 WRITE(6,810)A1,A2,A3,A4,A5
WRITE(6,810)A6,A7,HZR,HZE,HZJR
402 G2RR=SFACT*(C1+HZR*C5-HZE*C6-HZJR*C7+HZJE*C8)
G2RE=SFACT*(C2+HZR*C6+HZE*C5-HZJR*C8-HZJE*C7)
G2JR=SFACT*(C3+HZR*C7-HZE*C8+HZJR*C5-HZJE*C6)
G2JE=SFACT*(C4+HZR*C8+HZE*C7+HZJR*C6+HZJE*C5)
IF(KS) 259,257,259
257 G1RR=G2RR
G1RE=G2RE
G1JR=G2JR
G1JE=G2JE
KS=1
AS=0.0
AS1=0.0
BS=0.0
A1=SIG*FLX
DO 258 I=1,MT1
FRR(I)=0.0
FJR(I)=A1*TFE(I)
258 FJE(I)=-A1*TFR(I)
GO TO 252
259 CRR=E6*SPZ-E7*SFZR-E3*G1RR
CRJ=-E3*G1JR
DRR=-E3*G2RR+FTS
DRJ=-E3*G2JR
CTR=-E5*SFZE-E1*G1RE

```

```

CTJ=-E1*G1JE
DTR=-E1*G2RE-FRS
DTJ=-E1*G2JE
A1=(CRR+DTR)/2.0
A2=CRJ-DTJ
A3=0.5*A2
A4=DRR*CTJ+CTR*DRJ
A5=DRJ*CTJ-CRJ*DTJ-DRR*CTR
C3=(A1*A1-A3*A3+A5)/2.0
C4=(A1*(CRJ+DTJ)-A4)/2.0
C4=C3*C3+C4*C4
C4=SQRT (C4)
FFC=-C3+C4
FFC=SQRT (FFC)-A3
C3=CRJ+FFC
C4=FFC-DTJ
C5=C3+C4
EFC=(CRR*C4-DTR*C3+A4)/C5
IF(LC) 719,188,719
188 IF(KC) 190,189,190
189 FF(NS)=FFC
EF(NS)=EFC
190 WRT=(A4-CRR*DTJ-DTR*CRJ)/A2
C4=WRT
FEJL=(CRR-WRT)*(DTR+WRT)+A5
IF(NS-1) 510,510,511
510 CTR=-CTR
CTJ=-CTJ
DTR=-DTR
DTJ=-DTJ
WRITE(6,321)
WRITE(6,810)CRR,CRJ,DRR,DRJ
WRITE(6,322)
WRITE(6,810)CTR,CTJ,DTR,DTJ
C3=A3*A3-FEJL
IF(C3) 512,513,513
512 C1=-1.0
C2=-1.0
C3=-1.0
C4=-1.0
GO TO 514
513 C3=SQRT(C3)
C4=A3+C3
C5=A3-C3
C3=2.0*C3
C3=(A1*(CRJ-DTJ)-A4)/C3
C2=(CRR+DTR)/2.0
C1=C2+C3
C2=C2-C3
514 WRITE(6,323)
WRITE(6,810)C1,C2,C4,C5
GO TO 281
511 IF (NLB) 195,194,195
194 WRT1=WRT
WRT2=WRT/VMW
WRT3=WRT/SIG2*288.0
GO TO 196
195 WRT1=WRT
WRT=WRT1/SIG2
WRT2=WRT/VMW
WRT3=WRT/FLA2*72.0

```

```

196 IF(KK) 520,521,520
251 WRITE(6,804)SIG,WRT1,FEJL
GO TO 522
250 WRITE(6,803)SIG,WRT1,WRT,WRT2,WRT3,FEJL
KK=0
252 IF (KC) 273,260,254
260 IF(NS-2) 262,262,261
261 C1=Y1*FEJL
IF (C1) 263,273,262
262 Y1=FEJL
X1=SIG
W1=WRT
MS=MS+1
IF(MNS-MS) 571,281,281
571 IF(INT) 699,282,699
263 Y3=FEJL
W3=WRT
X3=SIG
KC=1
DSIG=X3-X1
SIG=SIG-0.5*DSIG
GO TO 250
264 Y2=FEJL
W2=WRT
X2=SIG
C3=X3-X2
C4=X2-X1
C5=X3-X1
C6=(Y3-Y2)/C5
C6=C6/C3
C7=(Y1-Y2)/C5
C7=C7/C4
C5=C6+C7
C4=C4*C6-C3*C7
D6=(W3-W2)/C5
D6=D6/C3
D7=(W1-W2)/C5
D7=D7/C4
A1=D6+D7
A2=C4*D6-C3*D7
A3=W2
IF(C5) 266,265,266
265 C3=-Y2/C4
GO TO 271
266 C4=C4/C5*0.5
C5=C4*C4-Y2/C5
C5=SQRT(C5)
IF(C4) 269,270,270
269 C5=-C5
270 C3=-C4+C5
271 SIG =X2+C3
WRT=(A1*C3+A2)*C3+A3
KC=-1
WRITE(6,810)SIG,WRT
KK=1
GO TO 250
273 KC=0
FFC1=FFC
EFC1=EFC
FKAP=C4
GAM=SIG

```

```

GAM2=SIG2
MC=MS
IF(INT) 290,282,699
290 Y1=Y3
    W1=W3
    X1=X3
    GO TO 281
699 IK=1
700 PDK=PDKL(IK)
    PDKQ=PDK*PDK
    IF(GAM) 703,704,703
703 C1=FKAP+PDK
    C1=FKAP/C1*PDK/GAM2
    WRITE(6,811)PDK,C1
704 IM=1
701 PDM=PDML(IM)
    PDM1=1.0+PDM
    PDM2=PDM1*PDM1
    IF(PDM) 705,706,705
705 IF(GAM) 698,706,698
698 C1=(PDK+FKAP*PDM1)/PDM*0.5
    C2=PDK/PDM*FKAP
    C3=C1*C1-C2
    C3=SQRT(C3)
    C2=(C1-C3)/GAM2
    C1=(C1+C3)/GAM2
    WRITE(6,814)
    WRITE(6,802)PDM,PDK,C1,C2
706 IF(ND) 741,741,707
707 ID=1
702 PDP1=PDL(ID)
    PDP=PDP1/12.0*FLA
    PDPQ=PDP*PDP
    WRITE(6,812)PDP1
    WRITE(6,314)
    NC=2
    JC=0
    LC=1
718 FFC=FF(NC)
    EFC=EF(NC)
    X=BSIG(NC)
719 C2=X*X
    C1=C2*PDPQ
    C4=PDP*X
    S3=C4-PDM1*FFC
    S3=(C4*EFC-PDK*FFC)/S3
    C3=PDK-PDM1*S3
    C3=C3*C3+C1
    ERR3=FFC-C4*S3/C3*S3
    IF(NLB) 501,502,501
502 RT1=S3
    RT2=S3/VMW
    RT3=S3/C2 *288.0
    GO TO 503
501 RT1=S3/C2
    RT2=RT1/VMW
    RT3=RT1/FLA2*72.0
503 IF(KK) 523,524,523
524 WRITE(6,804)X,S3,ERR3
    WRITE(6,805)EFC,FFC
    GO TO 525

```

```

523 WRITE(6,803)X,S3,RT1,RT2,RT3,ERR3
    WRITE(6,805)EFC,FFC
    KK=0
525 IF(JC) 760,728,720
720 JC=0
    GO TO 733
728 IF(NC-2) 729,729,730
729 X3=X
    Y3=ERR3
    NC=NC+1
    GO TO 718
730 X1=X3
    X3=X
    Y1=Y3
    Y3=ERR3
    C3=Y1*Y3
    IF(C3) 731,720,733
731 JC=-1
    X=(X1+X3)/2.0
    SIG=X
    GO TO 250
733 NC=NC+1
    IF(MC-NC) 740,734,718
734 IF(GAM) 735,718,735
735 X=GAM
    FFC=FFC1
    EFC=EFC1
    GO TO 719
760 X2=X
    Y2=ERR3
    C3=X3-X2
    C4=X2-X1
    C5=X3-X1
    C6=(Y3-Y2)/C5
    C6=C6/C3
    C7=(Y1-Y2)/C5
    C7=C7/C4
    C5=C6+C7
    C4=C4*C6-C3*C7
    IF(C5) 762,761,762
761 C3=-Y2/C4
    GO TO 765
762 C4=C4/C5*0.5
    C5=C4*C4-Y2/C5
    C5=SQRT(C5)
    IF(C4) 763,764,764
763 C5=-C5
764 C3=-C4+C5
765 X=X2+C3
    SIG=X
    JC=1
    KK=1
    GO TO 250
740 ID=ID+1
    IF(ND-ID) 741,702,702
741 IM=IM+1
    IF(NM-IM) 742,701,701
742 IK=IK+1
    IF(NK-IK) 281,700,700
281 CONTINUE
282 CONTINUE

```

```

283 CONTINUE
284 CONTINUE
285 CONTINUE
   IF(INP) 508,18,508
   18 WRITE(6,315)
      GO TO 13
508 STOP
300 FORMAT(72H1
      1
      )
301 FORMAT(5E14.6)
302 FORMAT(8I5)
303 FORMAT(6H0 NO.V7X5HN.L-S6X5HN.LAM6X4HN.EP7X5HN.SIG6X4HDIVS8X3HINP)
304 FORMAT(1XI4,7XI4,7XI4,7XI4,7XI4,7XI4,7XI4)
305 FORMAT(16HOPRESSURE RATIOS)
306 FORMAT(14HOLAMBDA-S LIST)
307 FORMAT(12HOLAMBDA LIST)
308 FORMAT(26HOLIST OF FREQUENCY RATIOS)
309 FORMAT(13H0 OR.RA.FCT5X8HINH.COMP6X8HFEED.VOL4X11HSP.HE.RATIO)
310 FORMAT(28HOVENA CONTRACTA COEFFICIENTS)
311 FORMAT(1H15X3HL/D9X8HPR.RATIO6X8HLAMBDA-S7X6HLAMBDA7X8HECCENTR.)
312 FORMAT(12H0 LAMBDA-T9X1HQ12X3HM-011X3HPSI6X13HORIF.PR.RATIO)
313 FORMAT(1H04X6HW/PALD8X6HW/DPLD7X7HATT.ANG7X7HFR/PALD7X7HFT/PALD)
314 FORMAT(11H0 FREQ/W7X8H(S*GAM)25X9HCMW2/PALD5X9HCMW2/DPLD3X14HMP
      1A/MU2L(R/C)54X5HERROR/29X13HEFF.STIFFNESS2X11HEFF.DAMPING)
315 FORMAT(1H1)
316 FORMAT(20HOECCENTRICITY RATIOS)
318 FORMAT(11H0 FREQ/W7X8H(S*GAM)25X9HCMW2/PALD5X9HCMW2/DPLD3X14HMP
      1A/MU2L(R/C)54X5HERROR)
321 FORMAT(55H0 CKXX/PALD CWCXX/PALD CKXY/PALD CWCXY/PALD)
322 FORMAT(55H0 CKYX/PALD CWCYX/PALD CKYY/PALD CWCYY/PALD)
323 FORMAT(55H0 EFF.STIFF-1 EFF.STIFF-2 EFF.DAMP-1 EFF.DAMP-2)
802 FORMAT(4(1PE15.7))
803 FCRMAT(6(1PE14.6))
804 FORMAT(1PE14.6,1PE14.6,42X1PE14.6)
805 FORMAT(28X1PE14.6,1PE14.6)
810 FORMAT(5(1PE14.6))
811 FORMAT(/16HOPEDEST.STIFFN.=,1PE13.6,14H MCW**2/PALD=,1PE13.6)
812 FORMAT(/20HC PEDESTAL DAMPING=,1PE13.6)
814 FORMAT(/14HO PEDEST.MASS5X9HPED.STIFF6X9HMASS RT.16X9HMASS RT.2)
      END

```

0.9985	0.9955	0.9915	0.9871	0.9824
0.9776	0.9726	0.9675	0.9623	0.957
0.9516	0.946	0.9402	0.9341	0.9276
0.9206	0.913	0.9046	0.895	0.8836
0.869	0.8477	0.8105	0.736	0.6

1.4  
 HYBRID-HYDROSTATIC RING BEARING , PS/PA=1.25 , 7-7-1967

1	1	7	1	33	15	1	0
1.0		1.5		1000.0		0.0	
1.25							
0.7							
0.3		1.0		2.0		5.0	10.0
30.0		100.0					
0.02							
1.0		0.00001		0.00005		0.0001	0.0005
0.001		0.003		0.006		0.01	0.03
0.06		0.1		0.15		0.2	0.25
0.3		0.35		0.4		0.42	0.44
0.46		0.48		0.485		0.49	0.492
0.494		0.496		0.497		0.498	0.499
0.5		0.501		0.51			
3	1	10					
0.05		0.038		0.019			
0.0							
0.2		0.5		2.0		5.0	20.0
50.0		100.		200.		500.	1000.

HYBRID-HYDROSTATIC RING BEARING , PS/PA=1.25 , 7-7-1967

NO.V	N.L-S	N.LAM	N.EP	N.SIG	DIVS	INP
1	1	7	1	33	15	0

OR.RA.FCT	INH.COMP	FEED.VOL	SP.HE.RATIO
1.500000E 00	1.000000E 03	0.	1.400000E 00

PRESSURE RATIOS  
1.250000E 00

LAMBDA-S LIST  
7.000000E-01

LAMBDA LIST

3.000000E-01	1.000000E 00	2.000000E 00	5.000000E 00	1.000000E 01
3.000000E 01	1.000000E 02			

ECCENTRICITY RATIOS  
2.000000E-02

LIST OF FREQUENCY RATIOS

1.000000E 00	1.000000E-05	5.000000E-05	10.000000E-05	5.000000E-04
10.000000E-04	3.000000E-03	6.000000E-03	10.000000E-03	3.000000E-02
6.000000E-02	1.000000E-01	1.500000E-01	2.000000E-01	2.500000E-01
3.000000E-01	3.500000E-01	4.000000E-01	4.200000E-01	4.400000E-01
4.600000E-01	4.800000E-01	4.850000E-01	4.900000E-01	4.920000E-01
4.940000E-01	4.960000E-01	4.970000E-01	4.980000E-01	4.990000E-01
5.000000E-01	5.010000E-01	5.100000E-01		

IBJOB VERSION 5 HAS CONTROL.  
\$IBJOB MTI  
\$IBLDR MTI

11/21/66

MTI 0000

VENA CONTRACTA COEFFICIENTS

9.985000E-01	9.955000E-01	9.915000E-01	9.871000E-01	9.824000E-01
9.776000E-01	9.726000E-01	9.675000E-01	9.623000E-01	9.570000E-01
9.516000E-01	9.460000E-01	9.402000E-01	9.341000E-01	9.276000E-01
9.206000E-01	9.130000E-01	9.046000E-01	8.950000E-01	8.836000E-01
8.690000E-01	8.477000E-01	8.105000E-01	7.360000E-01	6.000000E-01

L/D	PR.RATIO	LAMBDA-S	LAMBDA	ECCENTR.	
1.00000E-01	1.25000E-00	7.00000E-01	3.00000E-01	2.00000E-02	
LAMBDA-T	Q	M-O	PSI	ORIF.PR.RATIO	
8.75000E-01	2.76211E-01	2.52536E-01	1.33254E-00	9.51400E-01	
W/PALD	W/DPLD	ATT.ANG	FR/PALD	FT/PALD	
2.02286E-03	8.09146E-03	4.37088E-01	1.46225E-03	1.39778E-03	
CKXX/PALD	CWCXX/PALD	CKXY/PALD	CWCXY/PALD		
8.66624E-02	1.37786E-01	6.78691E-02	-1.35059E-02		
CKYX/PALD	CWCYX/PALD	CKYY/PALD	CWCYY/PALD		
-6.78835E-02	1.35032E-02	8.66158E-02	1.37758E-01		
EFF.STIFF-1	EFF.STIFF-2	EFF.DAMP-1	EFF.DAMP-2		
1.00350E-01	7.29274E-02	2.04624E-01	7.09214E-02		
FREQ/W	(S*GAM)2	CMW2/PALD	CMW2/DPLD	MPA/MU2L(R/C)5	ERROR
1.00000E-05	6.621407E-02				-4.933395E-03
5.00000E-05	6.621407E-02				-4.933395E-03
10.00000E-05	6.621407E-02				-4.933394E-03
5.00000E-04	6.621407E-02				-4.933397E-03
10.00000E-04	6.621408E-02				-4.933375E-03
3.00000E-03	6.621416E-02				-4.933216E-03
6.00000E-03	6.621457E-02				-4.932681E-03
10.00000E-03	6.621547E-02				-4.931412E-03
3.00000E-02	6.622655E-02				-4.915548E-03
6.00000E-02	6.626411E-02				-4.862009E-03
1.00000E-01	6.635310E-02				-4.735124E-03
1.50000E-01	6.652693E-02				-4.487395E-03
2.00000E-01	6.677020E-02				-4.140781E-03
2.50000E-01	6.708286E-02				-3.695483E-03
3.00000E-01	6.746478E-02				-3.151759E-03
3.50000E-01	6.791589E-02				-2.509956E-03
4.00000E-01	6.843601E-02				-1.770424E-03
4.20000E-01	6.866333E-02				-1.447346E-03
4.40000E-01	6.890169E-02				-1.108731E-03
4.60000E-01	6.915176E-02				-7.546133E-04
4.80000E-01	6.941139E-02				-3.850241E-04
4.85000E-01	6.947822E-02				-2.902138E-04
4.90000E-01	6.954571E-02				-1.944393E-04
4.92000E-01	6.957288E-02				-1.558591E-04
4.94000E-01	6.960014E-02				-1.171258E-04
4.96000E-01	6.962759E-02				-7.823831E-05
4.97000E-01	6.964126E-02				-5.873647E-05
4.98000E-01	6.965506E-02				-3.919589E-05
4.99000E-01	6.966892E-02				-1.961708E-05
5.00000E-01	6.968270E-02				3.224159E-05
4.99500E-01	6.967579E-02				-9.813994E-06
5.00000E-01	2.787861E-01				
5.00000E-01	6.968270E-02	2.787308E-01	1.114923E-00	2.229847E-02	-1.368790E-10

PEDEST.STIFFN.= 5.00000E-02 MCW\*\*2/PALD= 1.164457E-01

PEDESTAL DAMPING= 2.00000E-01

FREQ/W	(S*GAM)2	CMW2/PALD	CMW2/DPLD	MPA/MU2L(R/C)5	ERROR
1.00000E-05	4.999998E-02	EFF.STIFFNESS	EFF.DAMPING		-4.494735E-04

5.000000E-05	4.999992E-02	7.313440E-02	6.989497E-02	-9.009510E 03
10.000000E-05	4.999983E-02	7.313385E-02	6.988941E-02	-4.502197E 03
5.000000E-04	4.999917E-02	7.313316E-02	6.988245E-02	-9.010618E 02
10.000000E-04	4.999834E-02	7.312765E-02	6.982681E-02	-4.503558E 02
3.000000E-03	4.999501E-02	7.312078E-02	6.975726E-02	-1.499771E 02
6.000000E-03	4.998998E-02	7.309331E-02	6.947903E-02	-7.487353E 01
10.000000E-03	4.998320E-02	7.305239E-02	6.906166E-02	-4.483033E 01
3.000000E-02	4.994799E-02	7.299818E-02	6.850510E-02	-1.478160E 01
6.000000E-02	4.989048E-02	7.273359E-02	6.572138E-02	-7.259640E 00
1.000000E-01	4.980264E-02	7.235728E-02	6.154291E-02	-4.235936E 00
1.500000E-01	4.966765E-02	7.189382E-02	5.596658E-02	-2.700306E 00
2.000000E-01	4.948962E-02	7.137624E-02	4.898883E-02	-1.901080E 00
2.500000E-01	4.923927E-02	7.092734E-02	4.200385E-02	-1.380375E 00
3.000000E-01	4.885526E-02	7.054729E-02	3.501268E-02	-9.775532E-01
3.500000E-01	4.818385E-02	7.023618E-02	2.801635E-02	-6.177224E-01
4.000000E-01	4.669986E-02	6.999411E-02	2.101588E-02	-2.789018E-01
4.200000E-01	4.544253E-02	6.982114E-02	1.401231E-02	-1.610079E-01
4.400000E-01	4.300706E-02	6.977129E-02	1.121025E-02	-6.730940E-02
4.600000E-01	3.628871E-02	6.973254E-02	8.407920E-03	-1.006437E-02
4.800000E-01	-6.733018E-02	6.970487E-02	5.605391E-03	2.012720E-03
4.700000E-01	2.503681E-02	6.968825E-02	2.802725E-03	1.860958E-03
4.675185E-01	2.920510E-02	6.969517E-02	4.204076E-03	1.068935E 02
4.850000E-01	1.978179E-01	1.336168E-01	5.344673E-01	-1.417531E-06
4.825000E-01	-1.140688E 00	6.969735E-02	4.551807E-03	-2.239775E-03
4.827751E-01	1.270730E 03	6.968585E-02	2.102047E-03	2.382574E-04
4.900000E-01	9.598949E-02	6.968693E-02	2.452388E-03	4.361678E 06
4.920000E-01	8.616499E-02	5.452098E 03	2.180839E 04	-2.273591E-07
4.940000E-01	7.904167E-02	6.968678E-02	2.413838E-03	-9.241067E-03
4.960000E-01	7.543107E-02	6.968413E-02	1.401367E-03	-1.277892E-02
4.970000E-01	7.369077E-02	6.968361E-02	1.121090E-03	-1.672000E-02
		6.968319E-02	8.408194E-04	-2.105232E-02
		6.968294E-02	5.605491E-04	-2.336124E-02
		6.968278E-02	4.204111E-04	

4.980000E-01	7.217921E-02	6.968274E-02	2.802722E-04	-2.576278E-02
4.990000E-01	7.085406E-02	6.968276E-02	1.401352E-04	-2.825516E-02
5.000000E-01	6.968270E-02	6.968270E-02	0.	-3.083685E-02

PEDESTAL CAMPING= 5.000000E-01

FREQ/W	(S+GAM)Z	CMW2/PALD EFF. STIFFNESS	CMW2/DPLD EFF. DAMPING	MPA/MUZZL(R/C)5	ERROR
1.000000E-05	4.999996E-02	7.313440E-02	6.989497E-02		-1.801912E 04
5.000000E-05	4.999979E-02	7.313385E-02	6.988941E-02		-3.605347E 03
10.000000E-05	4.999959E-02	7.313316E-02	6.988245E-02		-1.802223E 03
5.000000E-04	4.999793E-02	7.312765E-02	6.982681E-02		-3.603328E 02
10.000000E-04	4.999586E-02	7.312078E-02	6.975726E-02		-1.800926E 02
3.000000E-03	4.998753E-02	7.309331E-02	6.947903E-02		-5.992807E 01
6.000000E-03	4.997494E-02	7.305239E-02	6.906166E-02		-2.988602E 01
10.000000E-03	4.995796E-02	7.299818E-02	6.850510E-02		-1.786884E 01
3.000000E-02	4.986954E-02	7.273359E-02	6.572138E-02		-5.850193E 00
6.000000E-02	4.972418E-02	7.235728E-02	6.154291E-02		-2.842366E 00
1.000000E-01	4.949983E-02	7.189382E-02	5.596658E-02		-1.633696E 00
1.500000E-01	4.914928E-02	7.137624E-02	4.898883E-02		-1.019420E 00
2.000000E-01	4.867561E-02	7.092734E-02	4.200385E-02		-6.980372E-01
2.500000E-01	4.798636E-02	7.054729E-02	3.501268E-02		-4.856614E-01
3.000000E-01	4.687280E-02	7.023618E-02	2.801635E-02		-3.175511E-01
3.500000E-01	4.474341E-02	6.999411E-02	2.101588E-02		-1.662452E-01
4.000000E-01	3.900330E-02	6.982114E-02	1.401231E-02		-3.811148E-02
4.200000E-01	3.258475E-02	6.977129E-02	1.121025E-02		-5.637898E-03
4.400000E-01	1.267814E-02	6.973254E-02	8.407920E-03		7.786740E-03
4.300000E-01	2.605859E-02	6.975052E-02	9.809118E-03		3.746990E-03
4.252980E-01	2.960905E-02	1.636959E-01	6.547835E-01	1.309567E 02	-2.791046E-05
4.600000E-01	8.335150E-01	6.975993E-02	1.046793E-02		-9.015465E-04
4.500000E-01	-3.027189E-02	6.970487E-02	5.605391E-03		6.210613E-03
4.590629E-01	7.155573E 01	6.971728E-02	7.006675E-03		
4.800000E-01	8.694693E-02	3.395471E 02	1.358188E 03	2.716377E 05	-9.609095E-06
		6.970591E-02	5.736705E-03		-2.957141E-02

4.850000E-01	8.013430E-02	6.968825E-02	2.802725E-03	-3.910153E-02
4.900000E-01	7.552384E-02	6.968585E-02	2.102047E-03	-4.930543E-02
4.920000E-01	7.407165E-02	6.968413E-02	1.401367E-03	-5.354350E-02
4.940000E-01	7.278582E-02	6.968361E-02	1.121090E-03	-5.785708E-02
4.960000E-01	7.163938E-02	6.968319E-02	8.408194E-04	-6.223691E-02
4.970000E-01	7.111142E-02	6.968294E-02	5.605491E-04	-6.444930E-02
4.980000E-01	7.061071E-02	6.968278E-02	4.204111E-04	-6.667459E-02
4.990000E-01	7.013513E-02	6.968274E-02	2.802722E-04	-6.891187E-02
5.000000E-01	6.968270E-02	6.968276E-02	1.401352E-04	-7.116072E-02
		6.968270E-02	0.	

PEDESTAL DAMPING= 2.000000E 00

FREQ/W	(S*GAM)Z	CMW2/PALD EFF. STIFFNESS	CMW2/DPLD EFF. DAMPING	MPA/MU2L(R/C)5	ERROR
1.000000E-05	4.999983E-02	7.313440E-02	6.989497E-02		-4.504705E 03
5.000000E-05	4.999917E-02	7.313385E-02	6.988941E-02		-9.010617E 02
10.000000E-05	4.999834E-02	7.313316E-02	6.988245E-02		-4.504810E 02
5.000000E-04	4.999172E-02	7.312765E-02	6.982681E-02		-9.000745E 01
10.000000E-04	4.998342E-02	7.312078E-02	6.975726E-02		-4.494466E 01
3.000000E-03	4.995003E-02	7.309331E-02	6.947903E-02		-1.490265E 01
6.000000E-03	4.989942E-02	7.305239E-02	6.906166E-02		-7.392185E 00
10.000000E-03	4.983091E-02	7.299810E-02	6.850510E-02		-4.388043E 00
3.000000E-02	4.946902E-02	7.273359E-02	6.572130E-02		-1.384065E 00
6.000000E-02	4.885431E-02	7.235728E-02	6.154291E-02		-6.327760E-01
1.000000E-01	4.785214E-02	7.189382E-02	5.596658E-02		-3.306548E-01
1.500000E-01	4.613578E-02	7.137624E-02	4.898883E-02		-1.752784E-01
2.000000E-01	4.346099E-02	7.092734E-02	4.200395E-02		-9.030746E-02
2.500000E-01	3.859127E-02	7.054729E-02	3.501268E-02		-2.998548E-02
3.000000E-01	2.667990E-02	7.023618E-02	2.801635E-02		1.412863E-02
2.750000E-01	3.422371E-02	7.038309E-02	3.151510E-02		-5.257838E-03
2.811421E-01	3.276969E-02	4.145918E-01	1.658367E 00	3.316734E 02	1.284359E-04
3.500000E-01	-4.951887E-02	7.034542E-02	3.065562E-02		1.681304E-02
		6.999411E-02	2.101588E-02		

#### REFERENCES

1. C.W. Ng and C.H.T. Pan, "A Linearized Turbulent Lubrication Theory". *Journal of Basic Engineering*, TRANS. ASME, Series D, vol. 87, 1965 pp. 675-688
2. J.W. Lund, "A Theoretical Analysis of Whirl Instability and Pneumatic Hammer for a Rigid Rotor in Pressurized Gas Journal Bearings". *Journal of Lubrication Technology*, TRANS, ASME, Series F, vol. 89, 1967, pp. 154-166
3. J.W. Lund and F. Orcutt, "Calculations and Experiments on the Unbalance Response of a Flexible Rotor". ASME Paper No. 67-Vibr-27, presented at the ASME Vibrations Conference, Boston, Mass., March 1967

UNCLASSIFIED

Security Classification		
DOCUMENT CONTROL DATA - R & D		
<i>(Security classification of title, body of abstract and indexing annotation must be entered when the overall report is classified)</i>		
1. ORIGINATING ACTIVITY (Corporate author) Mechanical Technology Incorporated 968 Albany-Shaker Rd. Latham, New York 12110		2a. REPORT SECURITY CLASSIFICATION Unclassified
		2b. TOUP N/A
3. REPORT TITLE Rotor Bearing Dynamic Design Technology PART VII: The Three Lobe Bearing and Floating Ring Bearing		
4. DESCRIPTIVE NOTES (Type of report and inclusive dates) Final Report for Period 1 August 1966 to 1 August 1967.		
5. AUTHOR(S) (First name, middle initial, last name) J. W. Lund		
6. REPORT DATE February, 1968	7a. TOTAL NO. OF PAGES 272	7b. NO. OF REFS 3
8a. CONTRACT OR GRANT NO.	8b. ORIGINATOR'S REPORT NUMBER(S)	
a. PROJECT NO. 3048 c. Task Nr. 304806 d.	8b. OTHER REPORT NO(S) (Any other numbers that may be assigned this report) AFAPL-TR-65-45, Part VII	
10. DISTRIBUTION STATEMENT This document is subject to special export controls and each transmittal to foreign governments or foreign nationals may be made only with the prior approval of the Air Force Aero Propulsion Laboratory, Wright-Patterson AFB, Ohio.		
11. SUPPLEMENTARY NOTES None	12. SPONSORING MILITARY ACTIVITY USAF AFSC, Air Force Aero Propulsion Laboratory Wright-Patterson AFB, Ohio 45433	
13. ABSTRACT <p>This volume treats three special bearing types selected for study because of their favorable stability characteristics and, hence, their potential for use in high speed rotating machinery applications. The three bearing types are:</p> <ul style="list-style-type: none"><li>a. The Three Lobe Journal Bearing</li><li>b. The Floating Sleeve Bearing with an Incompressible Lubricant</li><li>c. The Floating Sleeve Bearing with a Compressible Lubricant.</li></ul> <p>In the floating sleeve bearings, the ring is prevented from rotating but is otherwise free to move. The ring is floated by pressurizing the outer film of the bearing. In the case of a compressible lubricant, the inner film is pressurized as well.</p> <p>The volume gives extensive design data in form of charts and tables from which the bearing dimensions can be obtained for a given application. Data are given for bearing flow, friction power loss and the speed at which hydrodynamic instability sets in. In addition, two computer programs accompany the volume, and instructions and listings of the programs are included. The programs may be used to obtain data for cases not covered by the presented design data.</p>		

DD FORM 1 NOV 65 1473

UNCLASSIFIED

Security Classification

UNCLASSIFIED

Security Classification

14. KEY WORDS	LINK A		LINK B		LINK C	
	ROLE	WT	ROLE	WT	ROLE	WT
Bearings Lobed Bearings Lubrication Fluid Film Floating Ring Hydrodynamic Hydrostatic Rotor-Bearing Dynamics Stability Critical Speed						

UNCLASSIFIED

Security Classification